TENSILE CAPACITY OF ANCHORS WITH PARTIAL OR OVERLAPPING FAILURE SURFACES: EVALUATION OF EXISTING FORMULAS ON AN LRFD BASIS

by

Charles Benjamin Farrow, B.S.E.

Thesis

Presented to the Faculty of the Graduate School of
The University of Texas at Austin
in Partial Fulfillment
of the Requirements
for the Degree of
Master of Science in Engineering

THE UNIVERSITY OF TEXAS AT AUSTIN
August 1992

ACKNOWLEDGEMENTS

The author would like to express his appreciation to his Supervising Professor, Dr. Richard E. Klingner, for his continuous guidance, constructive criticism, and encouragement throughout this research. It has been both an honor and a pleasure to work with him.

Sincere thanks are also extended to Dr. John E. Breen for serving on the supervising committee. I especially appreciate the collection of data points compiled by Dr. Werner Fuchs and Dr. Breen and essential information sent to the University of Texas by Robert Cannon, Rolf Eligehausen, and Richard Orr.

Much of the computer analysis on which this research is based has been facilitated by the preliminary work of Imed Frigui, who, with Dr. Klingner and this author, cooperatively evaluated existing formulas for tensile capacity of single anchors. Indeed, this study of multiple closely spaced anchors and single anchors near a free edge is an extension of initial investigations for the Tennessee Valley Authority. The author gratefully acknowledges the financial support of this governmental agency.

TENSILE CAPACITY OF ANCHORS WITH PARTIAL OR OVERLAPPING FAILURE SURFACES: EVALUATION OF EXISTING FORMULAS ON AN LRFD BASIS

by

Charles Benjamin Farrow, B.S.E.

Supervising Professor: Richard E. Klingner

This study concerns the prediction of the tensile capacity of anchors as governed by concrete failure. Approximately 1500 data points from information previously compiled by Fuchs and Breen furnish the initial basis for this research. Recent correspondence with Cannon, Eligehausen, and Orr has provided additional data. These tests include both single and multiple anchor tests, anchors near to a free edge as well as anchors remote from a free edge, concrete cone failures, and blow-out failures.

This thesis focuses on single anchors located close to a free edge failing by formation of a concrete cone, and multiple anchors located far from a free edge failing by formation of a concrete cone. A total of 160 points is available for single anchors close to a free edge, while 185 points are available for multiple anchors. A total of 31 data points consisting of data on high strength anchors previously compiled by Klingner et al, Collins et al, and Cannon is accessible from tests on single anchors failing by fracture of the anchor steel. Using common definitions

and nomenclature for all variables and material properties, each of these sets of data are placed in a data base in SI units and concrete cube strengths. For single anchors located close to a free edge the concrete failure data are then plotted against three existing methods: the 45° cone method of ACI 349-85, Appendix B; a variable-angle cone method (VCA); and the Concrete Capacity (CC) method. For multiple anchors isolated from other anchors, the ratio of actual load to predicted load is also plotted for each of the above methods.

Furthermore, observed data are compared against these existing methods in terms of average square error and in terms of Load and Resistance Factor Design (LRFD). In particular, for anchors designed according to each method, the probability of steel or concrete failure under known loads and the probability of concrete failure under unlimited loads are calculated. Based on those comparisons, each approach is evaluated with respect to accuracy and suitability for use in design.

Both for single anchors located near a free edge and for multiple closely spaced anchors, the Concrete Capacity method fits most of the data better than either the ACI 349-85 method or the variable-angle cone method. This is especially evident at very shallow or very deep embedments.

TABLE OF CONTENTS

1.0 INTRODUCTION 1
  1.1 General 1
  1.2 Scope and Objectives 1

2.0 BACKGROUND 4
  2.1 General 4
  2.2 Cone Theory 4
    2.2.1 Constant-Angle Cone Theory . . 5
    2.2.2 Variable-Angle Cone Theory . . 6
  2.3 Kappa Theory 7
    2.3.1 General Background of Kappa Theory 7
    2.3.2 Concrete Capacity Method . . . 8

3.0 REVIEW OF AVAILABLE ANCHOR FAILURE DATA . . . 10
  3.1 General Description of Available Anchor Failure Data 10
    3.1.1 Concrete Failure Data 10
    3.1.2 Steel Failure Data 15
  3.2 Operations Carried Out on Original Data Bases 16
    3.2.1 Placement of Data in Spreadsheet-Type Format 16
    3.2.2 Conversion of SI to U.S. Units and Vice-Versa 16
    3.2.3 Creation of SI Data Bases . . . 17
    3.2.4 Selection of Data to be Excluded 17
      3.2.4.1 Single Anchors Near a Free Edge 17
      3.2.4.2 Multiple Closely Spaced Anchors 18
    3.2.5 Normalization of Data by Concrete Strength 19
    3.2.6 Possible Non-Compliance of Data with Design Requirements: . . . 20

4.0 DESCRIPTIONS OF PRINCIPAL EXISTING METHODS . . 21
  4.1 General 21
  4.2 Description of the ACI 349-85, Appendix B Method [1] 21
    4.2.1 Single Anchors Far from a Free Edge, Remote from Other Anchors 21

4.2.2 Single Anchors Near a Free Edge, Far from Other Anchors 22
4.2.3 Multiple Closely Spaced Anchors Far from a Free Edge 24
4.2.4 General Equations Used with ACI 349-85 Method 31
4.3 Description of the Variable-Angle Cone Method 31
4.3.1 Single Anchors Far from a Free Edge, Remote from Other Anchors . 31
4.3.2 Single Anchors Near a Free Edge, Far from Other Anchors 32
4.3.3 Multiple Closely Spaced Anchors Far from a Free Edge 34
4.3.4 General Equations Used with Variable-Angle Cone Method . . 37
4.4 Description of the Concrete Capacity Method 38
4.4.1 Single Anchors Far from a Free Edge, Remote from Other Anchors 38
4.4.2 Single Anchors Near a Free Edge, Far from Other Anchors 39
4.4.3 Multiple Closely Spaced Anchors Far from a Free Edge 41
4.4.4 General Equations Used with Concrete Capacity Method . . . 47
4.5 Description of Peripheral Shear as a Possible Capacity Prediction Model . . . 48

5.0 COMPARISON OF EXISTING METHODS WITH AVAILABLE DATA 50
5.1 General 50
5.2 Graphical Comparison of Existing Methods 50
5.2.1 Graphical Comparison of ACI 349-85, Appendix B with Concrete Failure Data Base 52
5.2.2 Graphical Comparison of Variable-Angle Cone Angle Method with Concrete Failure Data Base . . 52
5.2.3 Graphical Comparison of Concrete Capacity Method with Concrete Failure Data Base 53
5.3 Evaluation of Error Associated with Each Method 54
5.4 Discussion of Error Evaluation by Sum of Squares Method 55

6.0 LRFD IMPLICATIONS OF EXISTING THEORIES 60
- 6.1 General 60
- 6.2 Background of Applicable ACI 349-85 Provisions [1] 60
- 6.3 Probability of Failure Under Known Loads 62
  - 6.3.1 Statistical Distribution of Applied Loading 62
  - 6.3.2 Statistical Distribution of Anchor Resistances as Governed by Steel 64
  - 6.3.3 Statistical Distribution of Anchor Resistances as Governed by Concrete 67
  - 6.3.4 Combining Load, Steel Resistance, and Concrete Resistance 71
- 6.4 Probability of Concrete Failure Under Unlimited Loads 73
  - 6.4.1 Statistical Distribution of Applied Loading 73
  - 6.4.2 Statistical Distribution of Anchor Resistances as Governed by Steel 74
  - 6.4.3 Statistical Distribution of Anchor Resistances as Governed by Concrete 74
  - 6.4.4 Combining Steel Resistance and Concrete Resistance 74
- 6.5 Summary of Numerical Results 76
  - 6.5.1 Probability of Failure Under Known Loads 76
  - 6.5.2 Probability of Concrete Failure Under Unlimited Loads 78
- 6.6 Discussion of LRFD Results 80
  - 6.6.1 Probability of Failure Under Known Loads 80
  - 6.6.2 Probability of Concrete Failure Under Unlimited Loads 81
- 6.7 General Limitations of These Analyses . . 91

7.0 SUMMARY, CONCLUSIONS, AND RECOMMENDATIONS . . 92
- 7.1 Summary 92
- 7.2 Conclusions 94
  - 7.2.1 Single Anchors Located Near a Free Edge 94
    - 7.2.1.1 Square Error 94
    - 7.2.1.2 Probability of Failure Under Known Loads for

Single Anchors Near a Free Edge 94
7.2.1.3 Probability of Concrete Failure Under Unlimited Loads for Single Anchors Near a Free Edge 95
7.2.2 Multiple Anchors 95
7.2.2.1 Square Error 95
7.2.2.2 Probability of Failure Under Known Loads for Multiple Closely Spaced Anchors 95
7.2.2.3 Probability of Concrete Failure Under Unlimited Loads for Multiple Closely Spaced Anchors . . 96
7.2.3 General Conclusions 97
7.2.4 Limitations of This Study . . . 97
7.3 Recommendations for Further Research . . 100

APPENDIX A: GRAPHICAL COMPARISON OF EXISTING METHODS FOR SINGLE ANCHORS NEAR A FREE EDGE, FAR FROM OTHER ANCHORS (SI UNITS) 101

APPENDIX B: GRAPHICAL COMPARISON OF EXISTING METHODS FOR MULTIPLE CLOSELY SPACED ANCHORS FAR FROM A FREE EDGE (SI UNITS) 123

APPENDIX C: ORIGINAL DATA BASE FOR CONCRETE FAILURES (SI UNITS) 157

APPENDIX D: ORIGINAL DATA BASE FOR STEEL FAILURES (U.S. UNITS) 240

APPENDIX E: SPREADSHEET DATA BASE FOR CONCRETE FAILURES OF SINGLE ANCHORS NEAR A FREE EDGE, FAR FROM OTHER ANCHORS (SI UNITS) 244

APPENDIX F: SPREADSHEET DATA BASE FOR CONCRETE FAILURES OF MULTIPLE CLOSELY SPACED ANCHORS FAR FROM A FREE EDGE (SI UNITS) 249

APPENDIX G: SPREADSHEET DATA BASE FOR HIGH STRENGTH STEEL FAILURES (SI UNITS) . 255

APPENDIX H: COMPUTER PROGRAMS FOR CONDUCTING MONTE CARLO ANALYSIS 257

REFERENCES 276

LIST OF FIGURES

Figure 1: Definition of Effective Embedment Depth for Anchors 11

Figure 2: Available European Failure Data for Single Anchors Far From a Free Edge, Far From Other Anchors 13

Figure 3: Available U.S. Failure Data for Single Anchors Far From a Free Edge, Far From Other Anchors 13

Figure 4: Projected Area of a Single Anchor Located Near a Free Edge (ACI 349-85 Method) 24

Figure 5: Projected Area for a 2 Anchor Group Under Tensile Loading (ACI 349-85 Method) 27

Figure 6: Projected Area for a 4 Anchor Group Under Tensile Loading, $s_1 \geq \sqrt{2}\ (h_e + d_h/2)$ (ACI 349-85 Method) 28

Figure 7: Projected Area for a 4 Anchor Group Under Tensile Loading, $s_1 < \sqrt{2}\ (h_e + d_h/2)$ (ACI 349-85 Method) 29

Figure 8: Projected Area for a 16 Anchor Group Under Tensile Loading, $s_1 < \sqrt{2}\ (h_e + d_h/2)$ (ACI 349-85 Method) 30

Figure 9: Projected Area of a Single Anchor Located Near a Free Edge (CC Method) . 40

Figure 10: Projected Area for a 2 Anchor Group Under Tensile Loading (CC Method) . . 44

Figure 11: Projected Area for a 4 Anchor Group Under Tensile Loading (CC Method) . . 45

Figure 12: Projected Area for a 16 Anchor Group Under Tensile Loading (CC Method) . . 46

Figure 13: Comparison of Error Using Each Theory for Single Anchors Near a Free Edge (Square Root of Sum of Square Error) . 58

Figure 14: Comparison of Error Using Each Method for Multiple Closely Spaced Anchors (Square Root of Sum of Square Error), SI Units 59

Figure 15: Assumed Statistical Distribution of Anchor Loads 63

Figure 16: Required Steel Resistance 65

Figure 17: Actual Steel Resistance 66

Figure 18: Theoretical Steel Resistance 67

Figure 19: Theoretical Concrete Resistance . . . 68
Figure 20: Actual Concrete Resistance, Single Anchor with Edge Distance to Embedment Depth Ratio = 0.601-0.75, CC Method . 69
Figure 21: Probability of Failure Under Known Loads 72
Figure 22: Probability of Concrete Failure Under Unlimited Loads 75
Figure 23: Load, Steel Resistance, and Concrete Resistance Distributions 77
Figure 24: Steel and Concrete Resistance Distributions 79
Figure 25: Definition of β or Safety Index . . . 80
Figure 26: Probability of Failure Under Known Loads for Single Anchors Near a Free Edge 87
Figure 27: Probability of Failure Under Known Loads for Multiple Closely Spaced Anchors 88
Figure 28: Probability of Failure Under Unlimited Loads for Single Anchors Near a Free Edge 89
Figure 29: Probability of Failure Under Unlimited Loads for Multiple Closely Spaced Anchors 90

TABLES

Table 1: Comparison of Error Using Each Theory for Single Anchors Near a Free Edge, Far from Other Anchors (Square Root of Sum of Square Error), SI Units 55

Table 2: Comparison of Error Using Each Theory for Multiple Closely Spaced Anchors, Far from a Free Edge (Square Root of Sum of Square Error), SI Units 56

Table 3: Mean and Coefficient of Variation of Actual Capacity Divided by Predicted Concrete Capacity for Each Method for Single Anchors Near a Free Edge 69

Table 4: Mean and Coefficient of Variation of Actual Capacity Divided by Predicted Concrete Capacity for Each Method for Multiple Closely Spaced Anchors 70

Table 5: Results of Monte Carlo Analysis for Probability of Failure Under Known Loads for Single Anchors Near a Free Edge 83

Table 6: Results of Monte Carlo Analysis for Probability of Failure Under Known Loads for Multiple Closely Spaced Anchors Near Other Anchors 84

Table 7: Results of Monte Carlo Analysis for Probability of Concrete Failure Under Unlimited Loads for Single Anchors Near a Free Edge 85

Table 8: Results of Monte Carlo Analysis for Probability of Concrete Failure Under Unlimited Loads for Multiple Closely Spaced Anchors 86

1.0 INTRODUCTION

1.1 General

One of today's most vexing problems in the design of anchorage to concrete involves the question of how to predict the tensile capacity of anchors as governed by failure of the concrete. Many sets of design recommendations exist. Some are derived primarily from a cone-based concept, long popular in the United States. Others originate from the Kappa theory method developed over the past decade in Europe. Both general theories are reasonably consistent with test data.

To determine which design method is most appropriate, the available data base must be carefully examined. Resolution of this issue will permit a rational, consistent evaluation of the capacity of existing anchors, will unify the code development process in the United States, and will stimulate the increased use of anchors both in this nation and abroad.

1.2 Scope and Objectives

The overall objective of this research is to evaluate the accuracy and suitability for use in design of specific methods for predicting anchor capacity as governed by concrete failure. A previous study by Klingner et al has focused on evaluating each of the methods for single anchors far from a free edge and far from other anchors [2]. In particular, this study focuses on single anchors located close to a free edge, and on multiple closely spaced anchors located far from a free edge.

The objectives are fulfilled as follows:

1) A total of 160 data points is available from tests on single anchors close to a free edge in which failure occurs by formation of a concrete cone. Using common definitions and nomenclature for all variables and material properties, those data are placed in a data base in SI units and concrete cube strengths.

2) A total of 185 data points is available from tests on multiple closely spaced anchors far from a free edge. In these tests failure occurs by formation of a concrete cone. These data on multiple anchors include a large number of data points on groups of both 2 and 4 anchors. In addition, 6 tests on groups of 16 anchors are included. Using common definitions and nomenclature for all variables and material properties, those data are placed on a data base in SI units and concrete cube strengths.

3) Data for single anchors located close to a free edge are plotted against three existing methods: the 45° cone method of ACI 349-85; a variable-angle cone method; and the Concrete Capacity method (exponent of 1.5). These plots show concrete capacity, normalized by $\sqrt{f_{cc}}$, as a function of embedment depth.

4) Data for multiple closely spaced anchors is also plotted against three existing methods: the 45° cone method of ACI 349-85; a variable-angle cone method; and the Concrete Capacity method (exponent of 1.5). These plots show ratios of actual capacity to predicted capacity as a function of embedment depth.

5) Distinct square errors are computed for different ranges of ratios of edge distance to embedment depth for single anchors near a free edge.

6) Distinct square errors are computed for different ranges of ratios of edge distance to embedment depth for multiple closely spaced anchors.

7) The probability of steel or concrete failure under known loads, and of concrete failure under unlimited loads, is determined for single anchors located near a free edge. Distinct probabilities of failure are defined for different ranges of ratios of edge distance to embedment depth.

8) The probability of steel or concrete failure under known loads, and of concrete failure under unlimited loads is determined for multiple closely spaced anchors distant from free edges. Distinct probabilities of failure are defined for different ranges of ratios of anchor spacing to embedment depth.

9) Based on the above comparisons of square error and probability of failure, each method is evaluated with respect to accuracy and design suitability for both single anchors located near a free edge and multiple closely spaced anchors.

2.0 BACKGROUND

2.1 General

To design headed anchors subjected to tension, either acting alone or in combination with other anchors, it is necessary to predict the load at which a single tensile anchor fails. This thesis focuses on predicting the failure load as governed by concrete. General principles available to the structural engineer include the cone theory and the Kappa theory. The former is the basis for one widely used U.S. anchor design code [1]. The latter is described in recent European technical literature [3,4,5].

2.2 Cone Theory

Most U.S. design recommendations are founded on the cone theory [1,6], named after the roughly conical shape of the piece of concrete which pulls out in this kind of failure. Although this theory is often used assuming a cone angle of 45°, it is applicable to arbitrary cone angles.

Calculations of the cone theory for a single anchor far from a free edge and remote from other anchors assume a uniform nominal stress f_t on the entire surface of a truncated cone. The nominal tensile strength f_t, usually taken as $4\sqrt{f'_c}$ in psi units, is about two-thirds the typical actual tensile strength of $6\sqrt{f'_c}$. The cone theory is therefore usually defended physically in terms of a tensile stress distribution which varies from a maximum of $6\sqrt{f'_c}$ at the anchor head to zero at the surface. However, it can also be justified physically in terms of a uniform stress of $6\sqrt{f'_c}$ acting over the uncracked portion of a slowly propagating conical failure surface.

The capacity of an anchor near a free edge or near another anchor is calculated by multiplying the predicted cone theory value by a reduction factor in order to account for overlapping or partial conical failure surfaces. This factor is commonly taken as the ratio of net projected area of the anchor or group of anchors of interest to the gross area of an equivalent number of anchors with no influences from either edges or the proximity of other anchors.

The cone theory has logical arguments in its favor: first, the final failure surface is approximately conical; and second, the theory is conceptually simple. The principal objection to the cone theory is that it does not account directly for experimental evidence from the U.S. and Europe which clearly not only shows that failure does not occur simultaneously over the entire surface but also that the cone angle is not constant along the surface of the failed piece of concrete [3,4,5,7,8]. Although cone theories can include both phenomena, they do not always follow this pattern. A second objection to its use in building codes is that its application in design is simple in concept but complex in numerical computation unless computers or design aids are used.

2.2.1 Constant-Angle Cone Theory

If the cone angle is assumed constant with embedment depth, the cone theory predicts that anchor capacity for a single anchor far from other anchors and far from a free edge increases as a function of the embedment depth squared (that is, raised to the power 2). Constant-angle cone theories are exemplified by the provisions of Appendix B of ACI 349-85 [1].

When multiple closely spaced anchors or anchors near a free edge are evaluated using the constant-angle cone theory, the predicted failure load increases as a function of the embedment depth squared only for a given ratio of edge distance to embedment depth or spacing to embedment depth. This is due to the fact that the ratio of net projected area to gross area is constant only for constant ratios of edge distance to embedment depth or spacing to embedment depth. In addition, the ratio of net to gross area remains constant only for a constant number of anchors. For example, consider two groups of anchors, each group having the same ratio of spacing to embedment depth. If one group has two anchors, and the other has four anchors, their ratios of net area to gross area differs.

2.2.2 Variable-Angle Cone Theory

Experimental observations confirm that the average cone angle decreases (that is, the cone becomes flatter) as the embedment depth decreases. Within each cone, the cone angle also decreases as the fracture propagates toward the surface. TVA design recommendations [9] have addressed this phenomenon by prescribing a cone angle which is equal to 45° for embedment depths equal to or greater than 5 inches; then this cone angle decreases linearly to 28° for embedment depths of zero. If a flatter cone angle is assumed for shallower embedments, calculated anchor capacity increases more slowly with embedment depth than the constant-angle cone theory predicts. Because the variable-angle cone theory modifies the original cone theory by a coefficient which decreases with increasing embedment, it simulates a constant-coefficient equation in which embedment depth is raised to a power less than 2 for single anchors remote from free edges and other anchors, for single anchors located near a free edge with a constant ratio of edge distance to embedment depth, and for multiple closely spaced anchors with a given configuration as well as a constant ratio of spacing to embedment depth.

2.3 Kappa Theory

2.3.1 General Background of Kappa Theory

The Kappa theory [3,4,5], based on a combination of empirical evidence plus some fracture mechanics, states that the anchor capacity, as governed by concrete failure, varies as a function of the embedment depth to the power 1.5 for single anchors located far from a free edge and far from other anchors. In addition, this theory assumes the slope of the failure cone surface to be 35°. Such a slope implies a minimum spacing between anchors of 3 times the embedment depth of the anchor and a minimum edge distance of 1.5 times the embedment depth in order to develop full anchor capacity.

The Kappa theory has several rational supporting arguments:

a) Reduced test data from Europe, obtained from tests in which all variables except embedment depth are maintained constant, suggest that capacity prediction formulas with an exponent of 1.5 are preferable to those with an exponent of 2 [10].

b) Some researchers suggest that fracture mechanics provides a theoretical basis for capacity prediction formulas with an exponent of 1.5 [8].

The principal objection to the Kappa theory has been that most European data have not been available in their original form. However, the recent work of Eligehausen, Fuchs and Breen in this area has overcome this difficulty by providing available test data for this current research [11]. Other researchers also argue that fracture mechanics theory does not provide unequivocal support for the exponent of 1.5 nor for the precise form of the Kappa theory equation.

If anchors are located close to a free edge, the Kappa theory reduces the predicted capacity of an equivalent single anchor far from a free edge and far from other anchors. This is done by multiplying by a factor which is determined from linear interpolation between a minimum at an edge distance of zero to a maximum at an edge distance equal to 1.5 times the embedment depth. A similar linear interpolation is performed to account for the case in which multiple anchors have a spacing within the group that is so small that the respective break-out cones overlap. This factor varies linearly from a minimum at a spacing of zero to a maximum at a spacing of 3 times the embedment depth.

2.3.2 Concrete Capacity Method

The Concrete Capacity method is an attempt to combine the design approaches of both the ACI 349-85 design approach and the Kappa theory. For single anchors far from other anchors and far from a free edge, the Concrete Capacity method is equivalent to the Kappa theory. However, when the approach is applied to multiple closely spaced anchors or anchors located near a free edge, the concept of multiplying by the ratio of net area to gross area is adopted from the ACI 349-85 approach. These area calculations are based on the idealization of the concrete failure surface as a truncated pyramid with an inclination of approximately 35°. One obvious advantage of this method is that it substantially reduces the complexity of computing the net area for a group of anchors or an anchor located near a free edge.

As is the case with multiple closely spaced anchors evaluated with the constant-angle cone theory, the predicted failure load increases as a function of the embedment depth to the 1.5 power only for a given ratio of edge distance to embedment depth or spacing to embedment depth. This is due to the fact that the ratio of net projected area to gross area is constant only for constant ratios of spacing to embedment depth. In addition, the ratio of net to gross area remains constant only for a constant number of anchors. For example, a group of two anchors with the same spacing and embedment depth as a group of four anchors does not have the same ratio of net area to gross area.

3.0 REVIEW OF AVAILABLE ANCHOR FAILURE DATA

3.1 General Description of Available Anchor Failure Data

3.1.1 Concrete Failure Data

All information on concrete failures has been obtained from a data base previously compiled by Fuchs and Breen using results of tests on anchor bolts, headed studs, undercut anchors, and expansion anchors [12]. Furthermore, additional test data have recently been provided through correspondence with Cannon, Eligehausen, and Orr [13,14,15]. The data base from Fuchs and Breen is presented in its original form in Appendix A of this thesis followed by the data received from the other sources. In Appendix A, each set of data is identified by a corresponding reference number. References for all data points are listed at the end of Appendix A.

Each line of the original data base describes a single test result in terms of the following information:

1) Syst.: test number as defined by Fuchs and Breen
2) d: diameter of the anchor
3) do or dh: diameter of the hole for metal anchors and diameter of anchor head for headed studs, respectively
4) hef or h_e: effective embedment depth (measured to the bearing surface and illustrated in Figure 1)
5) Tinst: tightening torque
6) fy: yield strength of the steel
7) ft: tensile strength of the steel

8) fcc200: compressive strength of 200 mm concrete cubes

9) fct: tensile strength of the concrete

10) dagg: diameter of the aggregate in the concrete

11) c1: edge distance as measured from center of anchor

12) s1: distance to nearest anchor (direction 1) measured center to center of anchors

13) s2: distance to nearest anchor (direction 2) measured center to center of anchors

14) Nu: actual failure load

15) Lit.: reference number

Data received through correspondence with Cannon, Eligehausen, and Orr are presented in a similar format at the end of Appendix A.

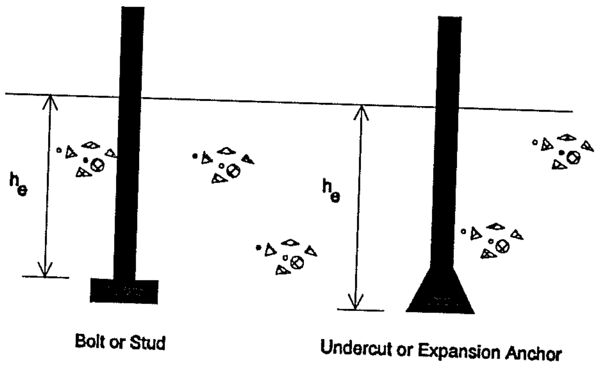

Figure 1: Definition of Effective Embedment Depth for Anchors

The original data base of Fuchs and Breen contains the results of over 1200 tests on anchors. These tests include anchors tested in shear and in tension for a wide range of anchor configurations. Recent correspondence with Cannon, Eligehausen, and Orr has provided data from approximately 50 additional tests on anchors loaded in tension. A total of 160 data points is available for single anchors located near a free edge, while 185 data points are available for multiple closely spaced anchors. Because most of the concrete failure results have been obtained from European tests, the original concrete data base has been prepared in SI units. Thus, concrete strength is expressed in terms of cube strength. Although the original data base contains tests conducted in both Europe and the United States, Eligehausen, Fuchs, and Breen report no difference in tension test results (Differences exists in shear tests due to differing friction between loading plates and concrete) [11]. This conclusion is supported by a graphical comparison of U.S. data and European data on single anchors far from a free edge and far from other anchors. Failure load is plotted as a function of embedment depth in Figures 2 and 3.

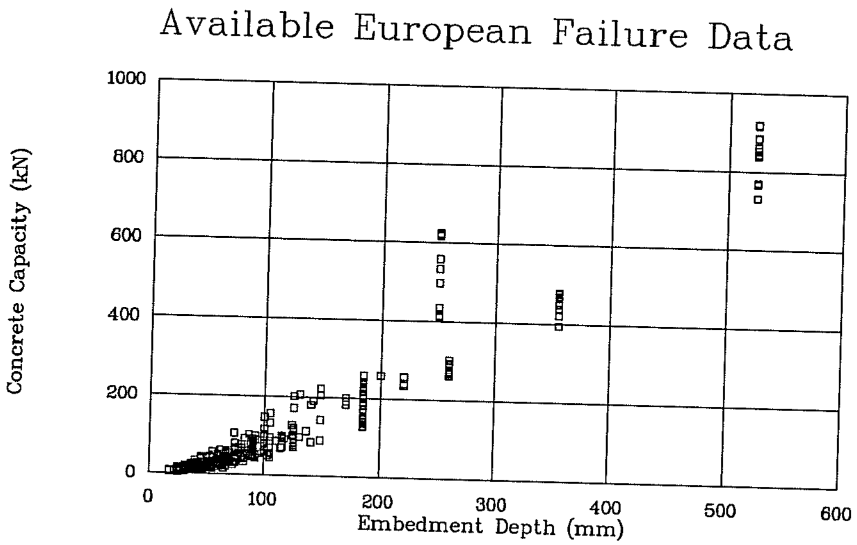

Figure 2: Available European Failure Data for Single Anchors Far From a Free Edge, Far From Other Anchors

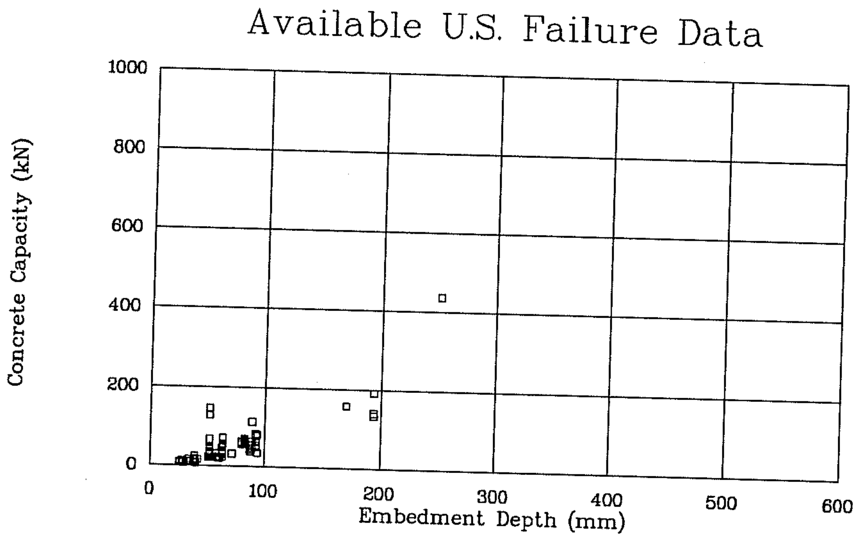

Figure 3: Available U.S. Failure Data for Single Anchors Far From a Free Edge, Far From Other Anchors

These data used in this evaluation of capacity prediction formulas focus on headed anchors and metal anchors. Headed anchors are either bolts or studs, usually installed by cast-in-place methods. Metal anchors are placed into pre-drilled holes in concrete and anchored by expansion or undercutting. Expansion anchors are anchored in holes by forced expansion. In contrast, undercut anchors are anchored mainly by undercutting of the concrete. Adhesive or bonded anchors are also included in the general category of metal anchors. However, no adhesive anchors are included in this study, since their use is prohibited in nuclear related structures [1].

All anchors included in this study have been subjected to static loading. The effect of cyclic loading is not considered. In addition, this loading is assumed to be applied concentrically. This factor is of special significance in comparing the Concrete Capacity method with either the ACI 349-85 or VCA method, since the Concrete Capacity method is the only one that considers the effects of eccentrically applied loading.

All tests have been performed in uncracked concrete. The presence of tensile cracks can substantially reduce the ultimate loads of concrete anchor bolts. Although this evaluation of available capacity methods does not consider the effects of tensile cracks on capacity, it seems reasonable to suggest compensating for this omission by reducing design capacity by an additional multiplicative factor. In addition, all tests have been performed in unreinforced concrete except for recent test results provided by Eligehausen [13]. Only tests in which the reinforcement does not intersect the failure surfaces are considered. Thus, each test is equivalent to experiments in unreinforced concrete.

3.1.2 Steel Failure Data

Data on steel failures are obtained from a data base previously published by Klingner et al [6], from tests performed by Collins [7], and from recent correspondence with Cannon [14] using results of tests on anchor bolts and headed studs. These data bases are presented in their original form in Appendix B of this thesis. In Appendix B, each set of data is identified by a corresponding reference number. The references are listed at the end of Appendix B.

Each line of the data base describes a single test result in terms of the following information:

1) test number as defined in Reference 5
2) reference number as listed in Reference 5
3) test number as defined in original reference
4) type of anchor
5) diameter of anchor
6) length of anchor
7) effective embedment depth of anchor
8) diameter of the anchor head
9) compressive strength of the concrete
10) type of concrete (normal or lightweight aggregate)
11) failure load
12) failure mode (steel or concrete)
13) remarks

These data refer to single anchor tests only. This data base includes tests on both high strength anchors and regular anchors. Since the nuclear industry is increasingly moving toward the use of high strength anchors, this study uses only the data available on high strength anchors in its evaluation of the probability of failure of each of the three methods. A total of 31 tests on high strength anchors is utilized. Because most of the steel failure data has been obtained from U.S. tests, the original steel data base has been prepared in U.S. units. Concrete strength is expressed in terms of cylinder strength.

3.2 Operations Carried Out on Original Data Bases

3.2.1 Placement of Data in Spreadsheet-Type Format

All data in Appendices A and B for tensile anchor tests are placed in spreadsheet form using SuperCalc 5.0©. They can be readily converted for use with Fortran or BASIC programs, other spreadsheets such as LOTUS*123©, and most common graphics packages.

3.2.2 Conversion of SI to U.S. Units and Vice-Versa

The original data base for concrete failures is obtained in SI units. In contrast, the original data base for steel failures is obtained in U.S. units. Using the conversion factors given below, all original data are manipulated to obtain all data bases in SI units:

1 in = 25.4 mm
1 psi = 0.006895 N/mm^2
1 lb = 4.448 N
f_{cc} (Cube) = 1.18 f_c (Cylinder)

After these conversions have been made, the predicted failure loads are computed separately for each data base, and are normalized for differences in concrete strengths.

U.S. practice bases the compressive strength of concrete on the strength of a 6- by 12-inch cylinder, while European practice uses a 200 mm cube. Because of its shape, a concrete cube normally has a central region subjected to biaxial lateral confinement due to platen restraint. When cubes and cylinders are cast from a single batch of concrete and cured identically, the cubes have a higher apparent strength than the cylinders. The cube strength is about 1.18 times the corresponding 6 x 12 cylinder strength [16]. This value is consistent with conversion factors used by Fuchs and Breen [11].

3.2.3 Creation of SI Data Bases

After selecting all data on single anchors with edge distances less than or equal to $2h_e$, these data are placed in spreadsheet form. Similarly, all data on multiple anchors with spacing less than or equal to $4h_e$ are presented in spreadsheet form. These distances have been chosen because they are consistent with the largest edge distance and largest spacing that would cause a reduction in predicted capacity by any of the three formulas. All capacities listed are normalized by the number of anchors within a group. Information presented here can be expressed and evaluated in either set of units and concrete compressive strength references.

3.2.4 Selection of Data to be Excluded

Some data on the original concrete data files have been excluded from further consideration based on the following criteria:

3.2.4.1 Single Anchors Near a Free Edge

1) Test data from single anchors failing by side blowout are excluded. Anchors placed close to a free edge can fail prematurely by creation of a partial cone [3,6], or by side blowout [3,6,17,18]. The edge distance within which a partial cone forms is far greater than that at which side blowout is a problem. This fact explains why this data base contains few points with very low ratios of edge distance to embedment.

2) Test data from anchors located sufficiently far from the edge so that a complete failure surface develops are not included in the data base. The limiting edge distance chosen is that distance at which all three methods - ACI 349-85, VCA, and CC - consider the anchor as a single anchor with no influence due to edge conditions. As previously stated, the shallowest cone angle predicted by the VCA method is 28°. This value is less than that of either the ACI 349-85 method (45° cone) or the CC method (35° pyramid). The 28° angle implies that anchors are affected by a free edge if they are placed closer to the free edge than $(h_e/\tan 28^\circ)+d/2$ or $(1.9\ h_e + d/2)$. However, no embedment depth is small enough to meet this limiting criterion; hence, the governing formula becomes the CC method and its assumption of approximately a 35° pyramid. This method is influenced by edge distances if anchors are less than $1.5h_e$ from the edge.

3.2.4.2 Multiple Closely Spaced Anchors

1) Test data from multiple anchors located sufficiently far from other anchors or located close to a nearby edge are not included in the data base. The limiting

center to center distance of the anchors chosen is the spacing at which all three methods - ACI 349-85, VCA, and CC - evaluate the group of anchors as an equivalent number of single anchors with no influence from other anchors. As previously stated, the shallowest cone angle predicted by the VCA method is 28°. This value is less than that of either the ACI 349-85 method (45° cone) or the CC method (35° pyramid). The 28° angle implies that anchors are affected by other anchors if they are placed closer to other anchors than $2((h_e/\tan 28°)+d/2)$, or $2(1.9\ h_e + d/2)$. However, no embedment depth is small enough to meet this limiting criterion; hence, the governing formula becomes the CC method and its assumption of approximately a 35° pyramid. This method is influenced by other anchors if anchors are less than $3.0h_e$ from adjacent anchors.

2) A series of approximately 10 tests is available involving unsymmetrically spaced group anchors. These data points are not included. Specifically, the tests are groups of 16 anchors in which the anchors are cast in groups of 4 symmetrically placed about a center point. Because the spacing between anchors within each group of 4 is not the same as the spacing between an anchor and the nearest anchor in an adjacent group, this pattern cannot be described by a single ratio of anchor spacing to embedment depth. These points are not included in the calculations in order to simplify the calculation process and to avoid the influence of possible eccentric load.

3.2.5 Normalization of Data by Concrete Strength

The available data are obtained from tests involving many different values of concrete strength. All three methods examined in this research predict that anchor capacity as governed by concrete failure is proportional to the square root of the concrete compressive strength. To permit the data to be plotted on a single graph as a function of embedment depth, actual and predicted failure loads are normalized by the square root of the concrete compressive strength.

3.2.6 Possible Non-Compliance of Data with Design Requirements

As discussed in detail in Section 7.2, ACI 349-85 has requirements for the minimum bearing area of the anchor head. The concrete data base has not been checked for compliance with those requirements. This is especially important to the single anchors located near a free edge since the design of some of the anchors may well be governed by this criteria. However, as previously stated, all "blow-out" failures are excluded from the data base.

Several design guides place minimum limitation on the diameter of the anchor shaft and the minimum anchorage depth. For instance, the UEAtc limits shaft diameter to 0.236 inches (6 mm) and embedment depth to 1.575 inches (40 mm) [19]. However, no check is made to insure that these criteria are met in this data base.

4.0 DESCRIPTIONS OF PRINCIPAL EXISTING METHODS

4.1 General

In this section the three principal existing methods introduced previously are described mathematically (SI units) for both single anchors near a free edge and for multiple closely spaced anchors. In evaluating the ACI 349-85 method and the variable-angle cone method for predicting concrete capacity, the head diameter d_h is assigned a value equivalent to the actual diameter of the anchor. This, it is believed, is consistent with the latest deliberations of ACI Committee 349. When capacity prediction methods are used for design, they are expressed in terms of specified concrete compressive strength (denoted by f'_{cc}). When capacity prediction methods are compared with test results, the actual concrete compressive strength is used (denoted by f_{cc}). In order for the equations to remain consistent with their original sources, they are written using the notation of f_{cc}.

4.2 Description of the ACI 349-85, Appendix B Method [1]

4.2.1 Single Anchors Far from a Free Edge, Remote from Other Anchors

The nominal cone capacity of the concrete is based on a maximum tensile strength of $4 \sqrt{f_c}$ (psi units). This tensile strength is assessed involving actions on the projected area of a 45° stress cone radiating toward the attachment from the bearing edge of the anchor (B.5.1.1) [1]:

$$4 \pi \sqrt{f_c}\, h_e \,(h_e + d_h)$$

where h_e = embedment length, measured from free surface to the bearing surface of the anchor head

d_h = diameter of anchor head (taken as anchor diameter)

Equivalently, this expression can be expressed in SI units (N, mm, and concrete cube strength) as follows:

$$0.96 \sqrt{f_{cc}}\, h_e \,(h_e + d_h)$$

4.2.2 Single Anchors Near a Free Edge, Far from Other Anchors

Locating an anchor near a free edge reduces the projected area of the 45° stress cone if the 45° cone intersects the edge of the concrete (Figure 4). ACI 349-85 takes this into account by multiplying the value obtained in the equation presented in Section 4.2.1 by the ratio of the actual projected area (net area) to the projected area of the anchor not limited by edge influences (gross area). Accordingly, the equation, expressed in SI units, is as follows:

$$\frac{A_p}{A_{p,o}}\, 0.96 \sqrt{f_{cc}}\, h_e \,(h_e + d_h)$$

where

A_p = actual projected area of anchor

$A_{p,o}$ = projected area of anchor not limited by edge influences

Note that the ratio of A_p to $A_{p,o}$ is non-dimensional and can be applied directly to the corresponding equation in U.S. units without using a conversion factor.

The ratio of A_p to $A_{p,o}$ for anchors located near a free edge is computed as follows:

1) Determine the radius of an equivalent full stress cone:

$$R = h_e + d_h/2$$

2) Partition the actual projected area of the anchor and determine appropriate geometric quantities: (Note: Measure all angles in degrees.)

$$\beta = Cos^{-1}\left[2\left(\frac{c_1}{R}\right)^2 - 1\right]$$

3) Find the projected area of one anchor not limited by edge influences:

$$A_{p,o} = \pi\, h_e\, (h_e + d_h)$$

4) Find the area lost due to the edge using the following:

$$A_{Lost} = \pi\, R^2\, \frac{\beta}{360} - c_1\, R\, Sin\left(\frac{\beta}{2}\right)$$

5) Finally, net projected area equals the difference between projected area of an anchor not limited by edge influences and the area of the segment formed by the edge of the concrete acting as a secant of the circle:

$$A_p = A_{p,o} - A_{Lost}.$$

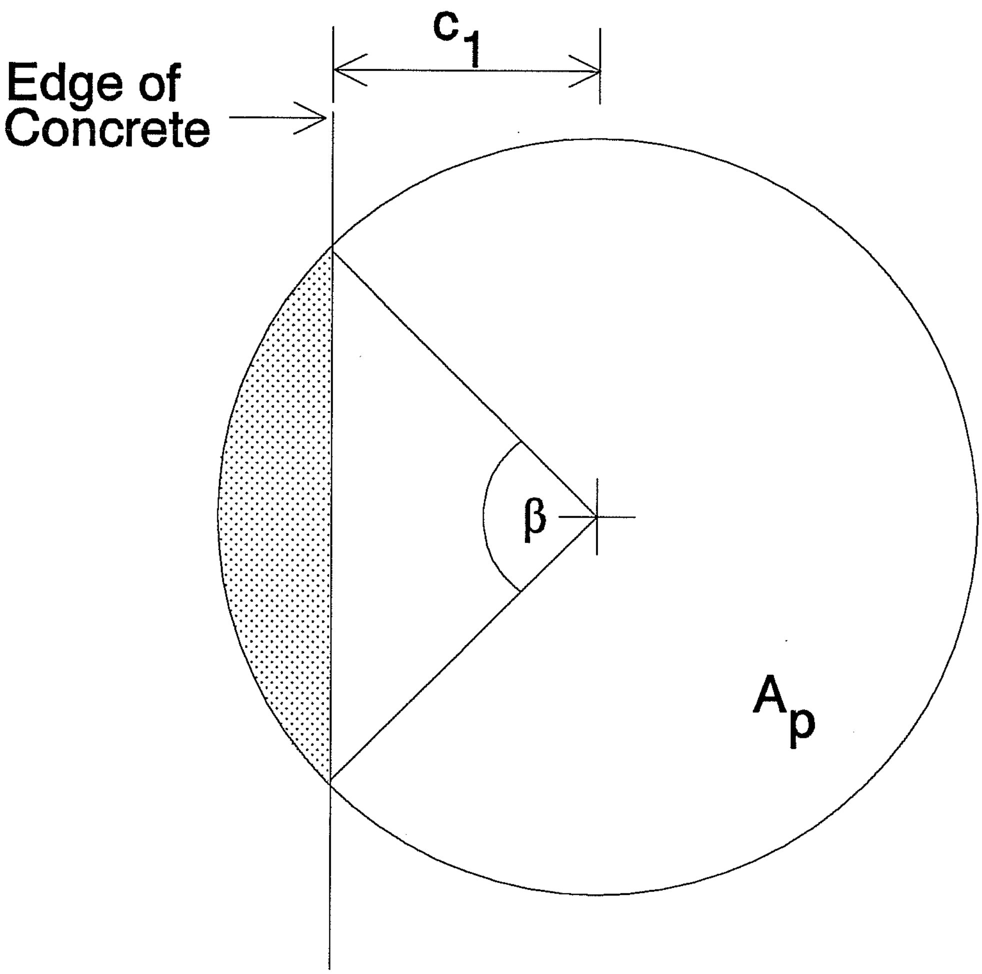

Figure 4: Projected Area of a Single Anchor Located Near a Free Edge (ACI 349-85 method)

This equation is valid until $c_1 = h_e + d_h/2$ or, equivalently, $A_p = A_{p,o}$.

4.2.3 Multiple Closely Spaced Anchors Far From a Free Edge

Locating anchors close to other anchors reduces the projected area of a single anchor due to overlapping of failure surfaces. ACI 349-85 takes this into account in the same way in which the problem of single anchors located near a free edge is evaluated for predicted capacity. Thus, the predicted capacity for each anchor within the group, expressed in SI units, is as follows:

$$\frac{A_p}{A_{p,o}}\ 0.96\ \sqrt{f_{cc}}\ h_e\ (h_e + d_h)$$

where

A_p = actual projected area of all anchors in the group

$A_{p,o}$ = projected area of all anchors in the group not limited by adjacent anchors

Note that the ratio of A_p to $A_{p,o}$ is non-dimensional and can be applied directly to the corresponding equation in U.S. units without employing a conversion factor.

The ratio of A_p to $A_{p,o}$ for multiple closely spaced anchors is calculated as follows:

1) Determine if all anchors in the group act as equivalent single anchors:
   Anchors behave as a group of single anchors if

   $$\left(\frac{s_1}{2} - h_e - \frac{d_h}{2}\right) \geq 0$$

   Otherwise, anchors have overlapping failure surfaces. If anchors act as a group of single anchors, then the ratio of A_p to $A_{p,o}$ is assigned a value of 1.0.
2) Find the projected area of all anchors not limited by edge influences:

$$A_{p,o} = n\pi\ h_e\ (h_e + d_h)$$

where

n = number of anchors within the group

3) Check to make sure that the projected failure surface does not intersect an edge:

If $(c_1/h_e) > 1$, then no edge problem exists.
If $(c_1/h_e) \leq 1$, then an edge problem results.

All points having edge problems according to these criteria have been removed from the data base.

4) Partition the actual projected area of the anchor group and determine appropriate geometric quantities. All anchor groups included in the data base have equal spacing between anchors for all anchors within the group. Thus, $s_1 = s_2$ for all anchor groups with $n > 2$. (Note: Measure all angles in degrees.)

5) Determine the actual projected area for the appropriate anchor configuration as defined in Figures 5 through 8. The equation presented at the beginning of Section 4.2.3 is valid until $(s_1/2) = h_e + d_h/2$ or, equivalently, $A_p = A_{p,o}$.

For a group of 2 fasteners the formula is as follows:

$$\beta = Cos^{-1}\left[2\left(\frac{s_1}{d_h+2\,h_e}\right)^2-1\right]$$

$$A_p = 2\pi h_e\,(h_e+d_h) - \left(h_e+\frac{d_h}{2}\right)^2 (\beta - Sin\beta)$$

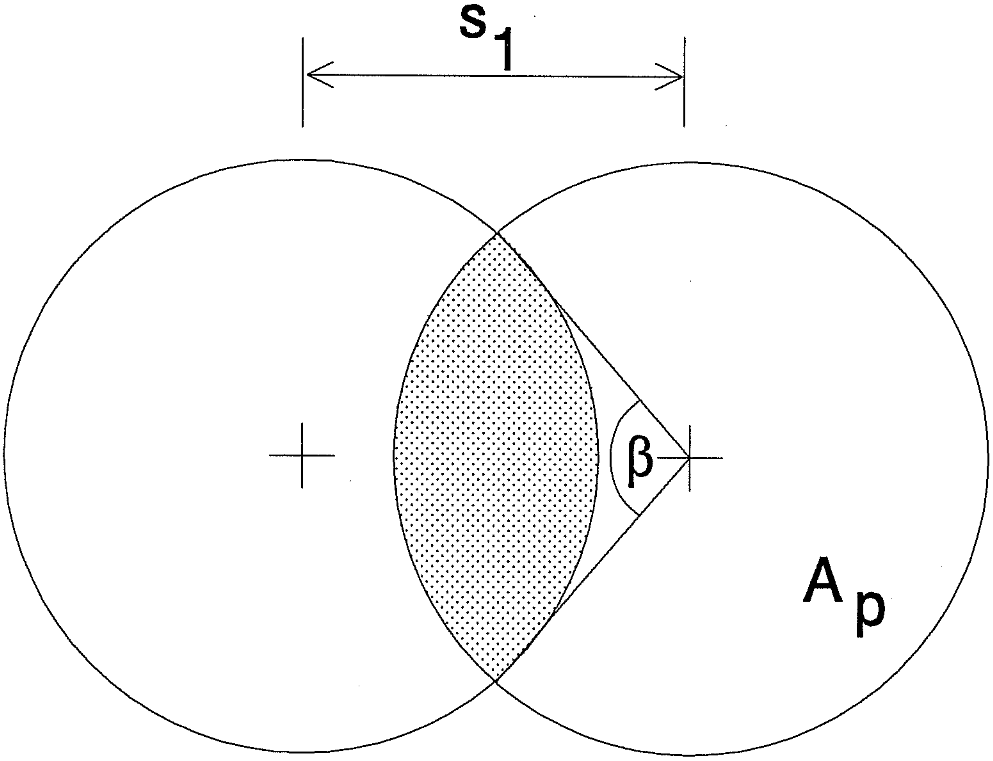

Figure 5: Projected Area for a 2 Anchor Group Under Tensile Loading (ACI 349-85 Method)

For a group of 4 fasteners where $s_1 = s_2$, the formulas are as follows:

$$\beta = Cos^{-1}\left[2\left(\frac{s_1}{d_h + 2h_e}\right)^2 - 1\right]$$

$$If\ s_1 \geq \sqrt{2}\left(h_e + \frac{d_h}{2}\right),\ then$$

$$A_p = 4\pi h_e (h_e + d_h) - 4\left(h_e + \frac{d_h}{2}\right)^2 (\beta - Sin\beta)$$

$$If\ s_1 < \sqrt{2}\left(h_e + \frac{d_h}{2}\right),\ then$$

$$A_p = s_1^2\left(1 + \tan\frac{\beta}{2}\right) + \left[\frac{270 - \beta}{90}\right]\pi\left(h_e + \frac{d_h}{2}\right)^2 - \pi d_h^2$$

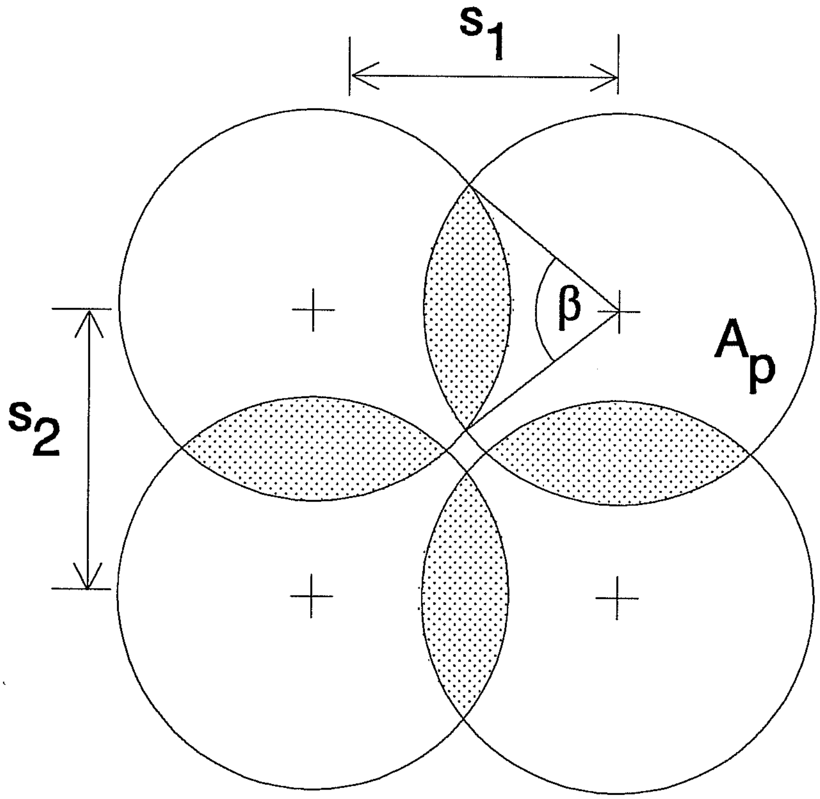

Figure 6: Projected Area for a 4 Anchor Group Under Tensile Loading, $s_1 \geq \sqrt{2}\ (h_e + d_h/2)$ (ACI 349-85 Method)

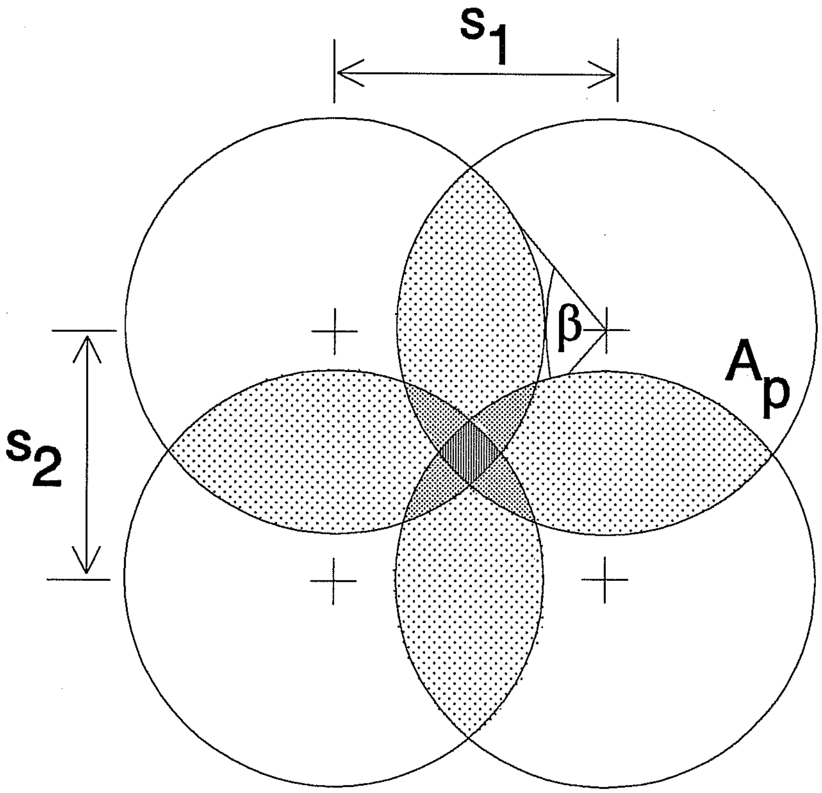

Figure 7: Projected Area for a 4 Anchor Group Under Tensile Loading, $s_1 < \sqrt{2}\ (h_e + d_h/2)$ (ACI 349-85 Method)

For a group of 16 anchors where $s_1 = s_2$, the only available data are for groups that have $s_1 < \sqrt{2}\ (h_e + d_h/2)$. The formula for determining the area of this type of configuration is as follows:

$$\beta = Cos^{-1}\left[2\left(\frac{s_1}{d_h + 2h_e}\right)^2 - 1\right]$$

$$A_p = s_1^2\left(1 + \tan\frac{\beta}{2}\right) + \left[\frac{270 - \beta}{90}\right]\pi\left(h_e + \frac{d_h}{2}\right)^2 - 16\pi d_h^2 + 4s_1^2 + 4s_1^2\left[1 + \tan\frac{\beta}{2} + \left(h_e + \frac{d_h}{2}\right)^2(\beta - Sin\beta)\right]$$

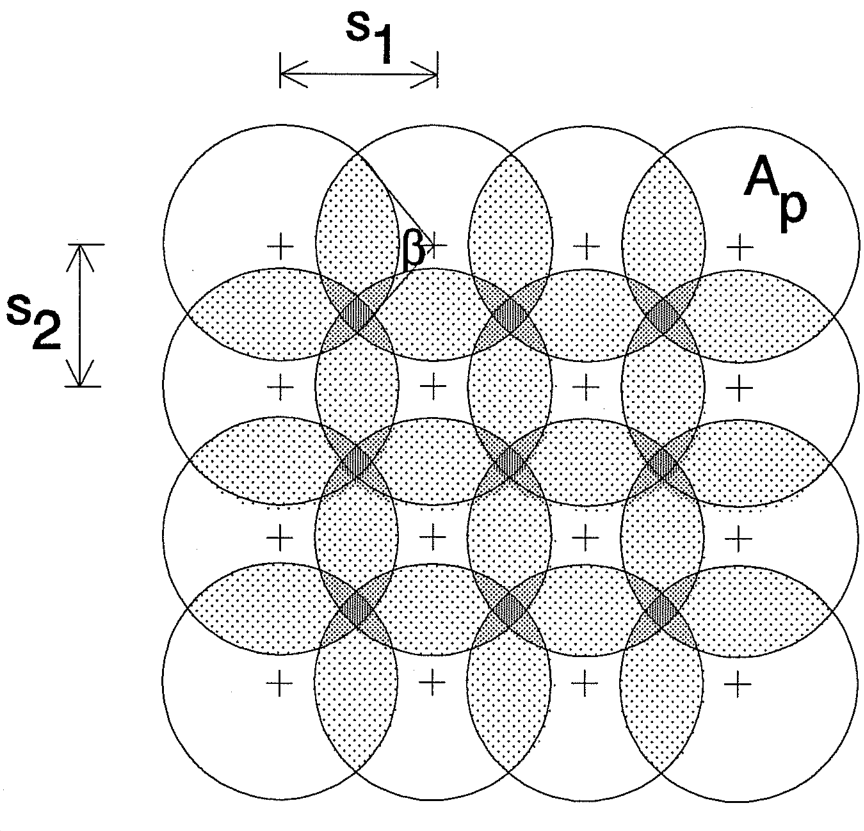

Figure 8: Projected Area for a 16 Anchor Group Under Tensile Loading, $s_1 < \sqrt{2}\ (h_e + d_h/2)$ (ACI 349-85 Method)

4.2.4 General Equations Used with ACI 349-85 Method

The equations for various cases of edge distance and spacing can be written in more general form. When using U.S. units (pounds, inches, and concrete cylinder strength), the concrete cone capacity is given by:

$$\frac{A_p}{A_{p,o}}\ 4\ \pi\ \sqrt{f_c}\ h_e\ [h_e + d_h]$$

When using SI units (N, mm, and concrete cube strength), the concrete cone capacity is determined by:

$$\frac{A_p}{A_{p,o}}\ 0.96\ \sqrt{f_{cc}}\ h_e [h_e + d_h]$$

In both cases, A_p and $A_{p,o}$ are defined as follows:

A_p = actual projected area of anchor or anchor group

$A_{p,o}$ = projected area of all anchors not limited by edge or spacing influences

4.3 Description of the Variable-Angle Cone Method

4.3.1 Single Anchors Far from a Free Edge, Remote from Other Anchors

The variable-angle cone method is identical to that of Appendix B of ACI 349-85 except for the way in which the available concrete cone capacity is calculated. The variable-angle cone method used here is based on one originally developed by the Tennessee Valley Authority [6,9]. The design pullout strength of the concrete is based on a maximum tensile strength of 4 $\sqrt{f_c}$ (psi units). Tensile strength is assessed involving actions on the projected area of a variable-angle stress cone radiating toward the attachment from the bearing edge of the anchor:

$$4\,\pi\sqrt{f_c}\left(\frac{h_e}{\tan\theta}\right)\left[\frac{h_e}{\tan\theta}+d_h\right]$$

where h_e = embedment length, measured from free surface to the bearing surface of the anchor head

d_h = diameter of anchor head (taken as anchor diameter)

θ = cone angle, measured from a plane perpendicular to the anchor axis

The cone angle varies as a function of the embedment depth:

$\theta = 45^o$ *for* $h_e \geq 5.0$ *inches* (127.0 *mm*)

$\theta = 28^o + (3.4\,h_e)^o$ *for* $h_e < 5.0$ *inches* (*U.S. Units*)

$\theta = 28^o + (0.13386\,h_e)^o$ *for* $h_e < 127.0$ *mm* (*SI Units*)

4.3.2 Single Anchors Near a Free Edge, Far from Other Anchors

Locating an anchor near a free edge reduces the projected area of the stress cone if the cone intersects the edge of the concrete (Figure 4). These researchers assume that the VCA method accounts for the reduction in projected area much the same as does the ACI 349-85 method. This assumption allows for a direct comparison between the ACI 349-85 method and a proposed variable-angle cone approach. Thus, the value obtained in the equation presented in Section 4.3.1 is multiplied by the ratio of the actual projected area (net area) to the projected area of the anchor not limited by edge influences (gross area). Thus, the equation, expressed in SI units, is as follows:

$$\frac{A_p}{A_{p,o}}\, 0.96\,\sqrt{f_{cc}}\,\frac{h_e}{\tan\theta}\left(\frac{h_e}{\tan\theta}+d_h\right)$$

where

A_p = actual projected area of anchor

$A_{p,o}$ = projected area of anchor not limited by edge influences

Again, note that the ratio of A_p to $A_{p,o}$ is non-dimensional and can be applied directly to the corresponding equation in U.S. units without employing a conversion factor.

The ratio of A_p to $A_{p,o}$ for anchors located near a free edge is calculated as follows:

1) Determine the radius of an equivalent full stress cone:

$$R = \frac{h_e}{\tan\theta} + \frac{d_h}{2}$$

2) Partition the actual projected area of the anchor and determine appropriate geometric quantities: (Note: Measure all angles in degrees.)

$$\beta = Cos^{-1}\left[2\left(\frac{c_1}{R}\right)^2 - 1\right]$$

3) Find the projected area of one anchor not limited by edge influences:

$$A_{p,o} = \pi \left(\frac{h_e}{\tan\theta}\right)\left[\frac{h_e}{\tan\theta} + d_h\right]$$

4) Find the area lost due to the proximity of an edge as follows:

$$A_{Lost} = \pi\ R^2\ \frac{\beta}{360} - c_1\ R\ Sin\left(\frac{\beta}{2}\right)$$

5) Finally, net projected area equals the difference between projected area of an anchor not limited by edge influences and the area of the segment formed by the edge of the concrete acting as a secant:

$$A_p = A_{p,o} - A_{Lost}.$$

This equation is valid until $c_1 = h_e/(\tan\ \theta) + d_h/2$, or, equivalently, $A_p = A_{p,o}$.

4.3.3 Multiple Closely Spaced Anchors Far from a Free Edge

Locating anchors close to other anchors reduces the projected area of a single anchor because of overlapping of failure surfaces. The variable-angle cone approach considers this in the same way in which single anchors located near a free edge are evaluated for predicted capacity. Thus, the predicted capacity for one of the anchors within the group, expressed in SI units, is as follows:

$$\frac{A_p}{A_{p,o}}\ 0.96\ \sqrt{f_{cc}}\left(\frac{h_e}{\tan\theta}\right)\left[\frac{h_e}{\tan\theta} + d_h\right]$$

where

A_p = actual projected area of all anchors in the group

$A_{p,o}$ = projected area of all anchors in the group not limited by adjacent anchors

Note that the ratio of A_p to $A_{p,o}$ is non-dimensional and can be applied directly to the corresponding equation in U.S. units without using a conversion factor.

The ratio of A_p to $A_{p,o}$ for multiple closely spaced anchors is computed as follows:

1) Determine if all anchors in the group act as equivalent single anchors:
Anchors behave as a group of single anchors if

$$\left[\frac{s_1}{2} - \left(\frac{h_e}{\tan\theta}\right) - \frac{d_h}{2}\right] \geq 0$$

Otherwise, anchors have overlapping failure surfaces. If multiple anchors act as a group of single anchors, then the ratio of A_p to $A_{p,o}$ is valued at 1.0.

2) Find the projected area of all anchors not limited by edge influences:

$$A_{p,o} = n\pi\left(\frac{h_e}{\tan\theta}\right)\left[\frac{h_e}{\tan\theta} + d_h\right]$$

where

n = number of anchors in the group

3) Check to make sure that the projected failure surface does not intersect an edge:

$$If \left[\frac{c_1}{\left(\dfrac{h_e}{\tan\theta}\right)}\right] > 1, \textit{ then no edge problem occurs.}$$

$$If \left[\frac{c_1}{\left(\dfrac{h_e}{\tan\theta}\right)}\right] \leq 1, \textit{ then edge problem results.}$$

All points having edge problems according to these criteria have been removed from the data base.

4) Partition the actual projected area of the anchor group and determine appropriate geometric quantities. All anchors groups included in the data base have equal spacing between anchors for all anchors within the group. Thus, $s_1 = s_2$ for all anchor groups with n > 2. (Note: Measure all angles in degrees.)

5) Determine the actual projected area for the appropriate anchor configuration as defined in Figures 5 through 8. The equation presented at the beginning of this section is valid until $(s_1/2) = (h_e/\tan\theta) + d_h/2$, or, equivalently, $A_p = A_{p,o}$.

For a group of 2 fasteners the formula is as follows:

$$\beta = Cos^{-1}\left[2\left(\frac{s_1}{d_h + \dfrac{2\,h_e}{\tan\theta}}\right)^2 - 1\right]$$

$$A_p = 2\pi\left(\frac{h_e}{\tan\theta}\right)\left[\frac{h_e}{\tan\theta} + d_h\right] - \left[\frac{h_e}{\tan\theta} + \frac{d_h}{2}\right]^2 (\beta - Sin\beta)$$

For a group of 4 fasteners where $s_1 = s_2$ the formulas are as follows:

$$\beta = Cos^{-1}\left[2\left(\frac{s_1}{d_h + \dfrac{2h_e}{\tan\theta}}\right)^2 - 1\right]$$

$$If\ s1 \geq \sqrt{2}\left(\frac{h_e}{\tan\theta} + \frac{d_h}{2}\right),\ then$$

$$A_p = 4\pi\left(\frac{h_e}{\tan\theta}\right)\left[\frac{h_e}{\tan\theta} + d_h\right] - 4\left(\frac{h_e}{\tan\theta} + \frac{d_h}{2}\right)^2 (\beta - Sin\beta)$$

$$If\ s1 < \sqrt{2}\left(\frac{h_e}{\tan\theta} + \frac{d_h}{2}\right),\ then$$

$$A_p = s_1^2\left(1 + \tan\frac{\beta}{2}\right) + \left[\frac{270-\beta}{90}\right]\pi\left(\frac{h_e}{\tan\theta} + \frac{d_h}{2}\right)^2 - \pi d_h^2$$

For a group of 16 anchors where $s_1 = s_2$, the only available data involve groups that have $s_1 < \sqrt{2}\ ((h_e/\tan\ \theta) + d_h/2)$. The formula for determining the area of this type of configuration is as follows:

$$\beta = Cos^{-1}\left[2\left(\frac{s_1}{d + 2\dfrac{h_e}{\tan\theta}}\right)^2 - 1\right]$$

$$A_p = s_1^2\left(1 + \tan\frac{\beta}{2}\right) + \left[\frac{270-\ \beta}{90}\right]\pi\left(\frac{h_e}{\tan\theta} + \frac{d}{2}\right)^2 - 16\pi d^2 +$$

$$4s_1^2 + 4s_1^2\left[1 + \tan\frac{\beta}{2} + \left(\frac{h_e}{\tan\theta} + \frac{d}{2}\right)^2 (\beta - Sin\beta)\right]$$

4.3.4 General Equations Used with Variable-Angle Cone Method

The equations presented in previous sections for various cases of edge distance and spacing can be written in more general form. When using U.S. units (pounds, inches, and concrete cylinder strength), the concrete cone capacity is given by:

$$\frac{A_p}{A_{p,o}}\ 4\ \pi\ \sqrt{f_c}\left(\frac{h_e}{\tan\theta}\right)\left[\frac{h_e}{\tan\theta} + d_h\right]$$

When using SI units (N, mm, and concrete cube strength), the concrete cone capacity is determined by:

$$\frac{A_p}{A_{p,o}}\ 0.96\ \sqrt{f_{cc}}\left(\frac{h_e}{\tan\theta}\right)\left[\frac{h_e}{\tan\theta} + d_h\right]$$

In both cases, A_p and $A_{p,o}$ are defined as follows:

A_p = actual projected area of anchor or anchor group

$A_{p,o}$ = projected area of all anchors not limited by edge influences or spacing influences

4.4 Description of the Concrete Capacity Method

4.4.1 Single Anchors Far from a Free Edge, Remote from Other Anchors

The Concrete Capacity method predicts that the concrete capacity increases with embedment length raised to the power 1.5 [4,5,10,11]. In addition, fracture mechanics has been used to provide some theoretical basis for capacity prediction formulas with an exponent of 1.5 [8]. In SI units the concrete capacity is as follows:

$$15.5\ h_e^{1.5}\ \textit{for headed studs}$$

$$13.5\ h_e^{1.5}\ \textit{for expansion or undercut anchors}$$

where h_e = embedment length, measured from free surface to the bearing surface of the anchor head

Expansion and undercut anchors are also denoted as metal anchors.

This method is equivalent to the Kappa method for single anchors remote from other anchors and far from a free edge [11,20].

4.4.2 Single Anchors Near a Free Edge, Far from Other Anchors

Locating an anchor near a free edge reduces the projected area of the 35° stress pyramid if the 35° pyramid intersects the edge of the concrete (Figure 9). The Concrete Capacity method multiplies the value obtained in the equation presented in Section 4.4.1 by the ratio of the actual projected area (net area) to the projected area of the anchor not limited by edge influences (gross area). Thus, the equation, expressed in SI units, is as follows:

$$\frac{A_p}{A_{p,o}} \psi_{SN} \psi_{ec} 15.5 h_e^{1.5} \qquad \textit{for headed studs}$$

$$\frac{A_p}{A_{p,o}} \psi_{SN} \psi_{ec} 13.5 h_e^{1.5} \qquad \textit{for expansion or undercut anchors}$$

where

A_p = actual projected area of anchor

$A_{p,o}$ = projected area of anchor not limited by edge influences

ψ_{SN} = factor that considers disturbance of radial symmetric stress distribution for anchors close to a free edge

ψ_{ec} = effect of eccentricity (assumed = 1)

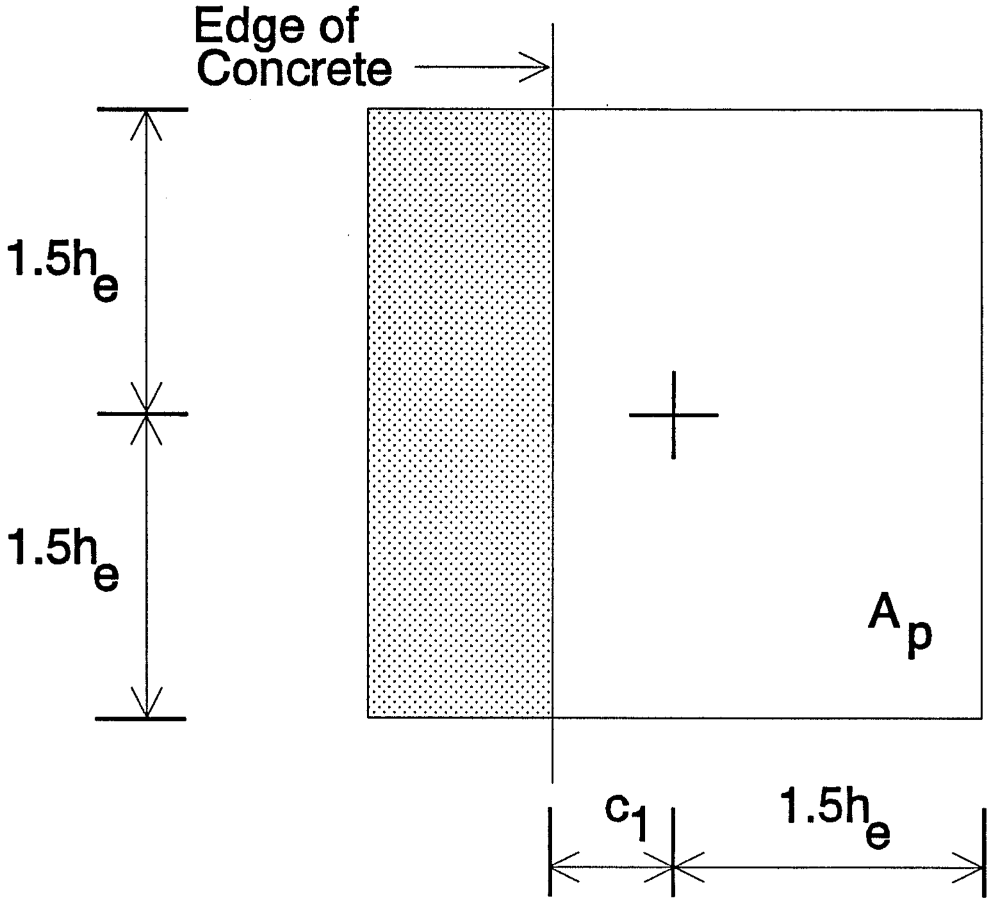

Figure 9: Projected Area of a Single Anchor Located Near a Free Edge (CC method)

Note that the ratio of A_p to $A_{p,o}$ is non-dimensional and can be applied directly to the corresponding equation in U.S. units without employing a conversion factor.

The predicted capacity for anchors located near a free edge is calculated as follows:

1) Determine Ψ_{SN}:

$$\text{If } \frac{c_1}{h_e} \leq 1.5, \qquad \psi_{SN} = \frac{1}{4}\,(2.5 + \frac{c_1}{h_e})$$

$$\text{If } \frac{c_1}{h_e} > 1.5, \qquad \psi_{SN} = 1$$

2) Find the actual projected area of the anchor:

$$A_p = 2\,(c_1 + 1.5 \times h_e) \times 1.5 \times h_e$$

3) Find the projected area of one anchor not limited by edge influences:

$$A_{p,o} = 9\,h_e^2$$

The equation presented in this section is valid until $c_1 = 1.5h_e$ or, equivalently, $A_p = A_{p,o}$.

4.4.3 Multiple Closely Spaced Anchors Far from a Free Edge

Locating anchors close to other anchors reduces the projected area of a single anchor due to overlapping of cones from single anchors. The Concrete Capacity method takes this rule into account by multiplying the value obtained in the equation presented in Section 4.4 by the ratio of the actual projected area (net area) to the projected area of the anchor not limited by edge influences (gross area). Thus the equation, expressed in SI units, is as follows:

$$\frac{A_p}{A_{p,o}}\,\psi_{SN}\,\psi_{ec}\,15.5\,h_e^{1.5} \qquad \textit{for headed studs}$$

$$\frac{A_p}{A_{p,o}}\,\psi_{SN}\,\psi_{ec}\,13.5\,h_e^{1.5} \qquad \textit{for expansion or undercut anchors}$$

where

A_p = actual projected area of anchor

$A_{p,o}$ = projected area of anchor not limited by edge influences

ψ_{SN} = factor that considers disturbance of radial symmetric stress distribution for anchors close to a free edge (Equal to 1 for all multiple anchor data considered)

ψ_{ec} = effect of eccentricity (assumed = 1)

Note that the ratio of A_p to $A_{p,o}$ is non-dimensional and can be applied directly to the corresponding equation in U.S. units without applying a conversion factor.

The predicted capacity for multiple closely spaced anchors located remote from a free edge is calculated as follows:

1) Determine if the projected failure surface intersects an edge:

   If $(c_1/h_e) \geq 1.5$, then no edge problem exists.

   If $(c_1/h_e) < 1.5$, then edge problem results.

   All points having edge problems according to these criteria have been removed from the data base.

2) Find the projected area of the anchor group not limited by overlapping failure surfaces:

$$A_{p,o} = 9nh_e^2$$

   where

   n = number of anchors in the group

3) Partition the actual projected area of the anchor group and determine appropriate geometric quantities.

All anchor groups included in the data base have equal spacing between anchors for all anchors within the group. Thus, $s_1 = s_2$ for all anchor groups with $n > 2$.

4) Determine the actual projected area for the appropriate anchor configuration as defined in Figures 10, 11, and 12. This equation is valid until $s_1 = s_2 = 3.0h_e$ or equivalently, $A_p = A_{p,o}$.

For a group of 2 fasteners the formula is as follows:

$$A_p = [2(1.5h_e) + s_1] \cdot 2(1.5h_e)$$

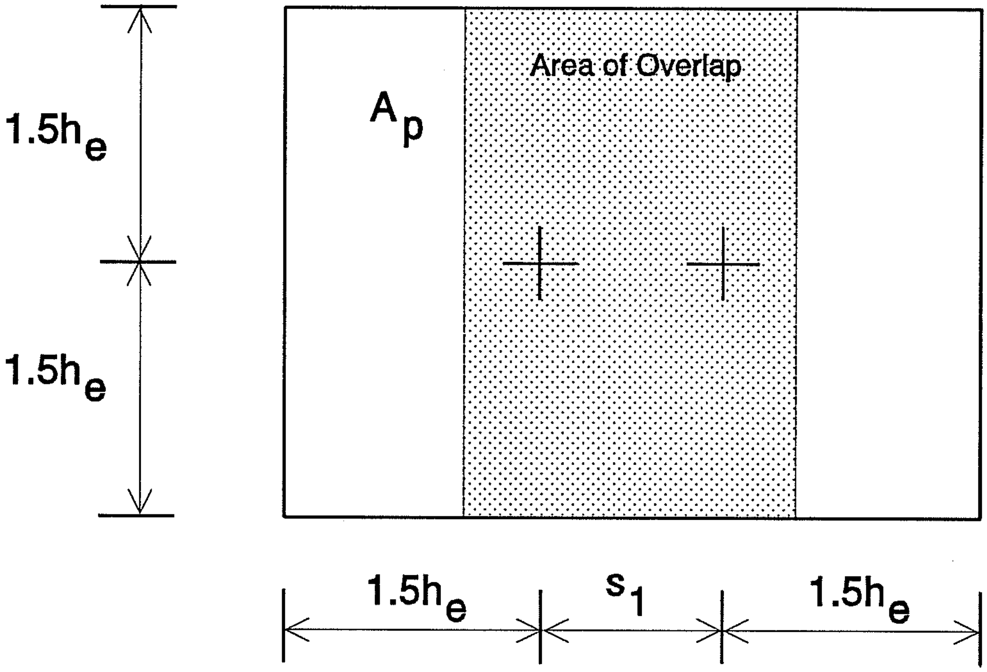
1.5h_e
1.5h_e
A_p
Area of Overlap
1.5h_e
s_1
1.5h_e

Figure 10: Projected Area for a 2 Anchor Group Under Tensile Loading (CC Method)

For a group of 4 fasteners the formula is as follows:

$$A_p = [2\,(1.5\,h_e) + s_1] \cdot [2\,(1.5\,h_e) + s_2]$$

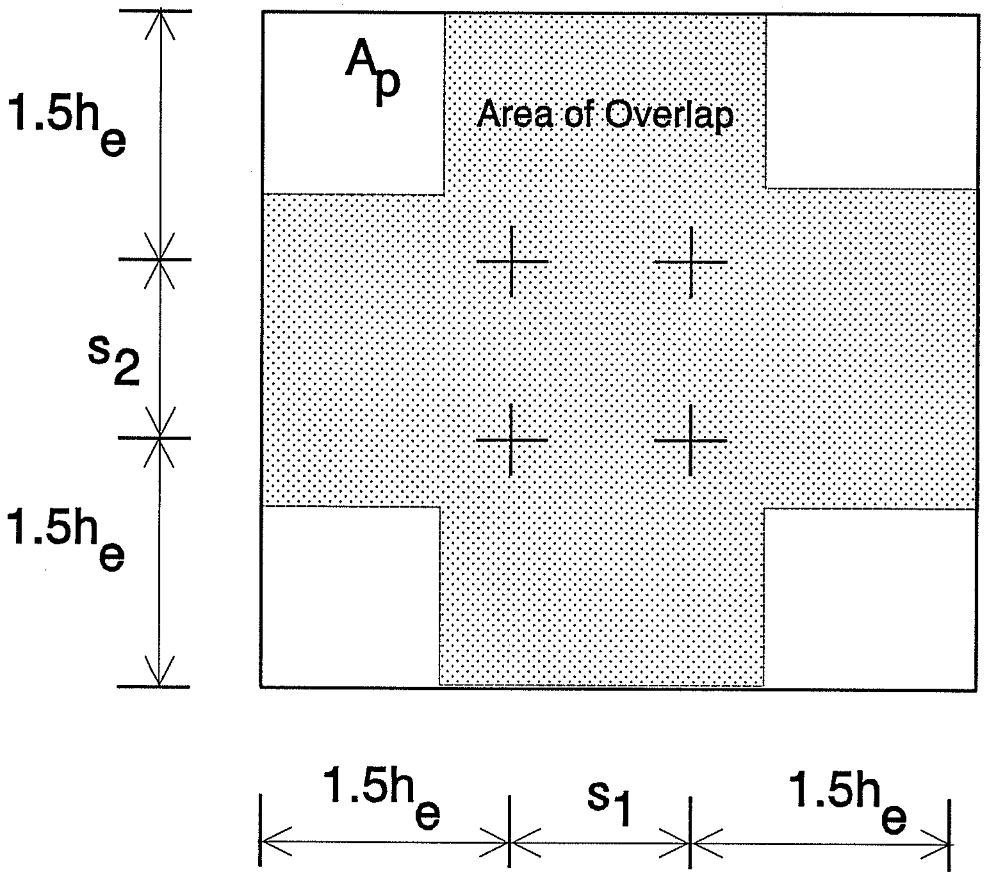

A_p
Area of Overlap
$1.5h_e$
s_2
$1.5h_e$
$1.5h_e$
s_1
$1.5h_e$

Figure 11: Projected Area for a 4 Anchor Group Under Tensile Loading (CC Method)

For a group of 16 fasteners the formula is as follows:

$$A_p = [2\,(1.5\,h_e) + 3\,s_1] \cdot [2\,(1.5\,h_e) + 3\,s_2]$$

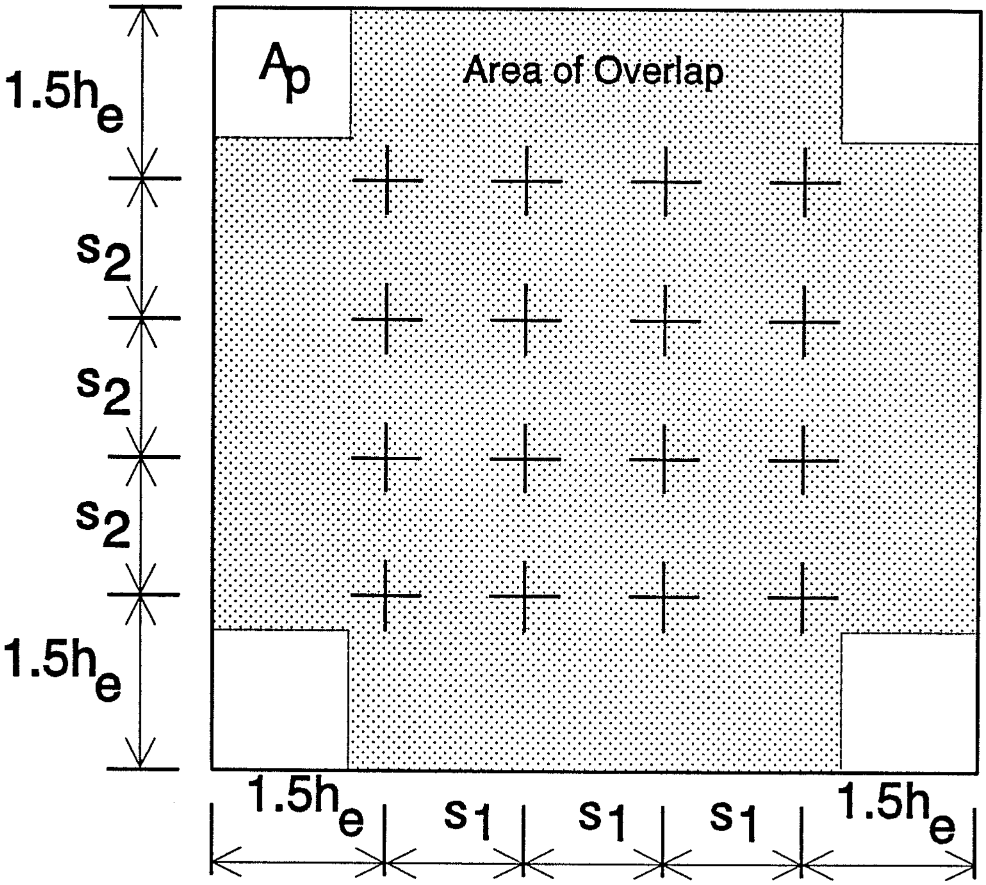
A_p
Area of Overlap
$1.5h_e$
s_2
s_2
s_2
$1.5h_e$
$1.5h_e$
s_1
s_1
s_1
$1.5h_e$

Figure 12: Projected Area for a 16 Anchor Group Under Tensile Loading (CC Method)

4.4.4 General Equations Used with Concrete Capacity Method

The equations presented in Sections 4.4.2 and 4.4.3 for various cases of edge distance and spacing can be written in more general form. When using U.S. units (pounds, inches, and concrete cylinder strength), the concrete capacity is determined by:

$$\frac{A_p}{A_{p,o}} \psi_{SN} \psi_{ec} \sqrt{f_c}\ 40.0\ h_e^{1.5} \qquad \textit{for headed studs}$$

$$\frac{A_p}{A_{p,o}} \psi_{SN} \psi_{ec} \sqrt{f_c}\ 35.0\ h_e^{1.5} \qquad \textit{for expansion or undercut anchors}$$

When using SI units (N, mm, and concrete cube strength), the concrete capacity is found by:

$$\frac{A_p}{A_{p,o}} \psi_{SN} \psi_{ec} \sqrt{f_{cc}}\ 15.5\ h_e^{1.5} \qquad \textit{for headed studs}$$

$$\frac{A_p}{A_{p,o}} \psi_{SN} \psi_{ec} \sqrt{f_{cc}}\ 13.5\ h_e^{1.5} \qquad \textit{for expansion or undercut anchors}$$

In both cases, A_p and $A_{p,o}$ are defined as follows:

A_p = actual projected area of anchor or anchor group

$A_{p,o}$ = projected area of all anchors not limited by edge influences or spacing influences

ψ_{SN} = 1 if $c_1/h_e \geq 1.5$

= $0.25 \times (2.5 + c_1/h_e)$ if $c_1/h_e < 1.5$

ψ_{ec} = $1/(1 + 2*e/(3*h_e)) \leq 1$

e = effect of eccentricity $\leq 1.5*h_e$

4.5 Description of Peripheral Shear as a Possible Capacity Prediction Model

Recent correspondence with Cannon [14] has suggested that the concept of peripheral shear can be used to compute an upper bound solution to capacities as predicted by either the ACI 349-85 method or VCA method for multiple closely spaced anchors. The basic assumption of the peripheral shear method is that the failure surface is a solid rectangular block of concrete around the group of anchors. The block has been modeled with a depth equal to the effective embedment depth of the anchor and perimeter (b_o) defined as follows:

For groups of 2 anchors: $b_o = 2s_1 + 4d$
For groups of 4 anchors: $b_o = 4(s_1 + d)$
For groups of 16 anchors: $b_o = 4(3s_1 + d)$

The predicted capacity, given in SI units (N), is expressed as follows:

$$\textit{Peripheral Shear Capacity} = 0.3057\ \sqrt{f_{cc}}\ b_o\ h_e$$

These calculations have been performed and are listed as the final column in Appendix F.

Peripheral shear calculations prove to be extremely conservative when compared to actual capacities for all cases except for 3 involving groups of 16 anchors. In addition, the normalized capacity as predicted by the peripheral shear method is lower than either the ACI 349-85 or the VCA method for every data point in the data base. Since the peripheral shear method is so conservative, one could argue that this method serves as a lower bound to concrete failure. However, this data indicates that the peripheral shear predicts an average capacity less than 1/2 of the actual mean capacity. This implies that such an approach, although conservative, is not the most exact method for calculating predicted capacity. Therefore, the calculated values for peripheral shear are not included in either the probability of failure calculations or the sum of the square calculations that are used to analyze the suitability for design for each of the three methods.

5.0 COMPARISON OF EXISTING METHODS WITH AVAILABLE DATA

5.1 General

The equations given in Chapter 4 for each of the three methods (SI units) are normalized by dividing by $\sqrt{f_{cc}}$ and the number of anchors in the group. These normalized results for both single anchors near a free edge and multiple closely spaced anchors are then compared with available failure data in two ways. First, results are presented graphically. Second, the square root of the sum of the squares error is evaluated for both single anchors near a free edge and multiple closely spaced anchors. All comparisons are presented graphically in terms of SI units.

5.2 Graphical Comparison of Existing Methods

Figures A-1 through A-21 contain observed failure points, denoted by charted values (squares), and best-fit curves of each of the available capacity prediction methods for single anchors near a free edge. Curves are plotted for the following ranges of embedment depth to edge distance:

0.45-0.60
0.601-0.75
0.751-0.90
0.901-1.05
1.051-1.20
1.201-1.35
1.351-1.50

These intervals are used in order to keep the ratio of A_p to $A_{p,o}$ approximately constant. The use of distinct intervals to keep the ratio of A_p to $A_{p,o}$ constant in the graphical presentation of data is an attempt to present the data in a form similar to the one used in the original study of single anchors far from a free edge and far from other anchors prepared for the Tennessee Valley Authority [2].

For multiple closely spaced anchors, results are presented in terms of the ratio of actual capacity to predicted capacity for the following ranges of spacing to embedment depth:

0.27-0.45
0.451-0.60
0.601-0.75
0.751-0.90
0.901-1.05
1.051-1.20
1.201-1.35
1.351-1.50
1.501-2.00
2.001-2.50
2.501-3.00

Figures B-1 through B-33 contain tabulations in which each value represents a ratio of actual capacity to predicted capacity. However, results are not plotted as for single anchors near a free edge because of the problem of maintaining a constant ratio of A_p to $A_{p,o}$. Although it is true that for a given spacing and a given configuration of the anchor group, the ratio of A_p to $A_{p,o}$ remains constant, this principle does not hold when various anchor configurations are introduced for a given ratio of spacing to embedment depth. For example, even with a constant ratio of edge depth to embedment depth the ratio of A_p to $A_{p,o}$ for a 2 anchor group is not the same as the ratio of A_p to $A_{p,o}$ for a 4 anchor group.

5.2.1 Graphical Comparison of ACI 349-85, Appendix B, with Concrete Failure Data Base

Nominal capacities computed according to ACI 349-85, Appendix B, are plotted against the data base of concrete failures. For single anchors near a free edge, a visual interpretation of results shows that the ACI 349-85 method is unconservative for large embedment depths. No variation in this statement is found for different ratios of edge distance to embedment depth. This concurs with the results found by Klingner et al [2] for single anchors far from a free edge and remote from other anchors. For multiple closely spaced anchors, a graphical comparison reveals no distinctive pattern over different ratios of spacing to embedment depth. This may partially be due to the fact that each graph includes data from several different configurations.

5.2.2 Graphical Comparison of Variable-Angle Cone Method with Concrete Failure Data Base

Nominal capacities computed according to the variable-angle cone method are plotted against the data base of concrete failures. For both single anchors close to a free edge and multiple closely spaced anchors, the variable-angle cone method is less conservative than the ACI 349-85 method for shallow embedment depths. For single anchors near a free edge, a visual interpretation of results shows that the variable-angle cone method is also unconservative for large embedment depths. This is due to the fact that the variable-angle cone method is identical to the ACI 349-85 approach for embedment depths greater than or equal to 127 mm. This concurs with the results found by Klingner et al [2] for single anchors far from a free edge and remote from other anchors. For multiple closely spaced anchors, no particular pattern is evident over different ratios of spacing to embedment depth. This may partially be due to the fact that each graph includes data from several different configurations.

5.2.3 Graphical Comparison of Concrete Capacity Method with Concrete Failure Data Base

Nominal capacities computed according to the Concrete Capacity method are plotted against the data base of concrete failures. For single anchors near a free edge and far from other anchors, the Concrete Capacity method provides a better fit to the actual failure points for all ranges of c_1/h_e, and a much better fit for most ranges, than either the ACI 349-85 method or the variable-angle cone method. For multiple closely spaced anchors, no such pattern of superiority is evident over different ratios of spacing to embedment depth. This may partially be due to the fact that each graph includes data from several different anchor configurations.

This study concurs with the findings of Eligehausen, Fuchs, and Breen that the CC method predicts load capacity more accurately for large groups of anchors; in contrast, ACI 349-85 is quite unconservative [21]. A typical example of this problem can be found by looking at one of the available data points on groups of 16 anchors. The following variables are defined:

d_h = 22
h_e = 185 mm
fcc200 = 26 MPa
c_1 =999mm
s_1 = 150 mm
s_2 =150 mm

$$Nu = 508 \text{ kN}$$

The normalized failure load indicates a failure load of 6227 √N × mm per anchor. This is reasonably close to the value of 7993 √N × mm predicted by the CC method. However, it is less than half the value of 12914 √N × mm predicted by the ACI 349-85 method. Although only 9 failure points are available, the ratio of actual to predicted failure load has a mean of 0.528 for the ACI 349-85 method, which implies that this approach may be unconservative for large groups of anchors.

5.3 Evaluation of Error Associated with Each Method

The error associated with each method is evaluated by computing the square root of the sum of the squares of the errors between the predicted and observed values. This numerical value is determined for each test in each data base. The results are expressed in Tables 1 and 2 in terms of SI units $(\sqrt{N} \cdot mm)$. Results are also illustrated in the form of bar graphs in Figures 13 and 14.

However, this method of error analysis does not present a complete picture of the reliability of a given formula. It assigns more weight to data points located far from the values predicted by the equation under consideration. A few data points lying far from the curve can have as much effect as a larger number of points close to the curve. Because each data point does not contribute equally in the error analysis, some distortion is created. Also, this method does not distinguish systematic error from random error. An examination of Figures A-1 through A-21 and Figures B-1 through B-33 shows that the ACI 349-85 method is consistently conservative for shallow embedments.

Table 1: Comparison of Error Using Each Method for Single Anchors Near a Free Edge, Far from Other Anchors (Square Root of Sum of Square Error), SI Units

Ratio of Spacing to Embedment Depth	Error, $\sqrt{N} \times mm$		
	ACI 349-85	VCA	CC
0.45-0.60	16770	16882	4955
0.601-0.75	12016	12096	5111
0.751-0.90	15555	15559	2696
0.901-1.05	22485	22495	5677
1.051-1.20	10693	10849	3554
1.201-1.35	32345	32286	1801
1.351-1.50	5960	5943	5319

That fact is not revealed in comparison of square error.

5.4 Discussion of Error Evaluation by Sum of Squares Method

Tables 1 and 2 (and Figures 13 and 14) demonstrate that for most embedment depths, the Concrete Capacity method has a square error lower than that of either ACI 349-85 or the variable-angle cone method. However, for multiple anchors with small ratios of spacing to embedment depth ($s_1/h_e \leq 0.75$), the ACI 349-85 method and the variable-angle cone method have a lower square error than the Concrete Capacity method.

The Concrete Capacity method seems particularly advantageous when examining the square root of the sum of the square error for single anchors near a free edge and

Table 2: Comparison of Error Using Each Method for Multiple Closely Spaced Anchors, Far from a Free Edge (Square Root of Sum of Square Error), SI Units

Ratio of Spacing to Embedment Depth	Error, √N × mm		
	ACI 349-85	VCA	CC
0.27-0.45	10081	10081	10128
0.451-0.60	2676	2795	3513
0.601-0.75	2577	2577	3150
0.751-0.90	4559	4524	1467
0.901-1.05	2687	2623	1900
1.051-1.20	1748	1827	1514
1.201-1.35	3522	2381	3018
1.351-1.50	5877	5850	2355
1.501-2.00	3374	2880	2393
2.001-2.50	3658	3004	2728
2.501-3.00	3384	2014	2433

far from other anchors. The Concrete Capacity method has a lower error than either of the other two methods. This is true mainly because of the effect of including all embedment depths in each range of edge distance to embedment depth. As stated previously, the ACI 349-85 method and the variable-angle cone method do not fit available failure data very well at large embedment depths. The effect of this divergence is to increase the sum of the square error for every range of edge distance to embedment depth.

No distinct conclusion can be drawn from the square error data for multiple anchors. There are only two cases in which the Concrete Capacity Method is noticeably different than either the ACI 349-85 or the variable-angle cone method ($0.75 \leq s_1/h_e \leq 0.90$ and $1.35 \leq s_1/h_e \leq 1.50$). In both cases, a large number of tests with large embedment depths and the same configuration are present in the available data. This seems to imply that the Concrete Capacity method best fits the available data for cases in which the embedment depth is large.

For single anchors located near a free edge, the variable-angle cone method has a square error only slightly different from that of the ACI 349-85. However, some advantage can be obtained for some ratios of spacing to embedment depth for the case of multiple anchors.

Tables 1 and 2 are consistent with Figures 13 and 14. However, this method of error analysis does not present a complete picture of the reliability of a given formula. It assigns more weight to data points located far from the values predicted by the equation under consideration. A few data points lying far from the curve can have as much effect as a larger number of points close to the curve. Because each data point does not contribute equally in the error analysis, some distortion is created. Also, this method does not distinguish systematic error from random error. Examination of Figures A-1 through A-21 and Figures B-1 through B-33 illustrates that the ACI 349-85 cone method is consistently conservative for shallow embedments. This fact is not disclosed in comparisons of square error.

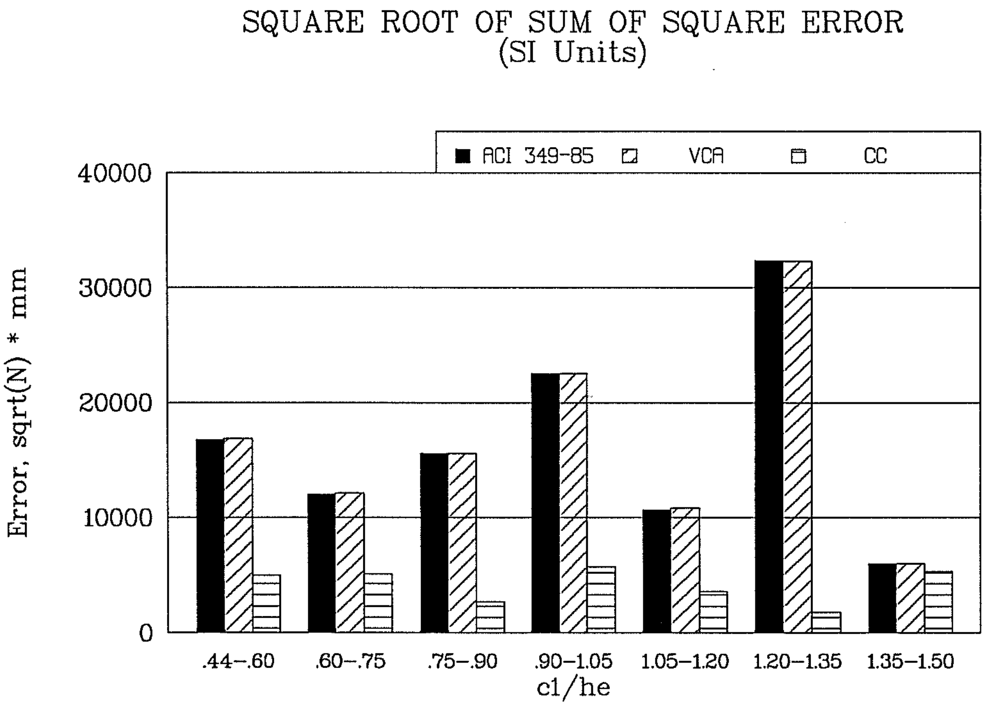

Figure 13: Comparison of Error Using Each Method for Single Anchors Near a Free Edge (Square Root of Sum of Square Error)

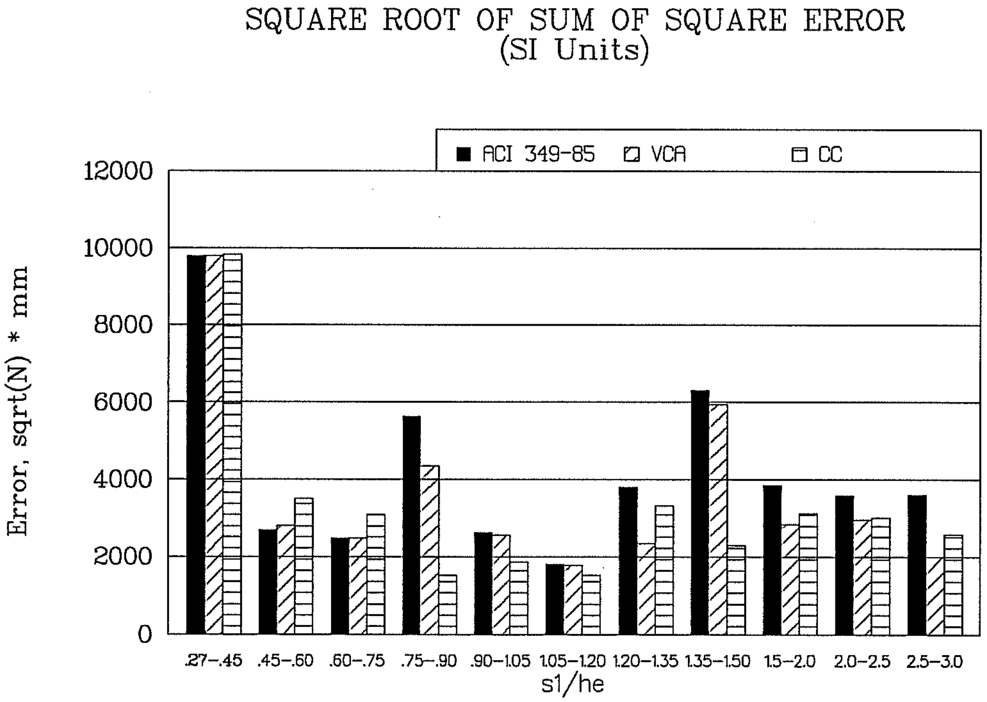

Figure 14: Comparison of Error Using Each Method for Multiple Closely Spaced Anchors (Square Root of Sum of Square Error)

6.0 LRFD IMPLICATIONS OF EXISTING METHODS

6.1 General

Each of the three capacity prediction methods is evaluated in terms of Load and Resistance Factor Design (LRFD) for both single anchors near a free edge and multiple closely spaced anchors. In particular, both the probability of steel or concrete failure under known loads and the probability of concrete failure under unlimited loads are calculated. Subsequently, each approach is compared on the basis of accuracy and suitability for use in design.

Several assumptions have been made to facilitate probability of failure calculations. First, all three methods are compared using the concrete cone understrength factor of ACI 349-85 ($\phi = 0.65$) as well as the corresponding load factor (1.7). The effect of both the understrength factor and the load factor is to decrease the probability of failure.

Second, both concrete and steel failure data are presumed to be normally distributed. This supposition is based on a previous report on single anchors far from a free edge and remote from other anchors prepared for the Tennessee Valley Authority [2]. For this thesis, the assumption of a normal distribution is judged reasonable if sufficient data are available for study.

6.2 Background of Applicable ACI 349-85 Provisions [1]

The design philosophy of Appendix B of ACI 349-85 is a strength design approach. In other words, anchors are designed to fail in a ductile manner; steel is expected to yield over a significant portion of the anchor length before steel fracture, concrete failure, or anchor pullout. In the design of an anchor for direct tension, this philosophy leads to the requirement that the concrete pullout strength must exceed the tensile strength of the anchor.

Design for tensile load involves specifying sufficient anchor area, so that the tensile capacity of the anchor, reduced by a capacity reduction factor, exceeds the factored design tension loading acting on the anchor (B.6.2):

$$\text{Factored Design Tension} \leq \phi A_s f_y$$

$$\text{but} \quad \text{Factored Design Tension} \leq A_s (0.8 f_{ut})$$

where A_s = tensile stress area of anchor steel

ϕ = 0.9 (capacity reduction factor)

f_y = specified minimum yield strength of anchor steel

f_{ut} = specified ultimate tensile strength of anchor steel

Once the necessary steel area has been computed, sufficient embedment must be provided, so that the pullout resistance of the concrete, reduced by a capacity reduction factor ($\phi = 0.65$), exceeds the ultimate tensile capacity of the anchor. The concrete capacity is computed using the method discussed in Section 4.2.4.

These design stipulations provide the basis on which the probability of failure calculations are based. For the probability of concrete failure under unlimited loads, the probability of failure is defined as the probability of concrete failure. For the probability of steel or concrete failure under known loads, the probability of failure is defined as the probability that either steel or concrete failure occurs under conditions consistent with the design load.

6.3 Probability of Failure Under Known Loads

The objective of calculating the probability of steel or concrete failure under known loads is to determine the safety of a single anchor near a free edge or of a group of multiple closely spaced anchors designed according to the load and understrength factors of ACI 349-85. These probabilities of failure are determined using both understrength and load factors of ACI 349-85.

In order to determine this probability of failure, three distinct distributions must be defined: the applied loading on the anchor; the resistance of a tensile anchor provided by steel; and the resistance of a tensile anchor as provided by concrete. As stated in Section 6.1, both steel resistance and concrete resistance are assumed to follow a normal distribution. In addition, this researcher assumes that the loading applied to the anchor follows a normal distribution. No research was performed to determine distributions of anchor loads. Note that these assumptions uniquely define the probabilities of failure. If loads or resistances were defined in some other way (log-normal) the probabilities of failure would change. However, the same principles in the computing the probability of failure would be followed.

6.3.1 Statistical Distribution of Applied Loading

For this analysis, the load is assumed to be known. All applied loads are assumed to be distributed according to available statistical data. Moreover, anchor loads are presumed to be distributed normally, with an arbitrary mean of 1.0 and an arbitrary coefficient of variation of 0.2 (Figure 15). No units are specified with this distribution because the distribution is independent of the units. Furthermore, the application of the loading curve is dependent only on the relationship of this curve to the curves of steel resistance and concrete resistance. Provided that units are consistent, they are otherwise unimportant.

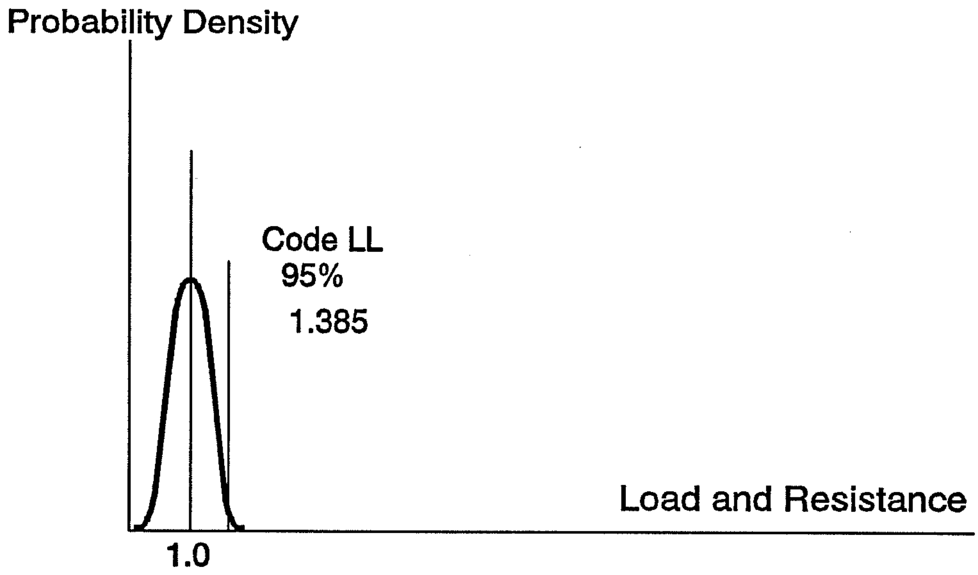

Figure 15: Assumed Statistical Distribution of Anchor Loads

Measurements of live load on typical office buildings have shown that building codes generally specify live loads at the 95-percentile value [21]. In other words, the prescribed value is greater than or equal to 95 percent of the observed load values. On that basis, the design load is fixed at the 95-percentile value of the assumed average load distribution. According to the assumed loading distribution, the 95 percentile load corresponds to a value of 1.385.

6.3.2 Statistical Distribution of Anchor Resistances as Governed by Steel

Because the nuclear industry is increasingly moving toward the use of high strength anchors, this study uses only data available on high strength anchors in its evaluation of the probability of failure of each of the three methods. These data on such high strength anchor steel failures have been adopted from previous work by Klingner and Mendonca [6] and Collins et al. [7]. This statistical distribution of actual resistances divided by the ACI 349-85 predictions has a mean value of 1.444. Assuming the use of a normal distribution for steel resistance, the corresponding coefficient of variation is 0.156. Note that load factors and ϕ factors are not used in computing the mean and coefficient of variation. However, these factors are included in the probability of failure calculations.

According to ACI 349-85, Appendix B, the required steel resistance must be greater than or equal to the factored load. Design values for anchor steel resistances are defined as the smaller of either $\phi\ A_s\ f_y$ or $0.8\ A_s\ f_{ut}$. Since the area of steel is constant for a given anchor, steel resistance is governed by the smaller of either f_y or $0.8\ f_{ut}$. For these high strength anchors, the value $\phi\ A_s\ f_y$ governs for every point in this data base. For example, consider a typical A193-B7 anchor bolt. This anchor has a yield strength of 105 ksi and an ultimate strength of 125 ksi. Since $\phi f_y = 94.5$ ksi $< 0.8 f_{ut} = 100.0$ ksi, the yield strength governs.

Because ϕf_y governs the design of every anchor in the data base, the required steel resistance is calculated based on the yield criterion. The required steel resistance is equal to the design load (the 95-percentile value of the load distribution = 1.385), multiplied by the load factor for live load (1.7), and divided by ACI 349-85's ϕ factor for the yield strength of steel (0.90):

$$\textit{Required Steel Resistance} = \frac{1.385 \times 1.7}{0.9} = 2.615$$

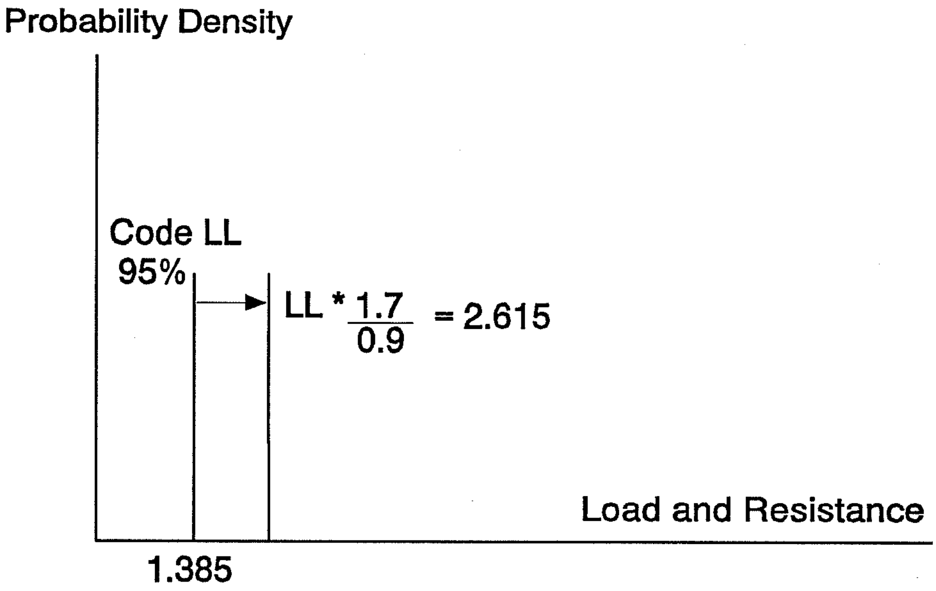

Figure 16: Required Steel Resistance

This required steel resistance is then shown in Figure 16.

Thus, the mean of the actual steel resistance can be defined as the product of the required steel resistance (2.615) and the calculated mean of the actual capacity to predicted capacity of the high strength steel data (1.444):

$$\textit{Actual Steel Resistance Mean} = 2.615 \times 1.444 = 3.78$$

Depicted in Figure 17, the coefficient of variation of the actual steel resistance is the same as the coefficient of variation for available data on high strength anchors.

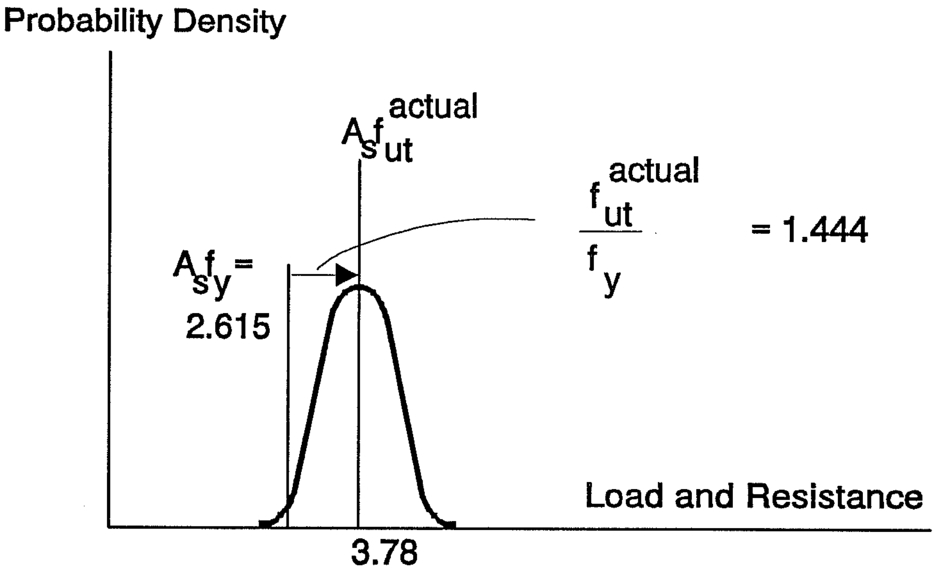

Figure 17: Actual Steel Resistance

In addition to the required steel resistance, one can define a theoretical steel resistance which is equal to the greater of either $\phi\ A_s\ f_y$ or $A_s\ f_{ut}$. If the required steel resistance is governed by f_y, then theoretical steel resistance is equal to the required steel resistance multiplied by the ratio of f_{ut} to f_y:

$$\textit{Theoretical Steel Resistance} = 2.615 \times 1.2 = 3.138$$

For purposes of this thesis, the ratio of f_{ut} to f_y is taken as 1.2. A comparison of the theoretical steel resistance and the steel resistance required by $0.8\ A_s\ f_{ut}$ is shown in Figure 18. Observe that these values are relatively close

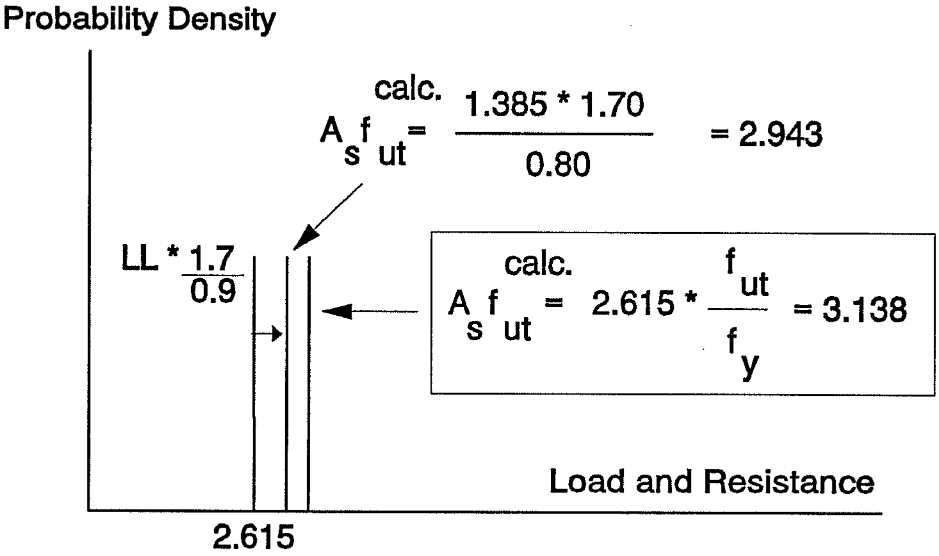
Probability Density
$A_s f_{ut}^{calc.} = \frac{1.385 * 1.70}{0.80} = 2.943$
$LL * \frac{1.7}{0.9}$
$A_s f_{ut}^{calc.} = 2.615 * \frac{f_{ut}}{f_y} = 3.138$
Load and Resistance
2.615

Figure 18: Theoretical Steel Resistance

and that neither governs if compared to $A_s f_y$.

6.3.3 Statistical Distribution of Anchor Resistances as Governed by Concrete

According to the provisions of ACI 349-85, the required nominal concrete strength of the anchor, reduced by an understrength factor of 0.65, must at least equal the specified ultimate tensile capacity of the anchor steel. From Section 6.3.2, the required nominal yield capacity of the anchor steel (yield strength of the anchor steel multiplied by the tensile stress area) is 2.615. Thus, the required nominal concrete capacity of the anchor is 2.615, multiplied by the ratio of specified ultimate strength to specified yield strength and reduced by the ϕ factor for concrete. As stated in Section 6.3.2, the ratio of ultimate strength to yield strength is taken as 1.2. This theoretical concrete resistance is calculated as follows:

$$\textit{Theoretical Concrete Resistance} = 2.615 \times 1.2 \times \frac{1}{0.65} = 4.83$$

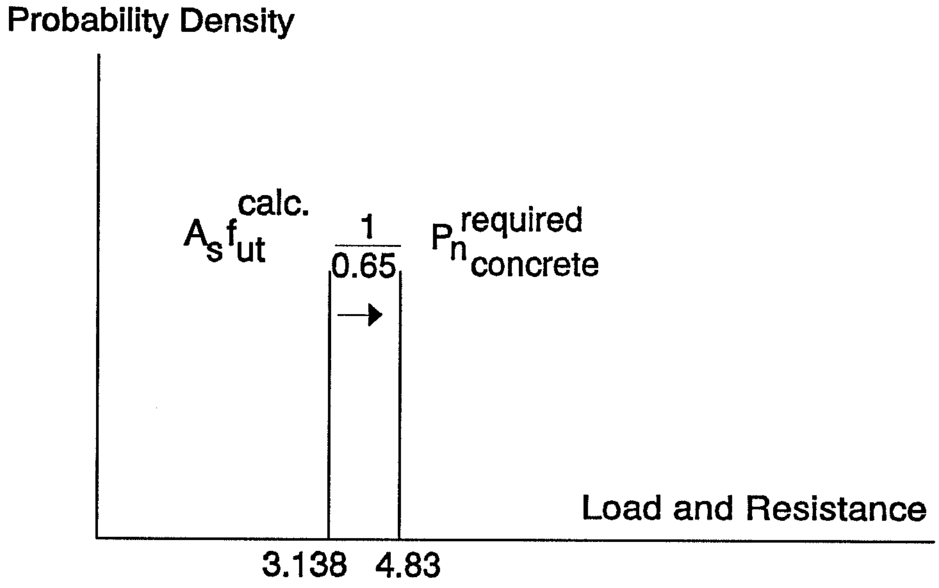
Probability Density
$A_s f_{ut}^{calc.}$
$\frac{1}{0.65}$
$P_n{}^{required}_{concrete}$
Load and Resistance
3.138
4.83

Figure 19: Theoretical Concrete Resistance

These results are illustrated in Figure 19.

The actual concrete resistance mean is figured by multiplying the theoretical concrete resistance (4.83) by the ratio of actual concrete resistance to predicted concrete resistance. The ratio of actual concrete resistance to predicted concrete resistance is found from available concrete failure data (Figure 20). Consider the Concrete Capacity method for single anchors near a free edge with edge distance to embedment depth ratios of 0.601-0.75:

$$\textit{Actual Mean Concrete Resistance} = 4.83 \times 1.093 = 5.28$$

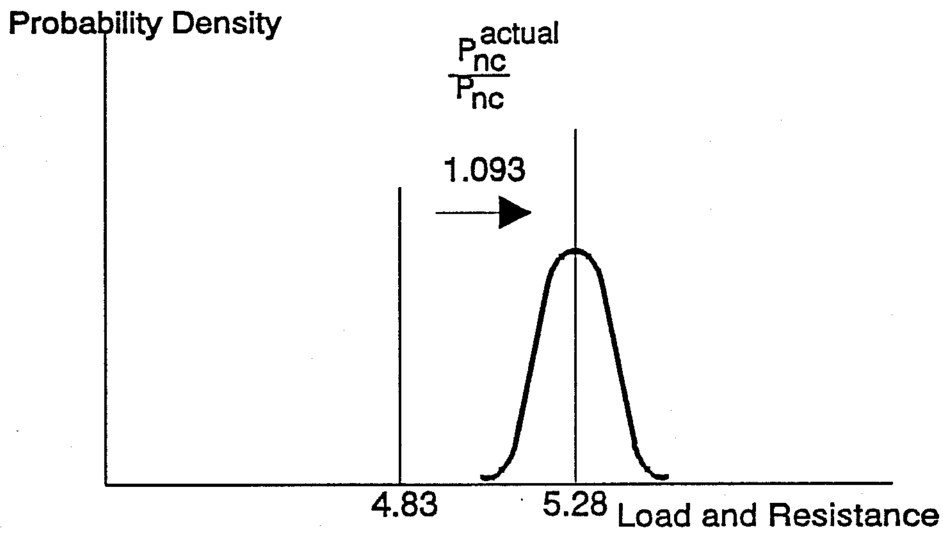

Figure 20: Actual Concrete Resistance, Single Anchor with Edge Distance to Embedment Depth Ratio = 0.601-0.75, CC Method

Table 3: Mean and Coefficient of Variation of Actual Capacity Divided by Predicted Concrete Capacity for Each Method for Single Anchors Near a Free Edge

c_1/h_e	Method					
	ACI 349-85		Variable Cone		Concrete Capacity	
	Mean	COV	Mean	COV	Mean	COV
0.44-0.60	0.843	0.323	0.715	0.311	1.146	0.234
0.601-0.75	0.918	0.284	0.728	0.245	1.093	0.249
0.751-0.90	0.869	0.315	0.764	0.212	1.075	0.163
0.901-1.05	1.033	0.327	0.780	0.243	1.151	0.232
1.051-1.20	1.194	0.233	0.785	0.291	0.972	0.251
1.201-1.35	1.208	0.182	0.815	0.263	0.981	0.170
1.351-1.50	1.267	0.332	0.764	0.220	0.884	0.222

Table 4: Mean and Coefficient of Variation of Actual Capacity Divided by Predicted Concrete Capacity for Each Method for Multiple Closely Spaced Anchors

s_1/h_e	Method					
	ACI 349-85		Variable Cone		Concrete Capacity	
	Mean	COV	Mean	COV	Mean	COV
0.27-0.45	1.061	0.255	1.061	0.255	1.400	0.254
0.451-0.60	0.931	0.188	0.910	0.210	1.060	0.255
0.601-0.75	0.994	0.200	0.994	0.200	1.151	0.234
0.751-0.90	0.845	0.379	0.804	0.249	1.023	0.189
0.901-1.05	1.161	0.158	0.873	0.214	1.052	0.163
1.051-1.20	1.242	0.310	0.886	0.235	1.108	0.246
1.201-1.35	1.434	0.236	1.119	0.156	1.478	0.183
1.351-1.50	1.141	0.496	0.857	0.299	1.191	0.283
1.501-2.00	1.322	0.278	0.968	0.218	1.248	0.222
2.001-2.50	1.441	0.310	0.946	0.174	1.177	0.187
2.501-3.00	1.515	0.150	0.992	0.163	1.155	0.146

In order to evaluate each method, the predicted concrete capacity is determined by each of the three methods. For single anchors near a free edge, the following ratio ranges of edge distance to embedment depth are considered:

0.45-0.60
0.601-0.75
0.751-0.90
0.901-1.05
1.051-1.20
1.201-1.35
1.351-1.50

The mean and coefficient of variation of actual capacity divided by predicted capacity are calculated for each method (Table 3). For multiple closely spaced anchors, the following ratio ranges of spacing to embedment depth are examined:

0.27-0.45
0.451-0.60
0.601-0.75
0.751-0.90
0.901-1.05
1.051-1.20
1.201-1.35
1.351-1.50
1.501-2.00
2.001-2.50
2.501-3.00

The mean and coefficient of variation of actual capacity divided by predicted concrete capacity are calculated for each method (Table 4). Determining the probability of failure for each discrete embedment depth and each discrete ratio of edge distance to embedment depth or spacing to embedment depth would produce more exact results than shown in these two tables. However, this precision has not been possible due to a limited amount of available data.

6.3.4 Combining Load, Steel Resistance, and Concrete Resistance

Based on the calculated distributions for load, concrete resistance, and steel resistance, a distinct set of numbers can be selected that represent some combination of load, concrete resistance, and steel resistance. Each of these points is selected randomly based on the experimentally determined normal distributions. After comparing concrete resistance and steel resistance, the minimum of these values is selected. The quantity (Resistance minus Load) is then computed for distinct values of load, concrete resistance, and steel resistance. This process is repeated 10,000 times. The frequency for which the resistance is less than the load, divided by the total number of cases, represents the probability of failure. This can also be viewed graphically as the area under the (Resistance minus Load) curve (Figure 21).

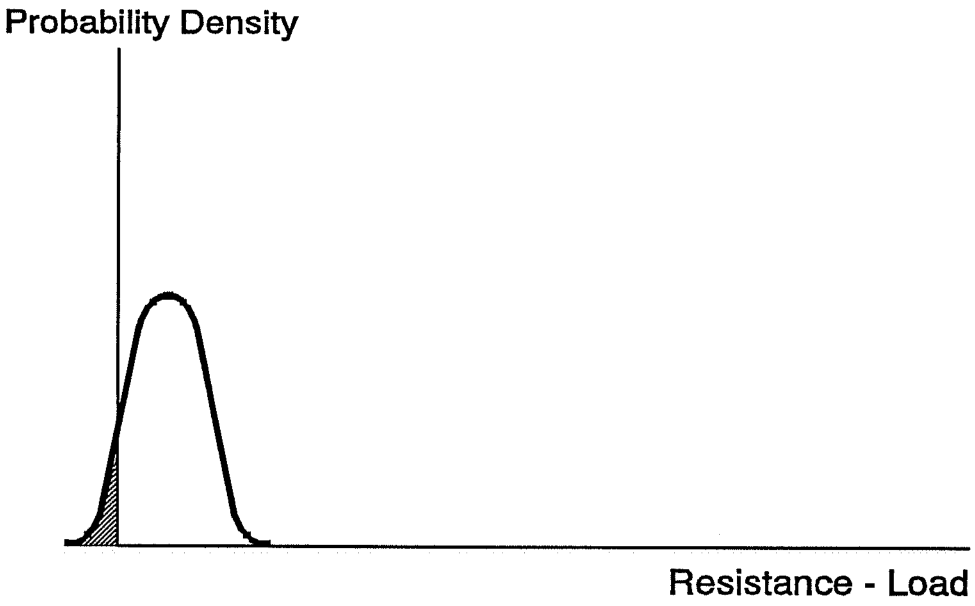

Figure 21: Probability of Failure Under Known Loads

6.4 Probability of Concrete Failure Under Unlimited Loads

The objective of calculating the probability of concrete failure under unlimited loads is to determine the probability of a failure when loads applied to a single anchor near a free edge or to a group of multiple closely spaced anchors exceed those assumed during design. Such a probability of failure is of interest when the structure is subjected to a catastrophic event such as a strong earthquake or extreme heat release. Such loads are highly unpredictable in magnitude. Because of this, design loads for extreme events are often based on the structural actions associated with the formation of a plastic mechanism, since the formation of such a mechanism sets an effective upper limit on the capacity. Thus, the phrase "unlimited loads" refers to loads that are limited only by the capacity of the weakest element in the anchoring system. The probability of concrete failure under unlimited loads is equivalent to the probability that steel capacity exceeds concrete capacity. In order to accomplish this task, distributions are designated for applied loading, steel resistance, and concrete resistance.

6.4.1 Statistical Distribution of Applied Loading

Although the loading to which the anchor in this probability analysis is unlimited, a distribution of loading must be assumed in order to obtain an initial design of the anchor. As in Section 6.3.1, all applied loads are assumed to be distributed normally, with an arbitrary mean of 1.0 and an arbitrary coefficient of variation of 0.2. According to the assumed loading distribution, the 95 percentile load corresponds to a value of 1.385.

6.4.2 Statistical Distribution of Anchor Resistances as Governed by Steel

The following procedure used to find the position of the normal curve is equivalent to the procedure followed in Section 6.3.2:

$$\mathit{Required\ Steel\ Resistance} = \frac{1.385 \times 1.7}{0.9} = 2.615$$

$$\mathit{Actual\ Mean\ Steel\ Resistance} = 2.615 \times 1.444 = 3.76$$

As stated in Section 6.3.2, the coefficient of variation of the actual steel resistance is the same as the coefficient of variation of the available data on high strength anchors.

6.4.3 Statistical Distribution of Anchor Resistances as Governed by Concrete

The procedure used to find the position of the normal curve is equivalent to the procedure followed in Section 6.3.2:

$$\mathit{Theoretical\ Concrete\ Resistance} = 2.615 \times \frac{1}{0.65} \times 1.2 = 4.83$$

As stated in Section 6.3.2, the coefficient of variation of the actual steel resistance is identical to the coefficient of variation of the available data on high strength anchors.

6.4.4 Combining Steel Resistance and Concrete Resistance

Given the distributions of steel resistance and concrete resistance, the probability of having a concrete capacity less than steel capacity can be calculated. Based on the calculated distributions for concrete resistance and steel resistance, a distinct pair of numbers can be selected that represent some combination of concrete strength and steel strength. Each of these points is selected randomly based on the experimentally determined normal distributions. The quantity (Concrete Resistance minus Steel Resistance) is computed for distinct values of concrete resistance and steel resistance. The process is repeated 10,000 times. The frequency for which concrete resistance is less than steel resistance, divided by the total number of cases, represents the probability of concrete failure. This can also be viewed graphically as the area under the (Concrete minus Steel) curve (Figure 22).

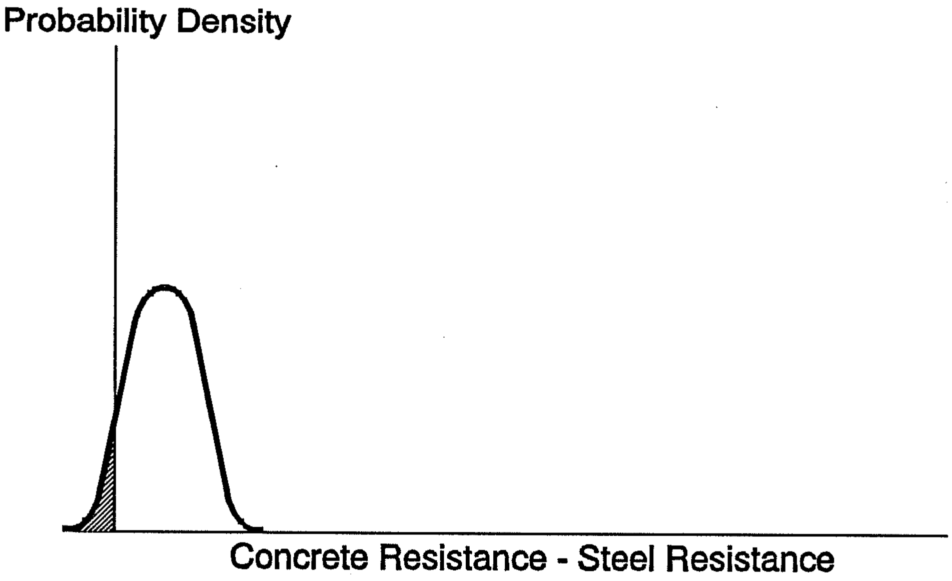

Figure 22: Probability of Concrete Failure Under Unlimited Loads

6.5 Summary of Numerical Calculations [22]

6.5.1 Probability of Failure Under Known Loads

Details of the numerical calculations, executed by computer as described in Appendix G, are as follows:

1) For each ratio range of edge distance to embedment depth or spacing to embedment depth the statistical distribution is discretized into a histogram. Each discrete load or resistance value is assigned a cardinal number of cells, in proportion to the probability of occurrence of that load or resistance value in the original statistical distribution. A total of 201 discrete values of load or resistance is selected, and the cardinal number of cells corresponding to each value is selected; accordingly, the total histogram contains 10,000 cells. The result is three sets of values: one for loads; one for probable steel resistances; and one for probable concrete resistances. These sets are assigned ordinal numbers.
2) Three sets of 10,000 random integers between 1 and 10,000 are created, using a pseudo-random number generation utility with three different seeds. Each combination of random integers, one from each set, represents a combination of load, steel resistance, and concrete resistance (Figure 23). In order to select these the i^{th} value of each set of random numbers is chosen. Suppose, for example, that this i^{th} value corresponds to the three ordinal numbers: 203, 999, and 5. Therefore, the 203rd value of the load is combined with the 999th value of the steel resistance and the 5th value of the concrete resistance. Because

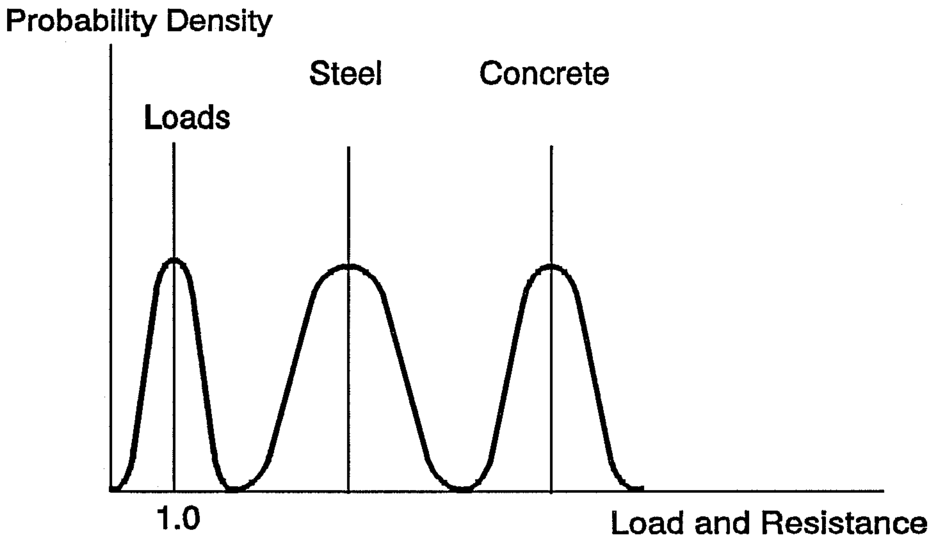

Figure 23: Load, Steel Resistance, and Concrete Resistance Distributions

each load and resistance value occurs in proportion to its relative probability, the combinations so obtained represent real combinations of load and resistance. The minimal value of resistance (lesser of steel and concrete), minus the value of load, represents a real (Resistance minus Load) value.

3) This process is repeated for each of the 10,000 sets of three random integers, and 10,000 (Resistance minus Load) values are obtained. These values are checked to ensure that the means and standard deviations of the discretized histograms match the target values.

4) The (Resistance minus Load) values so obtained are also assumed to be normally distributed. Their mean and standard deviation are calculated, as is the corresponding probability of failure (the area of the

probability distribution lying to the left of the vertical axis).

5) Because different combinations of random numbers are selected, each time the computer program of Appendix G is run, slightly different values of the safety index and the corresponding probability of failure are obtained. However, the values do not differ significantly.

6.5.2 Probability of Concrete Failure Under Unlimited Loads

The numerical calculations, carried out by computer as described in Appendix G, are outlined below:

1) For each ratio range of edge distance to embedment depth or spacing to embedment depth the statistical distribution is discretized into a histogram. Each discrete load or resistance value is assigned an integer number of cells, in proportion to the probability of occurrence of that load or resistance value.
2) Only two sets of 10,000 random numbers need to be generated to compute the histogram of (Concrete Resistance minus Steel Resistance). Each combination of random integers represents a combination of steel resistance and concrete resistance. Because each load and resistance value occurs in proportion to its relative probability, the combinations so obtained represent real combinations of steel resistance and concrete resistance.
3) This process is repeated for each of the 10,000 sets of two random integers, and 10,000 (Concrete Resistance minus Steel Resistance) are obtained.

These values are checked to ensure that the means and standard deviations (of the discretized histograms) match the target values.

4) The (Concrete Resistance minus Steel Resistance) values so obtained are also assumed to be normally distributed. Their mean and standard deviation are calculated, as is the corresponding probability of failure (the area of the probability distribution lying to the left of the vertical axis) (Figure 24).

5) Each time the computer program of Appendix G is run, slightly different values of the safety index and the corresponding probability of failure are obtained, because different combinations of random numbers are selected. However, the values do not differ significantly.

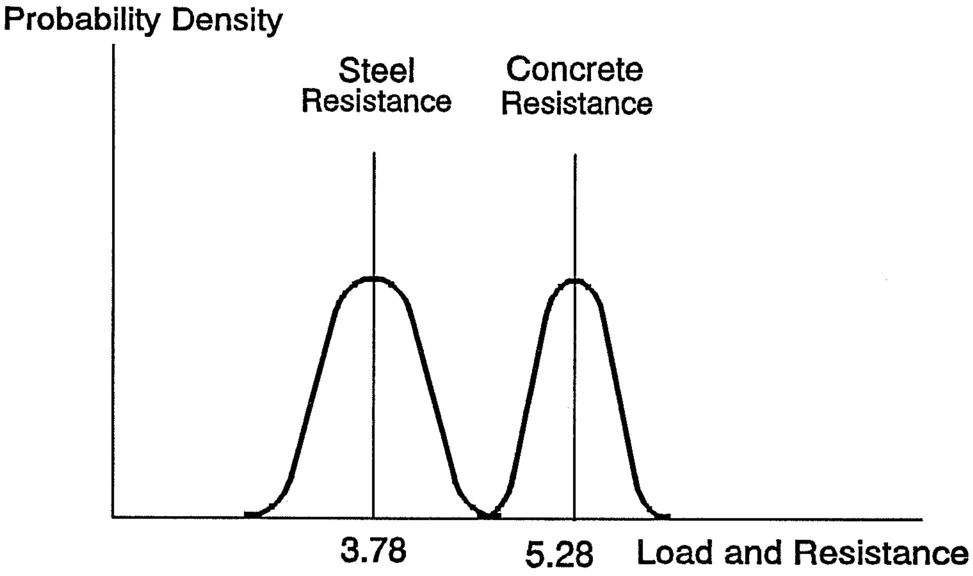

Figure 24: Steel and Concrete Resistance Distributions

6.6 Discussion of LRFD Results

6.6.1 Probability of Failure Under Known Loads

The probabilities of steel or concrete failure under known loads are detailed in Tables 5 and 6, and are illustrated in Figures 26 and 27. Current design practice for reinforced concrete structures with average consequences of failure accepts designs with probabilities of failure of about 0.0005, corresponding to β values of 3.0 to 3.5 [21]. The β value is defined as the safety index and is illustrated in Figure 25.

For single anchors located near a free edge and far from other anchors, the Concrete Capacity method has the lowest probability of failure for all except one range of edge distance to embedment depth ratios. The lowest value of β for any range of edge distance to embedment depth for the Concrete Capacity method is 3.97. In contrast, the ACI

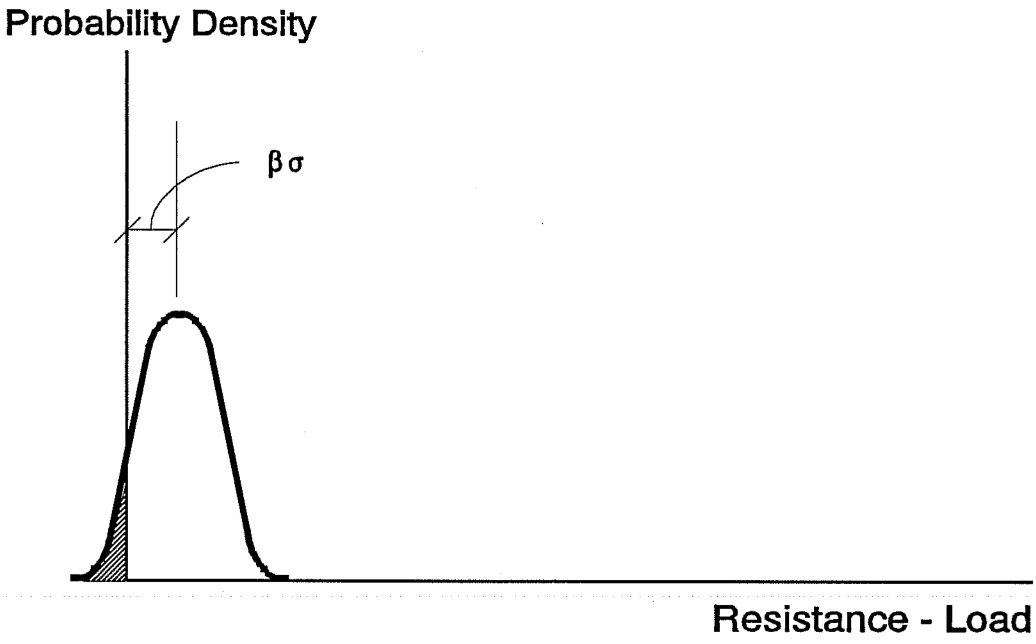

Figure 25: Definition of β or Safety Index

349-85 method's lowest value for β is 2.98. In addition, three ranges for the ACI 349-85 method have β values between 3.0 and 3.5 with all other β values greater than 3.5. For five of the seven ranges of edge distance to embedment depth no difference is evident between the ACI 349-85 method and the variable-angle cone method. In the remaining ranges, the ACI 349-85 method has a lower probability of failure than the variable-angle cone method.

As with single anchors near a free edge, the Concrete Capacity method generally has the lowest probability of failure for all ratio ranges of spacing to embedment depth for multiple closely spaced anchors. The lowest value of β for any range of edge distance to embedment depth for the Concrete Capacity method is 4.13. In contrast, the ACI 349-85 method has two ranges with values of β less than 2.5. All other ranges have β values greater than 3.5. The variable-angle cone method predicts probabilities of failure similar to the ACI 349-85 method except for two ranges of spacing to embedment depth where the β value is lowest. This is because the variable-angle cone predicts the failure load more consistently for various embedment depths.

6.6.2 Probability of Failure Under Unlimited Loads

The probabilities of concrete failure under unlimited loads are detailed in Table 7 and 8 and are illustrated in Figures 28 and 29. For single anchors near a free edge the variable-angle cone method is associated with a consistently larger probability of concrete failure than either the ACI 349-85 method or the Concrete Capacity method for all ranges of edge distance to embedment depth ratios. In addition, the ACI 349-85 method has a probability of failure much larger than the Concrete

Capacity method for the lowest four ratio ranges of edge distance to embedment depth.

For multiple closely spaced anchors, the ACI 349-85 method has probabilities of concrete failure within two orders of magnitude as those from the Concrete Capacity method for all but two segments of spacing to embedment depth ratios (s_1/h_e = 0.751-0.90 and s_1/h_e = 1.201-1.35). However, in those two ranges it is difficult to draw definitive conclusions regarding the relative merits of the ACI 349-85 method and the Concrete Capacity method. This is because both ranges contain a large number of points in which the embedment depth and the configuration of the anchor group are constant. Thus, if all variables affecting the actual failure load remain constant for these tests, the failure loads would be the same. Consequently, these results lead to a constant ratio of actual to predicted failure load. This provides an excellent approximation to the current use of an assumption of the normal curve. However, there are approximately three different groups of tests in each range of spacing to embedment depth, so the assumption of the normal distribution is no longer a strong premise. Examination of Figure 29 indicates that the Concrete Capacity method has more consistent probabilities of concrete failure under unknown loads than either the ACI 349-85 method or the variable-angle cone method.

Table 5: Results of Monte Carlo Analysis for Probability of Failure Under Known Loads for Single Anchors Near a Free Edge

c_1/h_e	Probability of Failure					
	ACI 349-85		Variable-Angle Cone		Concrete Capacity	
	β	P(f)	β	P(f)	β	P(f)
0.45-0.60	2.98	0.147 e-2	2.70	0.351 e-2	4.39	0.581 e-5
0.601-0.75	3.49	0.214 e-3	3.35	0.398 e-3	4.25	0.107 e-4
0.751-0.90	3.13	0.879 e-3	3.83	0.629 e-4	4.63	0.181 e-5
0.901-1.05	3.27	0.546 e-3	3.59	0.167 e-3	4.43	0.468 e-5
1.051-1.20	4.39	0.576 e-5	3.11	0.943 e-3	3.97	0.367 e-4
1.201-1.35	4.57	0.242 e-5	3.49	0.238 e-3	4.74	0.107 e-5
1.351-1.50	3.73	0.952 e-4	3.78	0.781 e-4	4.14	0.173 e-4

Table 6: Results of Monte Carlo Analysis for Probability of Failure Under Known Loads for Multiple Closely Spaced Anchors

s_1/h_e	Probability of Failure					
	ACI 349-85		Variable-Angle Cone		Concrete Capacity	
	β	P(f)	β	P(f)	β	P(f)
0.27-0.45	4.16	0.159 e-4	4.10	0.206 e-4	4.45	0.437 e-5
0.451-0.60	4.56	0.260 e-5	4.35	0.676 e-5	4.19	0.142 e-4
0.601-0.75	4.40	0.548 e-5	4.53	0.291 e-5	4.32	0.772 e-5
0.751-0.90	2.50	0.621 e-2	4.21	0.129 e-4	4.57	0.249 e-5
0.901-1.05	4.59	0.222 e-5	4.24	0.112 e-4	4.59	0.225 e-5
1.051-1.20	3.80	0.701 e-4	3.97	0.359 e-4	4.28	0.943 e-5
1.201-1.35	4.50	0.347 e-5	4.56	0.251 e-5	4.50	0.333 e-5
1.351-1.50	2.11	0.174 e-1	3.28	0.519 e-3	4.13	0.185 e-4
1.501-2.00	4.22	0.121 e-4	4.29	0.875 e-5	4.46	0.405 e-5
2.001-2.50	4.04	0.261 e-4	4.64	0.176 e-5	4.56	0.252 e-5
2.501-3.00	4.55	0.266 e-5	4.66	0.155 e-5	4.67	0.149 e-5

Table 7: Results of Monte Carlo Analysis for Probability of Concrete Failure Under Unlimited Loads for Single Anchors Near a Free Edge

c_1/h_e	Probability of Concrete Failure					
	ACI 349-85		Variable-Angle Cone		Concrete Capacity	
	β	P(f)	β	P(f)	β	P(f)
0.45-0.60	0.43	0.333	-0.69	0.754	2.52	0.592 e-2
0.601-0.75	1.01	0.156	-0.97	0.834	2.14	0.163 e-1
0.751-0.90	0.59	0.279	-0.43	0.666	5.59	0.112 e-7
0.901-1.05	1.19	0.117	-0.02	0.509	2.56	0.521 e-2
1.051-1.20	2.69	0.356 e-2	0.02	0.494	1.56	0.594 e-1
1.201-1.35	2.62	0.436 e-2	0.37	0.356	4.41	0.519 e-5
1.351-1.50	1.68	0.467 e-1	-0.37	0.645	1.37	0.851 e-1

Table 8: Results of Monte Carlo Analysis for Probability of Concrete Failure Under Unlimited Loads for Multiple Closely Spaced Anchors

s_1/h_e	Probability of Concrete Failure					
	ACI 349-85		Variable-Angle Cone		Concrete Capacity	
	β	P(f)	β	P(f)	β	P(f)
0.27-0.45	1.88	0.301 e-1	1.97	0.248 e-1	2.71	0.339 e-2
0.451-0.60	2.83	0.239 e-2	1.88	0.299 e-1	1.89	0.291 e-1
0.601-0.75	2.77	0.284 e-2	2.82	0.244 e-2	2.55	0.537 e-2
0.751-0.90	0.65	0.258	0.29	0.385	3.45	0.280 e-3
0.901-1.05	6.30	0.150 e-9	1.41	0.769 e-1	5.57	0.128 e-7
1.051-1.20	1.76	0.390 e-1	1.23	0.110	2.21	0.135 e-1
1.201-1.35	3.08	0.105 e-2	6.37	0.938 e-10	4.76	0.958 e-6
1.351-1.50	0.81	0.210	0.56	0.287	1.93	0.265 e-1
1.501-2.00	2.26	0.119 e-1	2.12	0.172 e-1	3.07	0.106 e-2
2.001-2.50	2.04	0.204 e-1	3.85	0.594 e-4	2.92	0.175 e-2
2.501-3.00	7.09	0.665 e-12	5.35	0.445 e-7	8.03	0.500 e-15

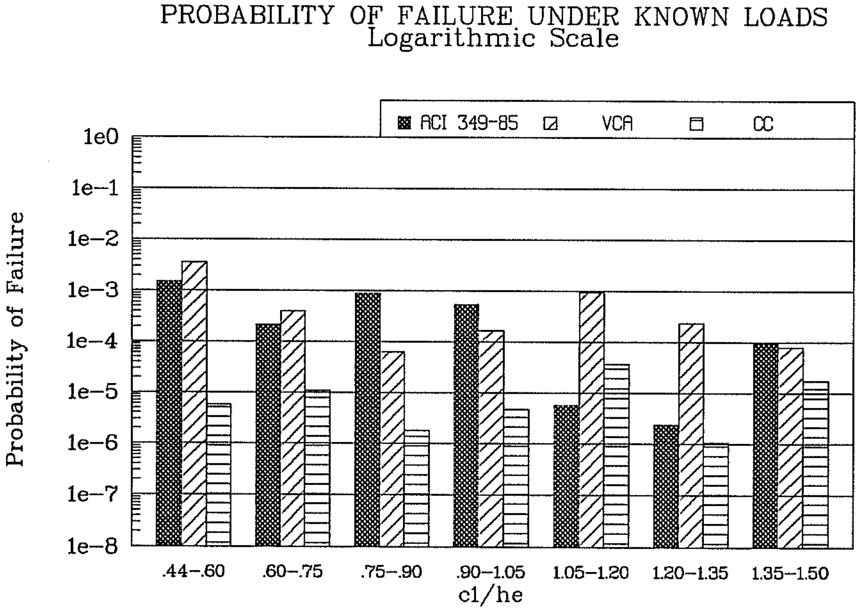

Figure 26: Probability of Failure Under Known Loads for Single Anchors Near a Free Edge

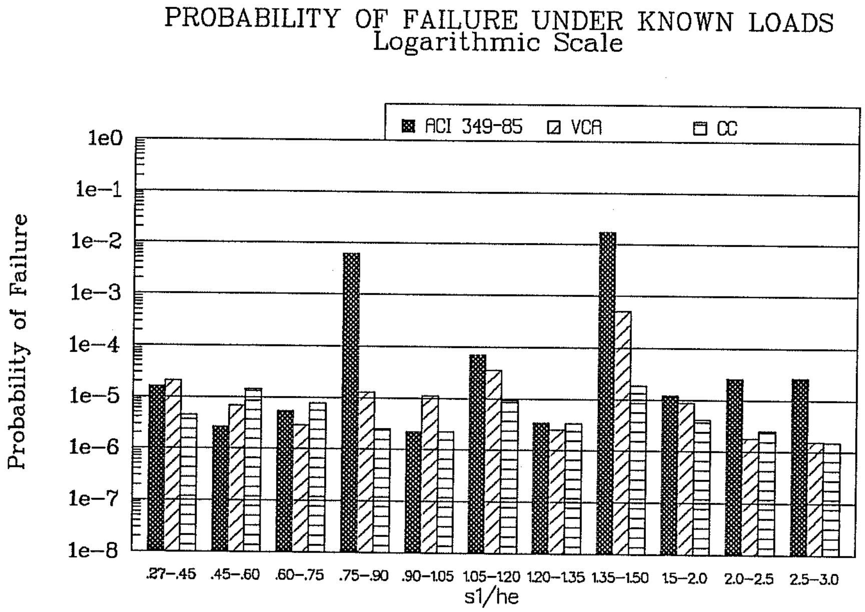

Figure 27: Probability of Failure Under Known Loads for Multiple Closely Spaced Anchors

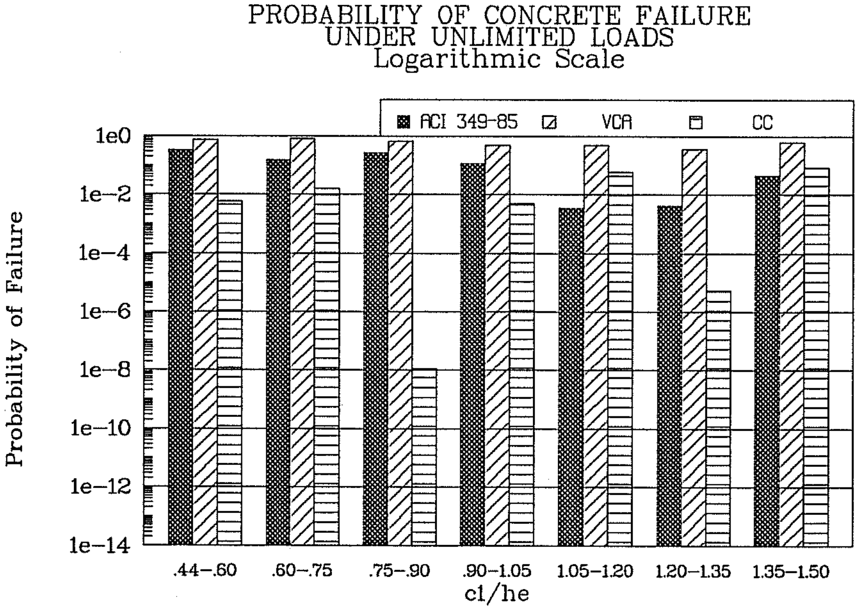

Figure 28: Probability of Concrete Failure Under Unlimited Loads for Single Anchors Near a Free Edge

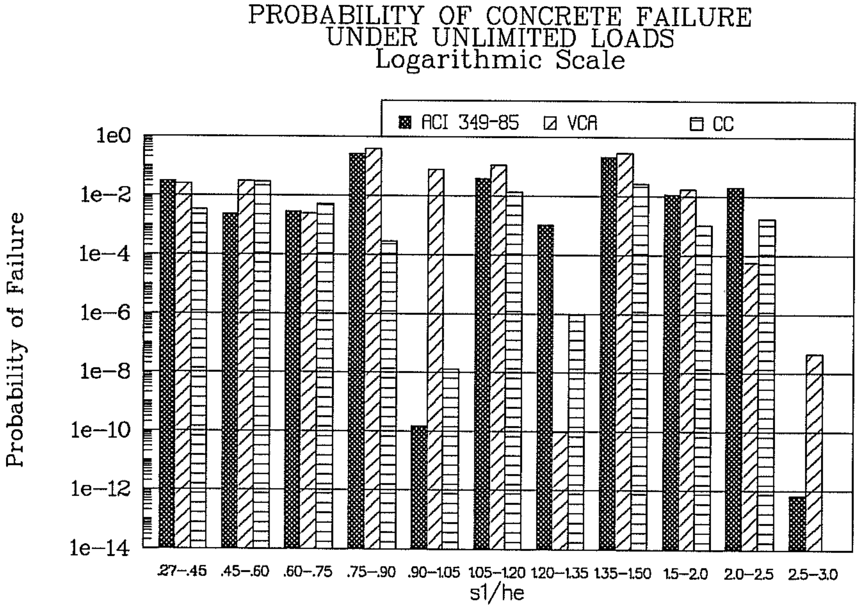

Figure 29: Probability of Concrete Failure Under Unlimited Loads for Multiple Closely Spaced Anchors

6.7 General Limitations of These Analyses

These analyses have the following limitations:

1) Loads and resistances are assumed to be normally distributed. Safety factors computed by the analysis could increase or decrease as a result of different presupposed distributions.
2) Actual concrete strength is presumed to equal the specified value. This premise is conservative, because actual concrete strength usually exceeds specifications.
3) A single representative value is assumed for the ratio of specified ultimate steel strength to specified yield strength. This value could be made more accurate by computing the ratio separately for each anchor in the data base.

7.0 SUMMARY, CONCLUSIONS, AND RECOMMENDATIONS

7.1 Summary

The overall objective of this research has been to evaluate the accuracy and suitability for design of three different methods for predicting anchor capacity as governed by concrete failure. In particular, this thesis has focused on single anchors located close to a free edge and multiple anchors located far from a free edge. That objective has been accomplished by the following steps:

1) A total of 160 data points is available from tests on single anchors close to a free edge in which failure occurs by formation of a concrete cone. Using common definitions and nomenclature for all variables and material properties, those data have been placed on a data base in terms of SI units and concrete cube strengths.
2) A total of 185 data points is available from tests on multiple anchors far from a free edge in which failure occurs by formation of a concrete cone. These data on multiple anchors include a large number of data points on both groups of 2 and 4 anchors. In addition, 9 tests on groups of 16 anchors are included. Using common definitions and nomenclature for all variables and material properties, those data are placed on a data base in SI units and in terms of concrete cube strengths.
3) Data for single anchors located close to a free edge have been plotted against three existing methods: the 45° cone method of ACI 349-85; a variable-angle cone method; and the Concrete Capacity method (exponent of

1.5). Plots show concrete capacity, normalized by $\sqrt{f'_c}$, as a function of embedment depth.

4) Data for multiple anchors have been plotted against three existing methods: the 45° cone method of ACI 349-85; a variable-angle cone method; and the Concrete Capacity method (exponent of 1.5). The plots show ratios of actual capacity to predicted capacity as a function of embedment depth.

5) Distinct square errors have been computed for different ratios of edge distance to embedment depth for single anchors near a free edge.

6) Distinct square errors have been computed for different ratios of edge distance to embedment depth for multiple closely spaced anchors.

7) The probability of steel or concrete failure under known loads, and of concrete failure under unlimited loads, has been determined for single anchors located near a free edge. Distinct probabilities of failure have been evaluated for different ratios of edge distance to embedment depth.

8) The probability of steel or concrete failure under known loads, and of concrete failure under unlimited loads, has been determined for multiple closely spaced anchors. Distinct probabilities of failure have been evaluated for different ratios of anchor spacing to embedment depth.

9) Based on the above comparisons of square error and probability of failure, each method has been evaluated with respect to accuracy and design suitability in terms of probability of failure for single anchors located near a free edge, and for multiple closely spaced anchors.

7.2 Conclusions

7.2.1 Single Anchors Located Near a Free Edge

7.2.1.1 Square Error

For all ratios of edge distance to embedment depth with single anchors near a free edge and far from other anchors, the Concrete Capacity method has a square error lower than that of either ACI 349-85 or the variable-angle cone methods. For most ratios of edge distance to embedment depth, the Concrete Capacity method has a square error lower than that of either the ACI 349-85 or the variable-angle cone method. However, the advantages of the Concrete Capacity method for multiple anchors are not as definitive as those for single anchors.

7.2.1.2 Probability of Failure Under Known Loads for Single Anchors Near a Free Edge

Current design practice for reinforced concrete structures with average consequences of failure accepts designs with probabilities of failure of about 0.0003, corresponding to β values of 3.0 to 3.5 [21].

For single anchors located near a free edge and far from other anchors, the Concrete Capacity method generally has the lowest probability of failure for most ranges of edge distance to embedment depth ratios. The lowest value of β for any range of edge distance to embedment depth for the Concrete Capacity method is 4.14. In contrast, the ACI 349-85 method's lowest value for β is 2.96. In addition, two ranges for the ACI 349-85 method have β values between 3.0 and 3.5 with all other β values greater than 3.5. No significant difference is evident between the ACI 349-85 method and the variable-angle cone method.

7.2.1.3 Probability of Concrete Failure Under Unlimited Loads for Single Anchors Near a Free Edge

The variable-angle cone method is associated with a much larger probability of concrete failure than either the ACI 349-85 method or the Concrete Capacity method for all ranges of edge distance to embedment depth. In addition, the ACI 349-85 method has a probability of failure much larger than the Concrete Capacity method for four of the seven edge distance to embedment depth segments.

7.2.2 Multiple Anchors

7.2.2.1 Square Error

No distinct conclusions can be made from the sum of the square error with multiple anchors. This may be due to the fact that data points from many different anchor configurations are included in this data base. This disorder would especially be true if one method proves exact for one anchor configuration but has a large error for another configuration.

7.2.2.2 Probability of Failure Under Known Loads for Multiple Closely Spaced Anchors

Current design practice for reinforced concrete structures with average consequences of failure accepts designs with probabilities of failure of about 0.0003, corresponding to β values of 3.0 to 3.5 [21]. As with single anchors near a free edge, the Concrete Capacity method has the lowest probability of failure for most ratio ranges of spacing to embedment depth for multiple closely spaced anchors. The lowest value of β for any range of edge distance to embedment depth for the Concrete Capacity method is 4.03. In contrast, the ACI 349-85 method has two ranges with values of β less than 2.5. All other ranges have β values greater than 3.5. The variable-angle cone method predicts probabilities of failure similar to the ACI 349-85 method except for two ranges of spacing to embedment depth where the β value is lowest. This is because the variable-angle cone predicts the failure load more consistently for various embedment depths.

7.2.2.3 Probability of Concrete Failure Under Unlimited Loads for Multiple Closely Spaced Anchors

For multiple closely spaced anchors, the ACI 349-85 method has probabilities of concrete failure within two orders of magnitude as those from the Concrete Capacity method for all but two segments of spacing to embedment depth ratios (s_1/h_e = 0.751-0.90 and s_1/h_e = 1.201-1.35). The problem with these ranges is that each contains a large number of points in which the embedment depth and the configuration of the anchor group are constant. Thus, if all variables affecting the actual failure load remain constant for these tests, the failure loads would be the same. Consequently, these results lead to a constant ratio of actual to predicted failure load. This would provide an excellent approximation to the current use of an assumption of the normal curve. However, there are approximately three different groups of tests in each range of spacing to embedment depth, so the assumption of the normal distribution is not a strong premise. Examination of Figure 29 indicates that the Concrete Capacity method has more consistent probabilities of concrete failure under unknown loads than either the ACI 349-85 method or the variable-angle cone method.

7.2.3 General Conclusions

1) For most embedment depths, the Concrete Capacity method has a square error lower than that of either ACI 349-85 or the variable-angle cone method. This is true both for single anchors located close to a free edge, and for multiple closely spaced anchors.
2) For single anchors located close to a free edge, and also for multiple closely spaced anchors, all three methods are associated with sufficiently low probabilities of failure under known loads for all ratios of edge distance to embedment depth and of spacing to embedment depth.
3) Under unlimited loads, the probability of concrete failure associated with the Concrete Capacity method is generally lower than that of either the variable-angle cone or the ACI 349-85 approach. This is true both for single anchors near a free edge, and for multiple closely spaced anchors.
4) The primary advantage of the ACI 349-85 approach is its conical idealization of the failure surface. However, calculations of net projected area for multiple anchors are very complex in practice. The Concrete Capacity method uses the basic principle of idealizing the failure surface along with a relatively simple calculation for net projected area. For this reason, the Concrete Capacity method can be regarded as much more designer-friendly.

7.2.4 Limitations of This Study

As detailed throughout, this study has the following limitations:

1) The Central Limit Theorem may not be valid for obtaining a normal distribution for the ratio of actual concrete strengths to predicted concrete strengths. Questions about this validity arise for two reasons.
   - First, a normal distribution has been assumed to be valid over a range of ratios of edge distance to embedment depth and of spacing to embedment depth in order to keep the number of failure points in each range of ratios large. For the normal distribution to be accurate, the ratio of actual capacity to predicted capacity should possess similar properties over the range of edge distance to embedment depth or spacing to embedment depth considered. No study has been performed to determine the variation of ratios from the smallest ratios of edge distance to embedment depth or spacing to embedment depth in the range of ratios considered to the largest embedment depth in a given range.
   - Second, the Central Limit Theorem requires a very large number of data points to determine the true normal distribution. As evident in Figures A-1 through A-21 and B-1 through B-33, a limited number of data points are available in each range of data considered. Ideal data for such a study consist of an infinite number of points at a given ratio of c_1/h_e or s_1/h_e.

2) Calculation of the net projected area for multiple anchors based on the ACI 349-85 and variable-angle cone methods are close approximations rather than exact calculations. This occurs because the net area (including the area due to the anchor shaft) is first

determined; then the area due to the number of shafts in the group is subtracted. This difference is exact except when the net projected area of one anchor overlaps the area projected by a shaft on another anchor in the group. However, this calculation is always conservative, since the effect is to reduce A_p, thus reducing predicted capacity.

3) ACI 349-85 has requirements for the minimum bearing area of the anchor head. The concrete data base has not been checked for compliance with those requirements.

4) Loads and resistances are assumed to be normally distributed. Safety factors computed by the analysis could increase or decrease as a result of different assumed distributions.

5) Actual concrete strength is assumed to equal the specified value. This assumption is conservative, because actual concrete strength usually exceeds that specified.

6) A single representative value is used for the ratio of specified ultimate steel strength to specified yield strength. This could be made more accurate by computing these ratios separately for each anchor in the data base.

7) Typical field construction variations in embedment depth and edge distance are not estimated.

8) The specimens comprising this data base involve essentially uncracked concrete. Effects of cracking would be expected to reduce the anchor capacity as governed by concrete; therefore, they would increase the probabilities of failure calculated in this study.

9) The representative value used for the ratio of specified ultimate steel strength to specified yield

strength is determined from data on high strength anchors only. This value changes if regular strength anchors are considered.

7.3 Recommendations for Further Research

1) Obtain additional data to increase the number of available results at particular ratios of edge distance to embedment depths for single anchors located near a free edge and for particular ratios of spacing to embedment depths for multiple anchors. If existing results are unavailable, it may be necessary to conduct additional tests.
2) Search for additional test data on large groups of anchors with overlapping failure surfaces. Limited results show that the ACI 349-85 approach is unconservative for large groups of anchors. This premise concurs with the results ascertained found by Fuchs, Breen, and Eligehausen [11].
3) Seek additional data to increase the number of high strength steel failure data points. Additional data points would provide a better estimate of the actual distribution of steel failure.
4) Extend this analysis to the following cases:

    - lightweight concrete
    - high strength concrete
    - adhesive anchors
    - eccentrically loaded anchors
    - cyclically loaded anchors

APPENDIX A: GRAPHICAL COMPARISON OF EXISTING METHODS FOR SINGLE ANCHORS NEAR A FREE EDGE, FAR FROM OTHER ANCHORS (SI UNITS)

TENSILE CAPACITY vs. EMBEDMENT DEPTH
Concrete Capacity Method
Figure A-1

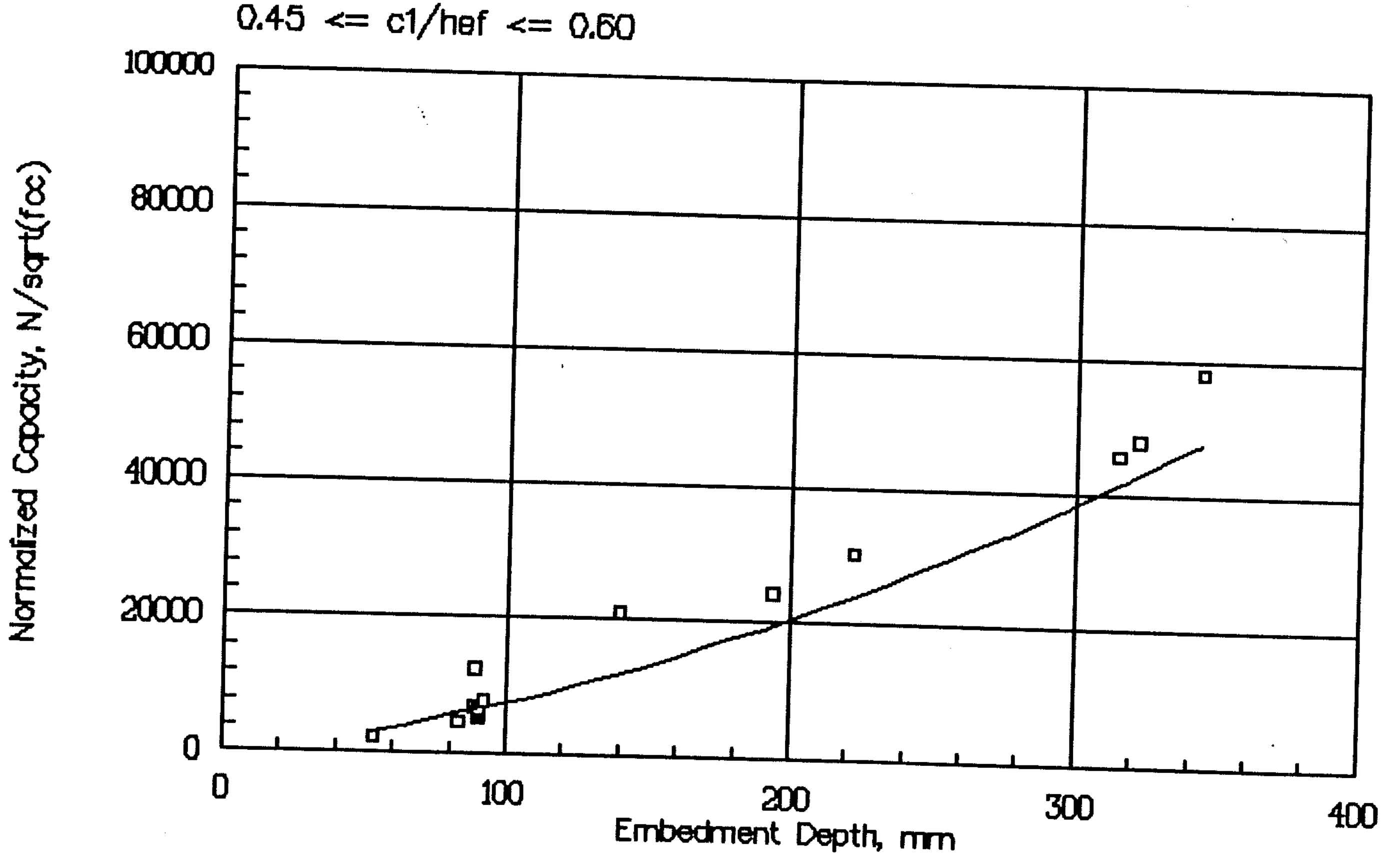

TENSILE CAPACITY vs. EMBEDMENT DEPTH
ACI 349-85 Method
Figure A-2

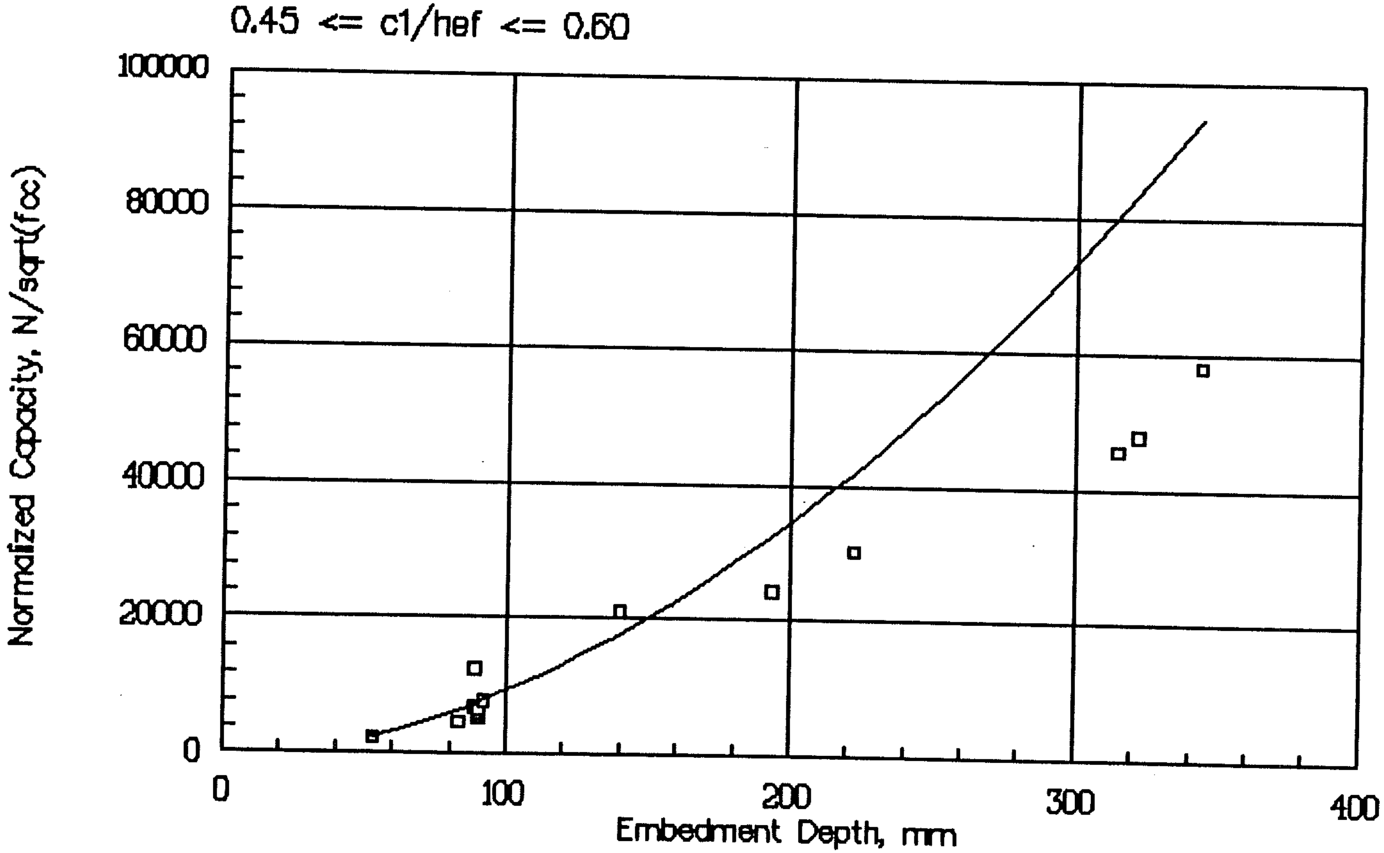

TENSILE CAPACITY vs. EMBEDMENT DEPTH
Variable–Angle Cone Method
Figure A–3

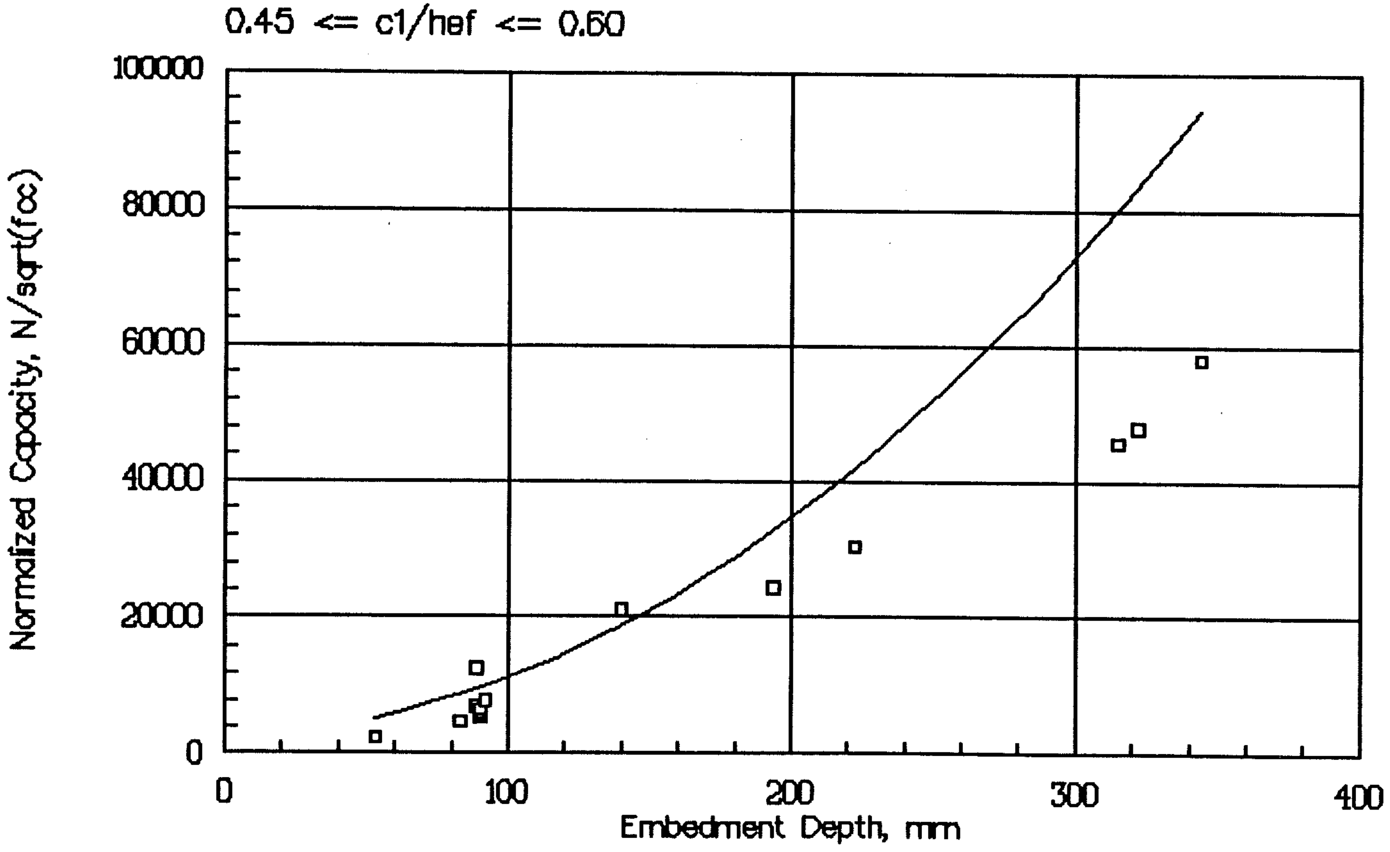

TENSILE CAPACITY vs. EMBEDMENT DEPTH
Concrete Capacity Method
Figure A–4

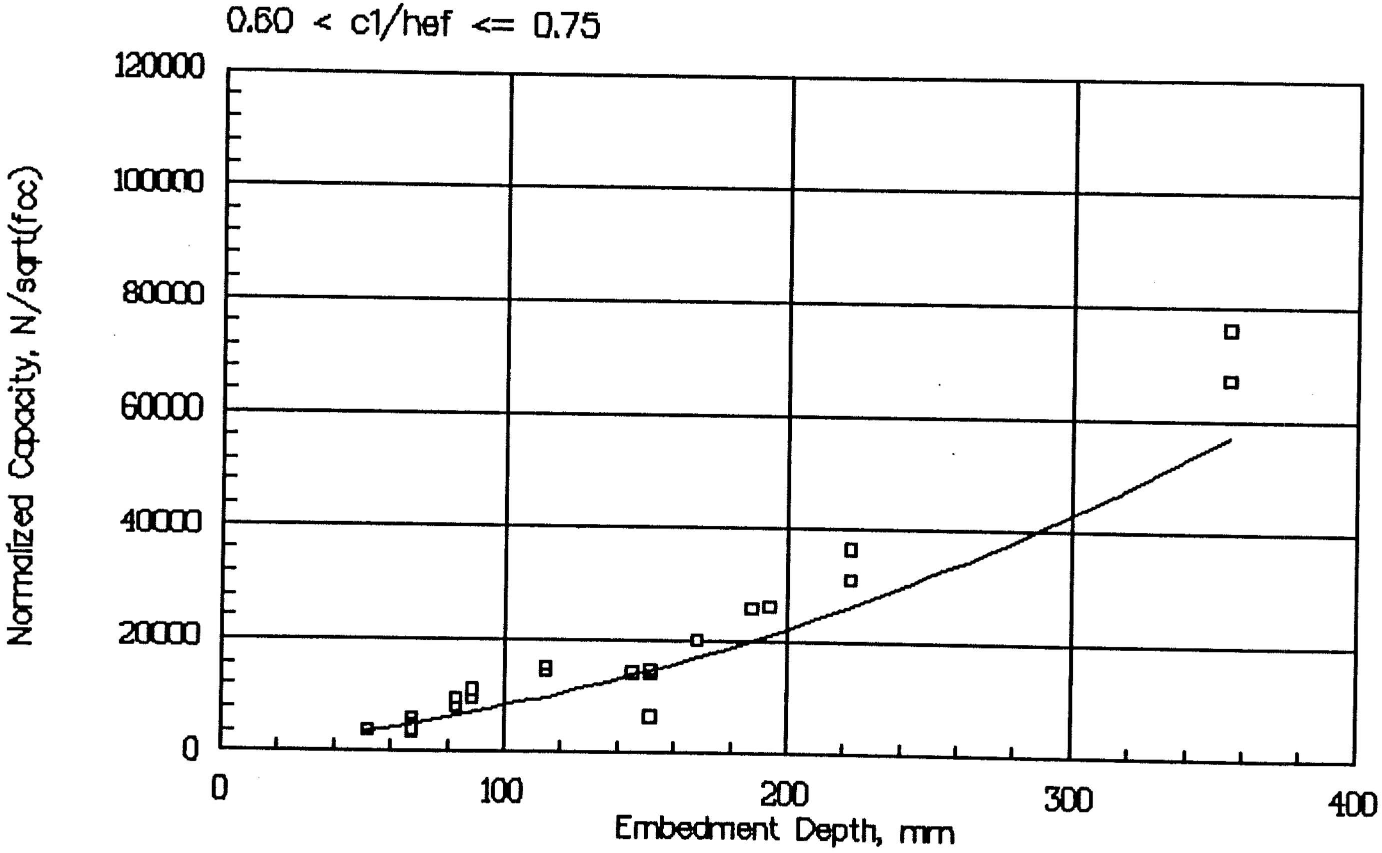

TENSILE CAPACITY vs. EMBEDMENT DEPTH
ACI 349-85 Method
Figure A-5

0.60 < c1/hef <= 0.75

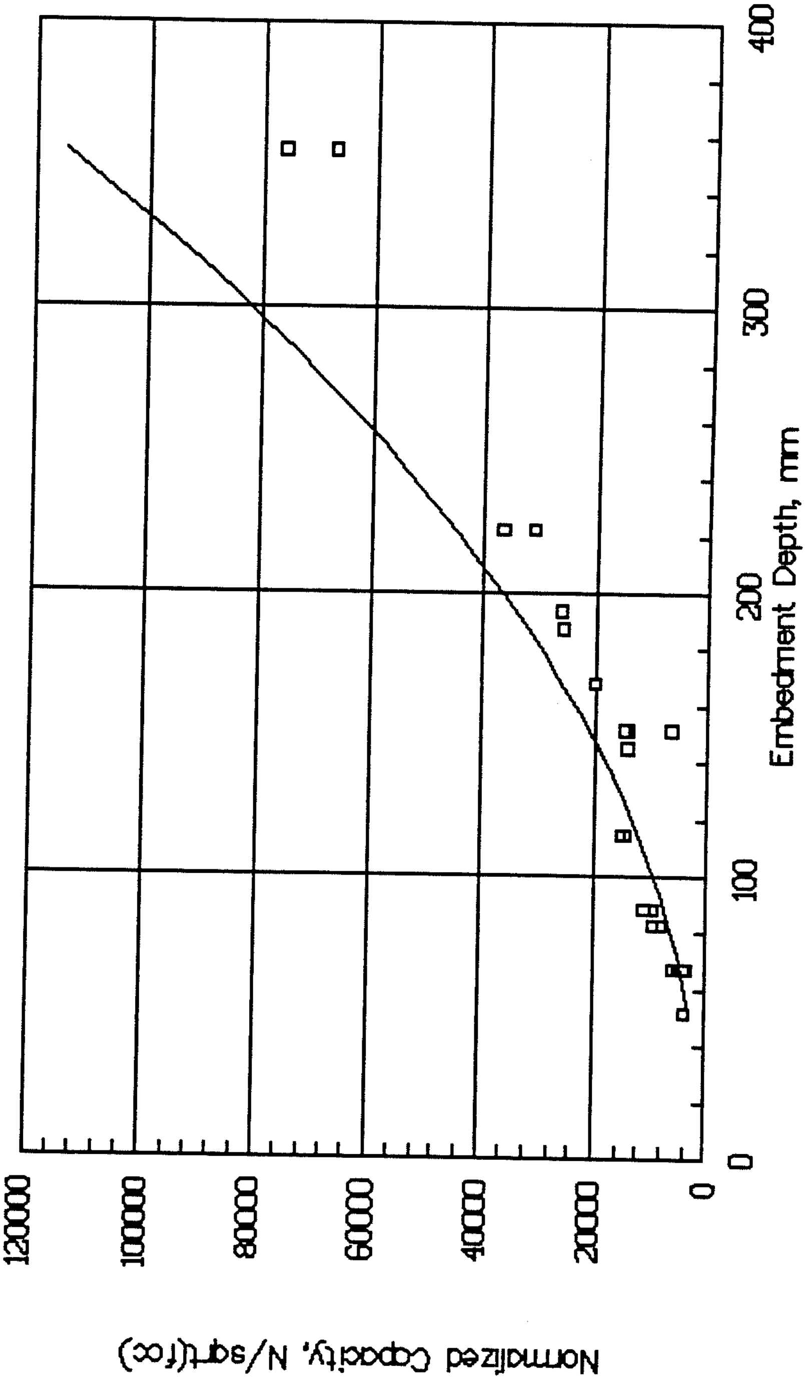

TENSILE CAPACITY vs. EMBEDMENT DEPTH
Variable-Angle Cone Method
Figure A-6

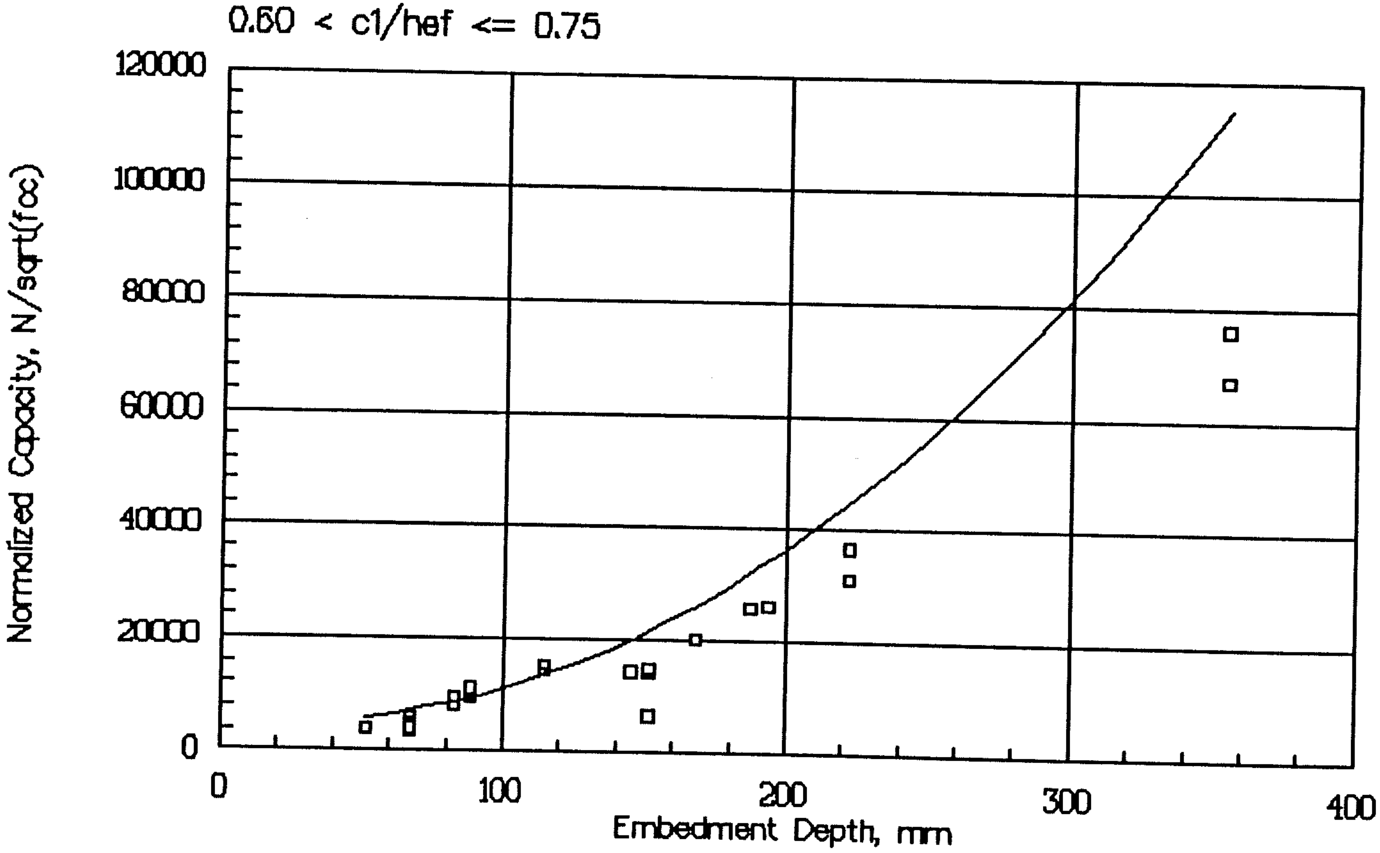

TENSILE CAPACITY vs. EMBEDMENT DEPTH
Concrete Capacity Method
Figure A-7

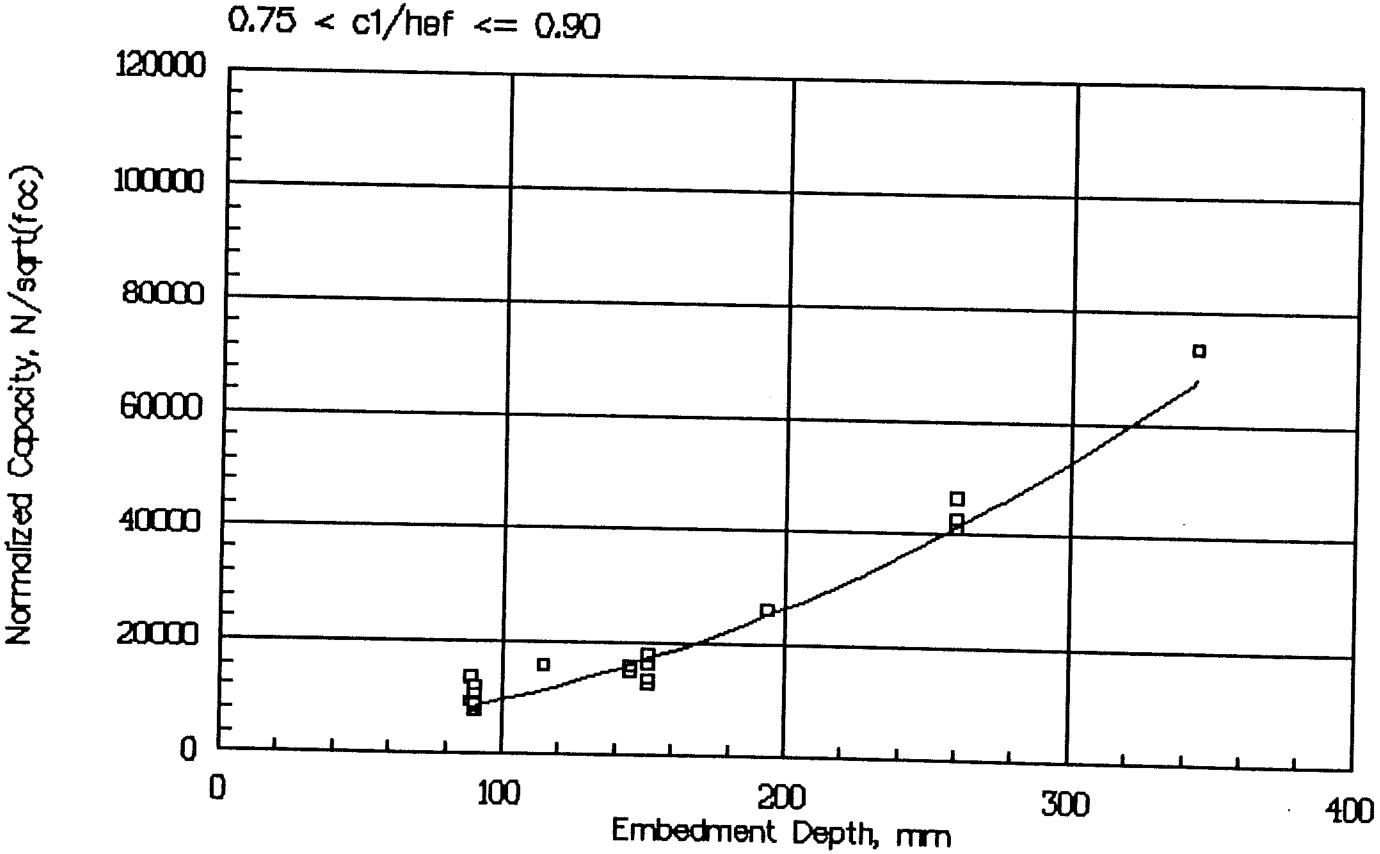

TENSILE CAPACITY vs. EMBEDMENT DEPTH
ACI 349–85 Method
Figure A–8

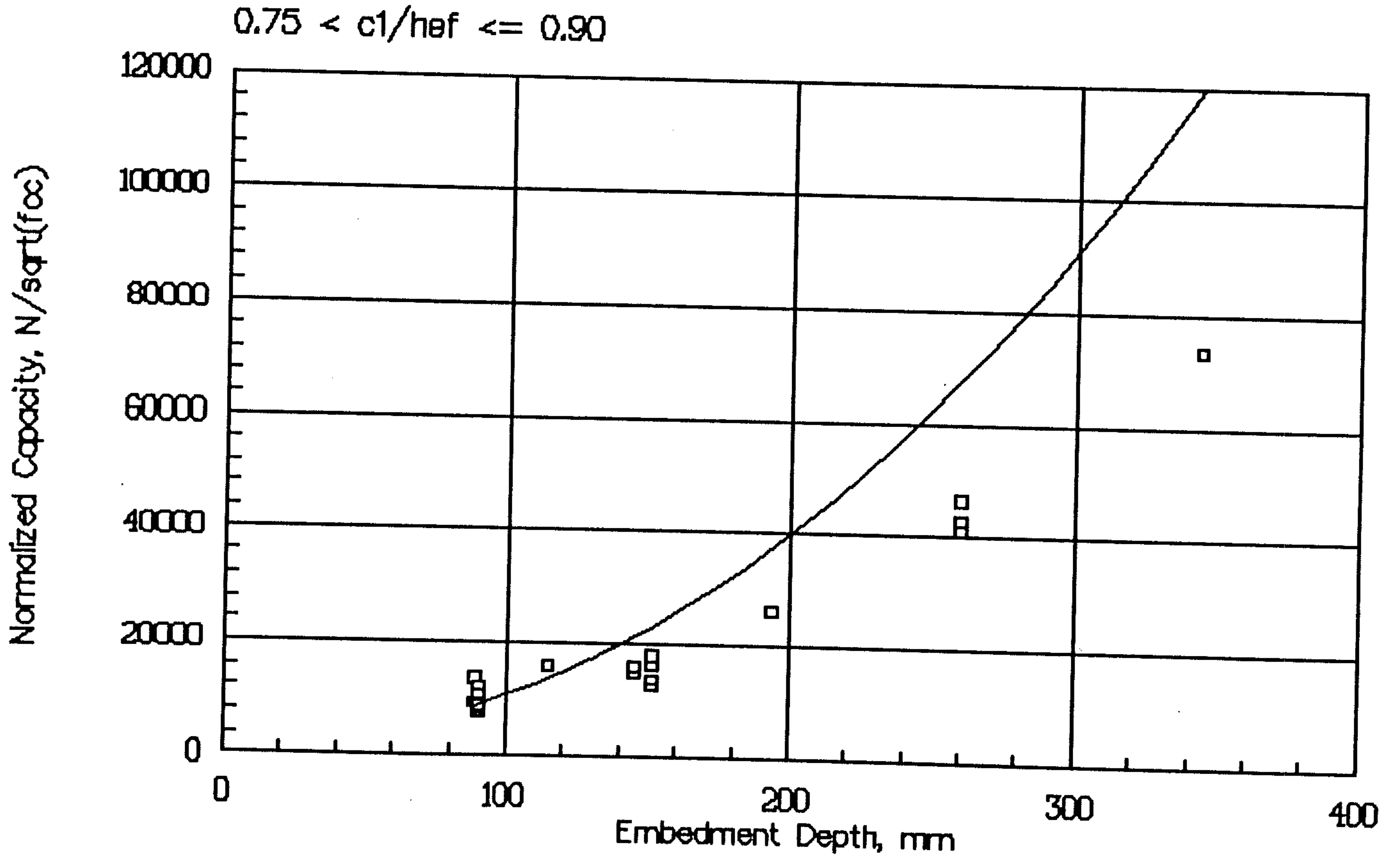

TENSILE CAPACITY vs. EMBEDMENT DEPTH
Variable–Angle Cone Method
Figure A–9

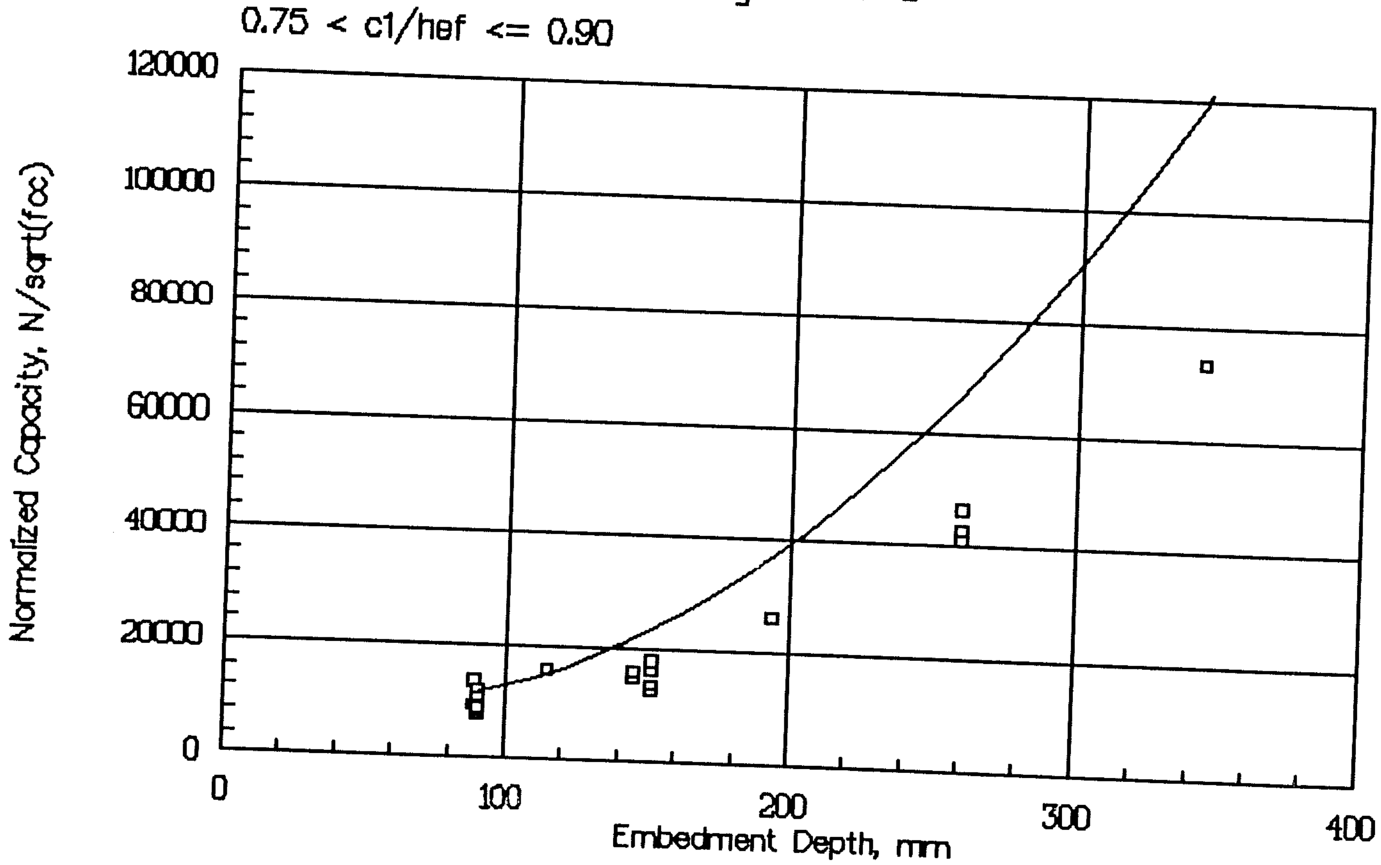

TENSILE CAPACITY vs. EMBEDMENT DEPTH
Concrete Capacity Method
Figure A–10

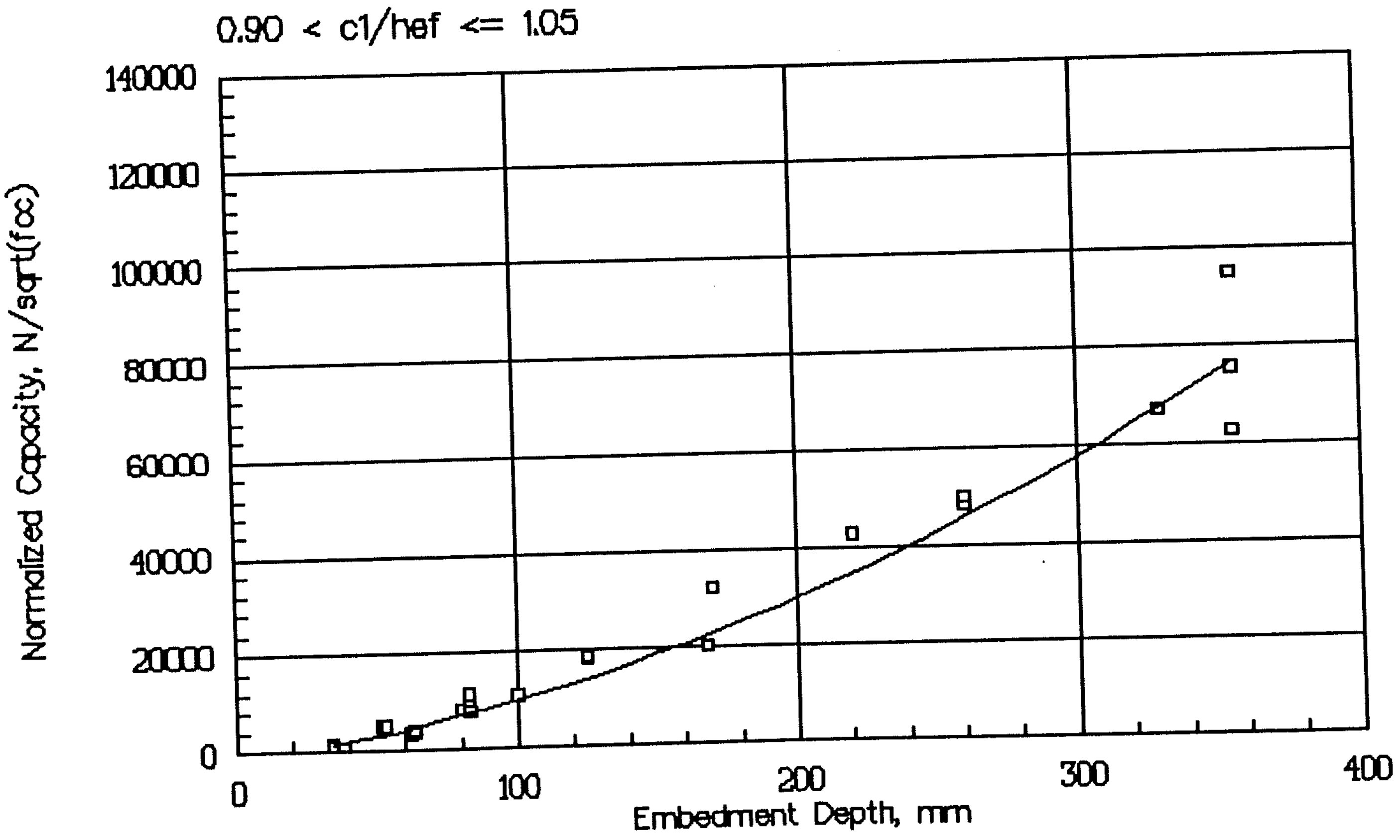

TENSILE CAPACITY vs. EMBEDMENT DEPTH
ACI 349–85 Method
Figure A–11

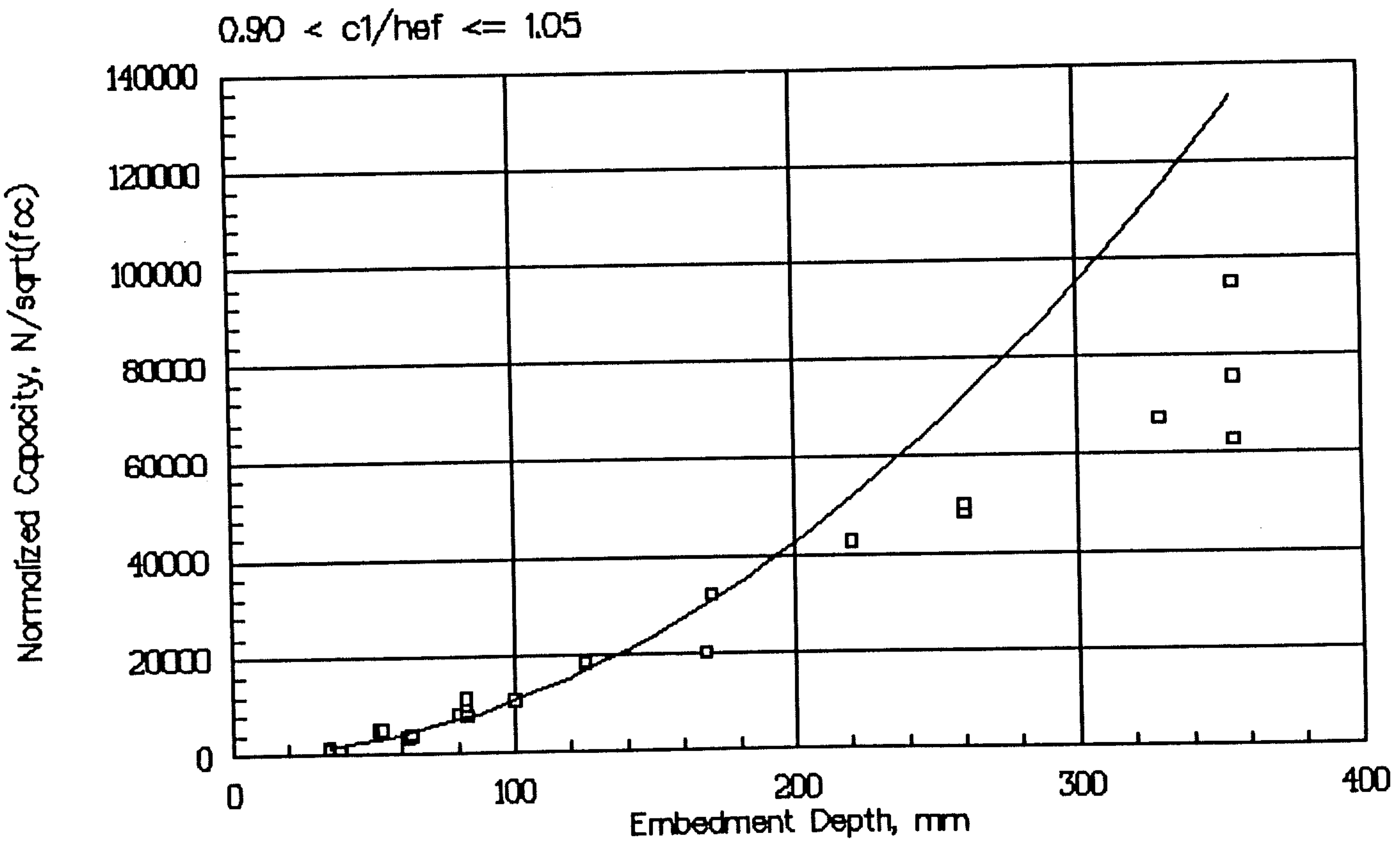

TENSILE CAPACITY vs. EMBEDMENT DEPTH
Variable–Angle Cone Method
Figure A–12

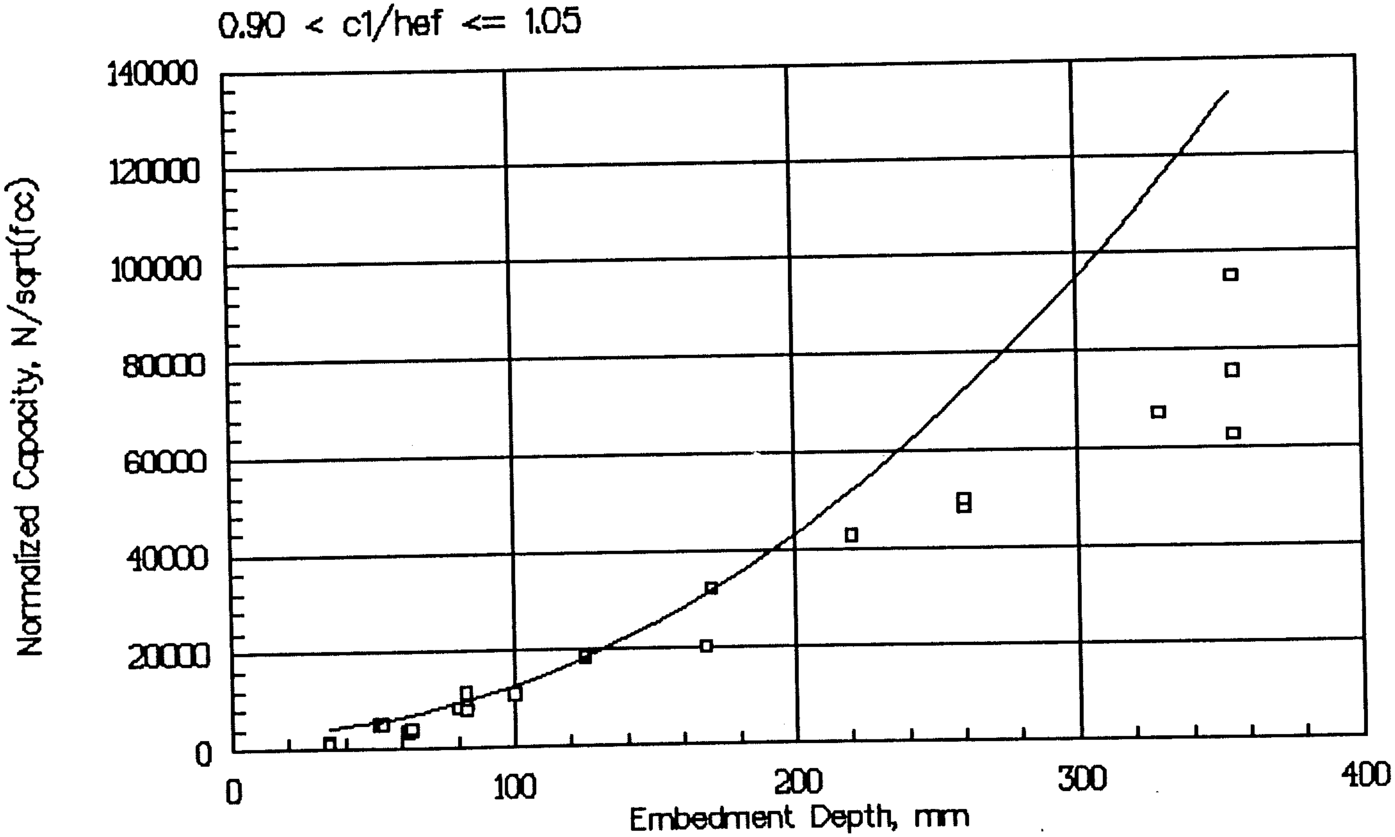

TENSILE CAPACITY vs. EMBEDMENT DEPTH
Concrete Capacity Method
Figure A—13

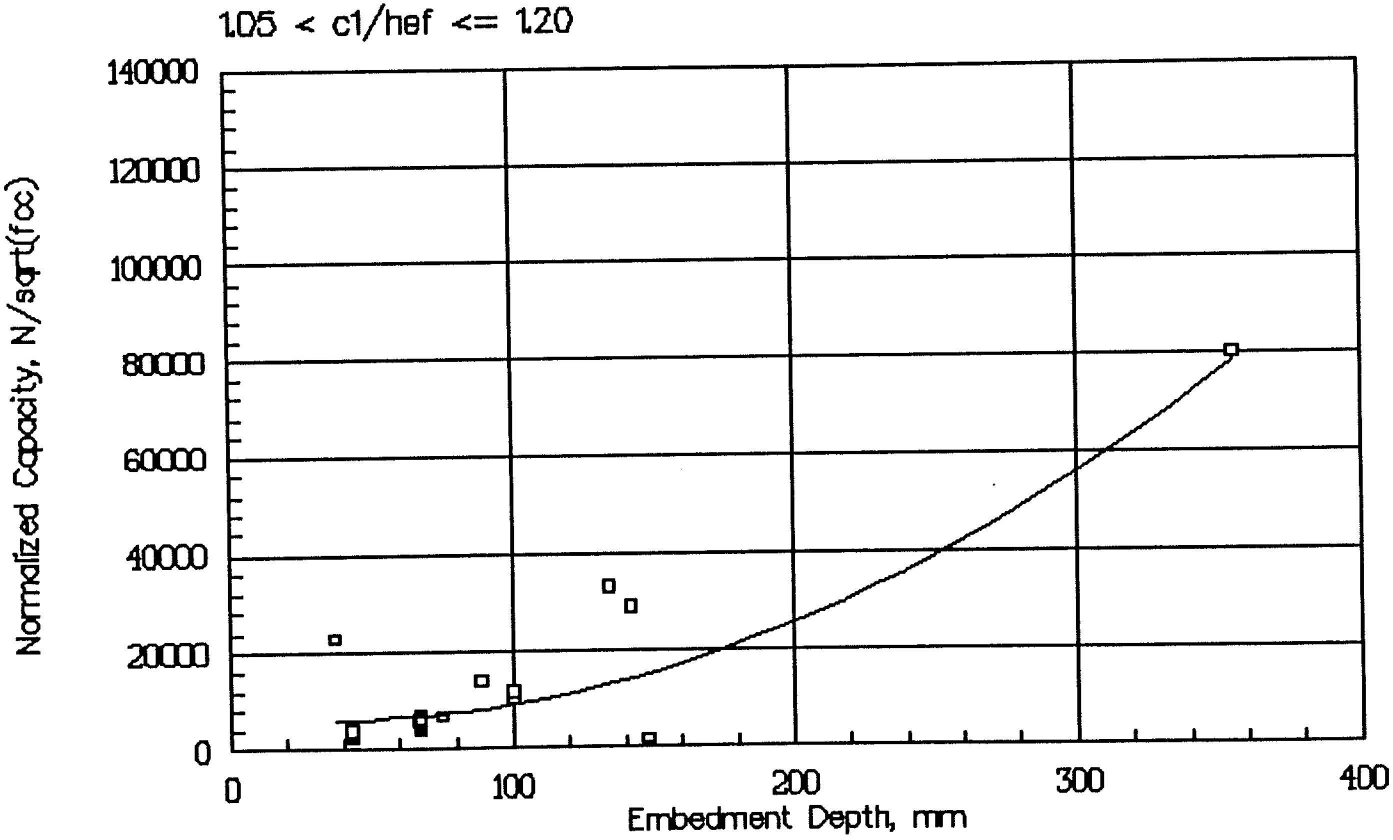

TENSILE CAPACITY vs. EMBEDMENT DEPTH
ACI 349-85 Method
Figure A-14

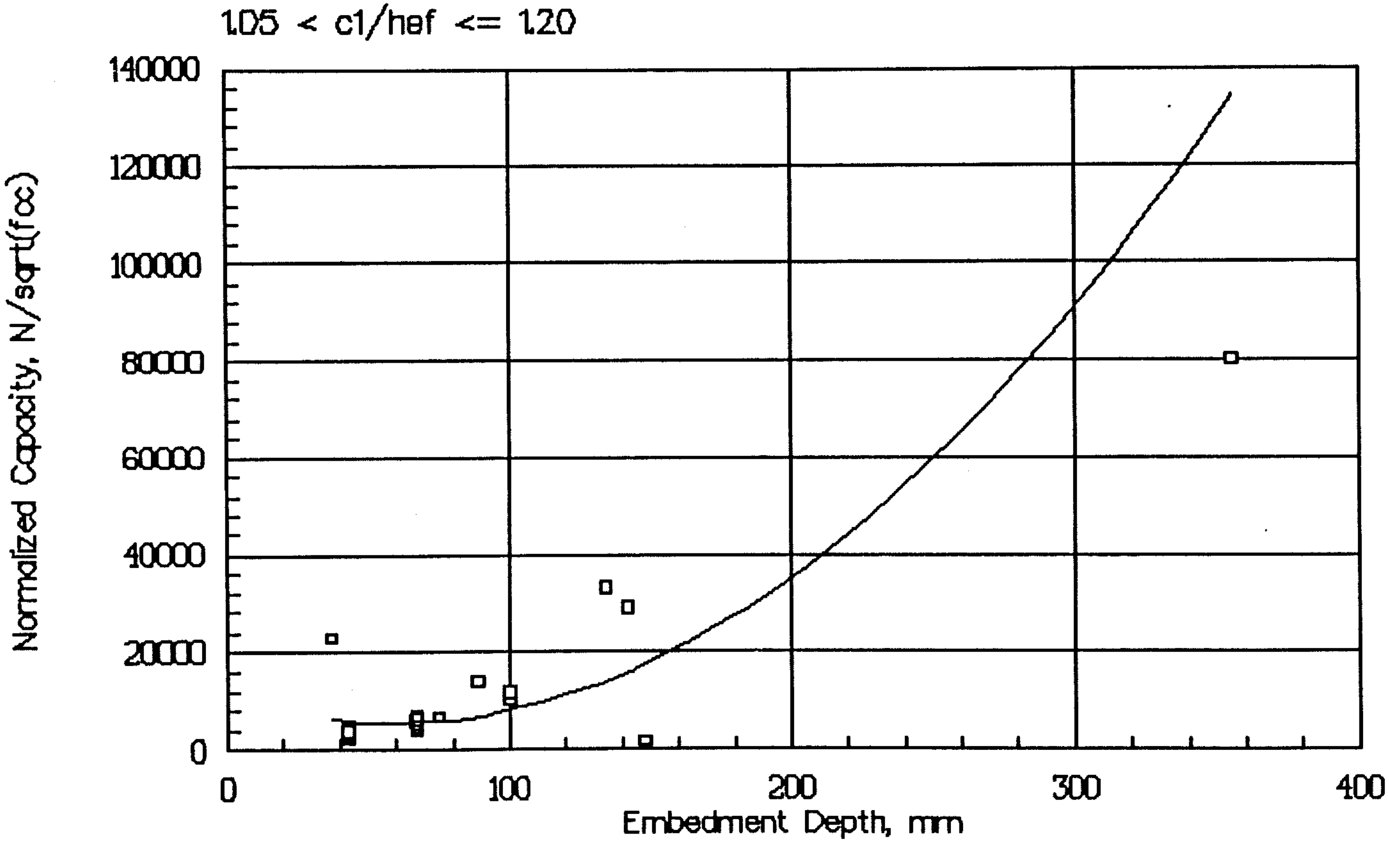

TENSILE CAPACITY vs. EMBEDMENT DEPTH
Variable-Angle Cone Method
Figure A-15

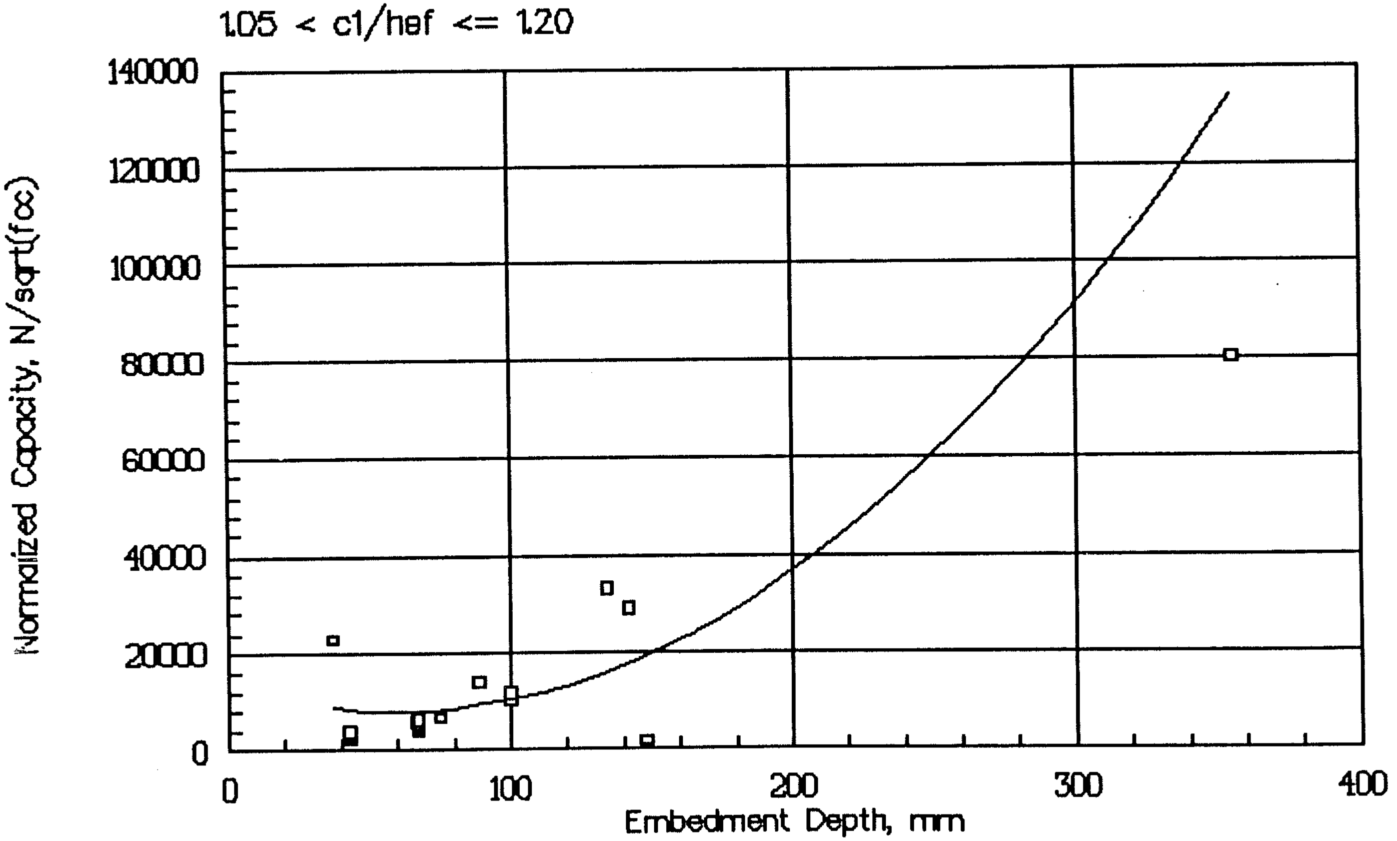

TENSILE CAPACITY vs. EMBEDMENT DEPTH
Concrete Capacity Method
Figure A–16

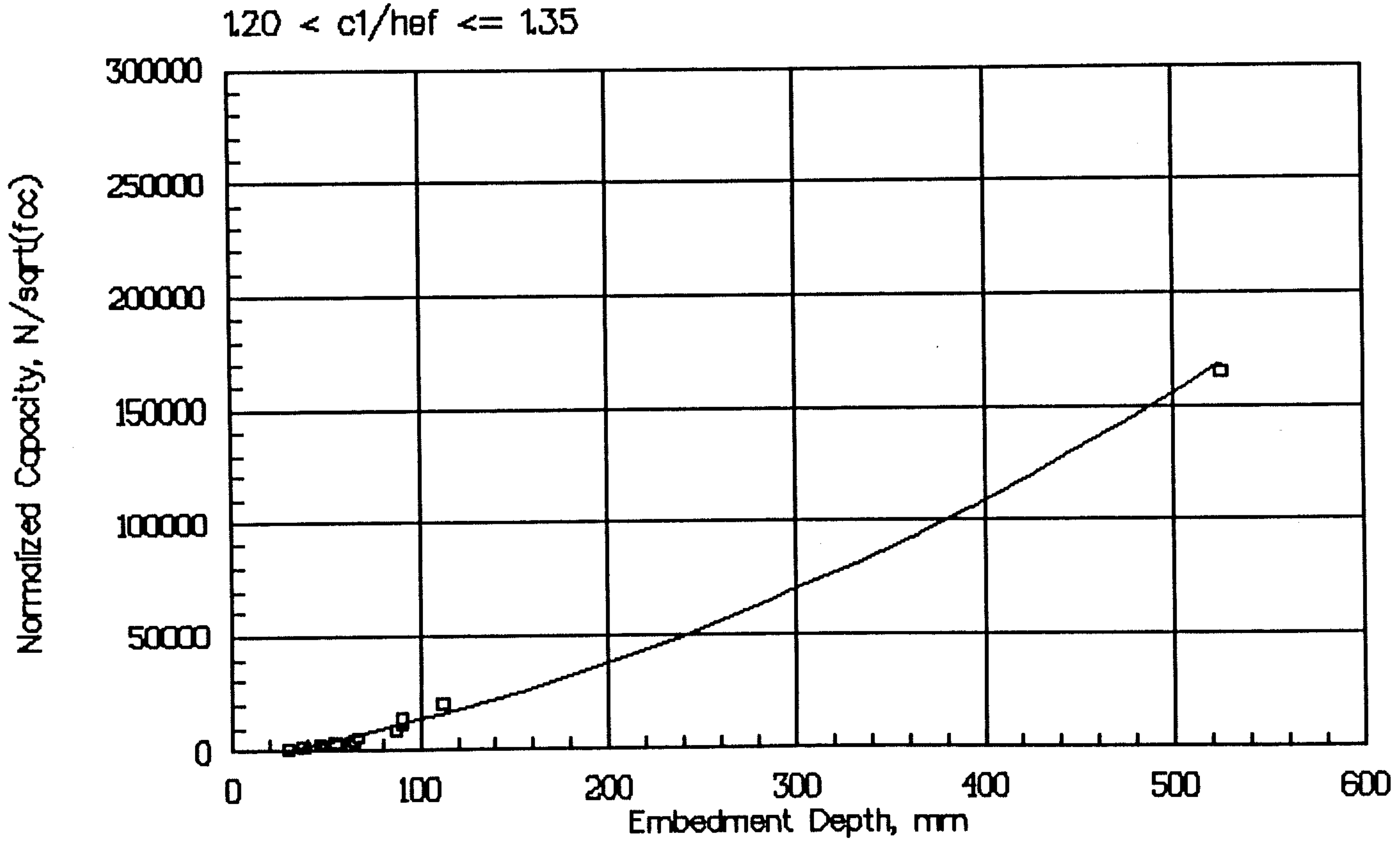

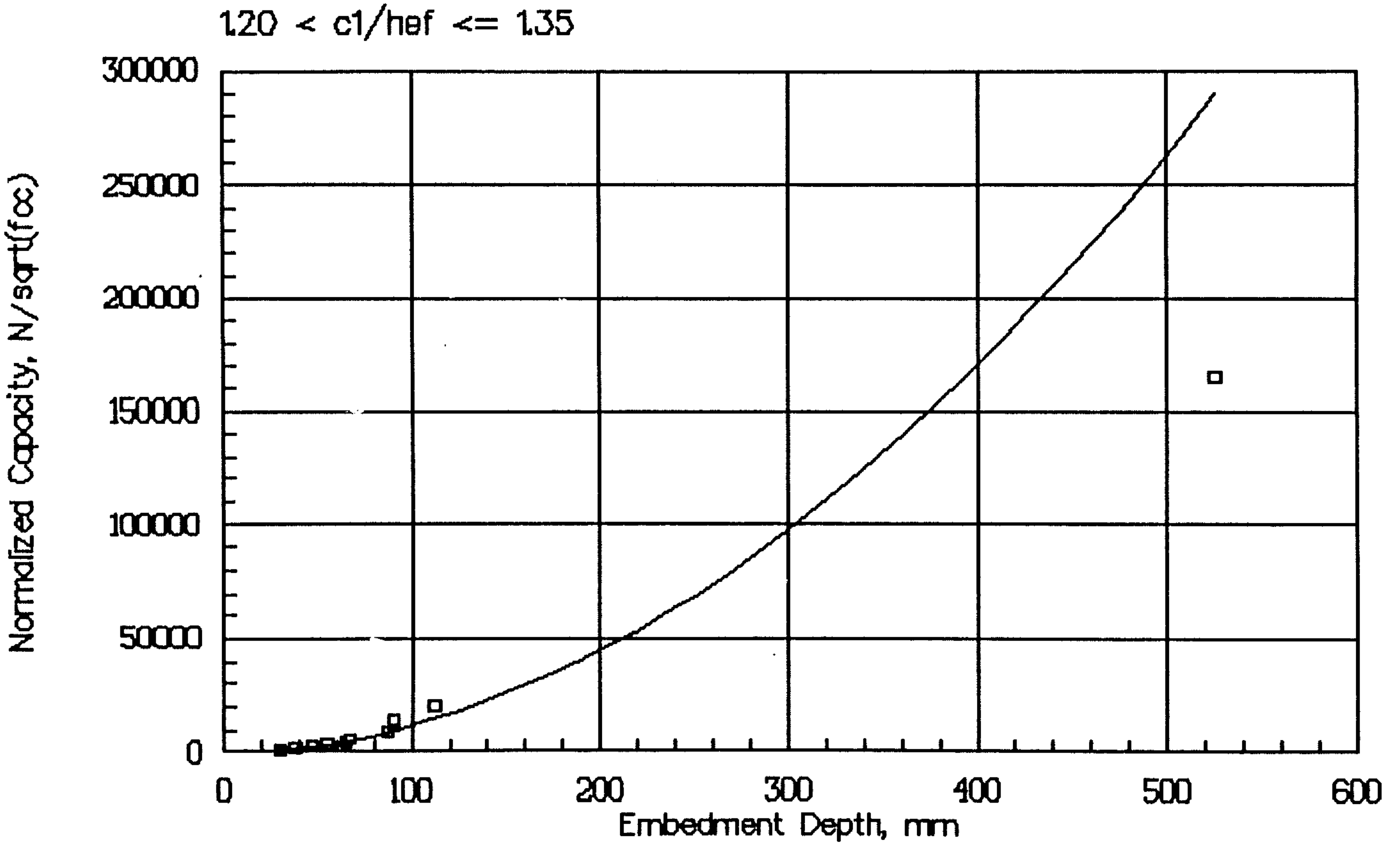

TENSILE CAPACITY vs. EMBEDMENT DEPTH
ACI 349-85 Method
Figure A-17

TENSILE CAPACITY vs. EMBEDMENT DEPTH
Variable–Angle Cone Method
Figure A–18

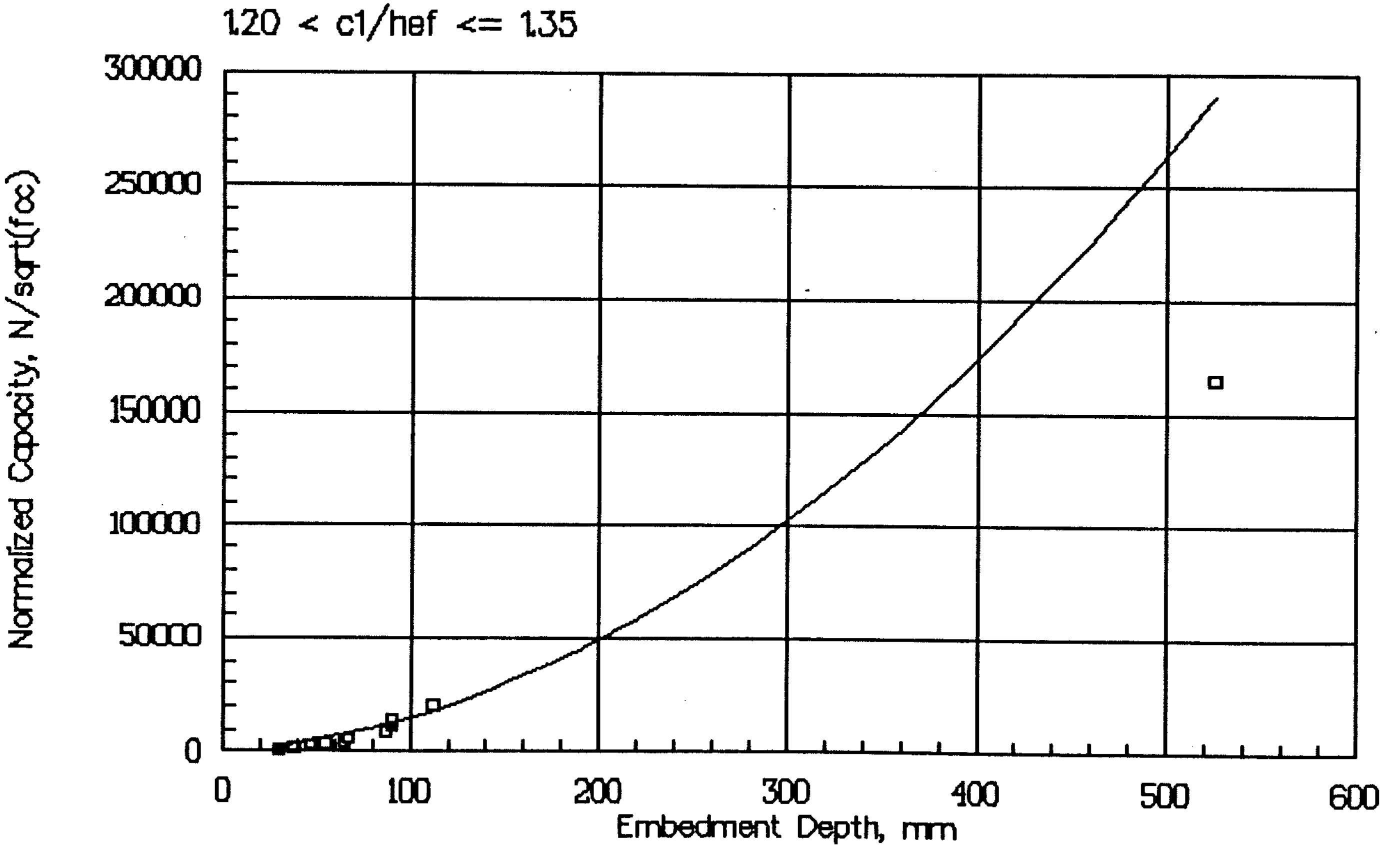

TENSILE CAPACITY vs. EMBEDMENT DEPTH
Concrete Capacity Method
Figure A–19

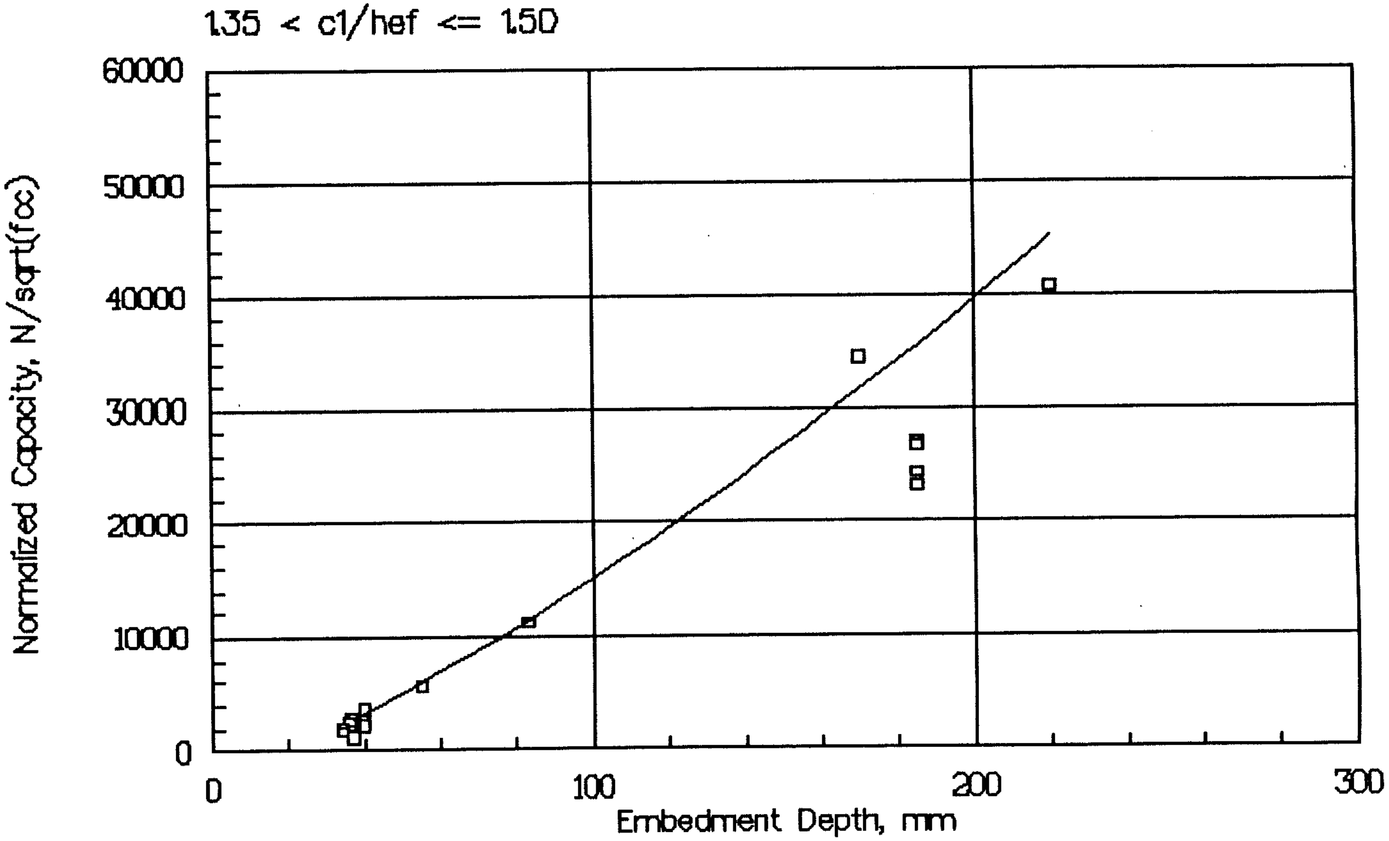

TENSILE CAPACITY vs. EMBEDMENT DEPTH
ACI 349–85 Method
Figure A–20

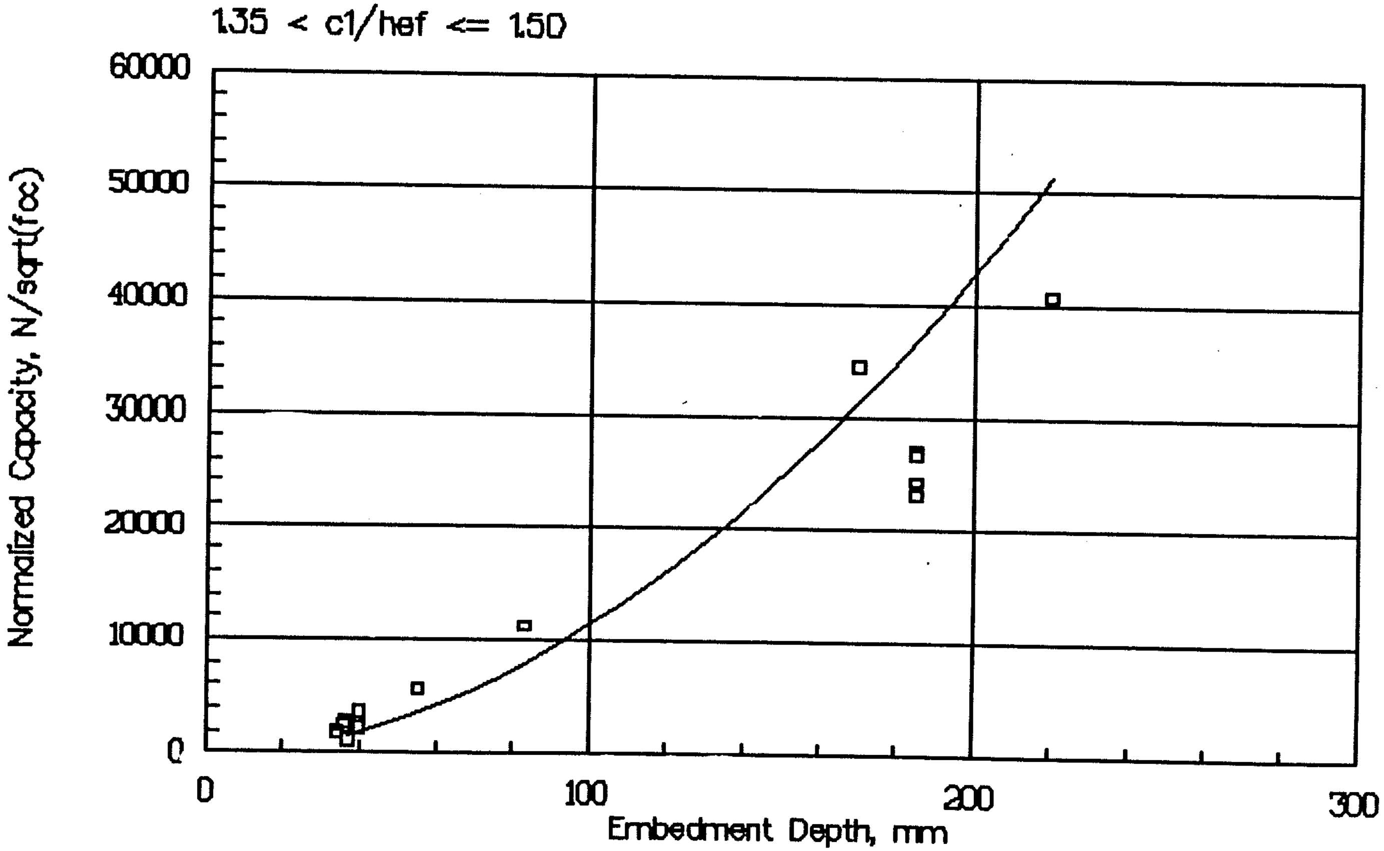

TENSILE CAPACITY vs. EMBEDMENT DEPTH
Variable-Angle Cone Method
Figure A-21

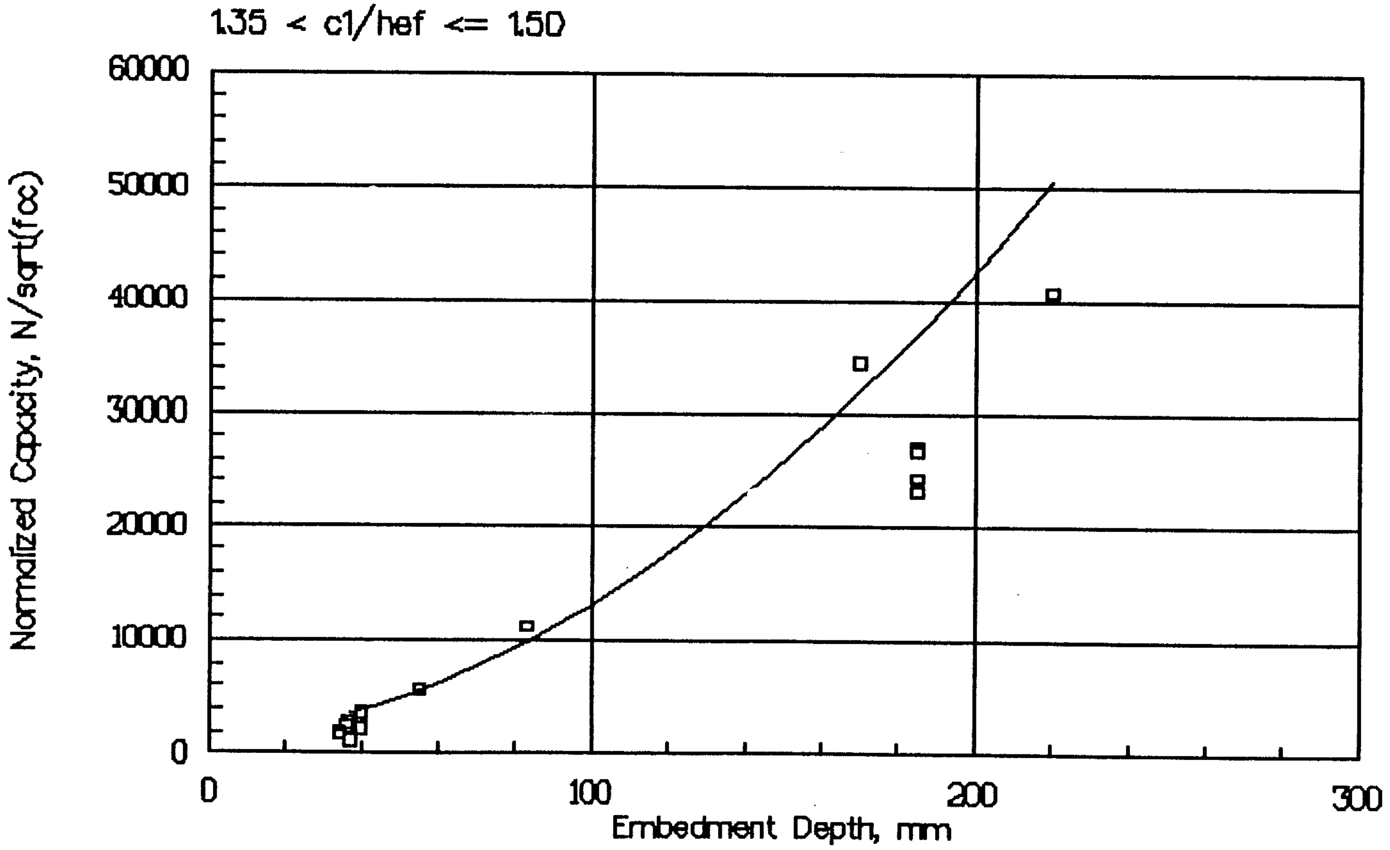

APPENDIX B: GRAPHICAL COMPARISON OF EXISTING METHODS FOR MULTIPLE CLOSELY SPACED ANCHORS FAR FROM A FREE EDGE (SI UNITS)

TENSILE CAPACITY vs EMBEDMENT DEPTH
Concrete Capacity Method
Figure B–1

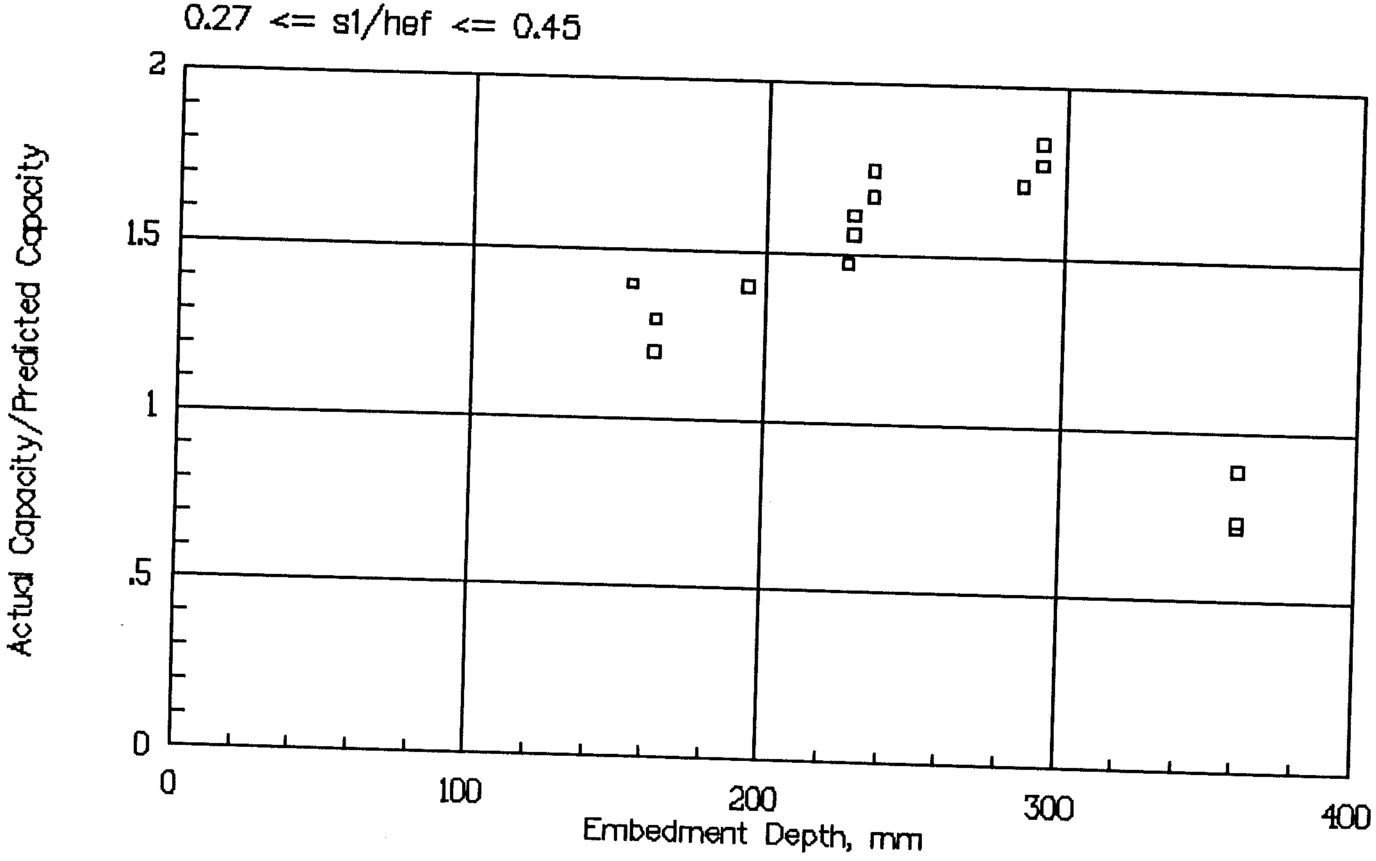

TENSILE CAPACITY vs EMBEDMENT DEPTH
ACI 349-85 Method
Figure B-2

0.27 <= s1/hef <= 0.45

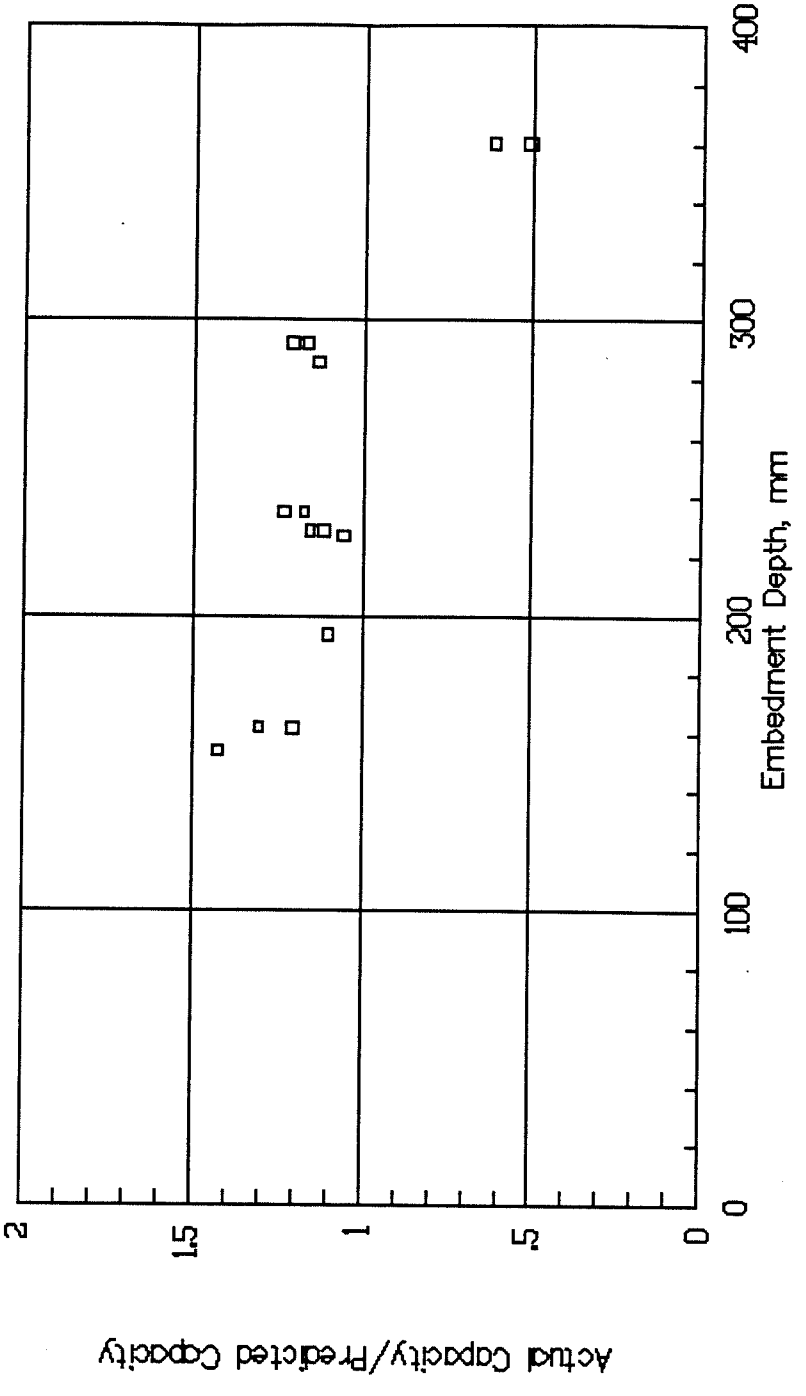

TENSILE CAPACITY vs EMBEDMENT DEPTH
Variable-Angle Cone Method
Figure B-3

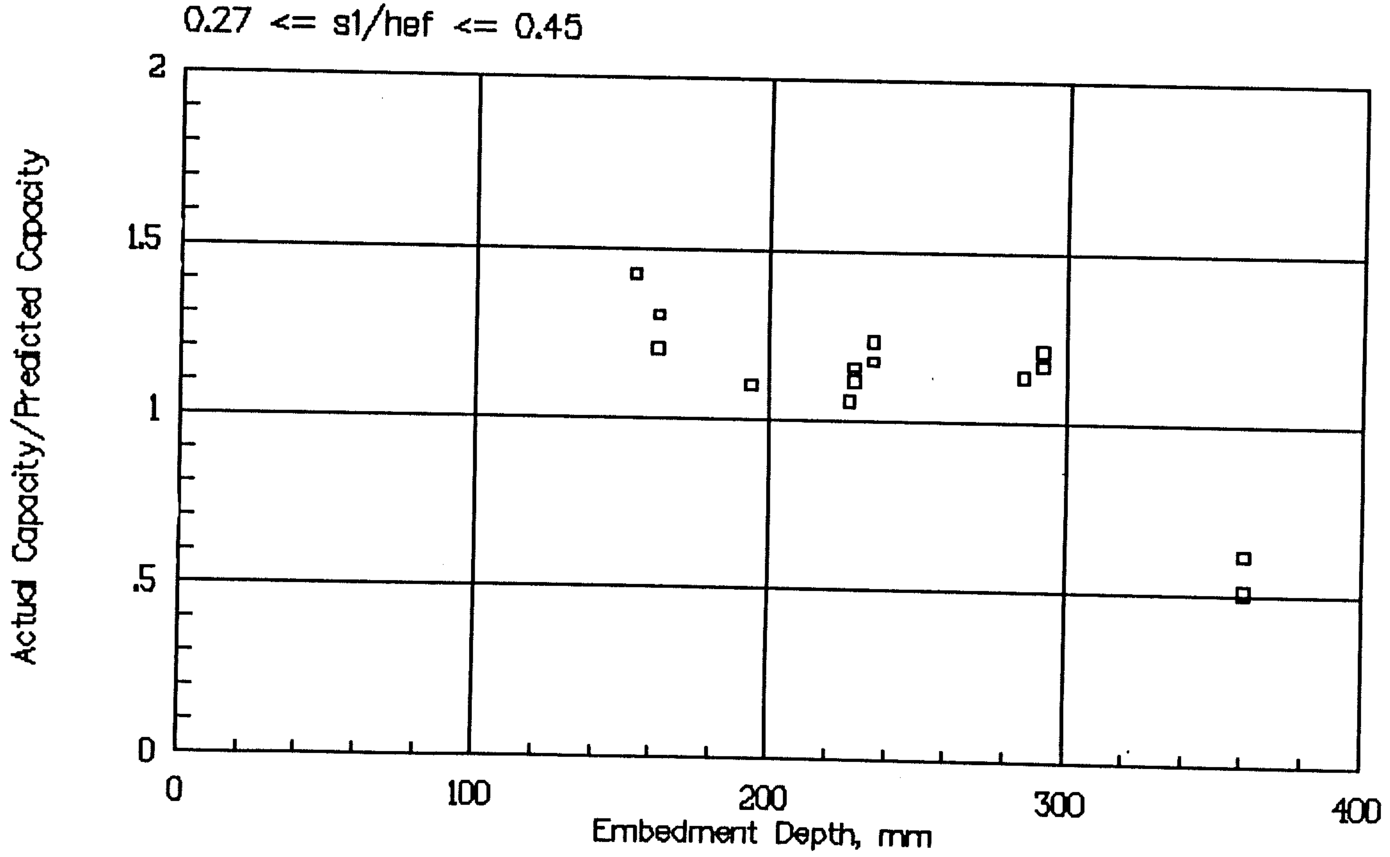

TENSILE CAPACITY vs EMBEDMENT DEPTH
Concrete Capacity Method
Figure B—4

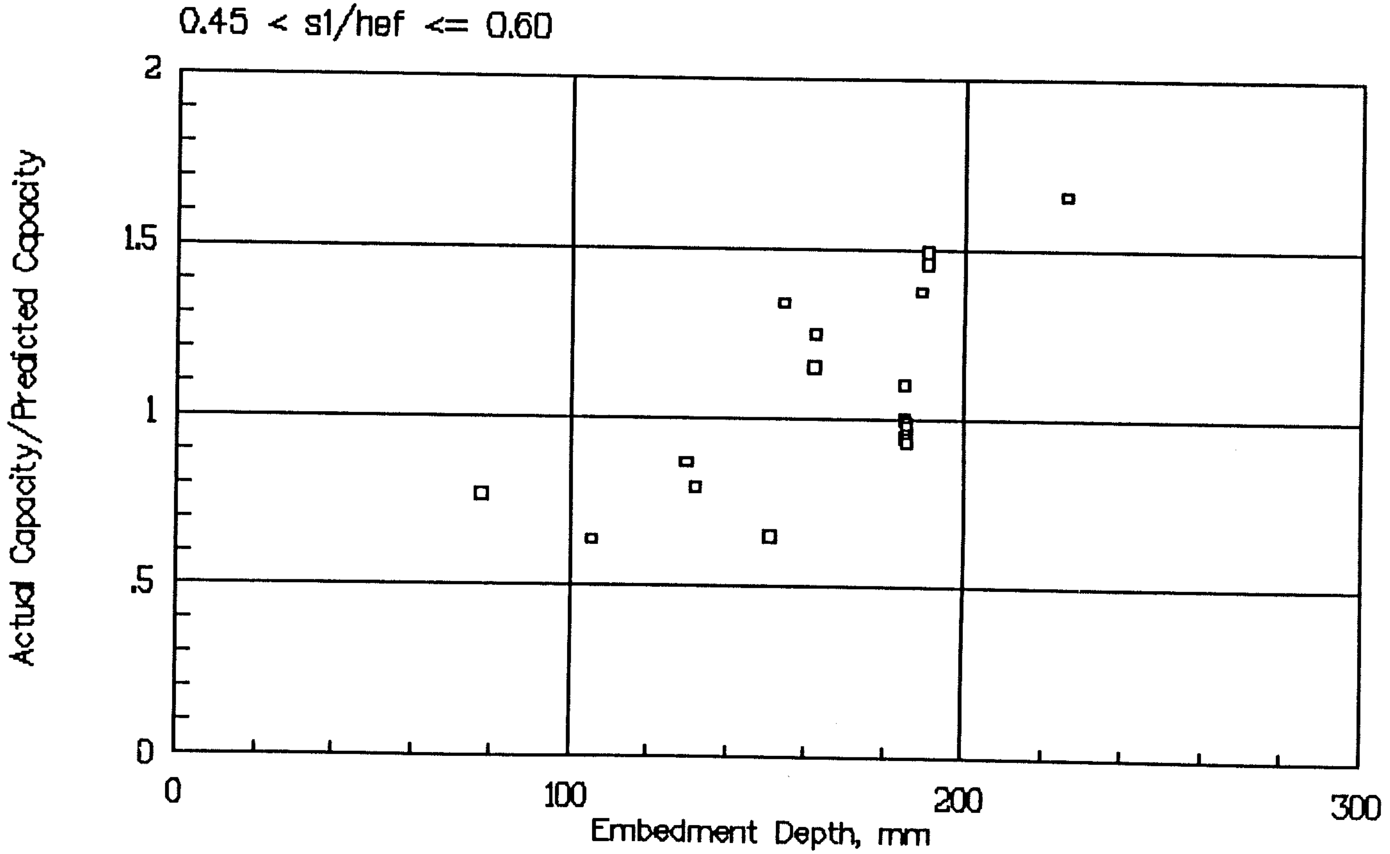

TENSILE CAPACITY vs EMBEDMENT DEPTH
ACI 349–85 Method
Figure B–5

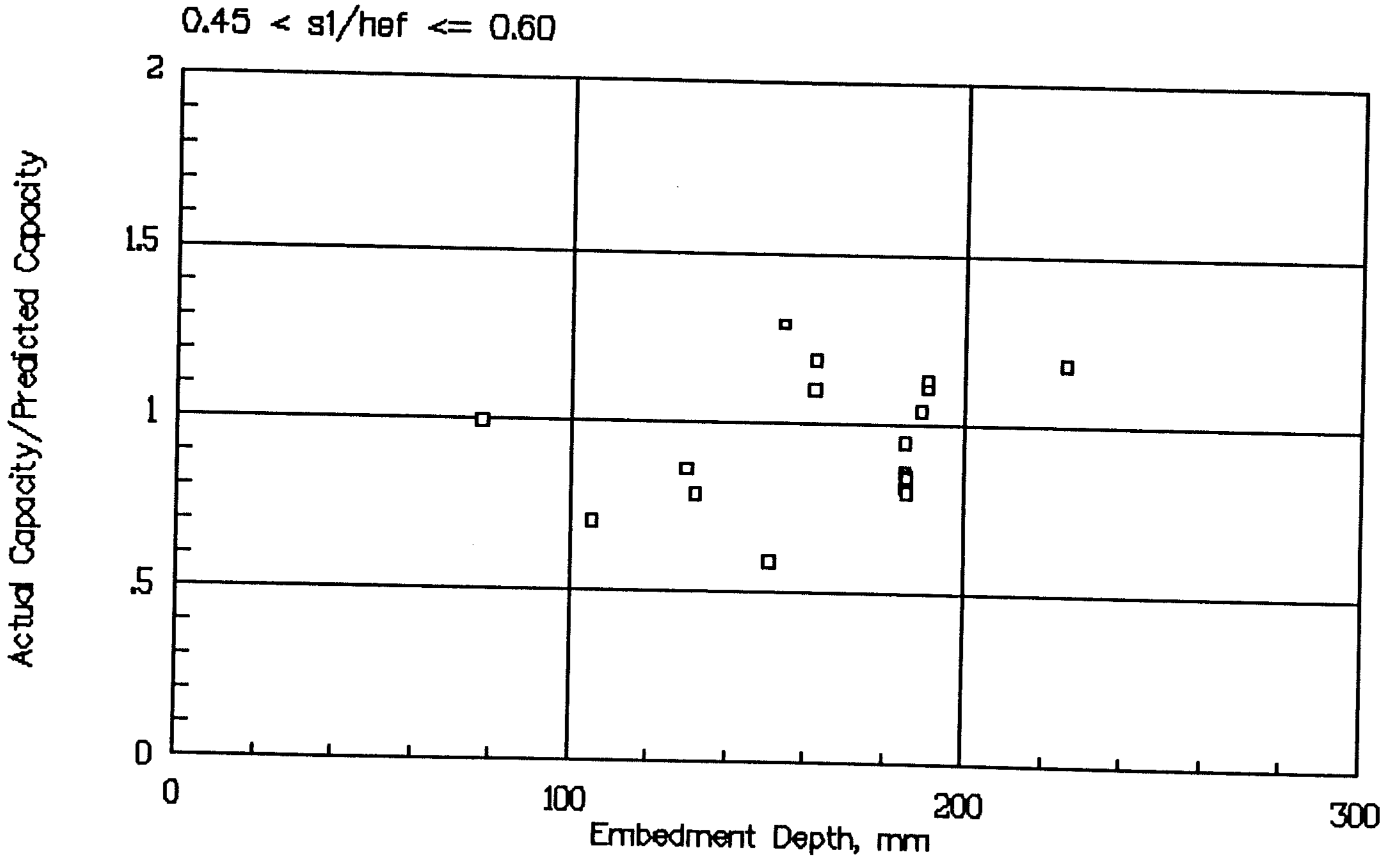

TENSILE CAPACITY vs EMBEDMENT DEPTH
Variable-Angle Cone Method
Figure B-6

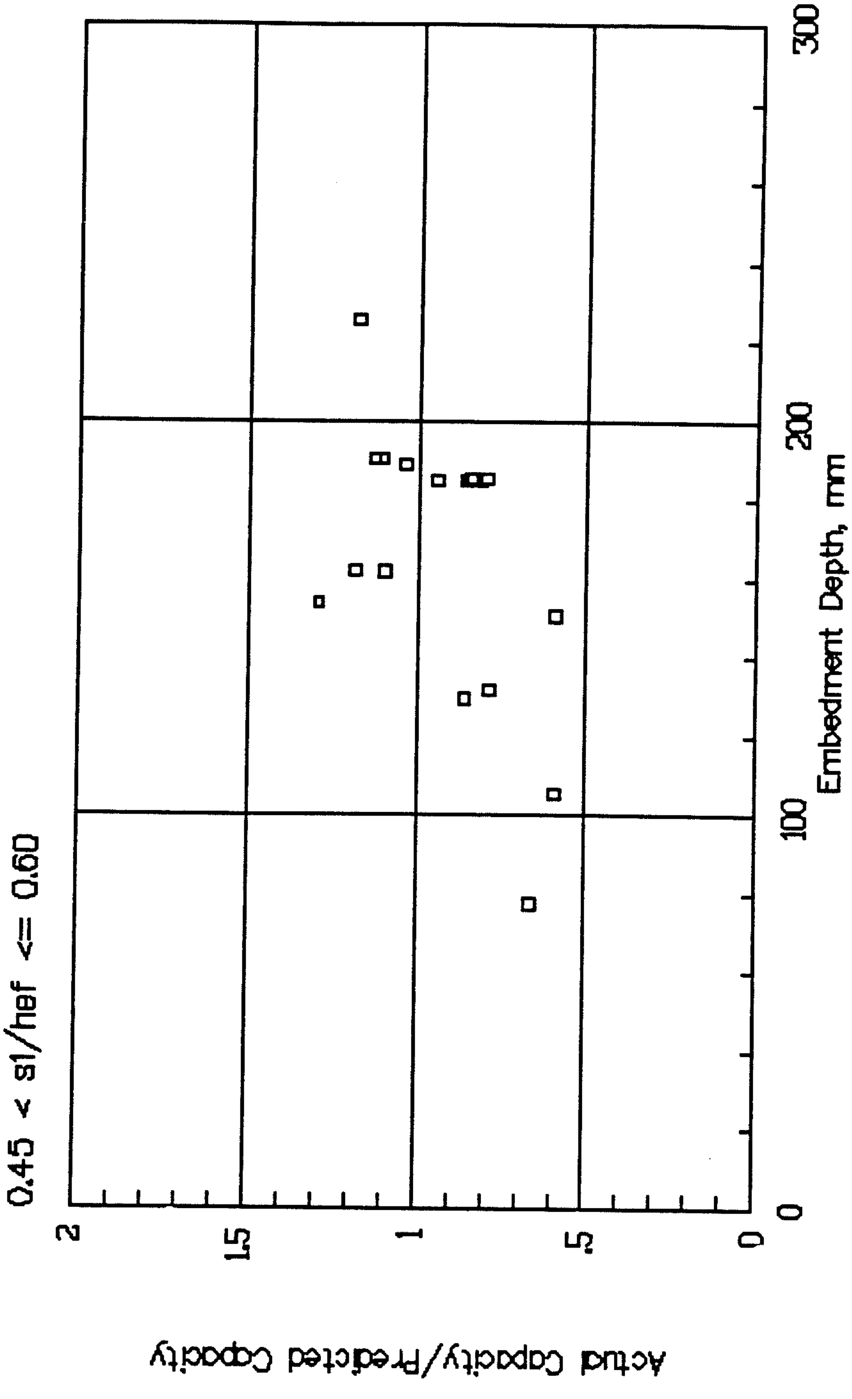

TENSILE CAPACITY vs EMBEDMENT DEPTH
Concrete Capacity Method
Figure B–7

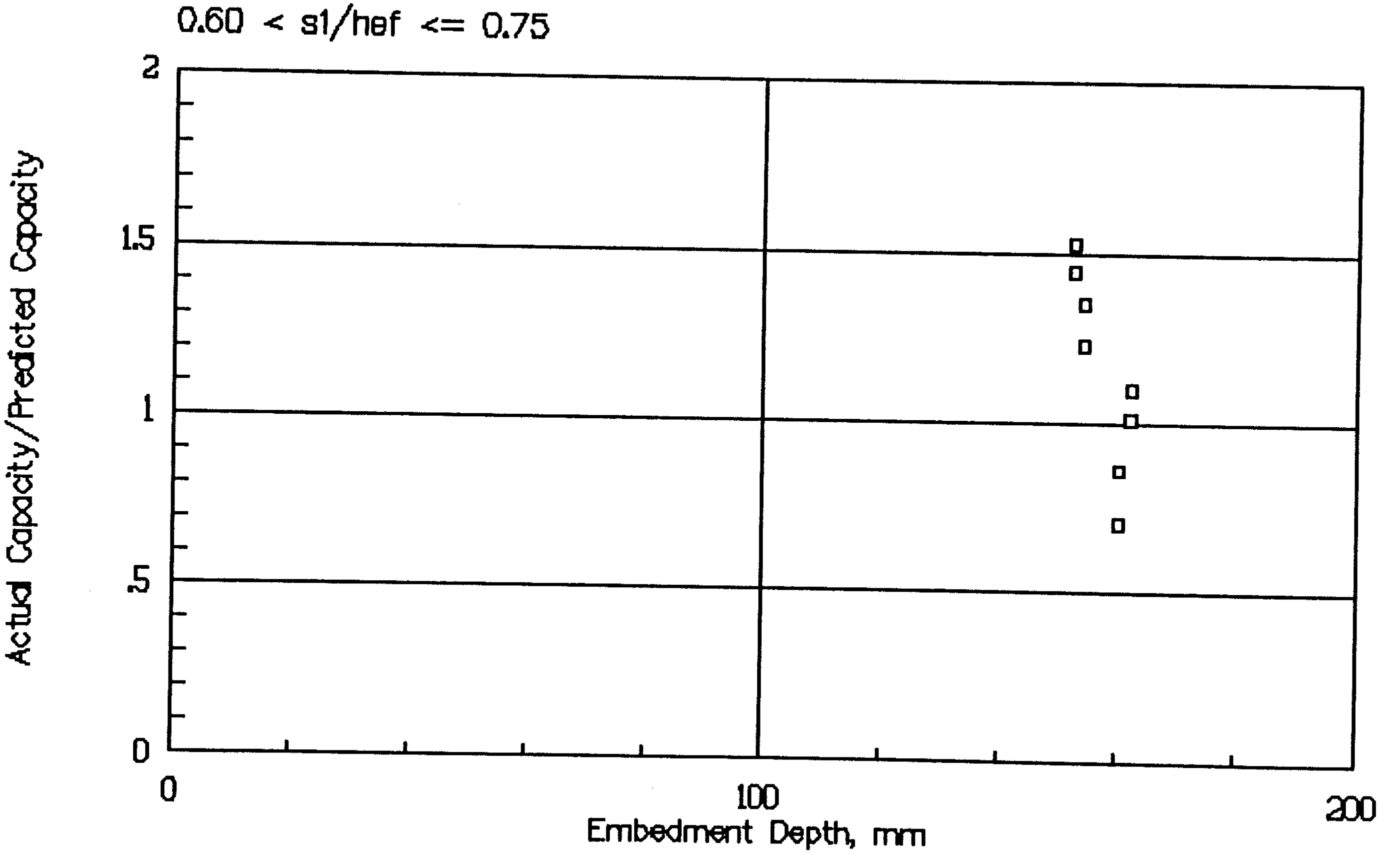

TENSILE CAPACITY vs EMBEDMENT DEPTH
ACI 349–85 Method
Figure B–8

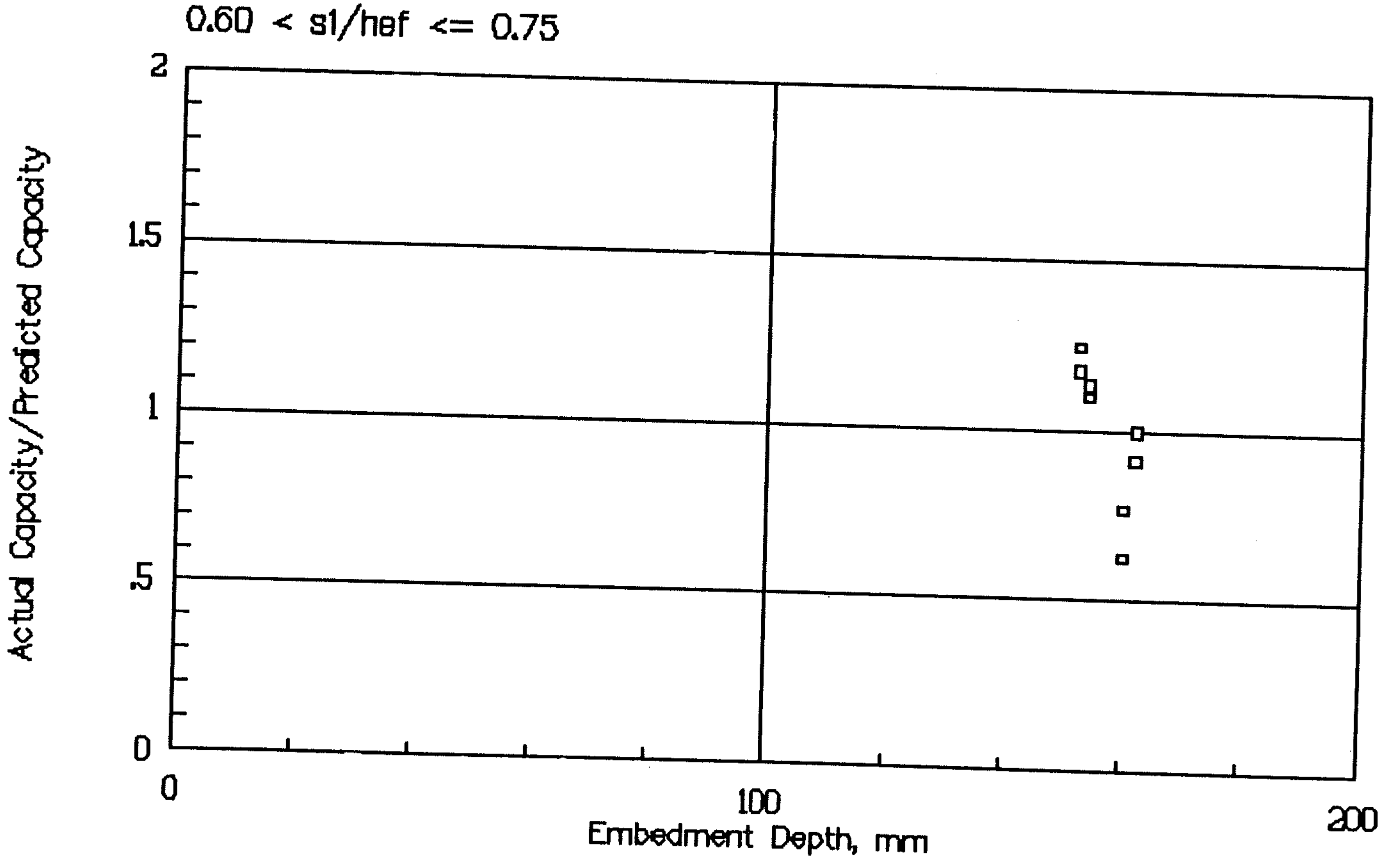

TENSILE CAPACITY vs EMBEDMENT DEPTH
Variable–Angle Cone Method
Figure B–9

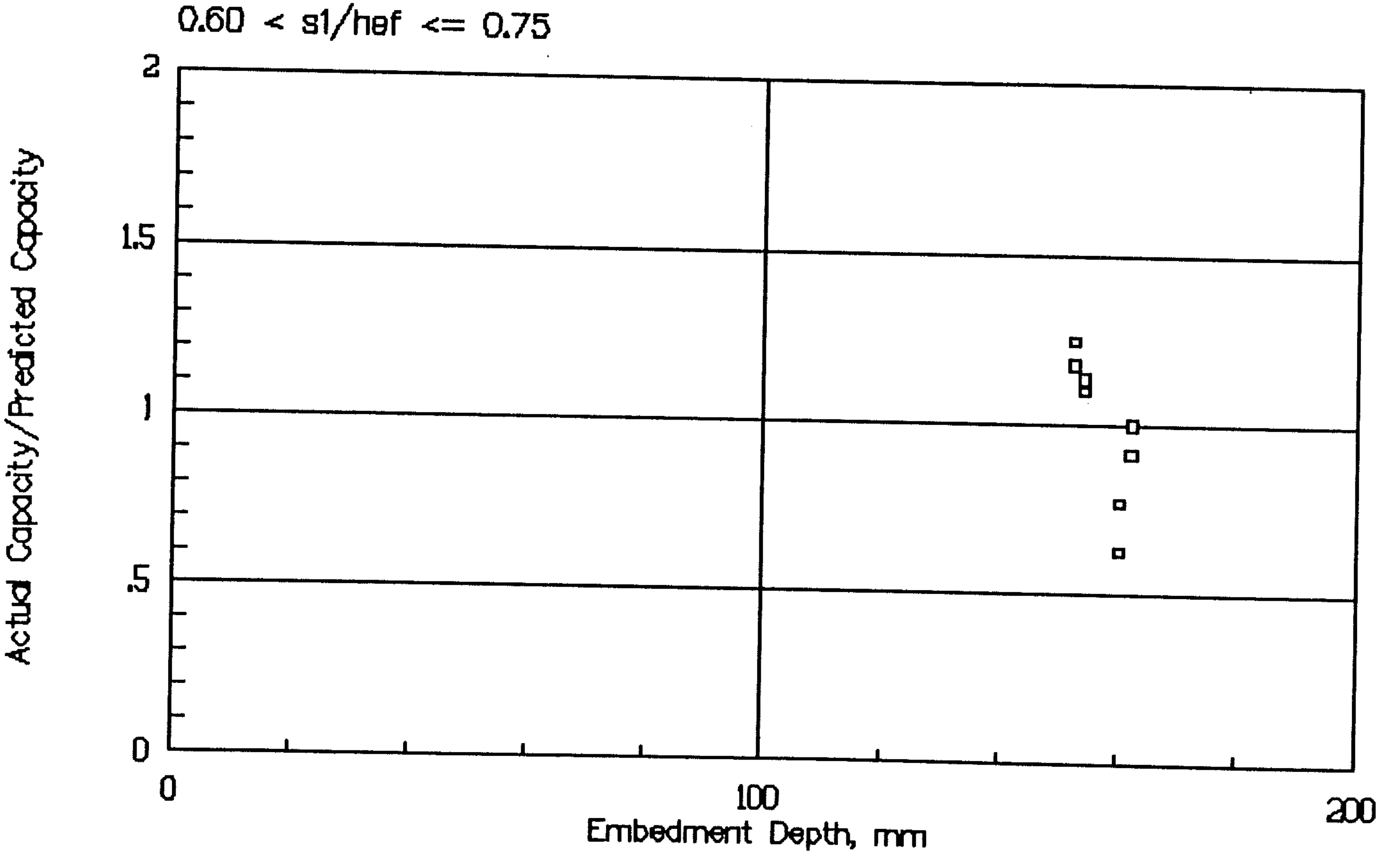

TENSILE CAPACITY vs EMBEDMENT DEPTH
Concrete Capacity Method
Figure B-10

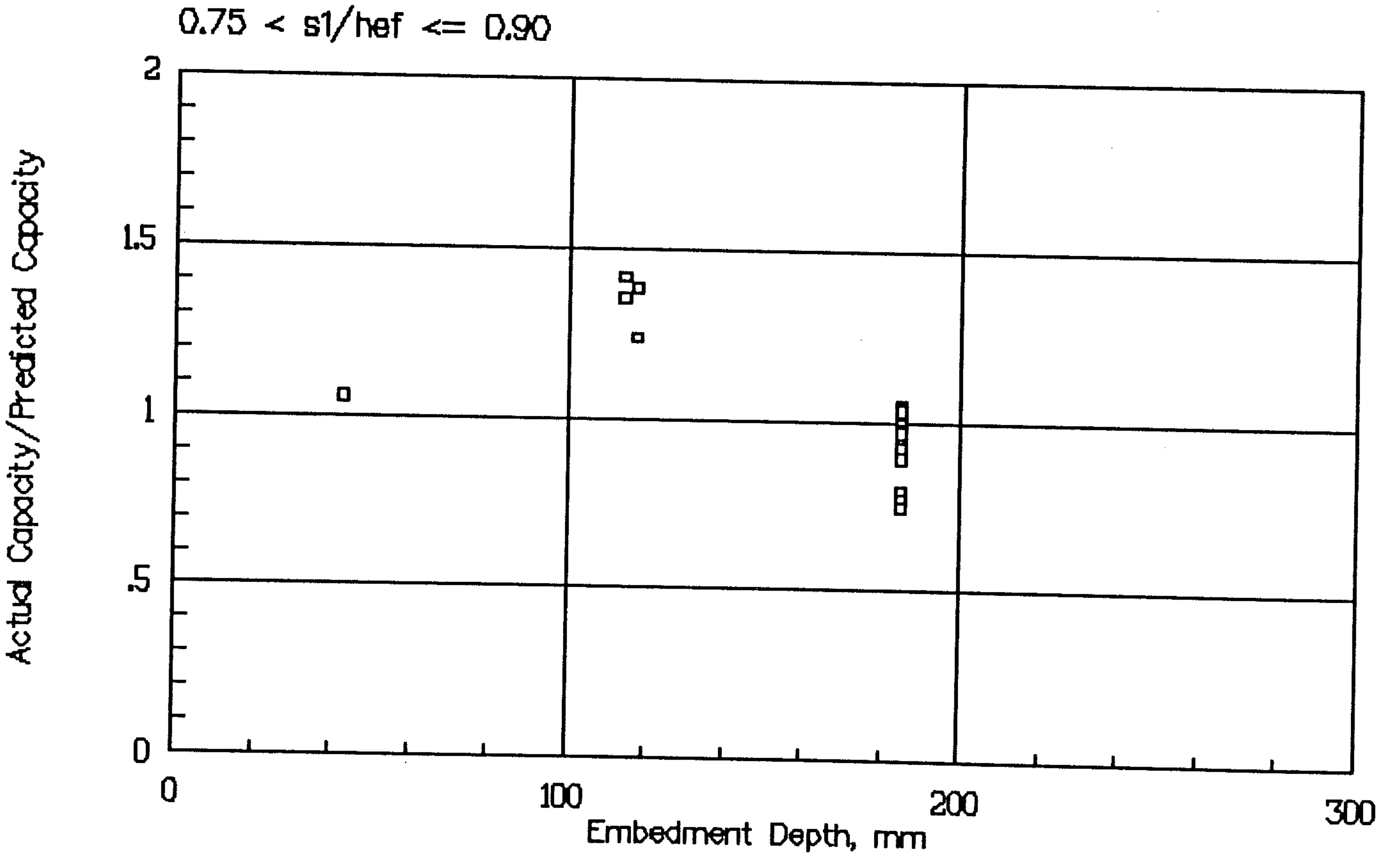

TENSILE CAPACITY vs EMBEDMENT DEPTH
ACI 349-85 Method
Figure B-11

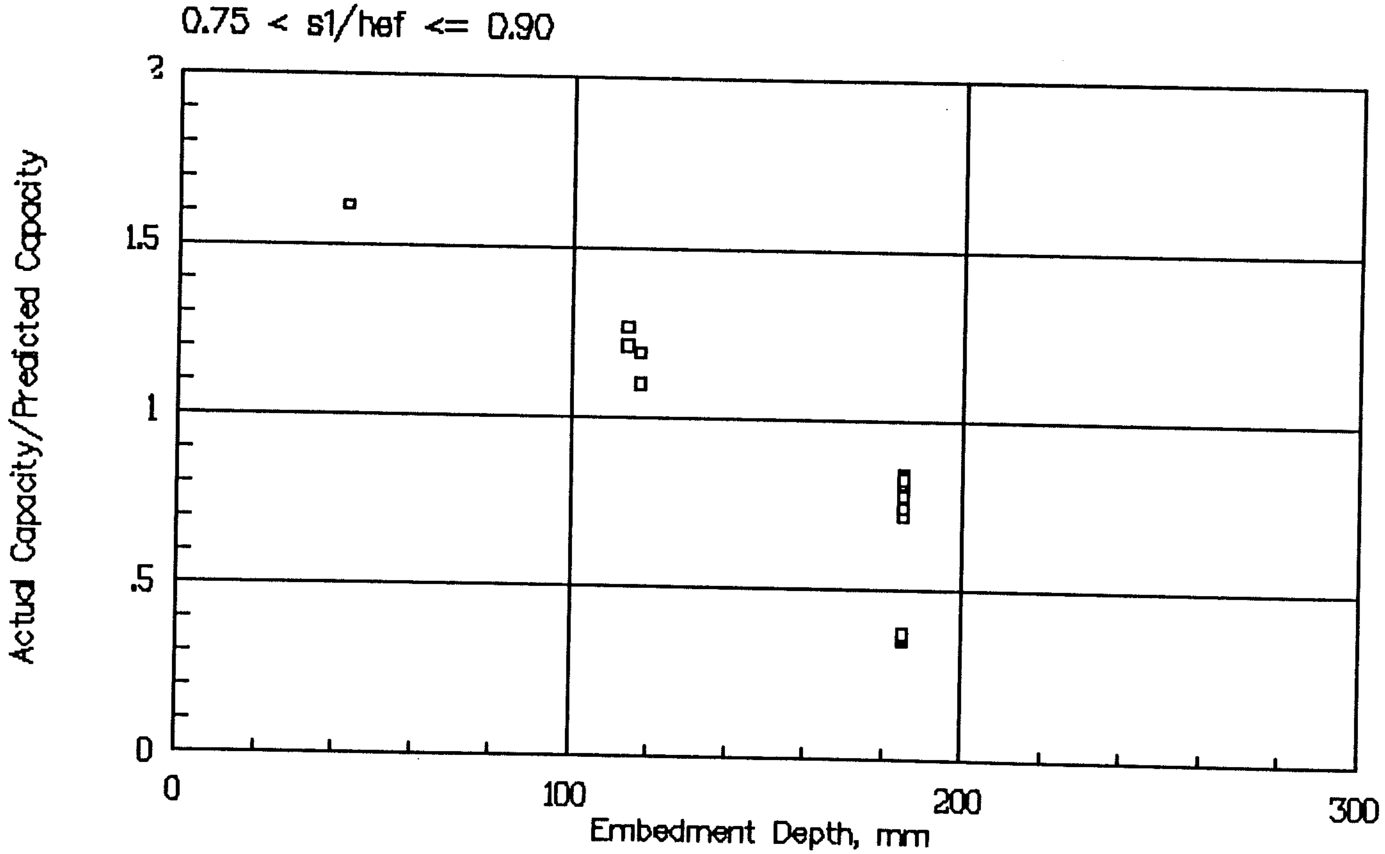

TENSILE CAPACITY vs EMBEDMENT DEPTH
Variable–Angle Cone Method
Figure B–12

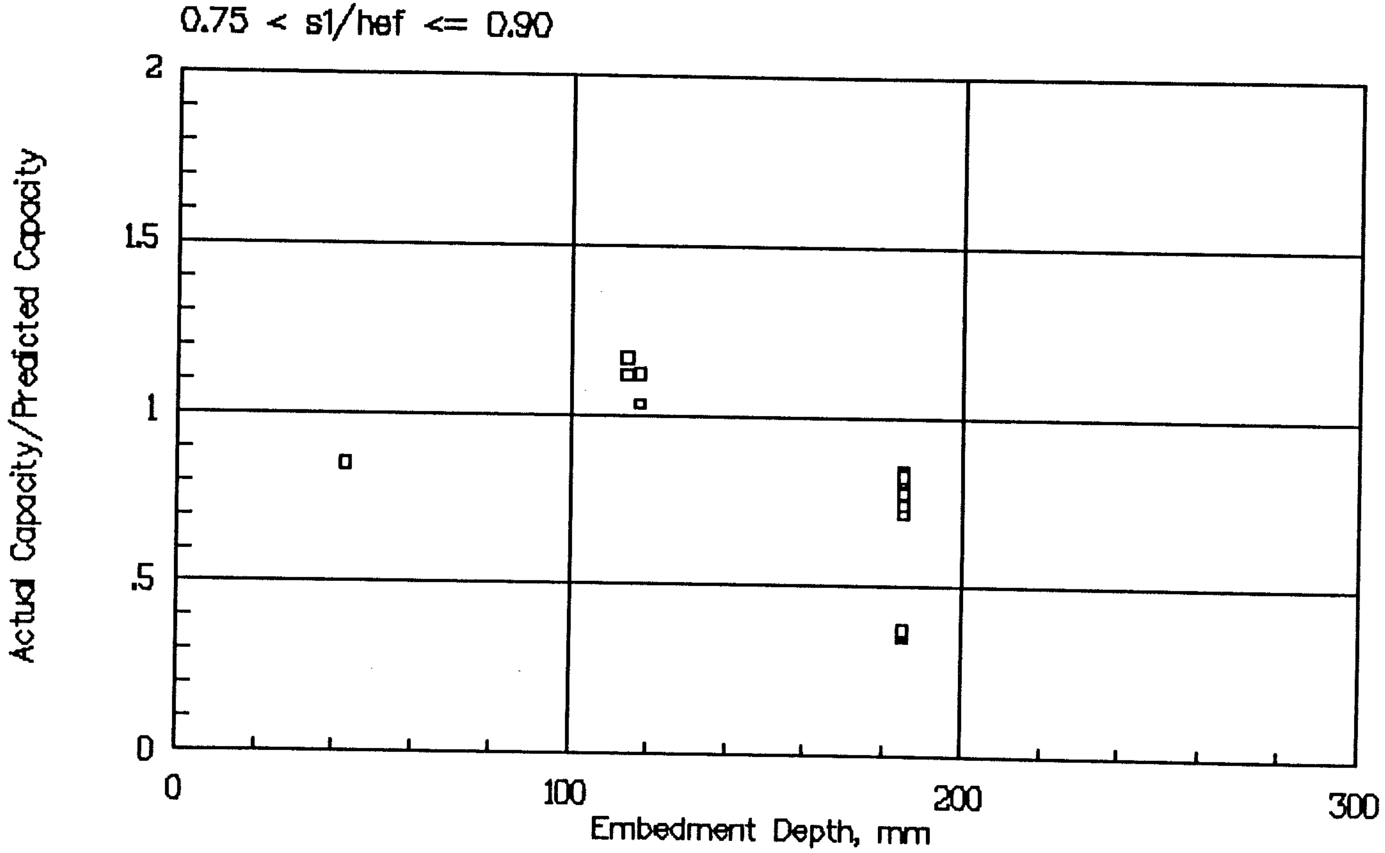

TENSILE CAPACITY vs EMBEDMENT DEPTH
Concrete Capacity Method
Figure B–13

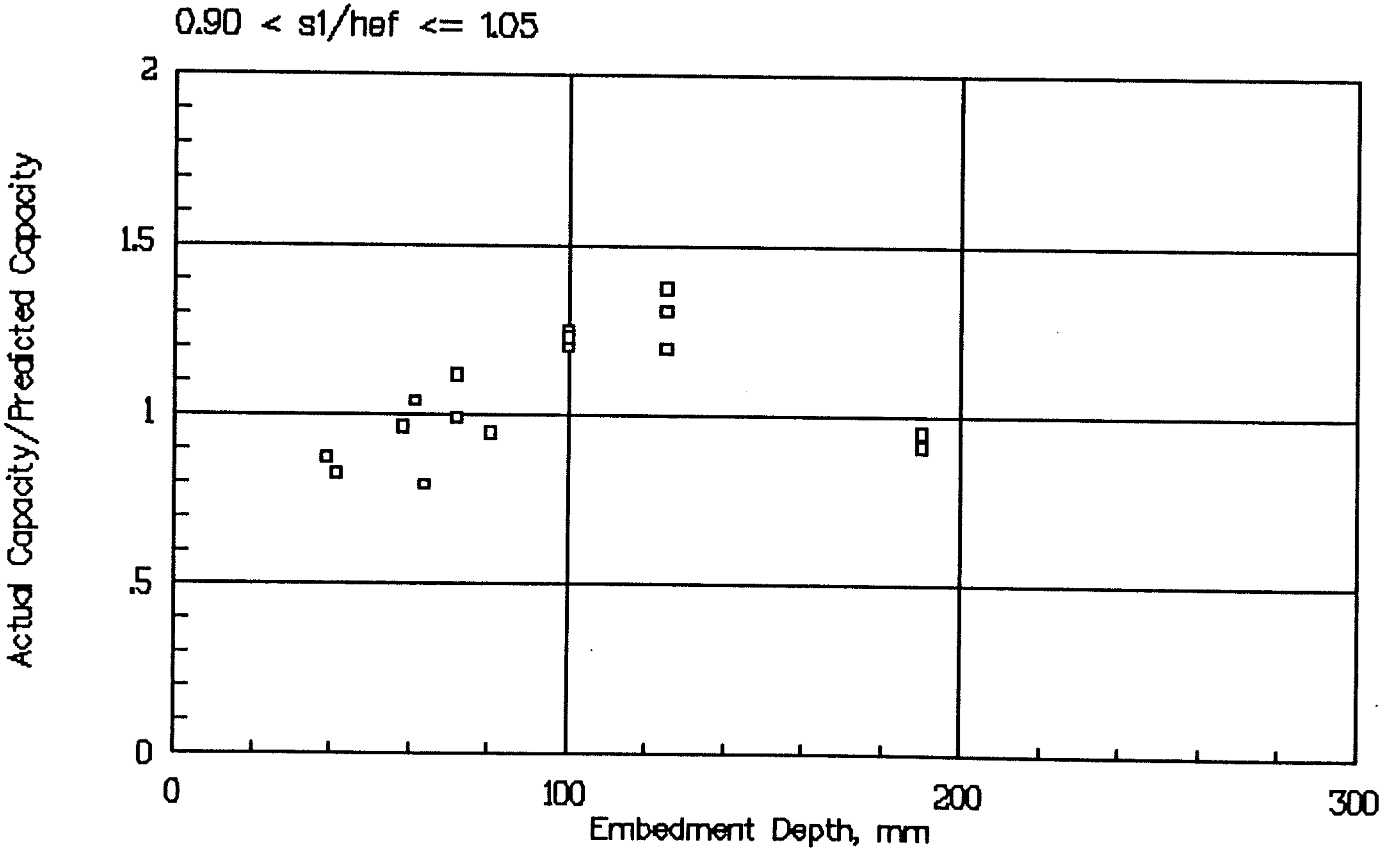

TENSILE CAPACITY vs EMBEDMENT DEPTH
ACI 349-85 Method
Figure B-14

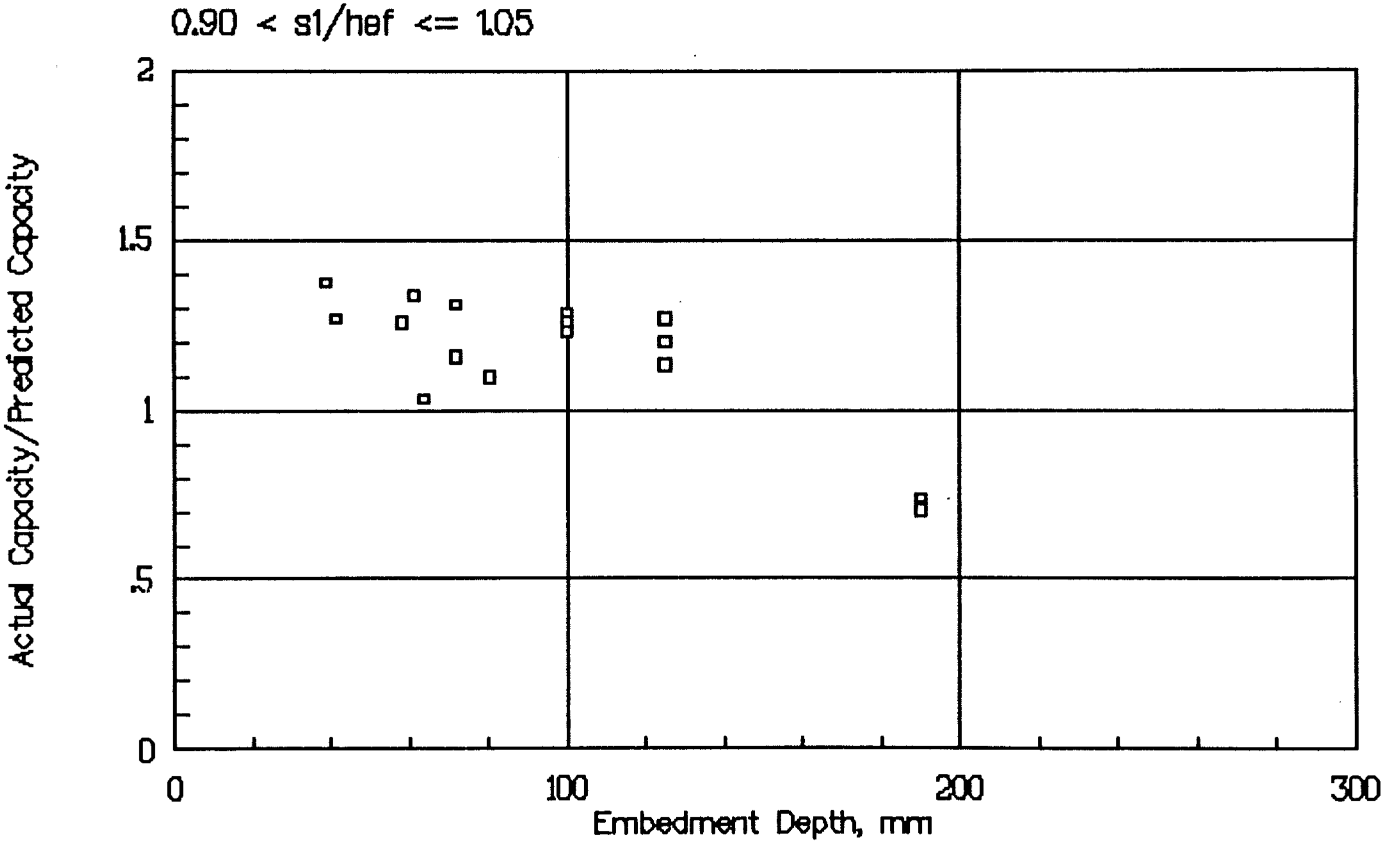

TENSILE CAPACITY vs EMBEDMENT DEPTH
Variable-Angle Cone Method
Figure B-15

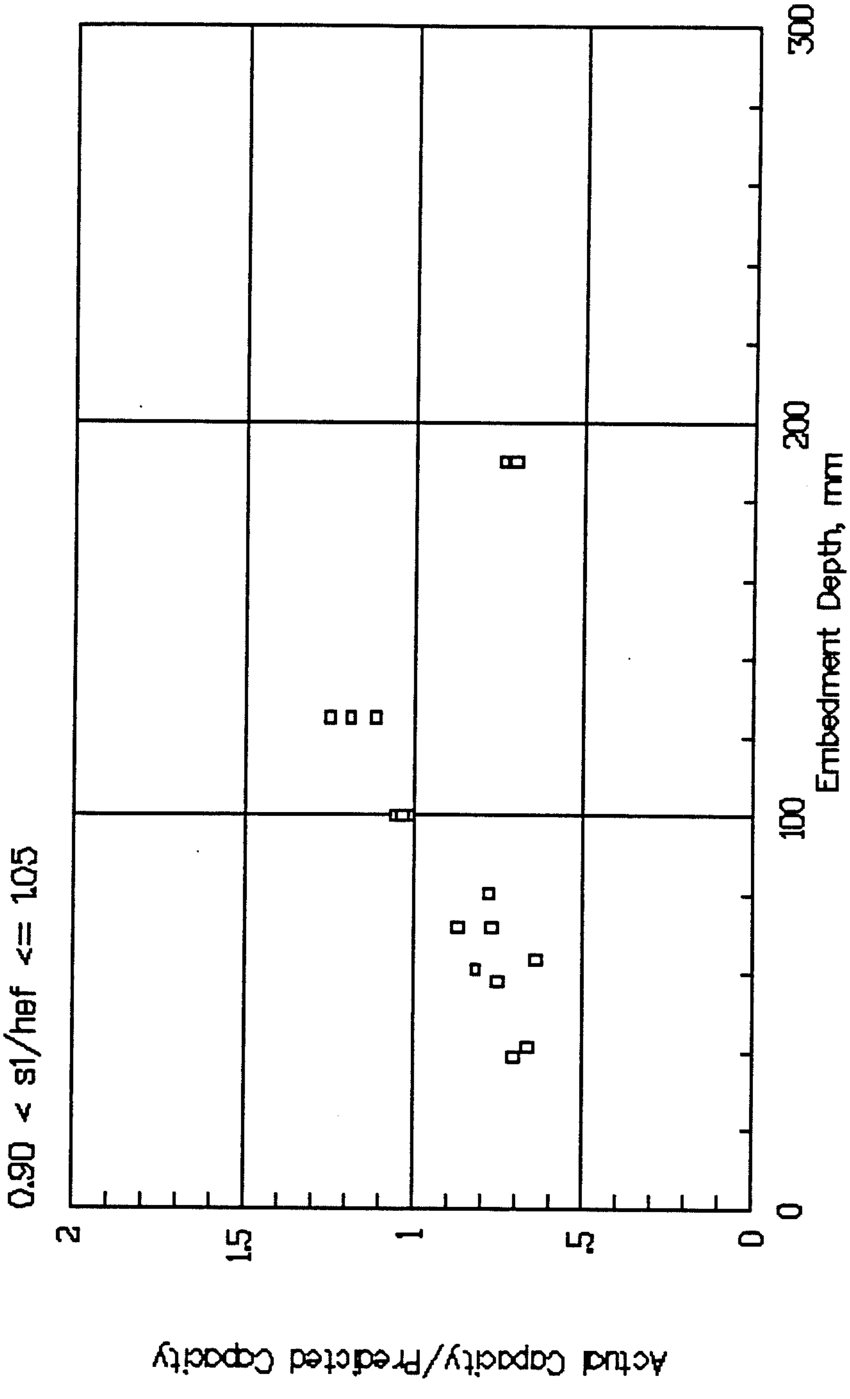

TENSILE CAPACITY vs EMBEDMENT DEPTH
Concrete Capacity Method
Figure B-16

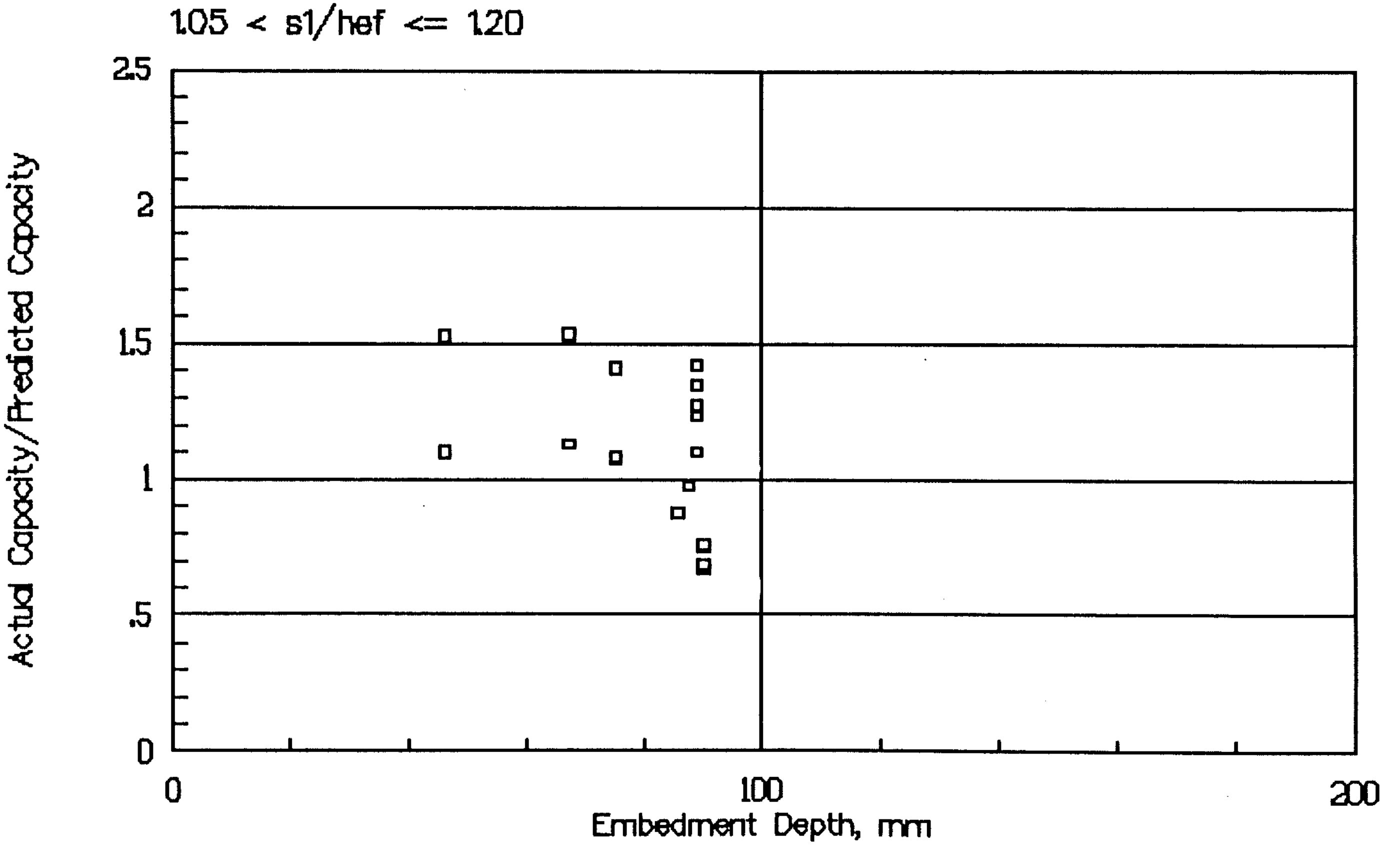

TENSILE CAPACITY vs EMBEDMENT DEPTH
ACI 349–85 Method
Figure B–17

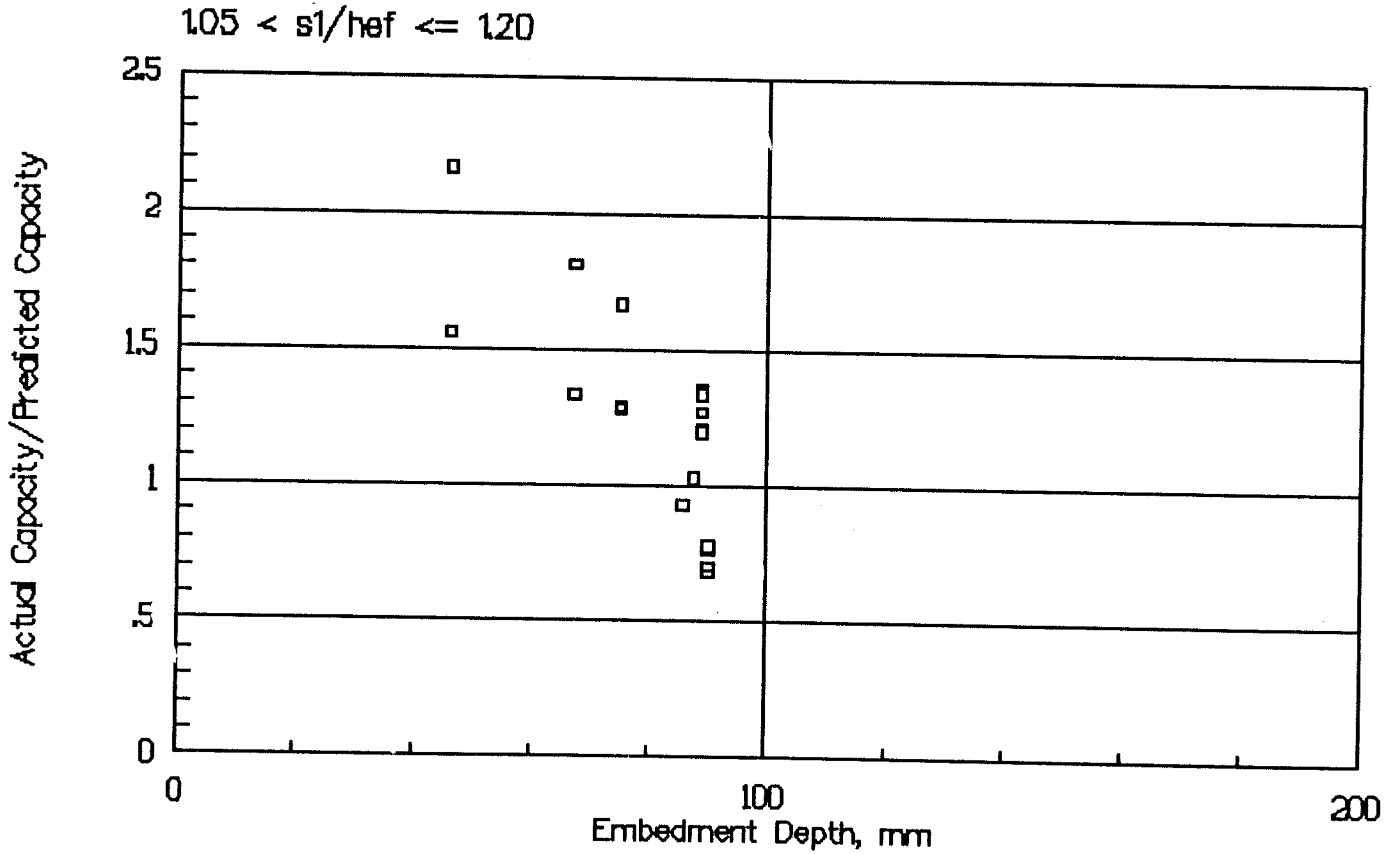

TENSILE CAPACITY vs EMBEDMENT DEPTH
Variable–Angle Cone Method
Figure B–18

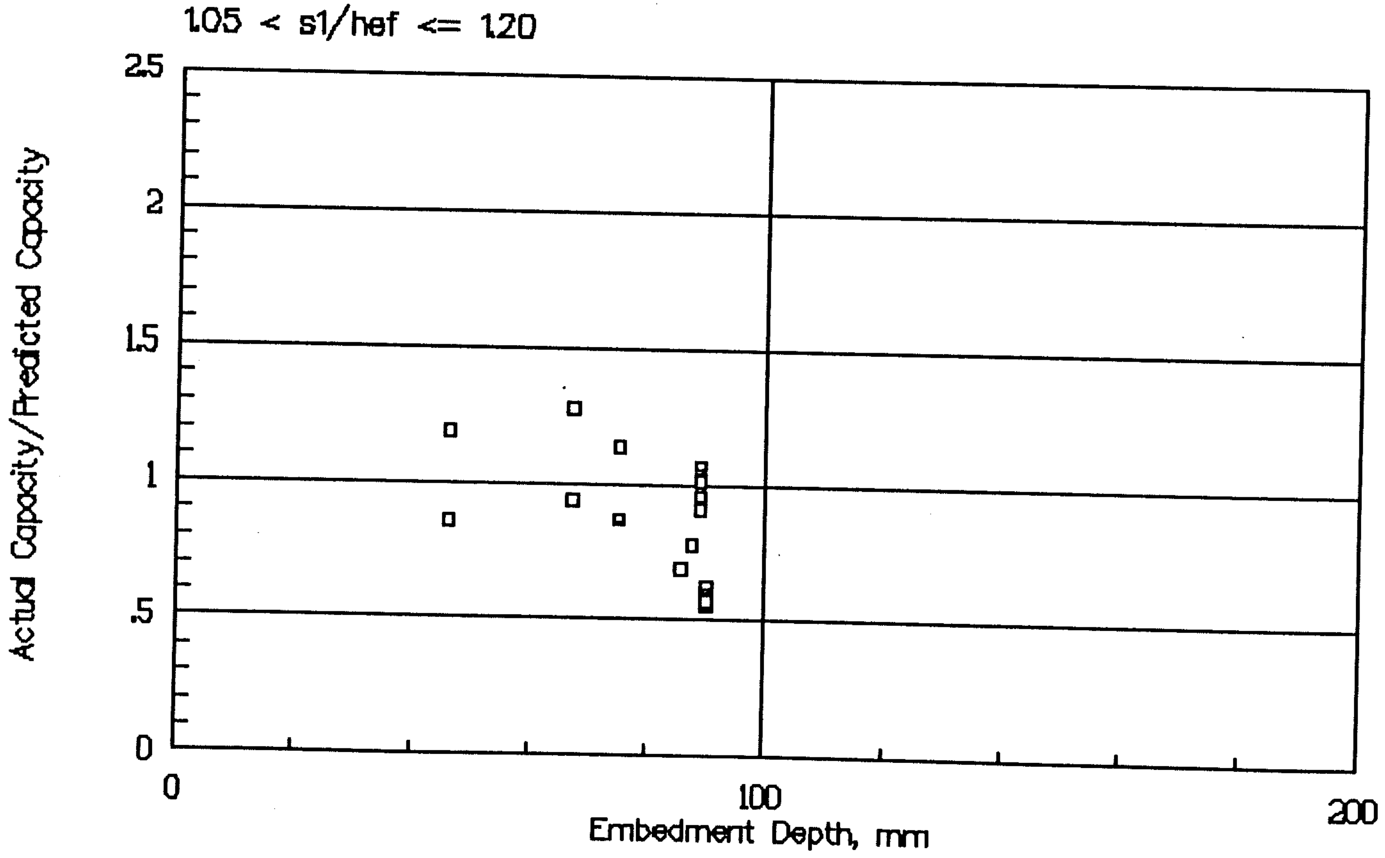

TENSILE CAPACITY vs EMBEDMENT DEPTH
Concrete Capacity Method
Figure B–19

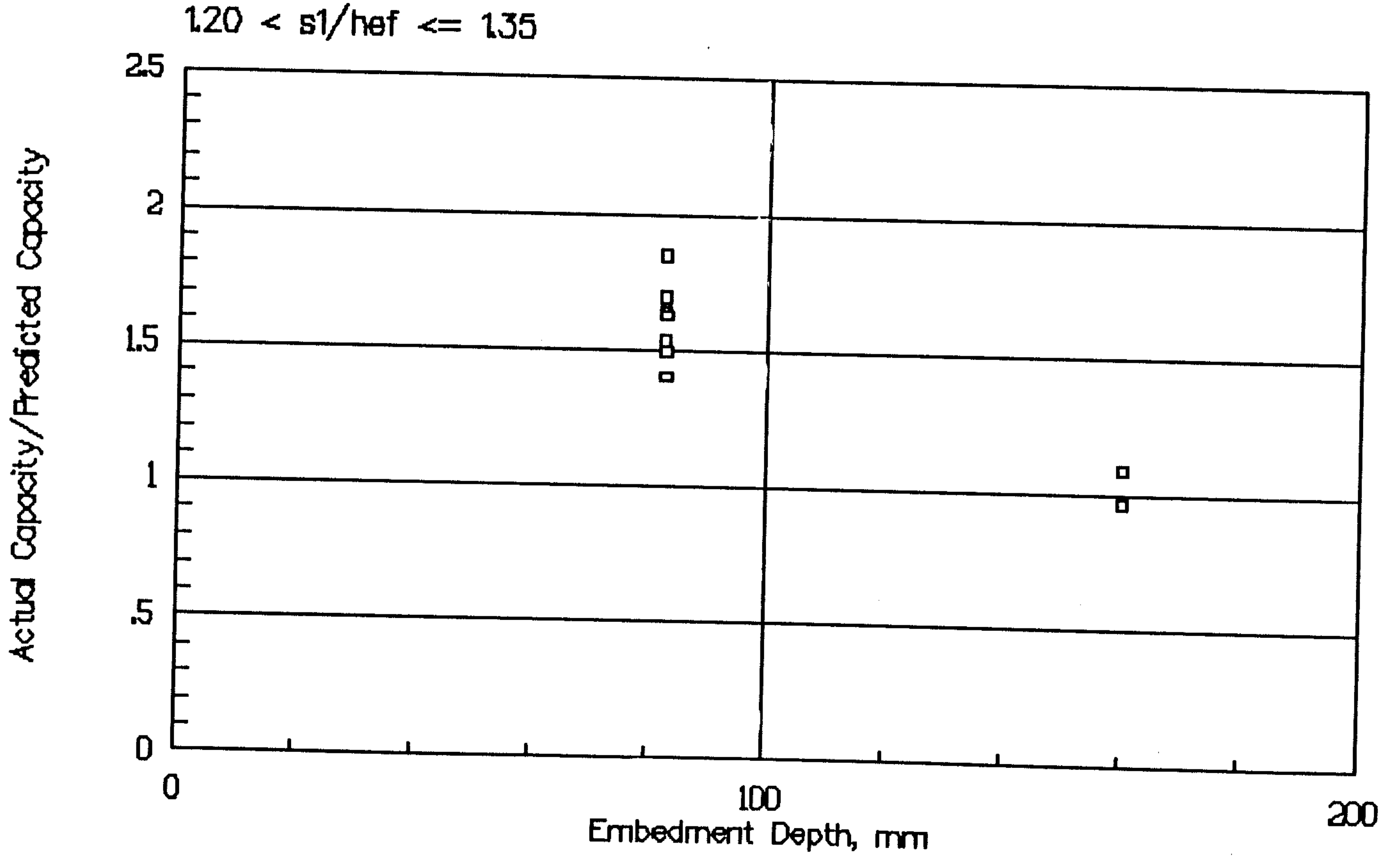

TENSILE CAPACITY vs EMBEDMENT DEPTH
ACI 349–85 Method
Figure B–20

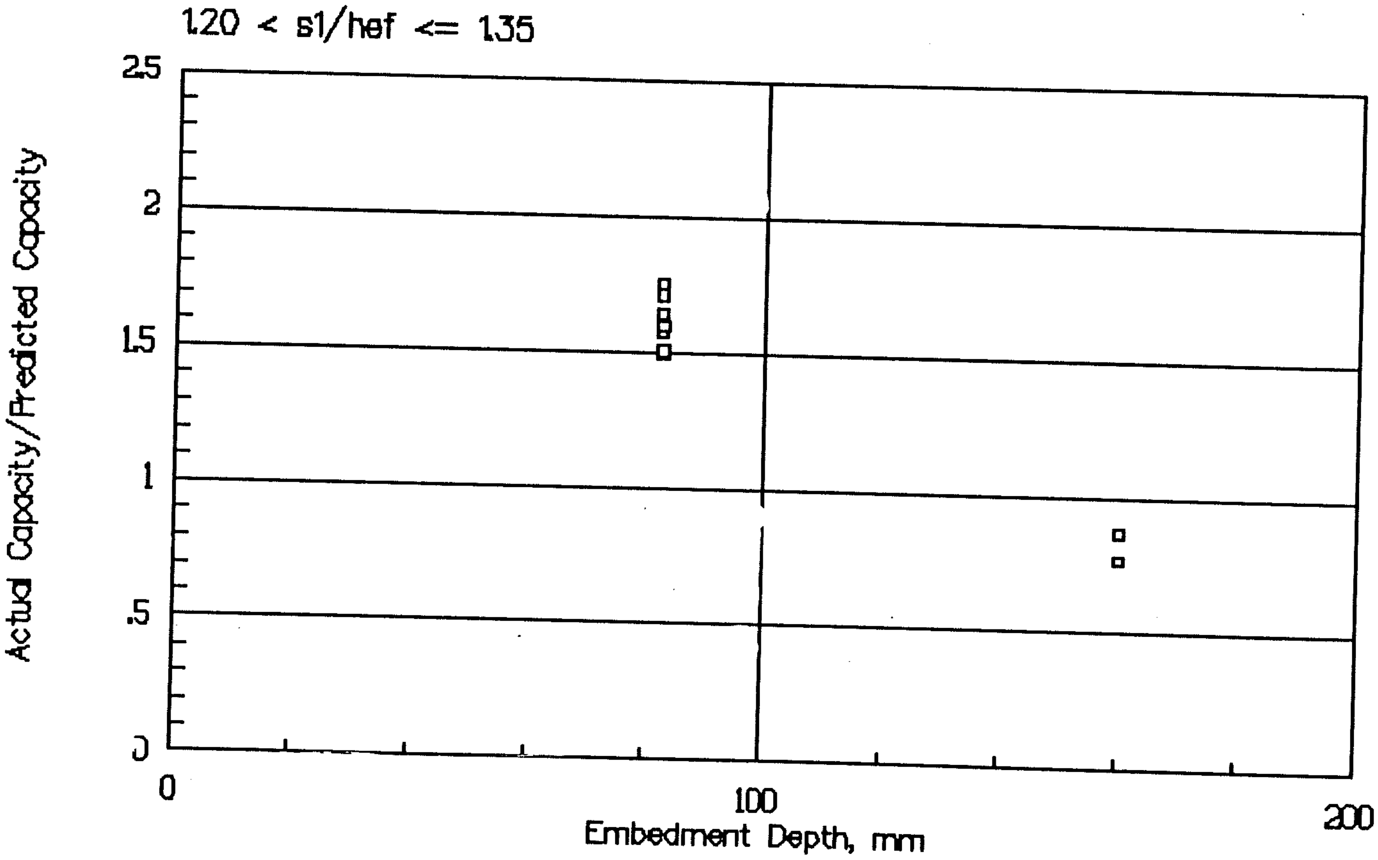

TENSILE CAPACITY vs EMBEDMENT DEPTH
Variable-Angle Cone Method
Figure B-21

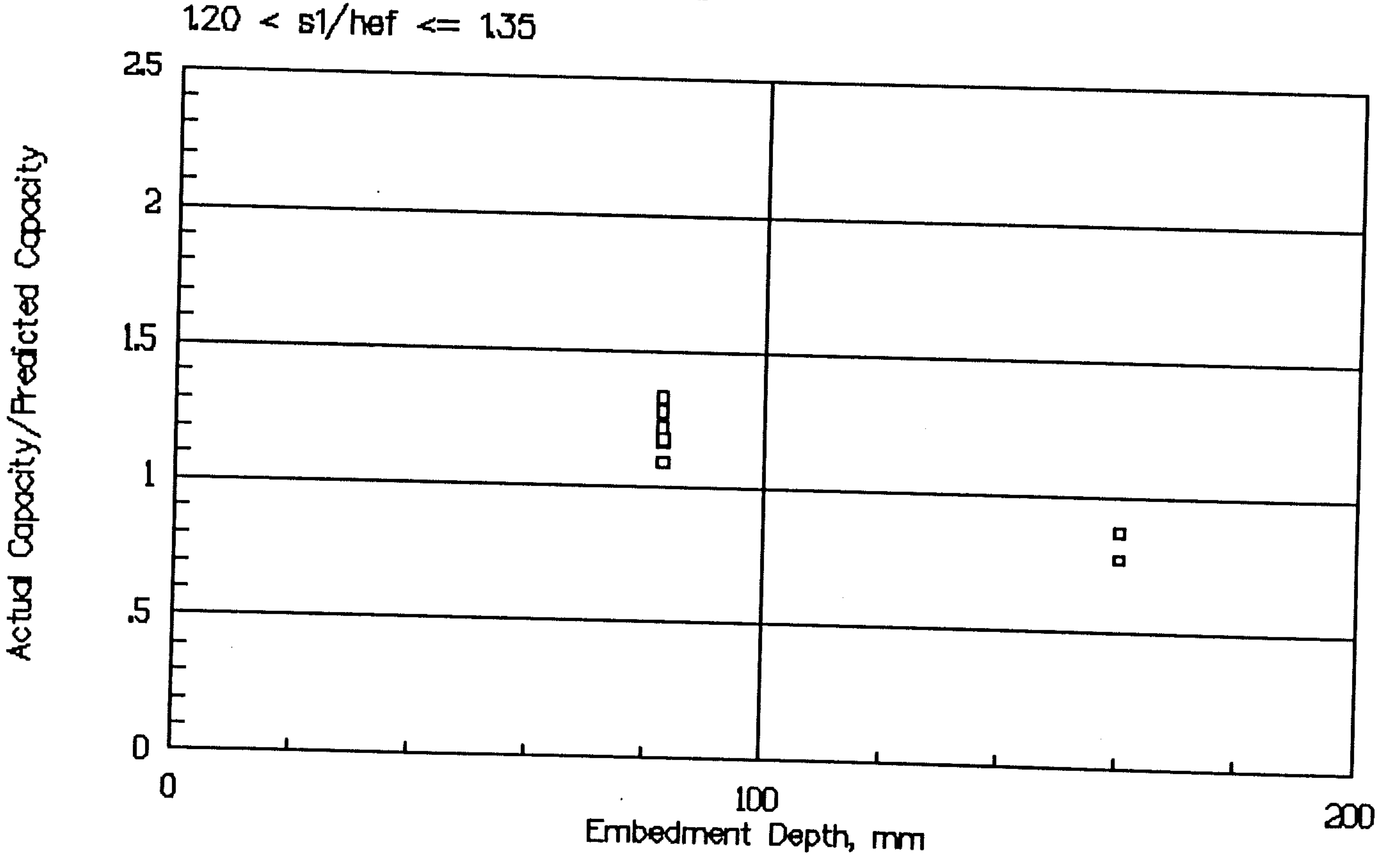

TENSILE CAPACITY vs EMBEDMENT DEPTH
Concrete Capacity Method
Figure B-22

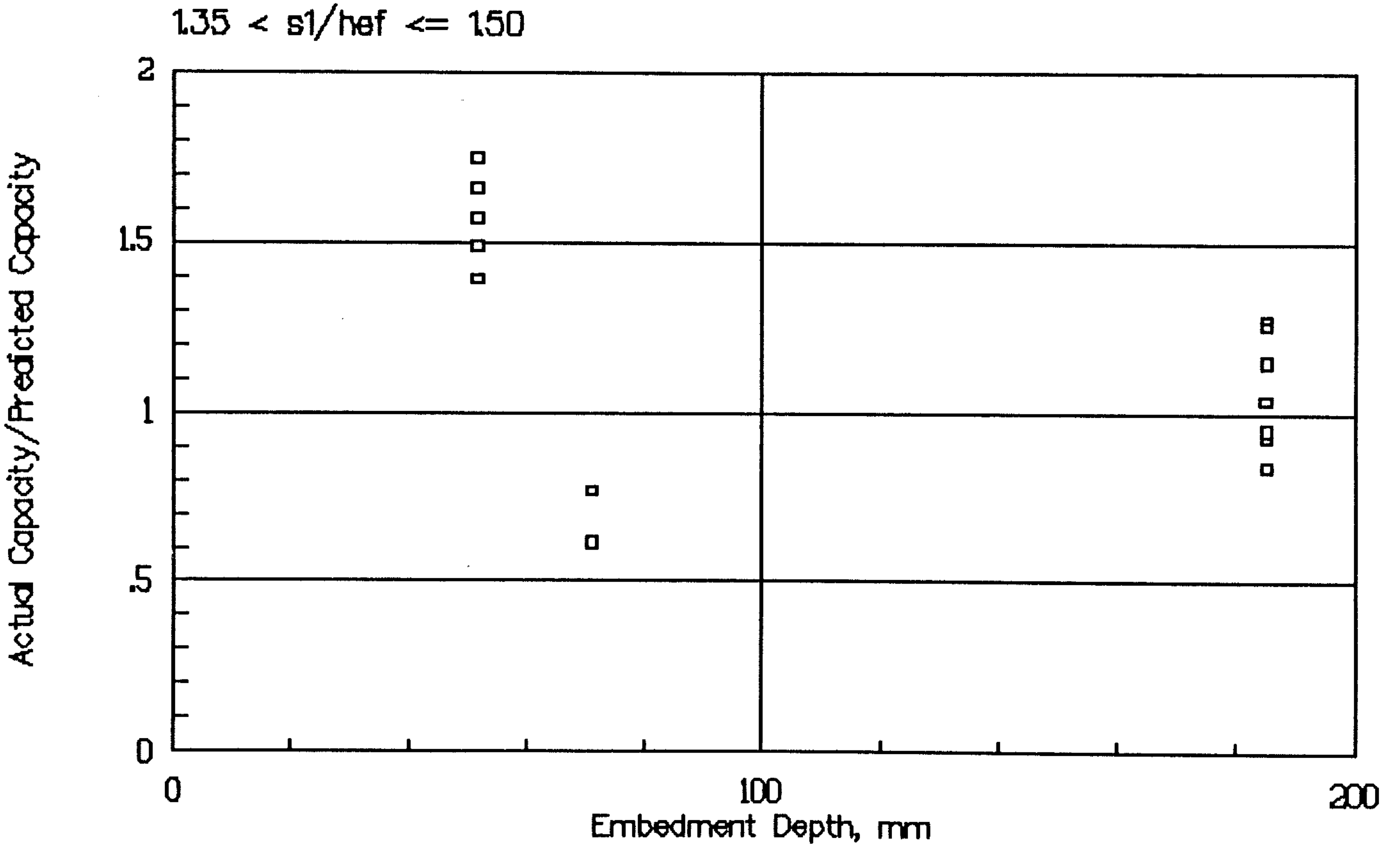

TENSILE CAPACITY vs EMBEDMENT DEPTH
ACI 349-85 Method
Figure B-23

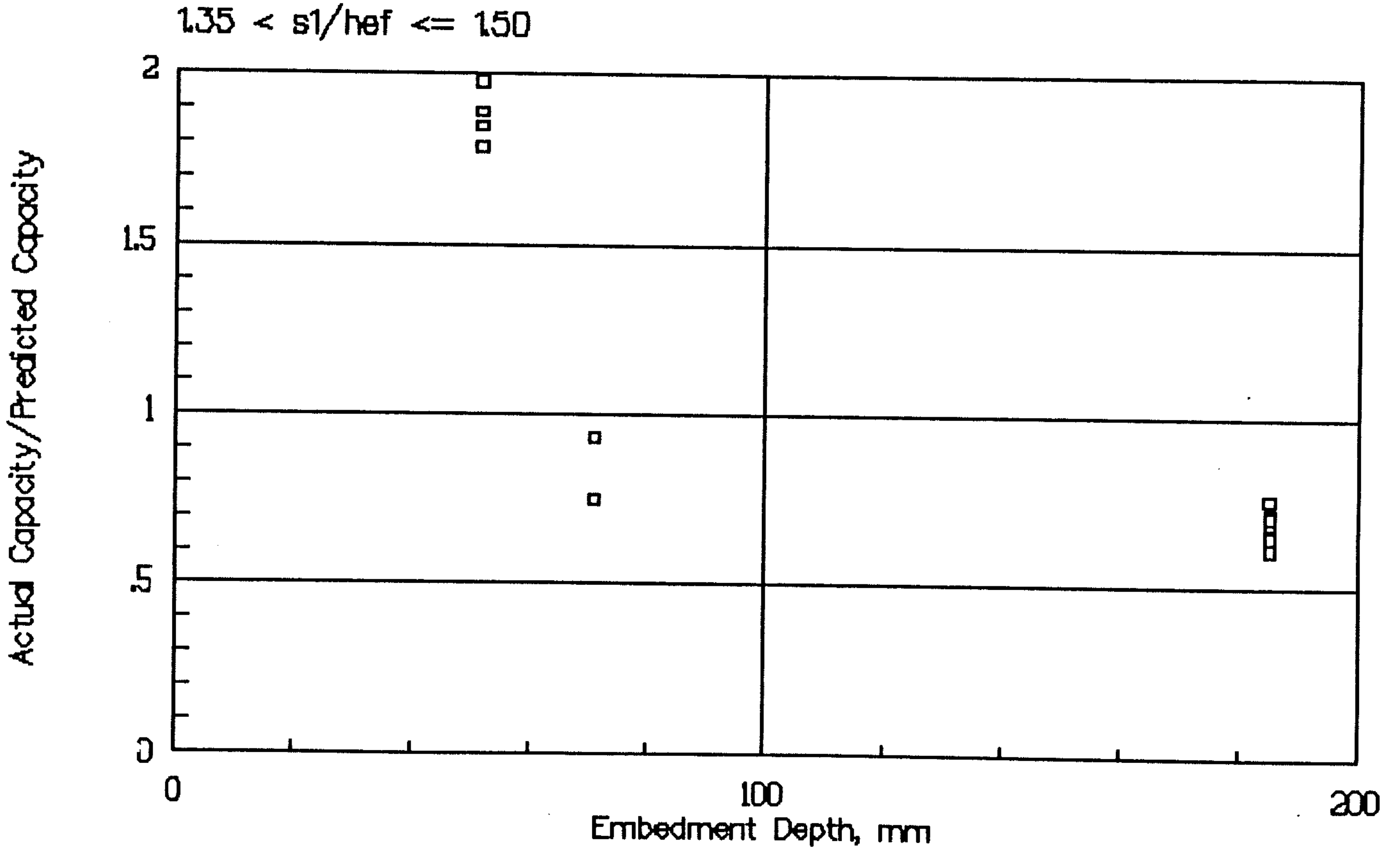

TENSILE CAPACITY vs EMBEDMENT DEPTH
Variable-Angle Cone Method
Figure B-24

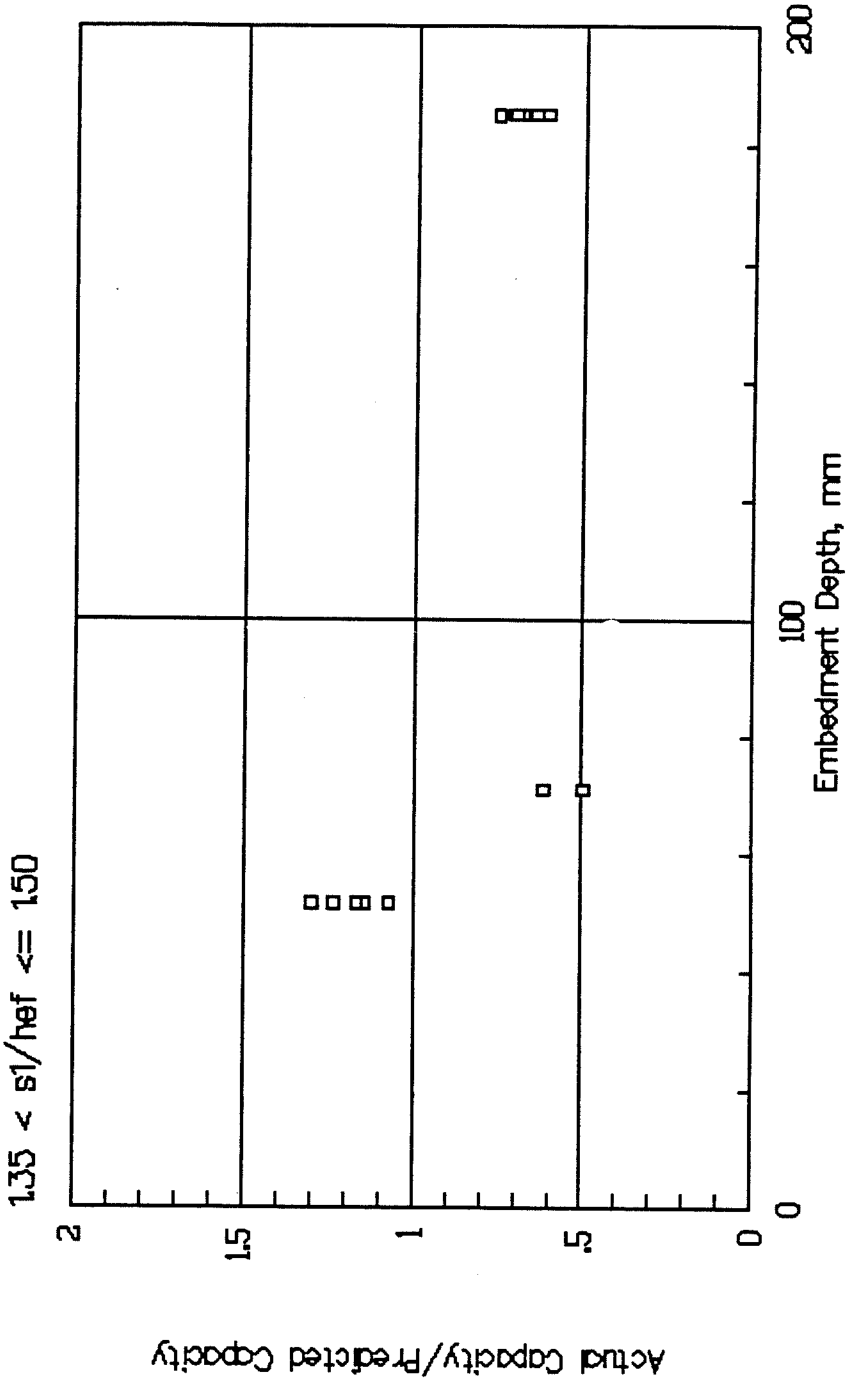

TENSILE CAPACITY vs EMBEDMENT DEPTH
Concrete Capacity Method
Figure B-25

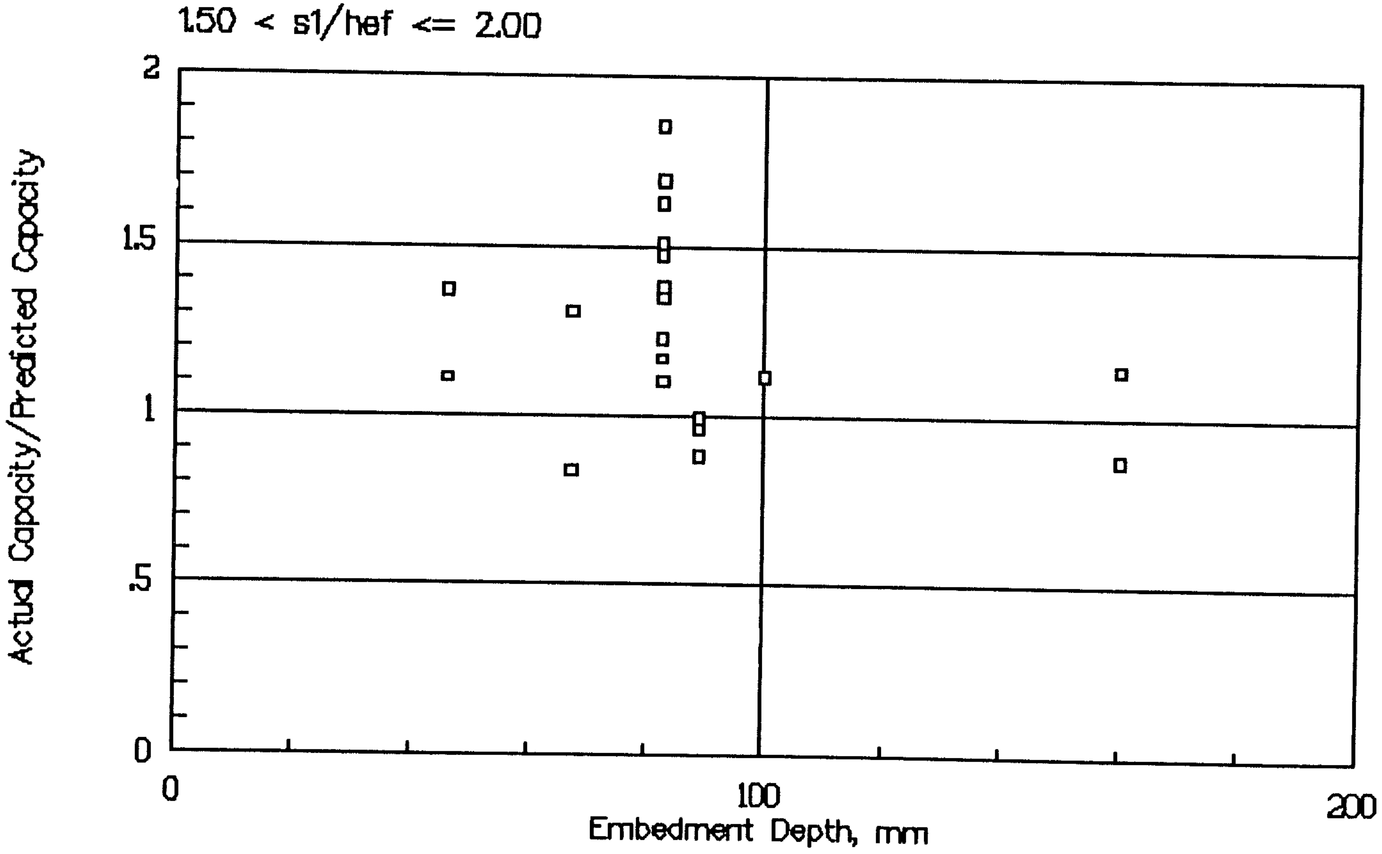

TENSILE CAPACITY vs EMBEDMENT DEPTH
ACI 349-85 Method
Figure B-26

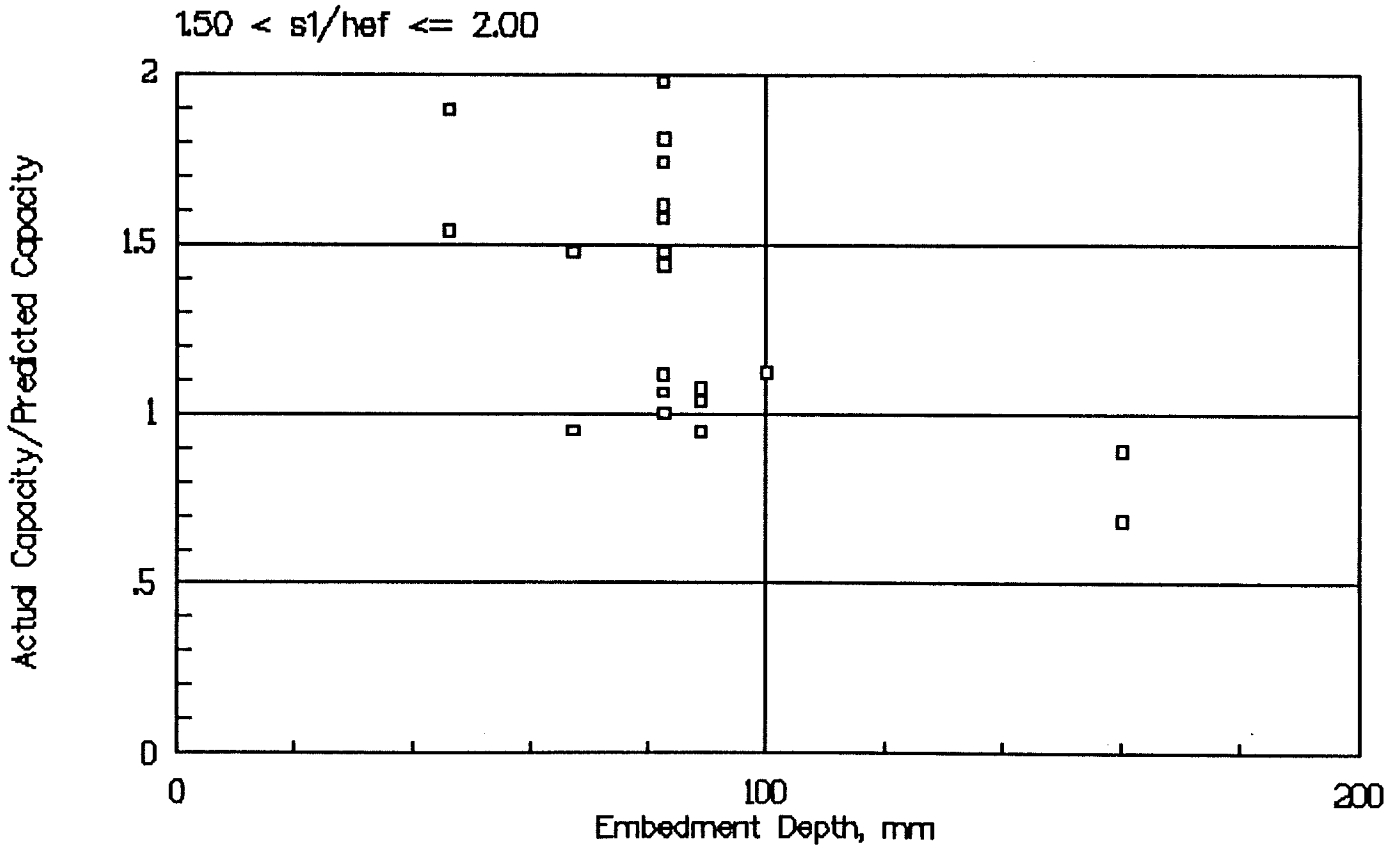

TENSILE CAPACITY vs EMBEDMENT DEPTH
Variable–Angle Cone Method
Figure B–27

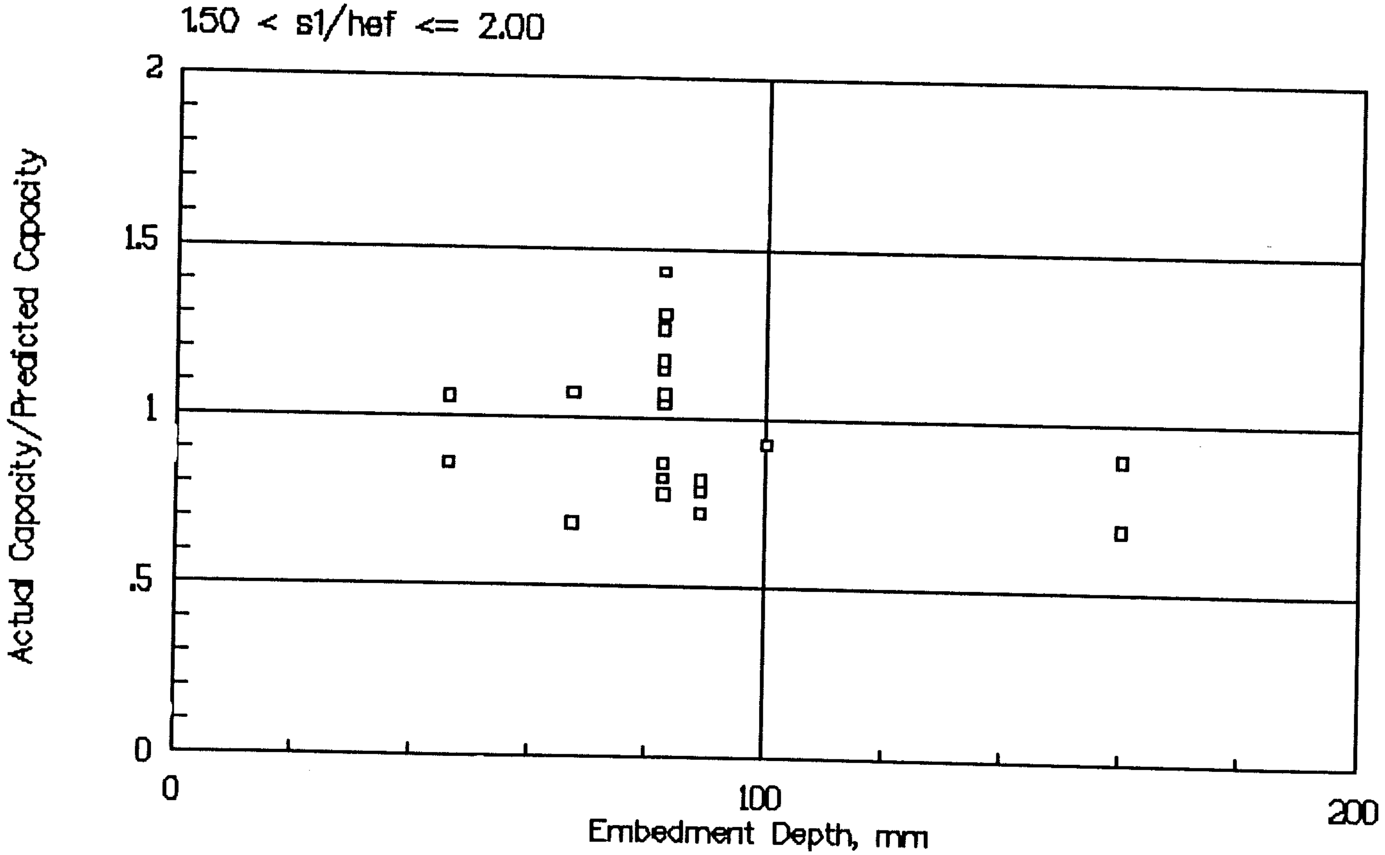

TENSILE CAPACITY vs EMBEDMENT DEPTH
Concrete Capacity Method
Figure B–28

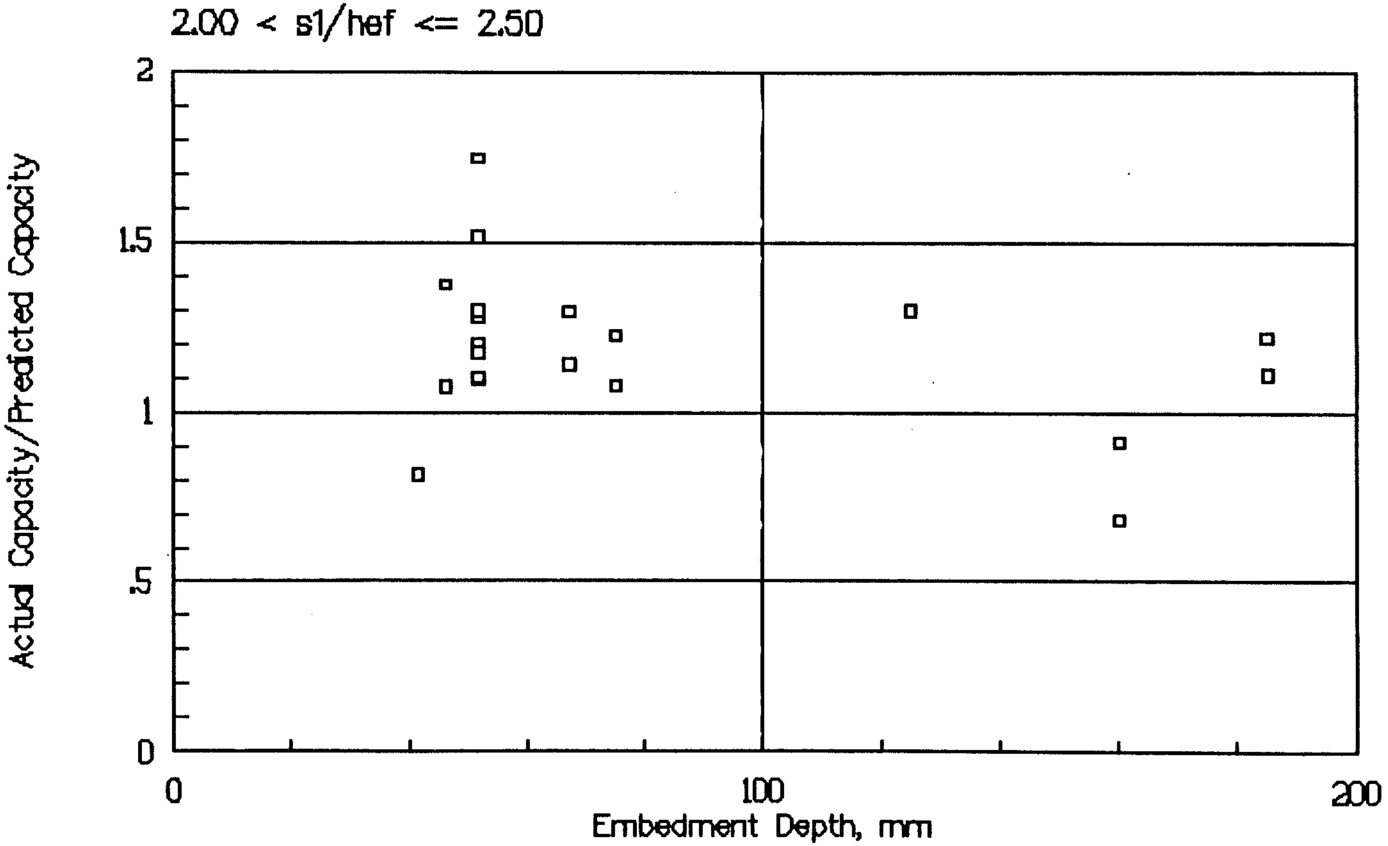

TENSILE CAPACITY vs EMBEDMENT DEPTH
ACI 349–85 Method
Figure B–29

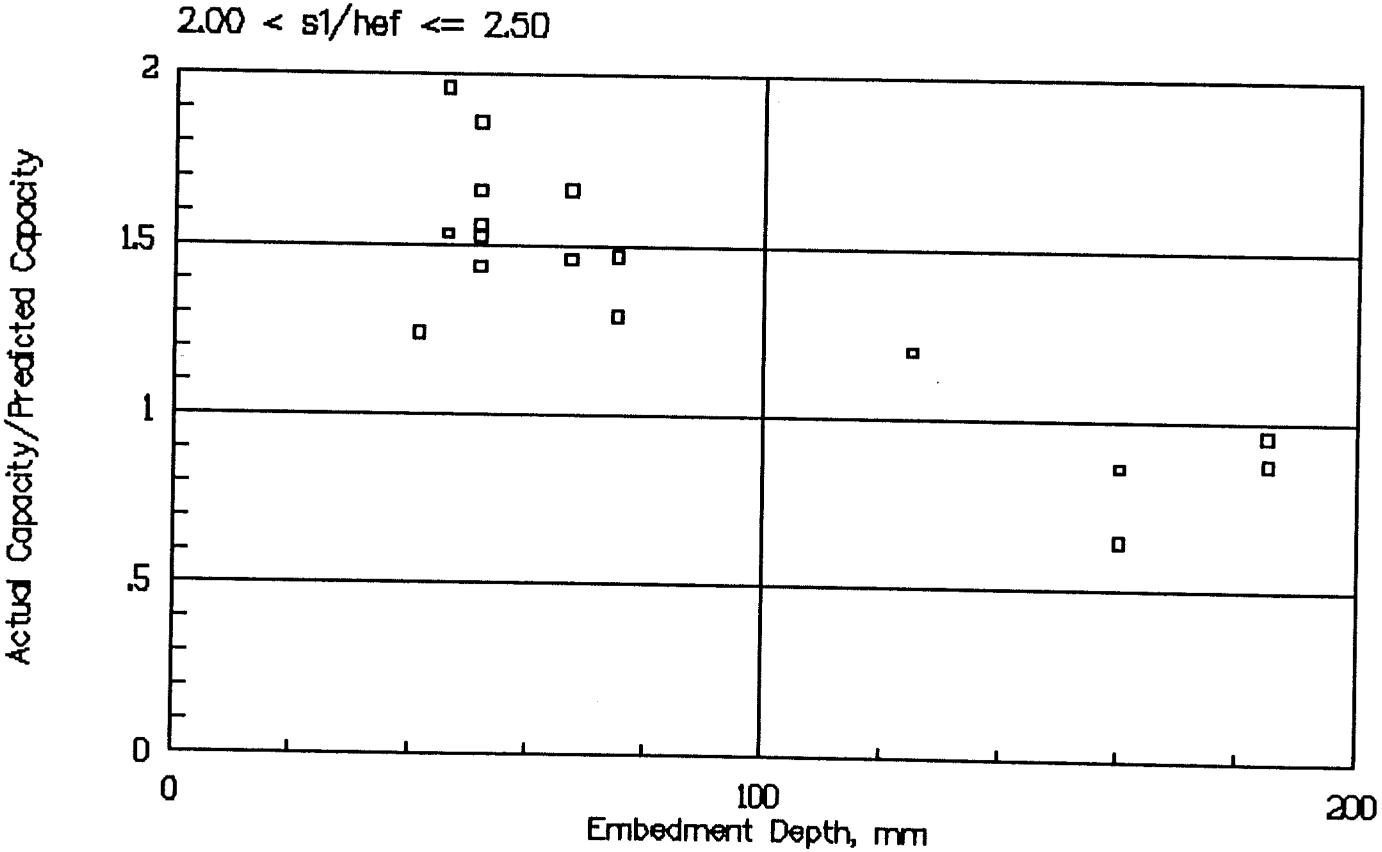

TENSILE CAPACITY vs EMBEDMENT DEPTH
Variable-Angle Cone Method
Figure B-30

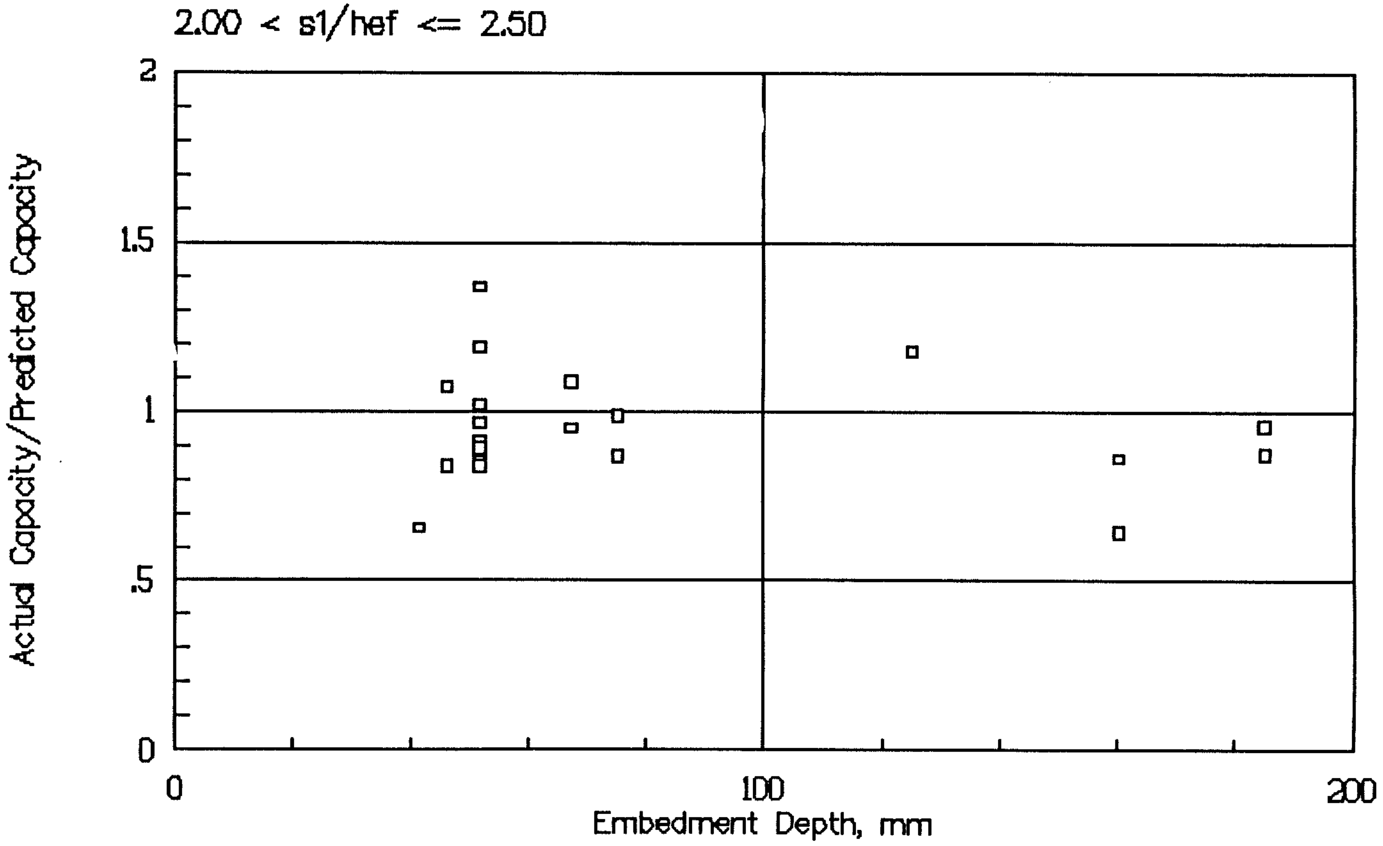

TENSILE CAPACITY vs EMBEDMENT DEPTH
Concrete Capacity Method
Figure B—31

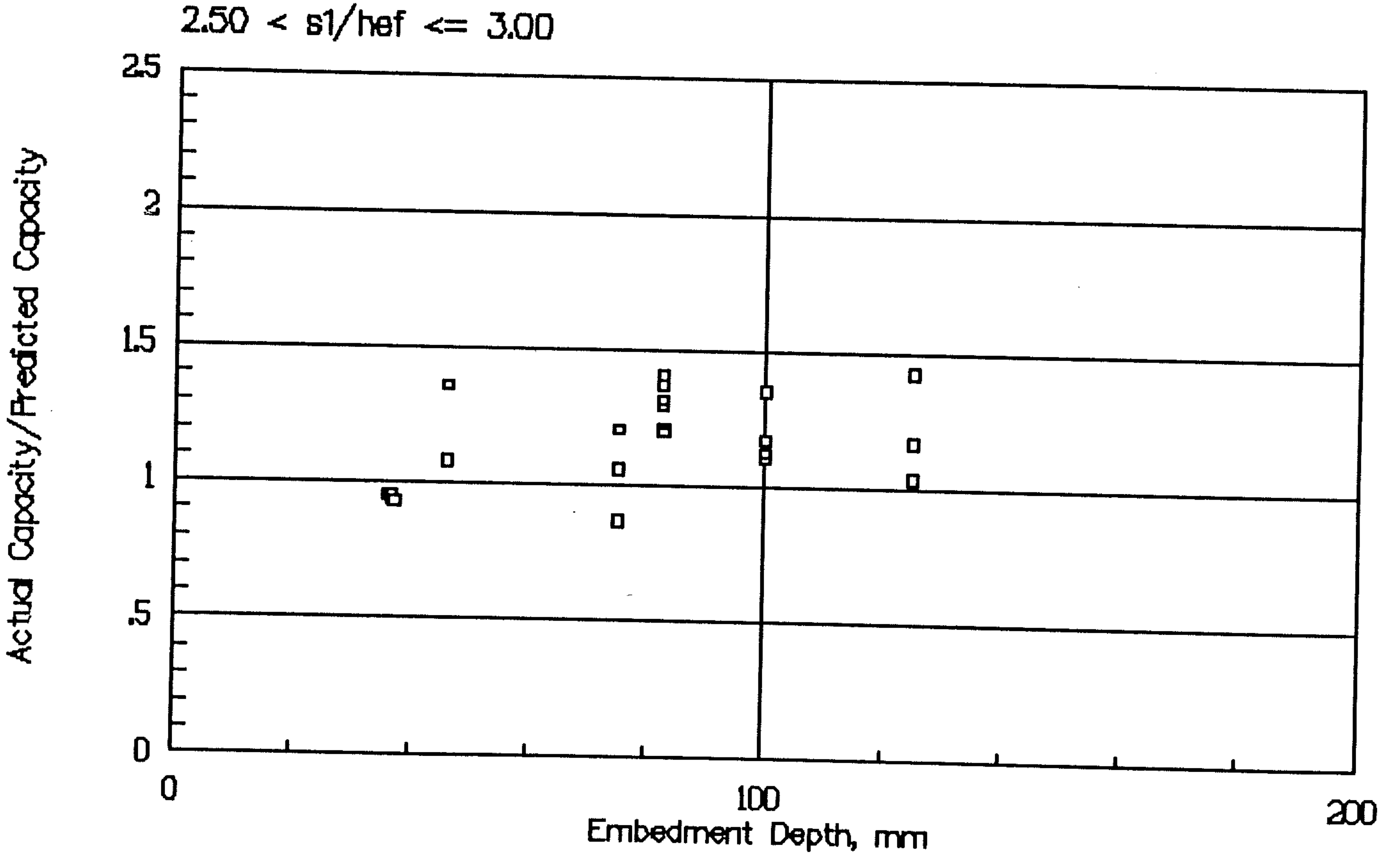

TENSILE CAPACITY vs EMBEDMENT DEPTH
ACI 349-85 Method
Figure B-32

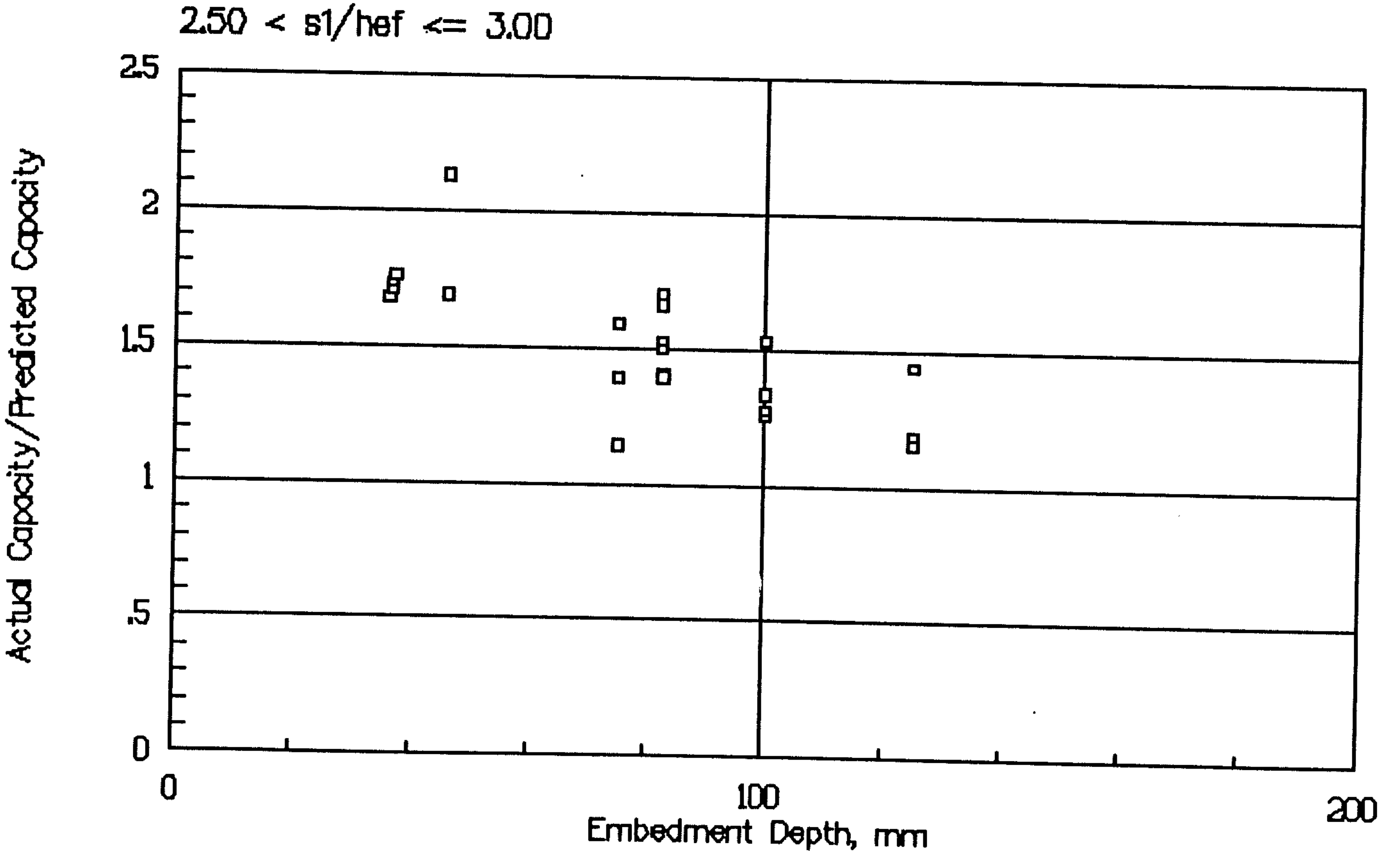

TENSILE CAPACITY vs EMBEDMENT DEPTH
Variable—Angle Cone Method
Figure B—33

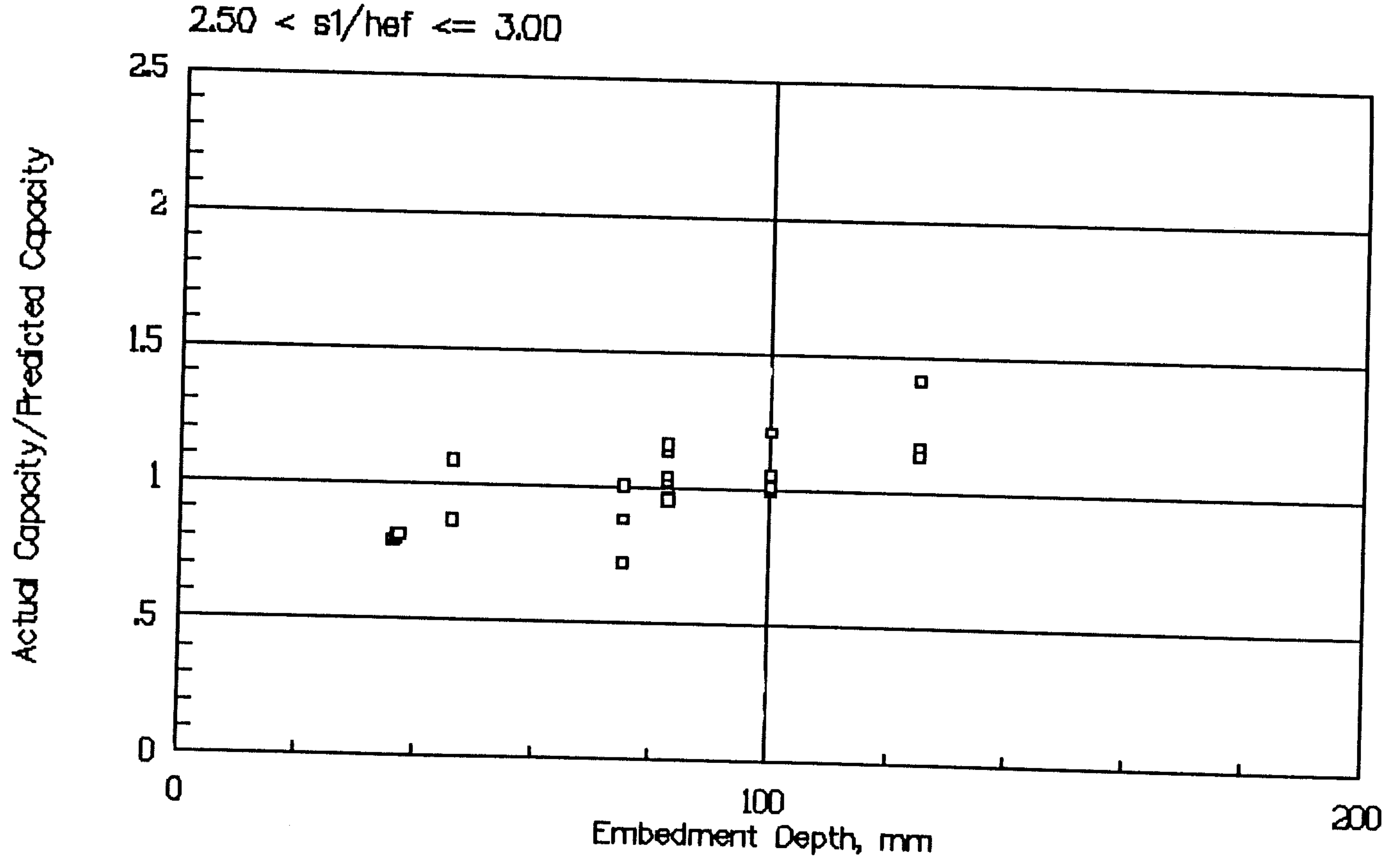

APPENDIX C: ORIGINAL DATA BASE FOR CONCRETE FAILURES (SI UNITS)

.ue
.nn 7.1
.sa 4

Syst. [-]	d [mm]	do [mm]	hef [mm]	Tinst [Nm]	fy [MPa]	ft [MPa]	fcc200 [MPa]	fct [MPa]	dagg [mm]	c1 [mm]	s1 [mm]	s2 [mm]	Nu,m [kN]	Lit.
A3	8.0	8.0	65.0	25.0	850.	950.	23.0	.	20.	80.	999.	999.	23.0	[1]
A3	12.0	12.0	100.0	100.0	850.	950.	23.0	.	20.	120.	999.	999.	50.0	[1]
A1	6.0	12.0	37.0	8.0	.	.	25.5	.	20.	50.	999.	999.	13.0	[1]

.fz 3
.sa 1
2Tabelle A$n2$1 Versuchsdaten, Axialzug, (GB), Einzelbefestigungen,
Dübel am Bauteilrand, c1 ≤ 1,5·hef

.ue
.nn 8.1
.sa 4

Syst. [-]	d [mm]	do [mm]	hef [mm]	Tinst [Nm]	fy [MPa]	ft [MPa]	fcc200 [MPa]	fct [MPa]	dagg [mm]	c1 [mm]	s1 [mm]	s2 [mm]	Nu,m [kN]	Lit.
A1	8.0	12.0	63.5	25.0	640.	800.	18.4	.	.	63.	999.	999.	18.0	[4]
A1	8.0	12.0	63.5	25.0	640.	800.	18.4	.	.	63.	999.	999.	17.3	[4]

.fz 3
.sa 1
Tabelle2 A$n2$1 Versuchsdaten, Axialzug, (F), Einzelbefestigungen,
Dübel mit kleinem Randabstand, c1≤1,5·hef

.ue
.nn 6.1
.sa 4

Syst. [-]	d [mm]	do [mm]	hef [mm]	Tinst [Nm]	fy [MPa]	ft [MPa]	fcc200 [MPa]	fct [MPa]	dagg [mm]	c1 [mm]	s1 [mm]	s2 [mm]	Nu,m [kN]	Lit.
D	6.0	10.7	37.0	.	640.	800.	24.0	.	.	50.	999.	999.	13.1	[2]
D	6.0	10.7	37.0	.	640.	800.	59.0	.	.	50.	999.	999.	17.9	[2]
D	8.0	12.7	36.5	.	640.	800.	56.0	.	.	50.	999.	999.	21.3	[2]
D	8.0	12.7	36.5	.	640.	800.	25.0	.	.	50.	999.	999.	13.9	[2]
A1	10.0	10.0	38.0	.	.	.	25.0	.	.	50.	999.	999.	11.1	[3]
A1	10.0	10.0	40.0	.	.	.	25.0	.	.	60.	999.	999.	10.9	[3]
B	10.0	10.0	30.0	.	.	.	25.0	.	.	40.	999.	999.	6.7	[3]
D	10.0	14.7	36.0	.	640.	800.	24.0	.	.	50.	999.	999.	11.9	[2]
D	10.0	14.7	36.0	.	640.	800.	59.0	.	.	50.	999.	999.	19.9	[2]
A1	12.0	12.0	62.0	.	.	.	25.0	.	.	60.	999.	999.	18.1	[3]
A1	12.0	12.0	47.0	.	.	.	25.0	.	.	60.	999.	999.	16.4	[3]
B	12.0	12.0	37.0	.	.	.	25.0	.	.	50.	999.	999.	5.6	[3]
B	12.0	12.0	37.0	.	.	.	25.0	.	.	40.	999.	999.	9.7	[3]
D	12.0	18.4	80.0	.	640.	800.	24.0	.	.	80.	999.	999.	39.7	[2]
D	12.0	18.4	80.0	.	640.	800.	24.0	.	.	80.	999.	999.	39.8	[2]
A1	14.0	14.0	55.0	.	.	.	25.0	.	.	70.	999.	999.	20.1	[3]
A1	14.0	14.0	55.0	.	.	.	25.0	.	.	80.	999.	999.	28.3	[3]
A1	16.0	16.0	67.0	.	.	.	25.0	.	.	80.	999.	999.	30.9	[3]
A1	16.0	16.0	67.0	.	.	.	25.0	.	.	90.	999.	999.	29.7	[3]
A1	16.0	16.0	75.0	.	.	.	25.0	.	.	80.	999.	999.	34.4	[3]
C	17.0	17.5	53.0	.	.	.	25.0	.	.	50.	999.	999.	26.7	[3]
C	17.0	17.5	53.0	.	.	.	25.0	.	.	30.	999.	999.	12.0	[3]
A1	22.0	22.0	87.0	.	.	.	25.0	.	.	110.	999.	999.	46.6	[3]
A1	24.0	24.0	100.0	.	.	.	25.0	.	.	110.	999.	999.	58.2	[3]
A1	24.0	24.0	100.0	.	.	.	25.0	.	.	105.	999.	999.	55.3	[3]

.fz3
.sa1
2Tabelle A$n21 Versuchsdaten, Axialzug, (D), Einzelbefestigungen,
Dübel am Bauteilrand, c1≤1,5 hef

.ns
.sa 4

Syst. [-]	d [mm]	do [mm]	hef [mm]	Tinst [Nm]	fy [MPa]	ft [MPa]	fcc200 [MPa]	fct [MPa]	dagg [mm]	c1 [mm]	s1 [mm]	s2 [mm]	Nu,m [kN]	Lit.
C	25.0	25.4	83.0	.	.	.	25.0	.	.	120.	999.	999.	56.1	[3]
C	25.0	25.4	83.0	.	.	.	25.0	.	.	80.	999.	999.	40.3	[3]
C	25.0	25.4	83.0	.	.	.	25.0	.	.	40.	999.	999.	24.2	[3]
A1	28.0	28.0	125.0	.	.	.	25.0	.	.	130.	999.	999.	91.2	[3]
A1	32.0	32.0	148.0	.	.	.	25.0	.	.	160.	999.	999.	114.6	[3]
D	16.0	.	125.0	100.0	902.	997.	37.7	3.3	16.	125.	999.	999.	114.3	[7]
D	16.0	.	125.0	100.0	902.	997.	37.7	3.3	16.	188.	999.	999.	120.9	[7]
D	20.0	.	170.0	200.0	1047.	1134.	24.7	2.5	16.	170.	999.	999.	159.8	[7]
D	20.0	.	170.0	200.0	1047.	1134.	28.3	2.6	16.	255.	999.	999.	183.2	[7]
D	24.0	.	220.0	300.0	1144.	1242.	27.6	2.8	16.	220.	999.	999.	223.4	[7]
D	24.0	.	220.0	300.0	1144.	1242.	33.2	3.0	16.	330.	999.	999.	235.3	[7]

.fz3
.sa1
2Tabelle A$n2$1 Versuchsdaten, Axialzug, (D), Einzelbefestigungen,
Dübel am Bauteilrand, c1≤1,5·hef

.ue
.nn 9.1
.sa 4

Syst. [-]	d [mm]	do [mm]	hef [mm]	Tinst [Nm]	fy [MPa]	ft [MPa]	fcc200 [MPa]	fct [MPa]	dagg [mm]	c1 [mm]	s1 [mm]	s2 [mm]	Nu,m [kN]	Lit.
A3	6.0	6.8	34.2	11.0	544.	634.	18.6	.	25.	32.	999.	999.	7.4	[38]
A3	6.0	6.8	34.2	11.0	544.	634.	34.1	.	25.	32.	999.	999.	7.6	[38]
C	12.7	.	51.6	.	.	.	24.4	.	.	38.	999.	999.	20.2	[6]
C	12.7	.	51.6	.	.	.	26.0	.	.	51.	999.	999.	25.8	[6]
C	12.7	.	51.6	.	.	.	24.4	.	.	51.	999.	999.	26.1	[6]
C	19.0	.	82.6	.	.	.	24.4	.	.	57.	999.	999.	41.6	[6]
A1	19.0	.	82.6	.	.	.	24.4	.	.	57.	999.	999.	47.2	[6]
C	19.0	.	82.6	.	.	.	24.4	.	.	76.	999.	999.	54.2	[6]
C	19.0	.	82.6	.	.	.	30.1	.	.	76.	999.	999.	55.0	[6]
A1	19.0	.	82.6	.	.	.	24.4	.	.	76.	999.	999.	57.1	[6]
D	12.7	.	151.4	.	.	.	32.9	.	.	102.	999.	999.	38.3	[6]
D	12.7	.	151.4	.	.	.	25.9	.	.	102.	999.	999.	74.7	[6]
D	12.7	.	145.0	.	.	.	29.6	.	.	102.	999.	999.	78.7	[6]
D	12.7	.	151.4	.	.	.	32.9	.	.	102.	999.	999.	80.1	[6]
D	12.7	.	151.4	.	.	.	29.6	.	.	102.	999.	999.	81.0	[6]
D	15.0	.	193.8	.	.	.	29.5	.	.	111.	999.	999.	131.4	[6]
D	12.7	.	151.4	.	.	.	32.9	.	.	114.	999.	999.	73.8	[6]
D	19.0	.	222.3	.	.	.	29.5	.	.	114.	999.	999.	164.6	[6]
D	12.7	.	151.4	.	.	.	32.9	.	.	127.	999.	999.	78.3	[6]
D	12.7	.	145.0	.	.	.	29.6	.	.	127.	999.	999.	81.0	[6]
D	12.7	.	151.4	.	.	.	25.9	.	.	127.	999.	999.	84.5	[6]
D	12.7	.	145.0	.	.	.	29.6	.	.	127.	999.	999.	85.9	[6]
D	12.7	.	151.4	.	.	.	25.9	.	.	127.	999.	999.	90.3	[6]
D	15.0	.	187.5	.	.	.	25.0	.	.	127.	999.	999.	129.7	[6]
D	15.0	.	193.8	.	.	.	25.2	.	.	127.	999.	999.	130.6	[6]

.fz 3
.sa 1
Tabelle $n2$1 Versuchsdaten, Axialzug, (USA), Einzelbefestigungen,
Dübel am Bauteilrand, c1≤1,0·hef

.ns
.sa 4

Syst. [-]	d [mm]	do [mm]	hef [mm]	Tinst [Nm]	fy [MPa]	ft [MPa]	fcc200 [MPa]	fct [MPa]	dagg [mm]	c1 [mm]	s1 [mm]	s2 [mm]	Nu,m [kN]	Lit.
D	19.0	.	222.3	.	.	.	29.5	.	.	133.	999.	999.	164.6	[6]
D	15.0	.	193.8	.	.	.	25.0	.	.	143.	999.	999.	129.9	[6]
D	19.0	.	222.3	.	.	.	29.5	.	.	152.	999.	999.	169.0	[6]
D	19.0	.	222.3	.	.	.	29.5	.	.	152.	999.	999.	197.9	[6]
D	15.0	.	193.8	.	.	.	25.2	.	.	159.	999.	999.	131.4	[6]

.fz 3
.sa 1
2Tabelle $n2$1 Versuchsdaten, Axialzug, (USA), Einzelbefestigungen,
Dübel am Bauteilrand, c1≤1,0hef

.ue
.nn 11.1
.sa 4

Syst. [-]	d [mm]	do [mm]	hef [mm]	Tinst [Nm]	fy [MPa]	ft [MPa]	fcc200 [MPa]	fct [MPa]	dagg [mm]	c1 [mm]	s1 [mm]	s2 [mm]	Nu,m [kN]	Lit.
A1	10.0	15.0	71.0	50.0	640.	800.	13.6	.	.	999.	100.	999.	33.6	[4]
A1	10.0	15.0	71.0	50.0	640.	800.	27.9	.	.	999.	100.	999.	38.7	[4]

.fz 3
.sa 1
Tabelle2 A$n2$1 Versuchsdaten, Axialzug, (F), Zweifachbefestigungen,
Dübel in der Fläche, c1≥1,5·hef

.ue
.nn 10.1
.sa 4

Syst. [-]	d [mm]	do [mm]	hef [mm]	Tinst [Nm]	fy [MPa]	ft [MPa]	fcc200 [MPa]	fct [MPa]	dagg [mm]	c1 [mm]	s1 [mm]	s2 [mm]	Nu,m [kN]	Lit.
B	12.0	15.0	46.0	.	.	.	20.0	.	.	999.	50.	999.	39.2	[3]
B	12.0	15.0	46.0	.	.	.	40.0	.	.	999.	50.	999.	40.0	[3]
B	12.0	15.0	46.0	.	.	.	20.0	.	.	999.	75.	999.	39.7	[3]
B	12.0	15.0	46.0	.	.	.	40.0	.	.	999.	75.	999.	45.6	[3]
D	12.0	18.0	80.0	.	640.	800.	25.0	2.1	29.	999.	80.	999.	60.9	[2]
A1	12.0	18.0	75.0	.	.	.	21.4	.	.	999.	80.	999.	59.4	[3]
C	12.0	18.4	80.0	.	640.	800.	25.0	.	.	999.	80.	999.	60.9	[2]
A1	12.0	18.0	75.0	.	.	.	29.3	.	.	999.	80.	999.	69.6	[3]
A1	12.0	18.0	75.0	.	.	.	57.0	.	.	999.	80.	999.	126.2	[3]
C	8.0	12.7	36.5	.	640.	800.	25.0	.	.	999.	100.	999.	26.6	[2]
C	10.0	14.7	36.0	.	640.	800.	28.0	.	.	999.	100.	999.	28.2	[2]
C	6.0	10.7	37.0	.	640.	800.	28.0	.	.	999.	100.	999.	28.4	[2]
C	10.0	14.7	36.0	.	640.	800.	56.0	.	.	999.	100.	999.	39.9	[2]
C	8.0	12.7	36.5	.	640.	800.	56.0	.	.	999.	100.	999.	40.4	[2]
B	12.0	15.0	46.0	.	.	.	20.0	.	.	999.	100.	999.	44.6	[3]
B	12.0	15.0	46.0	.	.	.	40.0	.	.	999.	100.	999.	49.4	[3]
A1	16.0	24.0	100.0	.	.	.	19.9	.	.	999.	105.	999.	101.2	[3]
A1	16.0	24.0	100.0	.	.	.	22.0	.	.	999.	105.	999.	102.6	[3]
A1	16.0	24.0	100.0	.	.	.	61.7	.	.	999.	105.	999.	175.2	[3]
B	12.0	15.0	46.0	.	.	.	20.0	.	.	999.	125.	999.	48.7	[3]
B	12.0	15.0	46.0	.	.	.	40.0	.	.	999.	125.	999.	54.6	[3]
D	16.0	.	125.0	100.0	902.	997.	34.1	2.9	16.	999.	125.	999.	175.7	[7]
A1	20.0	28.0	125.0	.	.	.	24.2	.	.	999.	130.	999.	163.2	[3]
A1	20.0	28.0	125.0	.	.	.	48.2	.	.	999.	130.	999.	242.4	[3]
B	12.0	15.0	46.0	.	.	.	20.0	.	.	999.	150.	999.	48.8	[3]

.fz3
.sa1
2Tabelle A$n2$1 Versuchsdaten, Axialzug, (D), Zweifachbefestigungen,
Dübel in der Fläche

.ns
.sa 4

Syst. [-]	d [mm]	do [mm]	hef [mm]	Tinst [Nm]	fy [MPa]	ft [MPa]	fcc200 [MPa]	fct [MPa]	dagg [mm]	c1 [mm]	s1 [mm]	s2 [mm]	Nu,m [kN]	Lit.
B	12.0	15.0	46.0	.	.	.	40.0	.	.	999.	150.	999.	59.0	[3]
A1	16.0	24.0	100.0	.	.	.	22.3	.	.	999.	158.	999.	108.6	[3]
A1	12.0	18.0	75.0	.	.	.	29.3	.	.	999.	160.	999.	87.6	[3]
A1	12.0	18.0	75.0	.	.	.	57.0	.	.	999.	160.	999.	138.8	[3]
B	12.0	15.0	46.0	.	.	.	20.0	.	.	999.	175.	999.	50.4	[3]
B	12.0	15.0	46.0	.	.	.	40.0	.	.	999.	175.	999.	62.5	[3]
C	8.0	12.7	36.5	.	640.	800.	25.0	.	.	999.	200.	999.	28.3	[2]
C	10.0	14.7	36.0	.	640.	800.	28.0	.	.	999.	200.	999.	31.5	[2]
C	8.0	12.7	36.5	.	640.	800.	56.0	.	.	999.	200.	999.	41.5	[2]
C	10.0	14.7	36.0	.	640.	800.	56.0	.	.	999.	200.	999.	42.2	[2]
A1	12.0	18.0	75.0	.	.	.	21.4	.	.	999.	200.	999.	66.4	[3]
A1	12.0	18.0	75.0	.	.	.	29.3	.	.	999.	200.	999.	94.4	[3]
A1	12.0	18.0	75.0	.	.	.	57.0	.	.	999.	200.	999.	150.4	[3]
A1	12.0	18.0	75.0	.	.	.	21.4	.	.	999.	240.	999.	67.6	[3]
A1	12.0	18.0	75.0	.	.	.	57.0	.	.	999.	240.	999.	149.0	[3]
A1	20.0	28.0	125.0	.	.	.	24.2	.	.	999.	260.	999.	204.0	[3]
A1	16.0	24.0	100.0	.	.	.	22.3	.	.	999.	263.	999.	132.3	[3]
A1	16.0	24.0	100.0	.	.	.	19.9	.	.	999.	263.	999.	132.4	[3]
A1	16.0	24.0	100.0	.	.	.	22.0	.	.	999.	263.	999.	133.3	[3]
A1	16.0	24.0	100.0	.	.	.	61.7	.	.	999.	263.	999.	268.0	[3]
D	12.0	18.0	80.0	.	640.	800.	26.0	2.2	29.	999.	280.	999.	103.6	[2]
C	12.0	18.4	80.0	.	640.	800.	25.0	.	.	999.	280.	999.	76.0	[2]
A1	12.0	18.0	75.0	.	.	.	57.0	.	.	999.	320.	999.	150.0	[3]
A1	20.0	28.0	125.0	.	.	.	24.2	.	.	999.	325.	999.	202.4	[3]
A1	20.0	28.0	125.0	.	.	.	48.2	.	.	999.	325.	999.	347.2	[3]
D	16.0	.	125.0	100.0	902.	997.	34.1	2.9	16.	999.	375.	999.	228.3	[7]

.fz 3
.sa 1
2Tabelle A$n2$1 Versuchsdaten, Axialzug, (D), Zweifachbefestigungen,
Dübel in der Fläche

.ue
.nn 12.1
.sa 4

Syst. [-]	d [mm]	do [mm]	hef [mm]	Tinst [Nm]	fy [MPa]	ft [MPa]	fcc200 [MPa]	fct [MPa]	dagg [mm]	c1 [mm]	s1 [mm]	s2 [mm]	Nu,m [kN]	Lit.
C	12.7	.	51.6	.	.	.	39.1	.	.	999.	76.	999.	64.9	[6]
C	12.7	.	51.6	.	.	.	39.1	.	.	999.	76.	999.	69.5	[6]
C	12.7	.	51.6	.	.	.	24.4	.	.	999.	127.	999.	49.1	[6]
C	12.7	.	51.6	.	.	.	24.4	.	.	999.	127.	999.	58.4	[6]
C	12.7	.	51.6	.	.	.	39.1	.	.	999.	127.	999.	86.3	[6]
C	12.7	.	51.6	.	.	.	39.1	.	.	999.	127.	999.	99.3	[6]
C	12.7	.	51.6	.	.	.	24.4	.	.	999.	178.	999.	66.8	[6]
A1	12.7	.	88.9	.	.	.	24.4	.	.	999.	152.	999.	77.0	[6]
A1	12.7	.	88.9	.	.	.	39.1	.	.	999.	102.	999.	107.6	[6]
A1	19.0	.	82.6	.	.	.	39.1	.	.	999.	102.	999.	133.7	[6]
A1	19.0	.	82.6	.	.	.	39.1	.	.	999.	102.	999.	125.3	[6]
A1	19.0	.	82.6	.	.	.	39.1	.	.	999.	165.	999.	178.3	[6]
A1	19.0	.	82.6	.	.	.	24.4	.	.	999.	165.	999.	112.3	[6]
A1	19.0	.	82.6	.	.	.	24.4	.	.	999.	165.	999.	115.1	[6]
A3	9.5	10.0	41.3	27.1	345.	483.	33.8	.	25.	999.	41.	999.	22.9	[44]
A3	9.5	10.0	41.3	27.1	345.	483.	33.8	.	25.	999.	83.	999.	28.4	[44]
A3	9.5	10.0	63.5	33.9	345.	483.	33.8	.	25.	999.	64.	999.	42.0	[44]
A3	9.5	10.0	42.6	41.0	483.	565.	14.9	.	25.	999.	38.	999.	19.8	[38]
A3	9.5	10.0	77.4	34.0	483.	565.	14.9	.	25.	999.	38.	999.	31.8	[38]
A3	9.5	10.0	38.5	41.0	483.	565.	36.2	.	25.	999.	38.	999.	22.5	[38]
A3	12.7	13.4	57.8	68.0	483.	565.	36.2	.	25.	999.	57.	999.	45.5	[38]
A3	12.7	13.4	105.4	68.0	483.	565.	14.9	.	25.	999.	51.	999.	41.8	[38]
A3	12.7	13.4	61.0	68.0	483.	565.	14.9	.	25.	999.	57.	999.	33.8	[38]
A3	15.9	16.6	71.5	122.0	483.	565.	14.9	.	25.	999.	70.	999.	46.6	[38]
A3	15.9	16.7	131.9	136.0	483.	565.	15.2	.	25.	999.	64.	999.	73.8	[38]
A3	15.9	16.7	71.4	122.0	483.	565.	36.2	.	25.	999.	70.	999.	64.1	[38]
A3	15.9	16.7	129.5	122.0	483.	565.	35.4	.	25.	999.	64.	999.	119.6	[38]
A3	19.0	19.8	87.6	163.0	483.	565.	14.9	.	25.	999.	95.	999.	56.7	[38]
A3	19.0	19.8	150.7	163.0	483.	565.	15.2	.	25.	999.	76.	999.	73.7	[38]
A3	19.0	19.9	85.7	190.0	483.	565.	36.2	.	25.	999.	95.	999.	77.3	[38]

.fz3
.sa1
2Tabelle$n2$1 Versuchsdaten, Axialzug, (USA), Zweifachbefestigungen,
Dübel in der Fläche

.ue
.nn 14.1
.sa 4

Syst. [-]	d [mm]	do [mm]	hef [mm]	Tinst [Nm]	fy [MPa]	ft [MPa]	fcc200 [MPa]	fct [MPa]	dagg [mm]	c1 [mm]	s1 [mm]	s2 [mm]	Nu,m [kN]	Lit.
C	12.7	.	51.6	.	.	.	40.7	.	.	999.	76.	76.	111.4	[6]
C	12.7	.	51.6	.	.	.	31.7	.	.	999.	127.	127.	109.4	[6]
C	12.7	.	51.6	.	.	.	33.0	.	.	999.	127.	127.	105.0	[6]
C	12.7	.	51.6	.	.	.	24.4	.	.	999.	178.	178.	128.1	[6]
C	12.7	.	51.6	.	.	.	39.1	.	.	999.	178.	178.	145.8	[6]
C	19.0	.	82.6	.	.	.	40.7	.	.	999.	102.	102.	209.8	[6]
C	19.0	.	82.6	.	.	.	33.0	.	.	999.	165.	165.	178.0	[6]
C	19.0	.	82.6	.	.	.	24.4	.	.	999.	229.	229.	223.4	[6]
C	19.0	.	82.6	.	.	.	39.1	.	.	999.	229.	229.	280.4	[6]
A1	12.7	.	88.9	.	.	.	40.7	.	.	999.	102.	102.	175.6	[6]
D	10.0	16.6	117.5	.	.	.	34.6	.	.	999.	102.	102.	208.1	[41]
D	15.9	24.8	227.0	.	.	.	34.6	.	.	999.	102.	102.	528.5	[41]
D	19.0	29.8	285.8	.	.	.	34.6	.	.	999.	102.	102.	820.9	[41]
D	12.7	19.8	154.0	.	.	.	34.6	.	.	999.	102.	102.	305.6	[41]
D	15.9	24.8	188.9	.	.	.	34.6	.	.	999.	102.	102.	394.2	[41]
D	19.0	29.8	225.4	.	.	.	34.6	.	.	999.	102.	102.	589.0	[41]
D	15.9	24.8	193.7	.	.	.	39.5	.	.	999.	76.	76.	409.0	[41]

.fz 3
.sa 1
2Tabelle $n2$1 Versuchsdaten, Axialzug, (USA), Vierfachbefestigungen,
Dübel in der Fläche

.ue
.nn 5.1
.sa 4

Syst. [-]	d [mm]	do [mm]	hef [mm]	Tinst [Nm]	fy [MPa]	ft [MPa]	fcc200 [MPa]	fct [MPa]	dagg [mm]	c1 [mm]	s1 [mm]	s2 [mm]	Nu,m [kN]	Lit.
A1	6.0	.	25.4	14.0	.	.	32.3	.	25.	999.	999.	999.	7.8	[33]
A1	6.0	.	25.4	14.0	.	.	32.3	.	25.	999.	999.	999.	8.7	[33]
A1	6.0	.	25.4	14.0	.	.	32.3	.	25.	999.	999.	999.	9.3	[33]
B	9.5	9.9	26.0	.	544.	634.	16.5	.	25.	305.	305.	305.	9.1	[38]
C	6.0	.	27.7	.	.	.	28.5	.	.	49.	999.	999.	10.7	[6]
C	6.0	.	28.0	5.0	393.	510.	45.9	.	.	999.	999.	999.	12.7	[32]
A1	6.0	6.7	28.9	.	544.	634.	16.5	.	25.	305.	305.	305.	6.6	[38]
A1	6.0	.	31.8	14.0	.	.	32.3	.	25.	999.	999.	999.	8.5	[33]
A1	6.0	.	31.8	14.0	.	.	32.3	.	25.	999.	999.	999.	10.5	[33]
C	8.9	.	33.3	.	.	.	28.5	.	.	58.	999.	999.	15.6	[6]
A3	8.9	8.5	34.2	27.0	483.	565.	18.6	.	25.	48.	999.	999.	8.9	[38]
A3	8.9	8.5	34.2	27.0	483.	565.	34.1	.	25.	48.	999.	999.	10.0	[38]
A3	9.5	10.0	35.5	41.0	483.	565.	16.1	.	25.	999.	999.	999.	10.9	[38]
A3	9.5	.	37.8	41.0	565.	.	34.5	.	25.	999.	999.	999.	13.6	[38]
C	10.0	.	38.9	.	.	.	28.5	.	.	113.	999.	999.	22.7	[6]
A3	9.5	9.9	38.9	54.0	483.	565.	18.6	.	25.	999.	999.	999.	14.4	[38]
C	10.0	.	39.0	17.0	393.	510.	45.9	.	.	999.	999.	999.	16.7	[32]
A3	9.5	.	39.3	41.0	745.	.	34.5	.	25.	999.	999.	999.	14.1	[38]
A3	9.5	.	40.0	.	745.	.	17.2	.	25.	57.	999.	999.	13.8	[38]
A3	9.5	.	40.0	.	565.	.	17.2	.	25.	57.	999.	999.	15.2	[38]
A1	8.9	.	40.0	.	393.	510.	31.8	.	.	999.	999.	999.	6.9	[32]
A1	8.9	.	40.0	.	393.	510.	31.8	.	.	999.	999.	999.	7.9	[32]
A1	8.9	.	40.0	.	393.	510.	31.8	.	.	999.	999.	999.	8.0	[32]
A1	8.9	.	40.0	.	393.	510.	31.8	.	.	999.	999.	999.	8.5	[32]
A1	8.9	.	40.0	.	393.	510.	31.8	.	.	999.	999.	999.	9.8	[32]

.fz 3
.sa 1
2Tabelle $n2$1 Versuchsdaten, Axialzug, (USA), Einzelbefestigungen,
Dübel in der Fläche, c1≥1,0·hef

.ns
.sa 4

Syst. [-]	d [mm]	do [mm]	hef [mm]	Tinst [Nm]	fy [MPa]	ft [MPa]	fcc200 [MPa]	fct [MPa]	dagg [mm]	c1 [mm]	s1 [mm]	s2 [mm]	Nu,m [kN]	Lit.
B	6.0	.	41.3	13.5	.	.	30.4	.	25.	999.	999.	999.	15.0	[33]
A3	12.7	13.4	50.8	48.0	483.	565.	18.0	.	25.	999.	999.	999.	21.0	[35]
A3	12.7	13.4	50.8	48.0	483.	565.	18.0	.	25.	999.	999.	999.	24.0	[35]
C	12.7	.	51.6	.	.	.	26.0	.	.	89.	999.	999.	23.8	[6]
C	12.7	.	51.6	.	.	.	25.2	.	.	90.	999.	999.	28.0	[6]
C	12.7	.	51.6	.	.	.	40.7	.	.	90.	999.	999.	32.7	[6]
C	12.7	.	51.6	.	.	.	25.2	.	.	90.	999.	999.	32.9	[6]
C	12.7	.	51.6	.	.	.	28.5	.	.	90.	999.	999.	34.7	[6]
C	12.7	.	51.6	.	.	.	25.2	.	.	90.	999.	999.	36.6	[6]
C	12.7	.	51.6	.	.	.	40.7	.	.	90.	999.	999.	40.9	[6]
C	12.7	.	51.6	.	.	.	50.4	.	.	90.	999.	999.	44.9	[6]
C	12.7	.	51.6	.	.	.	50.4	.	.	90.	999.	999.	46.3	[6]
C	12.7	.	51.6	.	.	.	40.7	.	.	90.	999.	999.	48.4	[6]
C	12.7	.	51.6	.	.	.	50.4	.	.	90.	999.	999.	49.8	[6]
C	12.7	.	51.6	.	.	.	26.0	.	.	102.	999.	999.	30.2	[6]
C	12.7	.	51.6	.	.	.	26.0	.	.	114.	999.	999.	31.7	[6]
C	12.7	.	51.6	.	.	.	26.0	.	.	127.	999.	999.	29.1	[6]
C	12.7	.	51.6	.	.	.	26.0	.	.	140.	999.	999.	27.9	[6]
C	12.7	.	51.6	.	.	.	26.0	.	.	152.	999.	999.	32.5	[6]
C	12.7	.	52.0	45.0	393.	510.	45.9	.	.	999.	999.	999.	35.0	[32]
A2	8.9	.	57.0	20.5	.	.	34.0	.	25.	999.	999.	999.	30.7	[33]
A2	15.9	.	57.0	110.0	.	.	31.6	.	25.	999.	999.	999.	33.4	[33]
A3	12.7	19.8	57.5	149.0	483.	565.	32.6	.	25.	999.	999.	999.	32.6	[35]
A3	12.0	.	58.2	68.0	745.	.	17.1	.	25.	999.	999.	999.	21.3	[38]
A3	12.0	.	58.9	68.0	565.	.	29.5	.	25.	999.	999.	999.	23.2	[38]

.fz 3
.sa 1
2Tabelle $n2$1 Versuchsdaten, Axialzug, (USA), Einzelbefestigungen,
Dübel in der Fläche, c1≥1,0·hef

.ns
.sa 4

Syst. [-]	d [mm]	do [mm]	hef [mm]	Tinst [Nm]	fy [MPa]	ft [MPa]	fcc200 [MPa]	fct [MPa]	dagg [mm]	c1 [mm]	s1 [mm]	s2 [mm]	Nu,m [kN]	Lit.
A3	12.0	.	60.2	68.0	565.	.	15.3	.	25.	999.	999.	999.	19.0	[38]
A3	12.0	.	60.7	68.0	745.	.	32.6	.	25.	999.	999.	999.	23.4	[38]
A3	12.0	13.4	60.8	65.0	483.	565.	16.1	.	25.	999.	999.	999.	19.0	[38]
C	15.9	.	62.7	.	.	.	28.5	.	.	110.	999.	999.	46.7	[6]
A1	15.9	16.6	63.5	.	.	.	35.7	.	9.	999.	999.	999.	33.9	[34]
A1	15.9	16.6	63.5	.	.	.	35.7	.	9.	999.	999.	999.	36.4	[34]
A1	15.9	16.6	63.5	.	.	.	35.7	.	9.	999.	999.	999.	36.4	[34]
A1	15.9	16.6	63.5	.	.	.	35.7	.	9.	999.	999.	999.	36.4	[34]
A1	15.9	16.6	63.5	.	.	.	51.9	.	9.	999.	999.	999.	49.6	[34]
A1	15.9	16.6	63.5	.	.	.	51.9	.	9.	999.	999.	999.	53.9	[34]
A1	15.9	16.6	63.5	.	.	.	51.9	.	9.	999.	999.	999.	56.4	[34]
A1	12.7	.	63.5	47.0	.	.	28.4	.	.	999.	999.	999.	29.8	[21]
A1	12.7	.	63.5	47.0	.	.	28.4	.	.	999.	999.	999.	30.3	[21]
A1	12.7	.	63.5	54.0	.	.	28.4	.	.	999.	999.	999.	22.3	[21]
A1	12.7	.	63.5	54.0	.	.	28.4	.	.	999.	999.	999.	29.6	[21]
A1	12.7	.	63.5	65.0	.	.	37.0	.	.	999.	999.	999.	32.7	[21]
A1	12.7	.	63.5	68.0	.	.	38.6	.	.	999.	999.	999.	35.9	[21]
A1	12.7	.	63.5	68.0	.	.	38.6	.	.	999.	999.	999.	37.0	[21]
A1	12.7	.	63.5	68.0	.	.	38.6	.	.	999.	999.	999.	37.0	[21]
A3	15.9	16.6	71.6	122.0	483.	565.	16.0	.	25.	999.	999.	999.	31.6	[38]
A1	12.0	.	80.0	45.0	393.	510.	47.1	.	.	999.	999.	999.	59.0	[32]
A1	12.0	.	80.0	45.0	393.	510.	35.3	.	.	999.	999.	999.	62.0	[32]
A1	12.0	.	80.0	77.0	393.	510.	47.1	.	.	999.	999.	999.	54.7	[32]
C	19.5	.	82.6	.	.	.	28.5	.	.	144.	999.	999.	66.3	[6]
C	19.5	.	82.6	.	.	.	30.1	.	.	210.	999.	999.	57.4	[6]

.fz 3
.sa 1
2Tabelle $n2$1 Versuchsdaten, Axialzug, (USA), Einzelbefestigungen,
Dübel in der Fläche, c1≥1,0·hef

.ns
.sa 4

Syst. [-]	d [mm]	do [mm]	hef [mm]	Tinst [Nm]	fy [MPa]	ft [MPa]	fcc200 [MPa]	fct [MPa]	dagg [mm]	c1 [mm]	s1 [mm]	s2 [mm]	Nu,m [kN]	Lit.
C	19.5	.	82.6	.	.	.	30.1	.	.	229.	999.	999.	69.4	[6]
C	19.5	.	83.0	145.0	248.	413.	45.9	.	.	999.	999.	999.	63.0	[32]
A3	19.5	19.7	87.4	163.0	483.	565.	16.0	.	25.	999.	999.	999.	37.3	[38]
C	22.2	.	93.7	.	.	.	28.5	.	.	164.	999.	999.	79.2	[6]
A1	20.0	.	170.0	150.0	248.	413.	27.1	.	.	999.	999.	999.	157.3	[32]

.fz 3
.sa 1
2Tabelle $n2$1 Versuchsdaten, Axialzug, (USA), Einzelbefestigungen,
Dübel in der Fläche, c1≥1,0·hef

.ue
.nn 2.1
.sa 4

Syst. [-]	d [mm]	do [mm]	hef [mm]	Tinst [Nm]	fy [MPa]	ft [MPa]	fcc200 [MPa]	fct [MPa]	dagg [mm]	c1 [mm]	s1 [mm]	s2 [mm]	Nu,m [kN]	Lit.
A3	8.0	8.0	50.0	25.0	850.	950.	23.0	.	20.	999.	999.	999.	15.0	[1]
A3	8.0	8.0	65.0	25.0	850.	950.	23.0	.	20.	999.	999.	999.	25.0	[1]
A3	12.0	12.0	75.0	100.0	850.	950.	23.0	.	20.	999.	999.	999.	29.0	[1]
A3	12.0	12.0	100.0	100.0	850.	950.	23.0	.	20.	999.	999.	999.	57.0	[1]
A3	12.0	12.0	75.0	100.0	850.	950.	23.0	.	20.	120.	999.	999.	33.0	[1]
A3	8.0	8.0	50.0	25.0	850.	950.	23.0	.	20.	80.	999.	999.	16.0	[1]
A3	16.0	16.0	53.0	67.0	.	.	34.0	.	20.	999.	999.	999.	43.0	[1]
A3	20.0	20.0	69.0	111.0	.	.	34.0	.	20.	999.	999.	999.	54.0	[1]
A3	25.0	25.4	76.0	204.0	.	.	34.0	.	20.	999.	999.	999.	68.0	[1]
A3	16.0	16.0	51.0	67.0	.	.	28.0	.	20.	999.	999.	999.	41.0	[1]
A3	6.0	6.0	22.0	.	.	.	26.4	.	20.	999.	999.	999.	7.0	[1]
A3	8.0	8.0	24.0	.	.	.	26.4	.	20.	999.	999.	999.	11.0	[1]
A3	10.0	10.0	30.0	.	.	.	26.4	.	20.	999.	999.	999.	16.0	[1]
A3	12.0	12.0	40.0	.	.	.	26.4	.	20.	999.	999.	999.	16.0	[1]
A3	16.0	16.0	53.0	.	.	.	26.4	.	20.	999.	999.	999.	28.0	[1]
A3	20.0	20.0	68.0	.	.	.	26.4	.	20.	999.	999.	999.	40.0	[1]
A1	6.0	10.0	37.0	8.0	.	.	25.5	2.1	20.	100.	999.	999.	13.0	[1]
A1	6.0	10.0	43.0	10.0	640.	800.	32.3	.	20.	999.	999.	999.	14.0	[1]
A1	8.0	12.0	43.0	18.0	.	.	24.7	2.3	20.	999.	999.	999.	13.0	[1]
A1	10.0	14.0	43.0	18.0	.	.	25.5	2.1	20.	65.	999.	999.	21.0	[1]
A1	8.0	12.0	47.0	25.0	640.	800.	32.3	.	20.	999.	999.	999.	21.0	[1]
A1	10.0	14.0	50.0	33.0	.	.	24.7	2.3	20.	999.	999.	999.	18.0	[1]
A1	10.0	14.0	50.0	33.0	.	.	24.7	2.3	20.	999.	999.	999.	23.0	[1]
A1	10.0	14.0	57.0	50.0	640.	800.	32.3	.	20.	999.	999.	999.	31.0	[1]
A1	12.0	18.0	58.0	80.0	640.	800.	32.3	.	20.	999.	999.	999.	35.0	[1]

.fz 3
.sa 1
2Tabelle A$n2$1 Versuchsdaten, Axialzug, (GB), Einzelbefestigungen,
Dübel in der Fläche, c1≥1,5 hef

.ns
.sa 4

Syst. [-]	d [mm]	do [mm]	hef [mm]	Tinst [Nm]	fy [MPa]	ft [MPa]	fcc200 [MPa]	fct [MPa]	dagg [mm]	c1 [mm]	s1 [mm]	s2 [mm]	Nu,m [kN]	Lit.
A1	8.0	12.0	62.0	25.0	640.	800.	32.3	.	20.	999.	999.	999.	29.0	[1]
A1	12.0	18.0	65.0	62.0	.	.	23.0	2.1	20.	999.	999.	999.	42.0	[1]
A1	10.0	14.0	72.0	50.0	640.	800.	32.3	.	20.	999.	999.	999.	42.0	[1]
A1	12.0	18.0	78.0	80.0	640.	800.	32.3	.	20.	999.	999.	999.	53.0	[1]
A1	16.0	24.0	90.0	150.0	.	.	23.0	2.1	20.	999.	999.	999.	57.0	[1]
A1	16.0	24.0	90.0	150.0	.	.	23.0	2.1	20.	999.	999.	999.	67.0	[1]
A1	20.0	28.0	110.0	280.0	.	.	25.5	2.3	20.	999.	999.	999.	86.0	[1]
A1	20.0	28.0	110.0	280.0	.	.	25.5	2.3	20.	999.	999.	999.	87.0	[1]
A1	16.0	24.0	117.0	200.0	640.	800	32.3	.	20.	999.	999.	999.	93.0	[1]
A1	20.0	28.0	136.0	400.0	640.	800.	32.3	.	20.	999.	999.	999.	113.0	[1]
B	6.0	8.0	25.0	.	.	.	26.4	.	20.	999.	999.	999.	9.0	[1]
B	6.0	8.0	25.0	.	.	.	28.1	.	20.	999.	999.	999.	10.0	[1]
B	8.0	10.0	30.0	.	.	.	26.4	.	20.	999.	999.	999.	11.0	[1]
B	8.0	10.0	30.0	.	.	.	28.1	.	20.	999.	999.	999.	13.0	[1]
B	8.0	10.0	30.0	.	.	.	26.4	.	20.	999.	999.	999.	13.0	[1]
B	10.0	12.0	40.0	.	.	.	26.4	.	20.	999.	999.	999.	16.0	[1]
B	10.0	12.0	40.0	.	.	.	28.1	.	20.	999.	999.	999.	19.0	[1]
B	10.0	12.0	40.0	.	.	.	29.8	.	20.	999.	999.	999.	19.0	[1]
B	10.0	12.0	43.0	.	.	.	26.4	.	20.	999.	999.	999.	23.0	[1]
B	12.0	15.0	50.0	.	.	.	26.4	.	20.	999.	999.	999.	24.0	[1]
B	12.0	15.0	50.0	.	.	.	28.1	.	20.	999.	999.	999.	28.0	[1]
B	12.0	15.0	50.0	.	.	.	29.8	.	20.	999.	999.	999.	40.0	[1]
B	12.0	15.0	53.0	.	.	.	26.4	.	20.	999.	999.	999.	32.0	[1]
B	16.0	20.0	60.0	.	.	.	26.4	.	20.	999.	999.	999.	29.0	[1]
B	16.0	20.0	60.0	.	.	.	29.8	.	20.	999.	999.	999.	47.0	[1]

.fz 3
.sa 1
2Tabelle A$n2$1 Versuchsdaten, Axialzug, (GB), Einzelbefestigungen,
Dübel in der Fläche, c1≥1,5 hef

.ns
.sa 4

Syst. [-]	d [mm]	do [mm]	hef [mm]	Tinst [Nm]	fy [MPa]	ft [MPa]	fcc200 [MPa]	fct [MPa]	dagg [mm]	c1 [mm]	s1 [mm]	s2 [mm]	Nu,m [kN]	Lit.
B	16.0	20.0	64.0	.	.	.	28.1	.	20.	999.	999.	999.	35.0	[1]
B	16.0	20.0	65.0	.	.	.	26.4	.	20.	999.	999.	999.	40.0	[1]
B	20.0	25.0	80.0	.	.	.	26.4	.	20.	999.	999.	999.	58.0	[1]
B	19.0	25.0	81.0	.	.	.	28.1	.	20.	999.	999.	999.	66.0	[1]
B	20.0	25.0	83.0	.	.	.	26.4	.	20.	999.	999.	999.	54.0	[1]

.fz 3
.sa 1
2Tabelle A$n2$1 Versuchsdaten, Axialzug, (GB), Einzelbefestigungen,
Dübel in der Fläche, c1≥1,5·hef

.ue
.nn 3.1
.sa 4

Syst. [-]	d [mm]	do [mm]	hef [mm]	Tinst [Nm]	fy [MPa]	ft [MPa]	fcc200 [MPa]	fct [MPa]	dagg [mm]	c1 [mm]	s1 [mm]	s2 [mm]	Nu,m [kN]	Lit.
A1	8.0	12.0	42.0	23.0	640.	800.	18.1	.	.	999.	999.	999.	13.8	[4]
A1	8.0	12.0	70.0	23.0	640.	800.	18.2	.	.	999.	999.	999.	20.6	[4]
A1	8.0	12.0	53.0	25.0	640.	800.	18.8	.	.	999.	999.	999.	18.7	[4]
A1	8.0	12.0	58.0	25.0	640.	800.	18.8	.	.	999.	999.	999.	19.4	[4]
A1	8.0	12.0	61.0	25.0	640.	800.	21.2	2.3	.	999.	999.	999.	19.7	[4]
A1	8.0	12.0	61.0	25.0	640.	800.	22.0	2.3	.	999.	999.	999.	21.7	[4]
A1	8.0	12.0	63.5	25.0	640.	800.	26.5	.	.	999.	999.	999.	24.8	[4]
A1	8.0	12.0	63.5	25.0	640.	800.	26.5	.	.	999.	999.	999.	24.8	[4]
A1	8.0	12.0	63.5	25.0	640.	800.	26.5	.	.	999.	999.	999.	26.8	[4]
A1	8.0	12.0	63.5	25.0	640.	800.	26.5	.	.	999.	999.	999.	26.8	[4]
A1	8.0	12.0	62.5	25.0	640.	800.	27.9	.	.	999.	999.	999.	25.4	[4]
A1	8.0	12.0	61.0	25.0	640.	800.	31.7	.	.	999.	999.	999.	33.5	[4]
A1	8.0	12.0	53.0	25.0	640.	800.	35.0	.	.	999.	999.	999.	23.0	[4]
A1	8.0	12.0	58.0	25.0	640.	800.	35.0	.	.	999.	999.	999.	26.2	[4]
A1	8.0	12.0	63.0	25.0	640.	800.	35.0	.	.	999.	999.	999.	28.7	[4]
A1	8.0	12.0	42.0	23.0	640.	800.	37.1	.	.	999.	999.	999.	20.3	[4]
A1	10.0	15.0	70.0	50.0	640.	800.	24.7	.	.	999.	999.	999.	30.5	[4]
A1	10.0	15.0	70.0	50.0	640.	800.	24.7	.	.	999.	999.	999.	32.6	[4]
A1	10.0	15.0	73.0	50.0	640.	800.	26.5	.	.	999.	999.	999.	33.5	[4]
A1	10.0	15.0	73.0	50.0	640.	800.	26.5	.	.	999.	999.	999.	38.2	[4]
A1	10.0	15.0	71.0	50.0	640.	800.	27.9	.	.	999.	999.	999.	38.7	[4]
A1	10.0	15.0	71.0	50.0	640.	800.	27.9	.	.	999.	999.	999.	38.9	[4]
A1	10.0	15.0	73.0	50.0	640.	800.	34.4	.	.	999.	999.	999.	47.9	[4]
A1	10.0	15.0	73.0	50.0	640.	800.	36.4	.	.	999.	999.	999.	49.6	[4]
A1	12.0	18.0	76.5	70.0	640.	800.	15.1	.	.	999.	999.	999.	28.4	[4]

.fz 3
.sa 1
2Tabelle A$n2$1 Versuchsdaten, Axialzug, (F), Einzelbefestigungen,
Dübel in der Fläche, c1≥1,5 hef

.ns
.sa 4

Syst. [-]	d [mm]	do [mm]	hef [mm]	Tinst [Nm]	fy [MPa]	ft [MPa]	fcc200 [MPa]	fct [MPa]	dagg [mm]	c1 [mm]	s1 [mm]	s2 [mm]	Nu,m [kN]	Lit.
A1	12.0	18.0	77.0	70.0	640.	800.	15.1	.	.	999.	999.	999.	26.6	[4]
A1	12.0	18.0	77.0	70.0	640.	800.	15.1	.	.	999.	999.	999.	28.3	[4]
A1	12.0	18.0	77.0	70.0	640.	800.	15.1	.	.	999.	999.	999.	32.8	[4]
A1	12.0	18.0	60.0	80.0	640.	800.	18.0	.	.	999.	999.	999.	24.7	[4]
A1	12.0	18.0	101.0	80.0	640.	800.	18.1	.	.	999.	999.	999.	44.1	[4]
A1	12.0	18.0	77.0	80.0	640.	800.	18.8	.	.	999.	999.	999.	35.1	[4]
A1	12.0	18.0	83.0	80.0	640.	800.	18.8	.	.	999.	999.	999.	38.9	[4]
A1	12.0	18.0	78.0	80.0	640.	800.	19.8	.	.	999.	999.	999.	40.2	[4]
A1	12.0	18.0	78.0	80.0	640.	800.	19.8	.	.	999.	999.	999.	41.1	[4]
A1	12.0	18.0	76.5	80.0	640.	800.	23.7	.	.	999.	999.	999.	49.6	[4]
A1	12.0	18.0	78.0	80.0	640.	800.	23.7	.	.	999.	999.	999.	52.8	[4]
A1	12.0	18.0	78.0	80.0	640.	800.	29.0	.	.	999.	999.	999.	58.1	[4]
A1	12.0	18.0	77.0	80.0	640.	800.	35.0	.	.	999.	999.	999.	66.7	[4]
A1	12.0	18.0	82.0	80.0	640.	800.	35.0	.	.	999.	999.	999.	71.9	[4]
A1	12.0	18.0	87.0	80.0	640.	800.	35.0	.	.	999.	999.	999.	74.8	[4]
A1	12.0	18.0	100.0	80.0	640.	800.	40.0	.	.	999.	999.	999.	73.6	[4]
A1	12.0	18.0	60.0	80.0	640.	800.	42.0	.	.	999.	999.	999.	46.4	[4]
A1	12.0	18.0	60.0	80.0	640.	800.	42.0	.	.	999.	999.	999.	47.5	[4]
A1	12.0	18.0	77.0	80.0	640.	800.	43.7	.	.	999.	999.	999.	62.1	[4]
A1	12.0	18.0	76.5	80.0	640.	800.	49.7	.	.	999.	999.	999.	67.3	[4]
A1	16.0	24.0	101.0	200.0	640.	800.	40.8	.	.	999.	999.	999.	91.8	[4]
A1	16.0	24.0	101.0	200.0	640.	800.	45.8	.	.	999.	999.	999.	92.7	[4]
A1	16.0	24.0	101.0	200.0	640.	800.	28.4	.	.	999.	999.	999.	82.4	[4]
A1	16.0	24.0	101.0	200.0	640.	800.	27.4	.	.	999.	999.	999.	74.4	[4]
A1	16.0	24.0	101.0	200.0	640.	800.	28.4	.	.	999.	999.	999.	78.0	[4]

.fz 3
.sa 1
2Tabelle A$n2$1 Versuchsdaten, Axialzug, (F), Einzelbefestigungen,
Dübel in der Fläche, c1≥1,5 hef

.ns
.sa 4

Syst. [-]	d [mm]	do [mm]	hef [mm]	Tinst [Nm]	fy [MPa]	ft [MPa]	fcc200 [MPa]	fct [MPa]	dagg [mm]	c1 [mm]	s1 [mm]	s2 [mm]	Nu,m [kN]	Lit.
A1	16.0	24.0	101.0	200.0	640.	800.	33.0	.	.	999.	999.	999.	81.3	[4]
A1	16.0	24.0	101.0	200.0	640.	800.	28.7	.	.	999.	999.	999.	62.7	[4]
A1	20.0	28.0	106.0	380.0	640.	800.	16.7	.	.	999.	999.	999.	81.4	[4]
A1	20.0	28.0	106.0	380.0	640.	800.	42.0	.	.	999.	999.	999.	120.0	[4]
A1	20.0	28.0	120.0	380.0	640.	800.	34.7	.	.	999.	999.	999.	129.3	[4]
A1	20.0	28.0	120.0	380.0	640.	800.	54.7	.	.	999.	999.	999.	149.7	[4]
A1	20.0	28.0	120.0	380.0	640.	800.	54.9	.	.	999.	999.	999.	156.4	[4]
A1	20.0	28.0	125.0	380.0	640.	800.	13.6	.	.	999.	999.	999.	66.3	[4]
A1	20.0	28.0	125.0	380.0	640.	800.	27.4	.	.	999.	999.	999.	130.2	[4]
A1	20.0	28.0	125.0	380.0	640.	800.	38.4	.	.	999.	999.	999.	163.2	[4]
A1	20.0	28.0	126.0	380.0	640.	800.	19.0	.	.	999.	999.	999.	80.2	[4]
A1	20.0	28.0	126.0	380.0	640.	800.	18.5	.	.	999.	999.	999.	98.7	[4]
A1	20.0	28.0	126.0	380.0	640.	800.	28.2	.	.	999.	999.	999.	117.9	[4]
A1	20.0	28.0	126.0	380.0	640.	800.	33.3	.	.	999.	999.	999.	120.1	[4]
A1	20.0	28.0	126.0	380.0	640.	800.	28.2	.	.	999.	999.	999.	131.2	[4]
A1	20.0	28.0	126.0	400.0	640.	800.	27.9	.	.	999.	999.	999.	101.0	[4]
A1	20.0	28.0	126.0	400.0	640.	800.	32.5	.	.	999.	999.	999.	104.5	[4]
A1	20.0	28.0	126.0	400.0	640.	800.	26.3	.	.	999.	999.	999.	110.3	[4]
A1	20.0	28.0	136.0	380.0	640.	800.	24.9	.	.	999.	999.	999.	114.8	[4]
A1	20.0	28.0	137.0	380.0	640.	800.	38.4	.	.	999.	999.	999.	141.6	[4]
A1	20.0	28.0	146.0	380.0	640.	800.	15.8	.	.	999.	999.	999.	97.2	[4]
A1	20.0	28.0	147.0	380.0	640.	800.	36.1	.	.	999.	999.	999.	153.2	[4]
A1	20.0	28.0	156.0	380.0	640.	800.	16.7	.	.	999.	999.	999.	116.2	[4]
A1	20.0	28.0	156.0	380.0	640.	800.	42.0	.	.	999.	999.	999.	189.2	[4]
B	8.0	12.0	60.0	25.0	640.	800.	27.9	.	.	999.	999.	999.	21.4	[4]

.fz 3
.sa 1
2Tabelle A$n2$1 Versuchsdaten, Axialzug, (F), Einzelbefestigungen,
Dübel in der Fläche, c1≥1,5·hef

.ns
.sa 4

Syst. [-]	d [mm]	do [mm]	hef [mm]	Tinst [Nm]	fy [MPa]	ft [MPa]	fcc200 [MPa]	fct [MPa]	dagg [mm]	c1 [mm]	s1 [mm]	s2 [mm]	Nu,m [kN]	Lit.
B	8.0	12.0	60.0	25.0	640.	800.	31.7	.	.	999.	999.	999.	30.3	[4]
B	10.0	15.0	69.0	50.0	640.	800.	24.7	.	.	999.	999.	999.	28.9	[4]
B	12.0	18.0	76.5	80.0	640.	800.	19.8	.	.	999.	999.	999.	33.5	[4]
B	12.0	18.0	76.5	80.0	640.	800.	49.7	.	.	999.	999.	999.	62.8	[4]

.fz 3
.sa 1
2Tabelle A$n2$1 Versuchsdaten, Axialzug, (F), Einzelbefestigungen,
DübelinderFläche, c1≥1,5·hef

.ue
.nn 1.1
.sa 4

Syst. [-]	d [mm]	do [mm]	hef [mm]	Tinst [Nm]	fy [MPa]	ft [MPa]	fcc200 [MPa]	fct [MPa]	dagg [mm]	c1 [mm]	s1 [mm]	s2 [mm]	Nu,m [kN]	Lit.
A1	6.0	6.3	17.6	.	630.	680.	22.0	1.5	.	999.	999.	999.	5.9	[8]
A1	6.0	6.3	17.6	.	630.	680.	49.0	3.1	.	999.	999.	999.	8.2	[8]
B	8.0	8.0	25.0	.	.	.	25.0	.	.	50.	999.	999.	6.6	[3]
B	8.0	8.0	25.0	.	.	.	25.0	.	.	63.	999.	999.	8.2	[3]
B	8.0	8.0	25.0	.	.	.	25.0	.	.	75.	999.	999.	7.5	[3]
B	6.0	9.5	25.0	.	.	.	22.0	1.5	.	999.	999.	999.	10.0	[8]
B	6.0	9.5	25.0	.	.	.	49.0	3.1	.	999.	999.	999.	15.4	[8]
B	8.0	8.0	25.0	.	.	.	11.2	.	.	999.	999.	999.	3.3	[3]
B	8.0	8.0	25.0	.	.	.	22.3	.	.	999.	999.	999.	5.6	[3]
B	8.0	8.0	25.0	.	.	.	12.5	.	.	999.	999.	999.	6.1	[3]
B	8.0	8.0	25.0	.	.	.	24.6	.	.	999.	999.	999.	7.2	[3]
B	8.0	8.0	25.0	.	.	.	29.6	.	.	999.	999.	999.	10.2	[3]
B	8.0	8.0	25.0	.	.	.	42.7	.	.	999.	999.	999.	10.6	[3]
B	8.0	8.0	25.0	.	.	.	50.7	.	.	999.	999.	999.	13.5	[3]
A1	9.0	9.5	26.6	.	684.	751.	22.0	1.5	.	999.	999.	999.	10.0	[8]
A1	9.0	9.5	26.6	.	684.	751.	49.0	3.1	.	999.	999.	999.	13.8	[8]
C	6.0	6.0	28.0	.	.	.	16.4	.	.	999.	999.	999.	6.3	[3]
C	6.0	6.0	28.0	.	.	.	20.5	.	.	999.	999.	999.	8.1	[3]
C	6.0	6.0	28.0	.	.	.	32.3	.	.	999.	999.	999.	9.1	[3]
C	10.0	10.4	28.0	.	.	.	45.8	.	.	999.	999.	999.	11.3	[3]
C	6.0	6.0	28.0	.	.	.	59.5	.	.	999.	999.	999.	12.4	[3]
C	10.0	10.4	28.0	.	.	.	56.8	.	.	999.	999.	999.	15.3	[3]
B	10.0	10.0	30.0	.	.	.	25.0	.	.	60.	999.	999.	9.6	[3]
B	10.0	10.0	30.0	.	.	.	25.0	.	.	75.	999.	999.	11.3	[3]
B	10.0	10.0	30.0	.	.	.	25.0	.	.	90.	999.	999.	11.4	[3]

.fz 3
.sa 1
2Tabelle A$n2$1 Versuchsdaten, Axialzug, (D), Einzelbefestigungen,
Dübel in der Fläche, c1≥1,5·hef

.ns
.sa 4

Syst. [-]	d [mm]	do [mm]	hef [mm]	Tinst [Nm]	fy [MPa]	ft [MPa]	fcc200 [MPa]	fct [MPa]	dagg [mm]	c1 [mm]	s1 [mm]	s2 [mm]	Nu,m [kN]	Lit.
B	10.0	10.0	30.0	.	.	.	13.1	.	.	999.	999.	999.	5.6	[3]
B	10.0	10.0	30.0	.	.	.	22.4	.	.	999.	999.	999.	9.8	[3]
B	10.0	10.0	30.0	.	.	.	20.6	.	.	999.	999.	999.	10.0	[3]
B	10.0	10.0	30.0	.	.	.	18.5	.	.	999.	999.	999.	11.8	[3]
B	10.0	10.0	30.0	.	.	.	26.4	.	.	999.	999.	999.	13.7	[3]
B	10.0	10.0	30.0	.	.	.	39.1	.	.	999.	999.	999.	17.9	[3]
C	12.0	12.0	31.0	.	.	.	25.0	.	.	60.	999.	999.	12.9	[3]
C	12.0	12.0	31.0	.	.	.	10.9	.	.	999.	999.	999.	6.7	[3]
C	12.0	12.0	31.0	.	.	.	14.3	.	.	999.	999.	999.	8.8	[3]
C	12.0	12.0	31.0	.	.	.	18.9	.	.	999.	999.	999.	9.0	[3]
C	12.0	12.0	31.0	.	.	.	26.7	.	.	999.	999.	999.	10.8	[3]
C	12.0	12.0	31.0	.	.	.	29.9	.	.	999.	999.	999.	15.1	[3]
C	12.0	12.0	31.0	.	.	.	43.1	.	.	999.	999.	999.	19.5	[3]
C	12.0	12.0	31.0	.	.	.	63.8	.	.	999.	999.	999.	20.3	[3]
A1	6.0	10.2	32.0	2.0	.	835.	23.2	2.0	.	999.	999.	999.	9.1	[2]
D	10.0	14.7	36.0	.	640.	800.	24.0	.	.	75.	999.	999.	12.9	[2]
D	10.0	14.7	36.0	.	640.	800.	59.0	.	.	75.	999.	999.	21.9	[2]
D	10.0	14.7	36.0	.	640.	800.	24.0	.	.	75.	999.	999.	16.1	[2]
D	10.0	14.7	36.0	.	640.	800.	59.0	.	.	75.	999.	999.	22.2	[2]
D	10.0	14.7	36.0	.	640.	800.	24.0	.	.	100.	999.	999.	16.9	[2]
D	10.0	14.7	36.0	.	640.	800.	59.0	.	.	100.	999.	999.	24.6	[2]
D	10.0	14.7	36.0	.	640.	800.	24.0	.	.	100.	999.	999.	18.4	[2]
D	10.0	14.7	36.0	.	640.	800.	59.0	.	.	100.	999.	999.	22.0	[2]
D	10.0	14.7	36.0	.	640.	800.	13.0	.	.	999.	999.	999.	10.4	[2]
D	10.0	14.7	36.0	.	640.	800.	38.0	.	.	999.	999.	999.	16.9	[2]

.fz 3
.sa 1
žTabelle A$n2$1 Versuchsdaten, Axialzug, (D), Einzelbefestigungen,
Dübel in der Fläche, c1≥1,5·hef

.ns
.sa 4

Syst. [-]	d [mm]	do [mm]	hef [mm]	Tinst [Nm]	fy [MPa]	ft [MPa]	fcc200 [MPa]	fct [MPa]	dagg [mm]	c1 [mm]	s1 [mm]	s2 [mm]	Nu,m [kN]	Lit.
D	10.0	14.7	36.0	.	640.	800.	28.0	.	.	999.	999.	999.	17.0	[2]
D	10.0	14.7	36.0	.	640.	800.	55.0	.	.	999.	999.	999.	23.5	[2]
D	8.0	12.7	36.5	.	640.	800.	25.0	.	.	75.	999.	999.	15.0	[2]
D	8.0	12.7	36.5	.	640.	800.	56.0	.	.	75.	999.	999.	22.3	[2]
D	8.0	12.7	36.5	.	640.	800.	25.0	.	.	75.	999.	999.	15.5	[2]
D	8.0	12.7	36.5	.	640.	800.	56.0	.	.	75.	999.	999.	24.2	[2]
D	8.0	12.7	36.5	.	640.	800.	25.0	.	.	100.	999.	999.	17.6	[2]
D	8.0	12.7	36.5	.	640.	800.	56.0	.	.	100.	999.	999.	25.5	[2]
D	8.0	12.7	36.5	.	640.	800.	25.0	.	.	100.	999.	999.	17.5	[2]
D	8.0	12.7	36.5	.	640.	800.	56.0	.	.	100.	999.	999.	25.7	[2]
D	8.0	12.7	36.5	.	640.	800.	13.0	.	.	999.	999.	999.	13.1	[2]
D	8.0	12.7	36.5	.	640.	800.	28.0	.	.	999.	999.	999.	16.2	[2]
D	8.0	12.7	36.5	.	640.	800.	38.0	.	.	999.	999.	999.	16.3	[2]
D	8.0	12.7	36.5	.	640.	800.	56.0	.	.	999.	999.	999.	20.3	[2]
B	12.0	12.0	37.0	.	.	.	25.0	.	.	70.	999.	999.	13.8	[3]
D	6.0	10.7	37.0	.	640.	800.	24.0	.	.	70.	999.	999.	14.3	[2]
D	6.0	10.7	37.0	.	640.	800.	24.0	.	.	75.	999.	999.	13.9	[2]
D	6.0	10.7	37.0	.	640.	800.	24.0	.	.	75.	999.	999.	16.1	[2]
D	6.0	10.7	37.0	.	640.	800.	24.0	.	.	80.	999.	999.	15.1	[2]
B	12.0	12.0	37.0	.	.	.	25.0	.	.	80.	999.	999.	15.8	[3]
D	6.0	10.7	37.0	.	640.	800.	24.0	.	.	100.	999.	999.	16.9	[2]
B	12.0	12.0	37.0	.	.	.	25.0	.	.	100.	999.	999.	16.2	[3]
D	6.0	10.7	37.0	.	640.	800.	24.0	.	.	100.	999.	999.	17.1	[2]
B	12.0	12.0	37.0	.	.	.	25.0	.	.	120.	999.	999.	16.8	[3]
D	6.0	10.7	37.0	.	640.	800.	13.0	.	.	999.	999.	999.	9.5	[2]

.fz 3
.sa 1
2Tabelle A$n2$1 Versuchsdaten, Axialzug, (D), Einzelbefestigungen,
Dübel in der Fläche, c1≥1,5·hef

.ns
.sa 4

Syst. [-]	d [mm]	do [mm]	hef [mm]	Tinst [Nm]	fy [MPa]	ft [MPa]	fcc200 [MPa]	fct [MPa]	dagg [mm]	c1 [mm]	s1 [mm]	s2 [mm]	Nu,m [kN]	Lit.
B	12.0	12.0	37.0	.	.	.	12.5	.	.	999.	999.	999.	11.7	[3]
A1	14.0	14.0	37.0	.	.	.	22.9	.	.	999.	999.	999.	14.5	[3]
D	6.0	10.7	37.0	.	640.	800.	28.0	.	.	999.	999.	999.	15.7	[2]
D	6.0	10.7	37.0	.	640.	800.	38.0	.	.	999.	999.	999.	16.1	[2]
B	12.0	12.0	37.0	.	.	.	26.4	.	.	999.	999.	999.	19.6	[3]
A1	14.0	14.0	37.0	.	.	.	63.5	.	.	999.	999.	999.	23.0	[3]
A1	10.0	10.0	38.0	.	.	.	25.0	.	.	100.	999.	999.	13.6	[3]
A1	10.0	10.0	38.0	.	.	.	25.6	.	.	999.	999.	999.	11.4	[3]
C	14.0	14.5	38.0	.	.	.	13.8	.	.	999.	999.	999.	11.9	[3]
C	14.0	14.5	38.0	.	.	.	20.5	.	.	999.	999.	999.	13.0	[3]
C	14.0	14.5	38.0	.	.	.	25.0	.	.	999.	999.	999.	15.7	[3]
C	14.0	14.5	38.0	.	.	.	27.2	.	.	999.	999.	999.	19.2	[3]
C	14.0	14.5	38.0	.	.	.	36.0	.	.	999.	999.	999.	19.9	[3]
C	14.0	14.5	38.0	.	.	.	44.1	.	.	999.	999.	999.	23.1	[3]
C	14.0	14.5	38.0	.	.	.	63.1	.	.	999.	999.	999.	25.9	[3]
A1	13.0	13.0	39.0	.	.	.	20.7	.	.	999.	999.	999.	14.7	[3]
A1	13.0	13.0	39.0	.	.	.	24.0	.	.	999.	999.	999.	17.5	[3]
A1	13.0	13.0	39.0	.	.	.	49.0	.	.	999.	999.	999.	27.9	[3]
D	8.0	12.0	40.0	4.0	640.	800.	23.0	.	.	.	.	.	15.0	[7]
D	8.0	12.0	40.0	4.0	640.	800.	59.0	.	.	.	.	.	26.2	[7]
D	8.0	12.0	40.0	12.5	640.	800.	26.0	.	.	.	.	.	16.0	[5]
D	8.0	12.0	40.0	12.5	640.	800.	29.8	.	.	.	.	.	18.1	[5]
D	8.0	12.0	40.0	12.5	640.	800.	45.7	.	.	.	.	.	23.0	[5]
B	9.0	12.7	40.0	.	.	.	22.0	1.5	.	999.	999.	999.	19.8	[8]
B	9.0	12.7	40.0	.	.	.	49.0	3.1	.	999.	999.	999.	34.1	[8]

.fz 3
.sa 1
2Tabelle A$n2$1 Versuchsdaten, Axialzug, (D), Einzelbefestigungen,
Dübel in der Fläche, c1≥1,5·hef

.ns
.sa 4

Syst. [-]	d [mm]	do [mm]	hef [mm]	Tinst [Nm]	fy [MPa]	ft [MPa]	fcc200 [MPa]	fct [MPa]	dagg [mm]	c1 [mm]	s1 [mm]	s2 [mm]	Nu,m [kN]	Lit.
A1	10.0	10.0	40.0	.	.	.	15.7	.	.	999.	999.	999.	10.6	[3]
A1	10.0	10.0	40.0	.	.	.	21.9	.	.	999.	999.	999.	10.8	[3]
B	12.0	12.0	40.0	.	.	.	13.1	.	.	999.	999.	999.	11.5	[3]
B	12.0	12.0	40.0	.	.	.	20.1	.	.	999.	999.	999.	13.2	[3]
B	12.0	12.0	40.0	.	.	.	20.6	.	.	999.	999.	999.	14.9	[3]
A1	10.0	10.0	40.0	.	.	.	39.9	.	.	999.	999.	999.	15.5	[3]
B	12.0	12.0	40.0	.	.	.	20.6	.	.	999.	999.	999.	16.3	[3]
A1	12.0	12.0	40.0	.	.	.	30.5	.	.	999.	999.	999.	16.8	[3]
B	12.0	12.0	40.0	.	.	.	26.2	.	.	999.	999.	999.	18.4	[3]
B	12.0	12.0	40.0	.	.	.	21.8	.	.	999.	999.	999.	18.6	[3]
B	12.0	12.0	40.0	.	.	.	26.2	.	.	999.	999.	999.	19.8	[3]
B	12.0	12.0	40.0	.	.	.	47.1	.	.	999.	999.	999.	21.4	[3]
A1	12.0	12.0	40.0	.	.	.	72.0	.	.	999.	999.	999.	24.6	[3]
D	8.0	14.2	40.0	4.0	640.	800.	30.1	2.4	.	999.	999.	999.	22.9	[7]
D	8.0	14.2	40.0	4.0	640.	800.	30.1	2.4	.	999.	999.	999.	23.6	[7]
D	8.0	14.2	40.0	4.0	640.	800.	64.1	3.9	.	999.	999.	999.	24.0	[7]
D	8.0	14.2	40.0	4.0	640.	800.	64.1	3.9	.	999.	999.	999.	27.4	[7]
D	6.0	10.9	40.0	5.0	.	812.	31.0	2.5	.	999.	999.	999.	14.5	[8]
A1	7.0	10.4	40.0	12.5	900.	1000.	35.0	1.9	.	999.	999.	999.	25.3	[2]
A1	7.0	10.4	40.0	12.5	900.	1000.	35.0	1.9	.	999.	999.	999.	25.3	[2]
D	8.0	12.7	40.0	20.0	640.	800.	26.5	2.2	.	999.	999.	999.	16.9	[2]
D	8.0	12.7	40.0	20.0	640.	800.	26.5	2.2	.	999.	999.	999.	16.9	[2]
D	8.0	12.7	40.0	20.0	640.	800.	29.4	2.3	.	999.	999.	999.	18.2	[2]
D	8.0	12.7	40.0	20.0	640.	800.	29.4	2.3	.	999.	999.	999.	18.2	[2]
A1	8.0	12.4	42.0	5.0	.	883.	23.2	2.0	.	999.	999.	999.	12.6	[2]

.fz 3
.sa 1
2Tabelle A$n2$1 Versuchsdaten, Axialzug, (D), Einzelbefestigungen,
Dübel in der Fläche, c1≥1,5·hef

.ns
.sa 4

Syst. [-]	d [mm]	do [mm]	hef [mm]	Tinst [Nm]	fy [MPa]	ft [MPa]	fcc200 [MPa]	fct [MPa]	dagg [mm]	c1 [mm]	s1 [mm]	s2 [mm]	Nu,m [kN]	Lit.
A1	10.0	10.0	44.0	.	.	.	21.9	.	.	999.	999.	999.	12.9	[3]
A1	10.0	10.0	44.0	.	.	.	27.5	.	.	999.	999.	999.	14.8	[3]
A1	16.0	16.0	45.0	.	.	.	21.5	.	.	999.	999.	999.	18.2	[3]
A1	17.0	17.0	45.0	.	.	.	20.7	.	.	999.	999.	999.	21.2	[3]
A1	17.0	17.0	45.0	.	.	.	24.0	.	.	999.	999.	999.	27.6	[3]
A1	17.0	17.0	45.0	.	.	.	49.0	.	.	999.	999.	999.	40.3	[3]
B	15.0	15.0	46.0	.	.	.	25.0	.	.	100.	999.	999.	22.3	[3]
B	15.0	15.0	46.0	.	.	.	25.0	.	.	125.	999.	999.	27.7	[3]
B	15.0	15.0	46.0	.	.	.	25.0	.	.	150.	999.	999.	26.7	[3]
B	15.0	15.0	46.0	.	.	.	25.0	.	.	175.	999.	999.	22.0	[3]
B	15.0	15.0	46.0	.	.	.	25.0	.	.	200.	999.	999.	27.8	[3]
B	15.0	15.0	46.0	.	.	.	12.4	.	.	999.	999.	999.	17.2	[3]
B	15.0	15.0	46.0	.	.	.	28.8	.	.	999.	999.	999.	30.6	[3]
B	15.0	15.0	46.0	.	.	.	36.3	.	.	999.	999.	999.	36.0	[3]
B	15.0	15.0	46.0	.	.	.	49.5	.	.	999.	999.	999.	43.3	[3]
A1	6.0	6.0	47.0	.	.	.	14.7	.	.	999.	999.	999.	9.8	[3]
A1	12.0	12.0	47.0	.	.	.	8.8	.	.	999.	999.	999.	11.0	[3]
A1	12.0	12.0	47.0	.	.	.	22.7	.	.	999.	999.	999.	13.1	[3]
A1	12.0	12.0	47.0	.	.	.	18.7	.	.	999.	999.	999.	13.8	[3]
A1	12.0	12.0	47.0	.	.	.	22.7	.	.	999.	999.	999.	15.1	[3]
A1	12.0	12.0	47.0	.	.	.	22.6	.	.	999.	999.	999.	15.8	[3]
A1	12.0	12.0	47.0	.	.	.	25.6	.	.	999.	999.	999.	19.9	[3]
A1	12.0	12.0	47.0	.	.	.	37.6	.	.	999.	999.	999.	20.8	[3]
A1	12.0	12.0	47.0	.	.	.	39.9	.	.	999.	999.	999.	26.6	[3]
D	8.0	12.0	50.0	12.5	640.	800.	26.0	.	.	.	.	.	21.2	[5]

.fz 3
.sa 1
2Tabelle A\$n2\$1 Versuchsdaten, Axialzug, (D), Einzelbefestigungen,
Dübel in der Fläche, c1≥1,5 hef

.ns
.sa 4

Syst. [-]	d [mm]	do [mm]	hef [mm]	Tinst [Nm]	fy [MPa]	ft [MPa]	fcc200 [MPa]	fct [MPa]	dagg [mm]	c1 [mm]	s1 [mm]	s2 [mm]	Nu,m [kN]	Lit.
B	15.0	15.0	50.0	.	.	.	13.1	.	.	999.	999.	999.	16.4	[3]
B	15.0	15.0	50.0	.	.	.	22.4	.	.	999.	999.	999.	19.1	[3]
B	15.0	15.0	50.0	.	.	.	24.1	.	.	999.	999.	999.	19.2	[3]
A1	13.0	13.0	50.0	.	.	.	24.0	.	.	999.	999.	999.	24.9	[3]
B	15.0	15.0	50.0	.	.	.	24.1	.	.	999.	999.	999.	25.8	[3]
D	8.0	14.3	50.0	4.0	640.	800.	28.2	2.9	.	999.	999.	999.	24.6	[7]
D	8.0	14.3	50.0	4.0	640.	800.	28.2	2.9	.	999.	999.	999.	27.2	[7]
D	8.0	14.3	50.0	4.0	640.	800.	60.7	3.1	.	999.	999.	999.	30.5	[7]
D	8.0	14.3	50.0	4.0	640.	800.	60.7	3.1	.	999.	999.	999.	30.8	[7]
D	8.0	12.8	50.0	10.0	.	812.	31.0	2.5	.	999.	999.	999.	20.7	[8]
D	8.0	14.4	50.0	10.0	640.	800.	35.0	1.9	.	999.	999.	999.	26.6	[7]
A1	10.0	16.4	51.0	10.0	.	906.	23.2	2.0	.	999.	999.	999.	22.0	[2]
C	17.0	17.5	53.0	.	.	.	25.0	.	.	100.	999.	999.	31.2	[3]
A1	12.0	12.0	53.0	.	.	.	25.0	.	.	130.	999.	999.	19.1	[3]
A1	12.0	12.0	53.0	.	.	.	17.3	.	.	999.	999.	999.	14.8	[3]
C	17.0	17.5	53.0	.	.	.	11.3	.	.	999.	999.	999.	19.1	[3]
C	17.0	17.5	53.0	.	.	.	14.4	.	.	999.	999.	999.	22.7	[3]
C	17.0	17.5	53.0	.	.	.	22.0	.	.	999.	999.	999.	26.6	[3]
C	17.0	17.5	53.0	.	.	.	29.1	.	.	999.	999.	999.	30.8	[3]
C	17.0	17.5	53.0	.	.	.	45.5	.	.	999.	999.	999.	44.6	[3]
B	20.0	20.0	55.0	.	.	.	25.0	.	.	120.	999.	999.	26.5	[3]
B	20.0	20.0	55.0	.	.	.	25.0	.	.	150.	999.	999.	30.5	[3]
B	20.0	20.0	55.0	.	.	.	25.0	.	.	180.	999.	999.	29.4	[3]
A1	10.0	10.0	55.0	.	.	.	20.5	.	.	999.	999.	999.	12.6	[3]
A1	10.0	10.0	55.0	.	.	.	20.9	.	.	999.	999.	999.	18.0	[3]

.fz 3
.sa 1
2Tabelle A$n2$1 Versuchsdaten, Axialzug, (D), Einzelbefestigungen,
Dübel in der Fläche, c1≥1,5 hef

.ns
.sa 4

Syst. [-]	d [mm]	do [mm]	hef [mm]	Tinst [Nm]	fy [MPa]	ft [MPa]	fcc200 [MPa]	fct [MPa]	dagg [mm]	c1 [mm]	s1 [mm]	s2 [mm]	Nu,m [kN]	Lit.
A1	12.0	12.0	55.0	.	.	.	26.1	.	.	999.	999.	999.	20.5	[3]
A1	14.0	14.0	55.0	.	.	.	22.5	.	.	999.	999.	999.	22.2	[3]
B	20.0	20.0	55.0	.	.	.	24.4	.	.	999.	999.	999.	29.5	[3]
A1	14.0	14.0	55.0	.	.	.	26.2	.	.	999.	999.	999.	29.8	[3]
B	20.0	20.0	55.0	.	.	.	26.4	.	.	999.	999.	999.	42.2	[3]
A1	14.0	14.0	55.0	.	.	.	55.4	.	.	999.	999.	999.	42.4	[3]
A1	14.0	14.0	55.0	.	.	.	70.3	.	.	999.	999.	999.	48.5	[3]
B	20.0	20.0	55.0	.	.	.	50.7	.	.	999.	999.	999.	57.3	[3]
A1	8.0	12.4	55.0	5.0	.	883.	23.2	2.0	.	999.	999.	999.	19.2	[2]
A1	14.0	14.0	57.0	.	.	.	22.7	.	.	999.	999.	999.	17.4	[3]
A1	20.0	20.0	57.0	.	.	.	19.2	.	.	999.	999.	999.	27.7	[3]
A1	20.0	20.0	57.0	.	.	.	48.8	.	.	999.	999.	999.	40.4	[3]
A1	20.0	20.0	57.0	.	.	.	63.5	.	.	999.	999.	999.	48.9	[3]
A1	16.0	16.0	59.0	.	.	.	15.7	.	.	999.	999.	999.	24.6	[3]
A1	16.0	16.0	59.0	.	.	.	63.0	.	.	999.	999.	999.	37.8	[3]
D	10.0	14.0	60.0	10.0	640.	800.	28.5	.	.	.	.	.	37.3	[8]
D	10.0	14.0	60.0	10.0	640.	800.	67.3	.	.	.	.	.	54.7	[8]
D	8.0	12.0	60.0	25.0	640.	800.	25.5	1.7	.	.	.	.	30.0	[8]
A1	14.0	14.0	60.0	.	.	.	25.0	.	.	140.	999.	999.	27.7	[3]
A1	19.0	19.0	60.0	.	.	.	68.5	.	.	999.	999.	999.	50.5	[3]
D	10.0	14.7	60.0	5.0	640.	800.	28.0	2.3	.	999.	999.	999.	35.6	[2]
D	10.0	14.7	60.0	5.0	640.	800.	28.0	2.3	.	999.	999.	999.	35.6	[2]
D	10.0	14.7	60.0	5.0	640.	800.	51.0	3.4	.	999.	999.	999.	43.8	[2]
D	10.0	14.7	60.0	5.0	640.	800.	51.0	3.4	.	999.	999.	999.	43.8	[2]
A1	10.0	16.3	60.0	10.0	.	.	56.0	3.1	.	999.	999.	999.	48.3	[0]

.fz 3
.sa 1
2Tabelle A$n2$1 Versuchsdaten, Axialzug, (D), Einzelbefestigungen,
Dübel in der Fläche, c1≥1,5hef

.ns
.sa 4

Syst. [-]	d [mm]	do [mm]	hef [mm]	Tinst [Nm]	fy [MPa]	ft [MPa]	fcc200 [MPa]	fct [MPa]	dagg [mm]	c1 [mm]	s1 [mm]	s2 [mm]	Nu,m [kN]	Lit.
A1	10.0	14.3	60.0	12.0	900.	1000.	31.0	2.6	.	999.	999.	999.	33.7	[3]
D	8.0	14.4	60.0	25.0	640.	800.	23.0	2.0	.	999.	999.	999.	27.7	[8]
D	8.0	14.4	60.0	25.0	640.	800.	25.5	1.8	.	999.	999.	999.	29.6	[8]
D	8.0	14.5	60.0	25.0	640.	800.	25.5	1.8	.	999.	999.	999.	30.5	[8]
D	10.0	16.3	60.0	30.0	833.	1022.	55.2	3.6	.	999.	999.	999.	50.7	[7]
D	10.0	14.7	60.0	40.0	886.	1036.	19.3	1.8	.	999.	999.	999.	22.5	[2]
D	10.0	14.7	60.0	40.0	886.	1036.	19.3	1.8	.	999.	999.	999.	22.5	[2]
D	10.0	14.7	60.0	40.0	.	812.	34.0	2.0	.	999.	999.	999.	29.7	[8]
D	10.0	16.0	60.0	50.0	640.	800.	28.5	2.3	.	999.	999.	999.	37.1	[8]
D	10.0	16.0	60.0	50.0	640.	800.	28.5	2.3	.	999.	999.	999.	37.4	[8]
D	10.0	16.0	60.0	50.0	640.	800.	28.5	2.3	.	999.	999.	999.	38.1	[8]
D	10.0	16.0	60.0	50.0	640.	800.	29.6	2.4	.	999.	999.	999.	49.1	[8]
A1	15.0	15.0	61.0	.	.	.	20.3	.	.	999.	999.	999.	29.4	[3]
A1	15.0	15.0	61.0	.	.	.	63.0	.	.	999.	999.	999.	45.8	[3]
B	15.0	22.2	62.0	.	.	.	22.0	1.5	.	999.	999.	999.	30.2	[8]
B	15.0	22.2	62.0	.	.	.	49.0	3.1	.	999.	999.	999.	61.0	[8]
C	21.0	21.5	63.0	.	.	.	25.0	.	.	120.	999.	999.	38.2	[3]
C	21.0	21.5	63.0	.	.	.	10.8	.	.	999.	999.	999.	19.4	[3]
C	21.0	21.5	63.0	.	.	.	13.8	.	.	999.	999.	999.	23.8	[3]
C	21.0	21.5	63.0	.	.	.	17.8	.	.	999.	999.	999.	33.5	[3]
C	21.0	21.5	63.0	.	.	.	21.9	.	.	999.	999.	999.	37.8	[3]
C	21.0	21.5	63.0	.	.	.	30.8	.	.	999.	999.	999.	44.0	[3]
C	21.0	21.5	63.0	.	.	.	42.8	.	.	999.	999.	999.	61.0	[3]
A1	10.0	10.0	65.0	.	.	.	14.7	.	.	999.	999.	999.	14.8	[3]
A1	10.0	10.0	65.0	.	.	.	30.5	.	.	999.	999.	999.	23.3	[3]

.fz 3
.sa 1
2Tabelle A$n2$1 Versuchsdaten, Axialzug, (D), Einzelbefestigungen,
Dübel in der Fläche, c1≥1,5 hef

.ns
.sa 4

Syst. [-]	d [mm]	do [mm]	hef [mm]	Tinst [Nm]	fy [MPa]	ft [MPa]	fcc200 [MPa]	fct [MPa]	dagg [mm]	c1 [mm]	s1 [mm]	s2 [mm]	Nu,m [kN]	Lit.
B	20.0	20.0	65.0	.	.	.	19.5	.	.	999.	999.	999.	29.6	[3]
B	20.0	20.0	65.0	.	.	.	20.5	.	.	999.	999.	999.	29.7	[3]
B	20.0	20.0	65.0	.	.	.	19.5	.	.	999.	999.	999.	36.5	[3]
B	20.0	20.0	65.0	.	.	.	27.1	.	.	999.	999.	999.	40.0	[3]
B	20.0	20.0	65.0	.	.	.	50.0	.	.	999.	999.	999.	52.0	[3]
A1	10.0	14.4	65.0	10.0	640.	800.	28.8	2.2	.	999.	999.	999.	36.4	[8]
A1	10.0	14.4	65.0	50.0	640.	800.	55.7	2.9	.	999.	999.	999.	37.1	[8]
A1	10.0	14.4	65.0	50.0	640.	800.	28.8	2.2	.	999.	999.	999.	38.1	[8]
A1	10.0	14.4	65.0	50.0	640.	800.	28.8	2.2	.	999.	999.	999.	38.1	[8]
A1	10.0	14.4	65.0	50.0	640.	800.	55.7	2.9	.	999.	999.	999.	39.7	[8]
A1	15.0	15.0	66.0	.	.	.	23.2	.	.	999.	999.	999.	30.5	[3]
A1	16.0	16.0	67.0	.	.	.	25.0	.	.	150.	999.	999.	29.0	[3]
A1	16.0	16.0	67.0	.	.	.	8.8	.	.	999.	999.	999.	19.2	[3]
A1	16.0	16.0	67.0	.	.	.	22.2	.	.	999.	999.	999.	33.1	[3]
A1	16.0	16.0	67.0	.	.	.	32.1	.	.	999.	999.	999.	45.5	[3]
A1	16.0	16.0	67.0	.	.	.	72.5	.	.	999.	999.	999.	59.9	[3]
A1	12.0	18.4	67.0	16.0	.	876.	22.0	1.9	.	999.	999.	999.	32.2	[2]
A1	18.0	18.0	70.0	.	.	.	22.6	.	.	999.	999.	999.	29.9	[3]
A1	18.0	18.0	70.0	.	.	.	25.6	.	.	999.	999.	999.	31.6	[3]
A1	18.0	18.0	70.0	.	.	.	37.6	.	.	999.	999.	999.	40.7	[3]
A1	10.0	15.4	70.0	10.0	640.	800.	48.0	3.3	.	999.	999.	999.	35.3	[7]
A1	10.0	15.4	70.0	50.0	640.	800.	36.0	2.7	.	999.	999.	999.	34.8	[7]
A1	10.0	15.4	70.0	50.0	640.	800.	48.0	3.3	.	999.	999.	999.	35.6	[7]
A1	19.0	19.0	71.0	.	.	.	25.0	.	.	160.	999.	999.	38.4	[3]
A1	19.0	19.0	71.0	.	.	.	17.6	.	.	999.	999.	999.	34.3	[3]

.fz 3
.sa 1
2Tabelle A$n2$1 Versuchsdaten, Axialzug, (D), Einzelbefestigungen,
Dübel in der Fläche, c1≥1,5·hef

.ns
.sa 4

Syst. [-]	d [mm]	do [mm]	hef [mm]	Tinst [Nm]	fy [MPa]	ft [MPa]	fcc200 [MPa]	fct [MPa]	dagg [mm]	c1 [mm]	s1 [mm]	s2 [mm]	Nu,m [kN]	Lit.
A1	19.0	19.0	71.0	.	.	.	24.0	.	.	999.	999.	999.	40.5	[3]
A1	19.0	19.0	71.0	.	.	.	24.0	.	.	999.	999.	999.	43.8	[3]
A1	14.0	14.0	73.0	.	.	.	20.5	.	.	999.	999.	999.	25.5	[3]
A1	14.0	14.0	73.0	.	.	.	23.0	.	.	999.	999.	999.	32.8	[3]
B	25.0	25.0	74.0	.	.	.	25.0	.	.	160.	999.	999.	41.9	[3]
B	25.0	25.0	74.0	.	.	.	25.0	.	.	200.	999.	999.	49.9	[3]
B	25.0	25.0	74.0	.	.	.	25.0	.	.	240.	999.	999.	65.0	[3]
B	25.0	25.0	74.0	.	.	.	12.2	.	.	999.	999.	999.	31.3	[3]
B	25.0	25.0	74.0	.	.	.	18.5	.	.	999.	999.	999.	39.3	[3]
B	25.0	25.0	74.0	.	.	.	29.4	.	.	999.	999.	999.	60.5	[3]
B	25.0	25.0	74.0	.	.	.	56.6	.	.	999.	999.	999.	105.0	[3]
A1	16.0	16.0	75.0	.	.	.	25.0	.	.	160.	999.	999.	43.7	[3]
A1	16.0	16.0	75.0	.	.	.	25.0	.	.	200.	999.	999.	46.4	[3]
A1	16.0	16.0	75.0	.	.	.	25.0	.	.	240.	999.	999.	48.3	[3]
A1	18.0	18.0	75.0	.	.	.	20.7	.	.	999.	999.	999.	40.1	[3]
A1	18.0	18.0	75.0	.	.	.	29.3	.	.	999.	999.	999.	54.2	[3]
A1	18.0	18.0	75.0	.	.	.	40.3	.	.	999.	999.	999.	62.6	[3]
A1	18.0	18.0	75.0	.	.	.	39.1	.	.	999.	999.	999.	67.6	[3]
A1	18.0	18.0	75.0	.	.	.	57.0	.	.	999.	999.	999.	79.3	[3]
A1	20.0	20.0	78.0	.	.	.	23.3	.	.	999.	999.	999.	39.1	[3]
A1	20.0	20.0	78.0	.	.	.	25.9	.	.	999.	999.	999.	46.6	[3]
A1	20.0	20.0	78.0	.	.	.	69.8	.	.	999.	999.	999.	68.9	[3]
C	12.0	18.4	80.0	.	640.	800.	24.0	.	.	140.	999.	999.	42.4	[2]
C	12.0	18.4	80.0	.	640.	800.	24.0	.	.	140.	999.	999.	45.5	[2]
C	12.0	18.4	80.0	.	640.	800.	24.0	.	.	160.	999.	999.	45.1	[2]

.fz 3
.sa 1
2Tabelle A$n2$1 Versuchsdaten, Axialzug, (D), Einzelbefestigungen,
Dübel in der Fläche, c1≥1,5·hef

.ns
.sa 4

Syst. [-]	d [mm]	do [mm]	hef [mm]	Tinst [Nm]	fy [MPa]	ft [MPa]	fcc200 [MPa]	fct [MPa]	dagg [mm]	c1 [mm]	s1 [mm]	s2 [mm]	Nu,m [kN]	Lit.
B	25.0	25.0	80.0	.	.	.	19.5	.	.	999.	999.	999.	48.8	[3]
C	12.0	18.4	80.0	.	640.	800.	49.0	.	.	999.	999.	999.	75.8	[2]
C	12.0	18.4	80.0	.	640.	800.	49.0	.	.	999.	999.	999.	76.0	[2]
A1	10.0	16.3	80.0	16.0	.	1139.	30.5	2.4	.	999.	999.	999.	46.4	[2]
A1	10.0	16.3	80.0	16.0	.	1139.	30.5	2.4	.	999.	999.	999.	46.4	[2]
A1	12.0	18.4	80.0	16.0	640.	800.	40.8	2.9	.	999.	999.	999.	52.8	[8]
A1	12.0	18.3	80.0	40.0	640.	800.	26.9	2.1	.	999.	999.	999.	45.6	[7]
A1	12.0	18.3	80.0	40.0	640.	800.	29.3	2.4	.	999.	999.	999.	53.2	[7]
A1	12.0	18.4	80.0	80.0	640.	800.	30.0	2.4	.	999.	999.	999.	38.4	[8]
A1	12.0	18.4	80.0	80.0	640.	800.	30.0	2.4	.	999.	999.	999.	40.8	[8]
A1	12.0	18.4	80.0	80.0	640.	800.	40.8	2.9	.	999.	999.	999.	49.3	[8]
A1	12.0	18.4	80.0	80.0	640.	800.	40.8	2.9	.	999.	999.	999.	51.6	[8]
D	12.0	18.3	80.0	80.0	978.	1101.	55.2	3.6	.	999.	999.	999.	75.8	[7]
A1	18.0	18.0	81.0	.	.	.	20.5	.	.	999.	999.	999.	40.7	[3]
A1	20.0	20.0	82.0	.	.	.	22.7	.	.	999.	999.	999.	32.8	[3]
A1	16.0	24.4	82.0	40.0	.	862.	23.2	2.0	.	999.	999.	999.	49.0	[2]
C	25.0	25.4	83.0	.	.	.	25.0	.	.	160.	999.	999.	60.5	[3]
C	25.0	25.4	83.0	.	.	.	17.9	.	.	999.	999.	999.	41.1	[3]
C	25.0	25.4	83.0	.	.	.	14.3	.	.	999.	999.	999.	41.4	[3]
C	25.0	25.4	83.0	.	.	.	19.5	.	.	999.	999.	999.	55.3	[3]
C	25.0	25.4	83.0	.	.	.	28.7	.	.	999.	999.	999.	67.7	[3]
C	25.0	25.4	83.0	.	.	.	50.9	.	.	999.	999.	999.	76.0	[3]
C	25.0	25.4	83.0	.	.	.	68.8	.	.	999.	999.	999.	92.4	[3]
A1	22.0	22.0	87.0	.	.	.	25.0	.	.	200.	999.	999.	48.2	[3]
A1	22.0	22.0	87.0	.	.	.	22.5	.	.	999.	999.	999.	47.4	[3]

.fz 3
.sa 1
2Tabelle A$n2$1 Versuchsdaten, Axialzug, (D), Einzelbefestigungen,
Dübel in der Fläche, c1≥1,5·hef

.ns
.sa 4

Syst. [-]	d [mm]	do [mm]	hef [mm]	Tinst [Nm]	fy [MPa]	ft [MPa]	fcc200 [MPa]	fct [MPa]	dagg [mm]	c1 [mm]	s1 [mm]	s2 [mm]	Nu,m [kN]	Lit.
A1	22.0	22.0	87.0	.	.	.	27.2	.	.	999.	999.	999.	53.3	[3]
A1	22.0	22.0	87.0	.	.	.	55.6	.	.	999.	999.	999.	102.2	[3]
A1	24.0	24.0	89.0	.	.	.	25.0	.	.	250.	999.	999.	58.7	[3]
A1	24.0	24.0	89.0	.	.	.	22.6	.	.	999.	999.	999.	46.5	[3]
A1	24.0	24.0	89.0	.	.	.	22.7	.	.	999.	999.	999.	50.5	[3]
A1	24.0	24.0	89.0	.	.	.	37.6	.	.	999.	999.	999.	62.9	[3]
A1	22.0	22.0	90.0	.	.	.	20.5	.	.	999.	999.	999.	51.0	[3]
A1	22.0	22.0	90.0	.	.	.	68.0	.	.	999.	999.	999.	90.9	[3]
A1	25.0	25.0	94.0	.	.	.	25.0	.	.	250.	999.	999.	53.5	[3]
A1	24.0	24.0	97.0	.	.	.	25.0	.	.	200.	999.	999.	58.5	[3]
A1	24.0	24.0	97.0	.	.	.	19.4	.	.	999.	999.	999.	53.9	[3]
A1	24.0	24.0	97.0	.	.	.	20.3	.	.	999.	999.	999.	70.6	[3]
A1	24.0	24.0	97.0	.	.	.	45.0	.	.	999.	999.	999.	87.6	[3]
D	16.0	24.0	100.0	200.0	640.	800.	35.0	.	.	.	.	.	82.2	[2]
A1	24.0	24.0	100.0	.	.	.	25.0	.	.	210.	999.	999.	77.7	[3]
A1	24.0	24.0	100.0	.	.	.	25.0	.	.	260.	999.	999.	80.3	[3]
A1	24.0	24.0	100.0	.	.	.	25.0	.	.	263.	999.	999.	79.0	[3]
A1	25.0	25.0	100.0	.	.	.	24.5	.	.	999.	999.	999.	60.7	[3]
A1	24.0	24.0	100.0	.	.	.	18.3	.	.	999.	999.	999.	62.1	[3]
A1	25.0	25.0	100.0	.	.	.	24.6	.	.	999.	999.	999.	65.5	[3]
A1	24.0	24.0	100.0	.	.	.	19.9	.	.	999.	999.	999.	72.2	[3]
A1	24.0	24.0	100.0	.	.	.	40.3	.	.	999.	999.	999.	96.6	[3]
A1	25.0	25.0	100.0	.	.	.	56.2	.	.	999.	999.	999.	102.9	[3]
A1	24.0	24.0	100.0	.	.	.	39.1	.	.	999.	999.	999.	117.2	[3]
A1	24.0	24.0	100.0	.	.	.	61.7	.	.	999.	999.	999.	147.3	[3]

.fz 3
.sa 1
2Tabelle A$n2$1 Versuchsdaten, Axialzug, (D), Einzelbefestigungen,
Dübel in der Fläche, c1≥1,5 hef

.ns
.sa 4

Syst. [-]	d [mm]	do [mm]	hef [mm]	Tinst [Nm]	fy [MPa]	ft [MPa]	fcc200 [MPa]	fct [MPa]	dagg [mm]	c1 [mm]	s1 [mm]	s2 [mm]	Nu,m [kN]	Lit.
D	12.0	18.0	105.0	80.0	640.	800.	41.0	2.4	.	.	.	.	83.5	[7]
A1	28.0	28.0	105.0	.	.	.	8.8	.	.	999.	999.	999.	45.1	[3]
A1	28.0	28.0	105.0	.	.	.	22.7	.	.	999.	999.	999.	54.5	[3]
A1	25.0	25.0	105.0	.	.	.	22.7	.	.	999.	999.	999.	57.4	[3]
A1	28.0	28.0	105.0	.	.	.	25.0	.	.	999.	999.	999.	86.2	[3]
A1	28.0	28.0	105.0	.	.	.	32.3	.	.	999.	999.	999.	95.7	[3]
A1	28.0	28.0	105.0	.	.	.	62.2	.	.	999.	999.	999.	133.0	[3]
A1	28.0	28.0	105.0	.	.	.	75.4	.	.	999.	999.	999.	157.0	[3]
A1	28.0	28.0	114.0	.	.	.	22.7	.	.	999.	999.	999.	68.8	[3]
D	16.0	24.4	123.9	180.0	640.	800.	63.0	3.9	.	999.	999.	999.	128.2	[8]
D	16.0	24.0	124.0	180.0	640.	800.	35.0	2.3	.	.	.	.	101.3	[8]
D	16.0	24.4	124.5	180.0	640.	800.	35.0	2.6	.	999.	999.	999.	101.8	[8]
D	16.0	.	125.0	100.0	902.	997.	37.7	3.3	16.	188.	999.	999.	120.9	[7]
D	16.0	.	125.0	100.0	902.	997.	37.7	3.3	16.	250.	999.	999.	120.6	[7]
A1	28.0	28.0	125.0	.	.	.	18.3	.	.	999.	999.	999.	84.5	[3]
A1	28.0	28.0	125.0	.	.	.	24.2	.	.	999.	999.	999.	114.6	[3]
A1	28.0	28.0	125.0	.	.	.	39.1	.	.	999.	999.	999.	171.6	[3]
A1	28.0	28.0	125.0	.	.	.	55.5	.	.	999.	999.	999.	201.8	[3]
A1	16.0	24.4	125.0	36.0	640.	800.	29.4	2.3	.	999.	999.	999.	81.8	[8]
D	16.0	.	125.0	100.0	902.	997.	37.7	3.3	16.	999.	999.	999.	121.2	[7]
A1	16.0	24.4	125.0	180.0	640.	800.	24.8	2.1	.	999.	999.	999.	72.3	[8]
A1	16.0	24.4	125.0	180.0	640.	800.	24.8	2.1	.	999.	999.	999.	76.5	[8]
A1	16.0	24.4	125.0	180.0	640.	800.	54.9	3.6	.	999.	999.	999.	93.5	[8]
A1	16.0	24.4	125.0	180.0	640.	800.	58.4	3.7	.	999.	999.	999.	100.5	[8]
A1	32.0	32.0	148.0	.	.	.	18.3	.	.	999.	999.	999.	90.4	[3]

.fz 3
.sa 1
2Tabelle A$n2$1 Versuchsdaten, Axialzug, (D), Einzelbefestigungen,
Dübel in der Fläche, c1≥1,5·hef

.ns
.sa 4

Syst. [-]	d [mm]	do [mm]	hef [mm]	Tinst [Nm]	fy [MPa]	ft [MPa]	fcc200 [MPa]	fct [MPa]	dagg [mm]	c1 [mm]	s1 [mm]	s2 [mm]	Nu,m [kN]	Lit.
A1	32.0	32.0	148.0	.	.	.	26.1	.	.	999.	999.	999.	142.0	[3]
A1	32.0	32.0	148.0	.	.	.	42.9	.	.	999.	999.	999.	204.6	[3]
A1	32.0	32.0	148.0	.	.	.	46.6	.	.	999.	999.	999.	222.6	[3]
D	20.0	.	170.0	200.0	1047.	1134.	28.3	2.6	16.	255.	999.	999.	183.2	[7]
D	20.0	.	170.0	200.0	1047.	1134.	28.3	2.6	16.	340.	999.	999.	190.7	[7]
D	20.0	.	170.0	200.0	1047.	1134.	28.3	2.6	16.	999.	999.	999.	199.6	[7]
D	24.0	32.0	200.0	150.0	640.	800.	42.0	2.0	.	.	.	.	258.8	[7]
D	24.0	.	220.0	300.0	1144.	1242.	33.2	3.0	16.	330.	999.	999.	235.3	[7]
D	24.0	32.3	220.0	60.0	900.	1000.	42.0	3.0	.	999.	999.	999.	257.2	[7]
D	24.0	.	220.0	300.0	1144.	1242.	27.6	2.8	16.	999.	999.	999.	240.3	[7]

.fz 3
.sa 1
2Tabelle A$n2$1 Versuchsdaten, Axialzug, (D), Einzelbefestigungen,
Dübel in der Fläche, c1≥1,5 hef

.ue
.nn 4.1
.sa 4

Syst. [-]	d [mm]	do [mm]	hef [mm]	Tinst [Nm]	fy [MPa]	ft [MPa]	fcc200 [MPa]	fct [MPa]	dagg [mm]	c1 [mm]	s1 [mm]	s2 [mm]	Nu,m [kN]	Lit.
A3	10.0	10.2	32.0	45.0	540.	610.	23.2	.	16.	100.	999.	999.	14.2	[31]
A3	10.0	10.4	32.0	20.0	560.	575.	26.7	.	16.	999.	999.	999.	12.6	[31]
A3	8.0	8.4	35.0	25.0	550.	620.	40.5	.	16.	80.	999.	999.	16.9	[31]
A3	8.0	8.2	36.0	25.0	550.	620.	26.0	.	16.	80.	999.	999.	14.1	[31]
A3	10.0	10.2	36.0	45.0	540.	610.	23.2	.	16.	100.	999.	999.	16.1	[31]
A3	8.0	8.2	37.0	25.0	550.	620.	40.6	.	16.	80.	999.	999.	16.6	[31]
A3	8.0	8.2	38.0	25.0	550.	620.	25.7	.	16.	80.	999.	999.	15.5	[31]
A3	10.0	10.2	39.0	45.0	540.	610.	40.6	.	16.	100.	999.	999.	19.5	[31]
A3	10.0	10.2	41.0	45.0	540.	610.	26.0	.	16.	100.	999.	999.	14.8	[31]
A3	10.0	10.2	41.0	45.0	540.	610.	40.5	.	16.	100.	999.	999.	21.3	[31]
D	6.0	10.7	43.0	8.5	855.	930.	23.1	.	16.	999.	999.	999.	13.7	[31]
D	6.0	10.7	44.0	8.5	855.	930.	25.8	.	16.	999.	999.	999.	15.0	[31]
A3	10.0	10.4	46.0	45.0	540.	610.	18.2	.	16.	100.	999.	999.	17.6	[31]
A3	16.0	16.4	48.0	90.0	425.	480.	24.9	.	16.	999.	999.	999.	26.8	[31]
A3	16.0	16.4	51.0	120.0	430.	500.	25.7	.	16.	160.	999.	999.	29.3	[31]
A3	10.0	10.3	55.0	20.0	560.	575.	23.4	.	16.	999.	999.	999.	17.9	[31]
A3	12.0	12.3	57.0	35.0	560.	575.	42.6	.	16.	999.	999.	999.	31.0	[31]
A3	16.0	16.4	58.0	120.0	430.	500.	25.7	.	16.	160.	999.	999.	33.4	[31]
D	8.0	14.0	60.0	25.0	795.	885.	26.9	.	16.	999.	999.	999.	26.7	[31]
D	10.0	14.7	63.0	40.0	855.	930.	42.6	.	16.	999.	999.	999.	35.0	[31]
D	10.0	14.7	64.0	40.0	855.	930.	23.1	.	16.	999.	999.	999.	23.7	[31]
A3	16.0	16.4	65.0	120.0	430.	500.	20.7	.	16.	160.	999.	999.	27.9	[31]
A3	16.0	16.3	67.0	120.0	430.	500.	40.5	.	16.	150.	999.	999.	47.1	[31]
D	12.0	18.0	72.0	80.0	795.	885.	26.9	.	16.	999.	999.	999.	40.0	[31]
D	12.0	18.0	72.0	80.0	795.	885.	43.7	.	16.	999.	999.	999.	46.3	[31]
D	16.0	22.7	103.0	130.0	815.	910.	28.9	.	16.	999.	999.	999.	49.6	[31]
D	16.0	22.7	104.0	130.0	815.	910.	42.8	.	16.	999.	999.	999.	69.0	[31]
D	16.0	24.0	125.0	180.0	660.	855.	16.3	.	16.	999.	999.	999.	76.2	[31]

.fz 3
.sa 1
2Tabelle $n2$1 Versuchsdaten, Axialzug, (S), Einzelbefestigungen,
Dübel in der Fläche

.ue
.nn 17.1
.sa 4

Syst.	d	dh	hef	Tinst	fy	ft	fcc200	fct	dagg	c1	s1	s2	Nu	Lit.	[-]
[mm]	[mm]	[mm]	[Nm]	[MPa]	[MPa]	[MPa]	[MPa]	[mm]	[mm]	[mm]	[mm]	[kN]			
Kb	19.5	31.8	193.6	.	345.	414.	43.1	.	.	305.	999.	999.	133.8	[14]	
Kb	19.5	31.8	92.1	.	345.	414.	24.4	.	.	305.	999.	999.	53.3	[14]	
Kb	19.5	31.8	193.6	.	345.	414.	43.1	.	.	305.	999.	999.	140.1	[14]	
Kb	19.5	31.8	92.1	.	345.	414.	42.1	.	.	305.	999.	999.	82.2	[14]	
Kb	19.5	28.5	63.5	.	345.	414.	25.3	.	.	381.	999.	999.	71.1	[14]	
Kb	19.5	31.8	92.1	.	345.	414.	24.4	.	.	305.	999.	999.	48.9	[14]	
Kb	19.5	31.8	92.1	.	345.	414.	42.1	.	.	305.	999.	999.	82.2	[14]	
Kb	19.5	28.5	88.9	.	345.	414.	25.3	.	.	381.	999.	999.	112.9	[14]	
Kb	19.5	31.8	92.1	.	345.	414.	24.4	.	.	305.	999.	999.	62.2	[14]	
Kb	19.5	31.8	92.1	.	345.	414.	42.1	.	.	305.	999.	999.	76.9	[14]	
Kb	19.5	28.5	88.9	.	345.	414.	39.6	.	.	102.	999.	999.	88.5	[14]	
Kb	22.2	34.9	193.6	.	345.	414.	39.8	.	.	305.	999.	999.	191.2	[14]	
Kb	25.4	41.2	251.4	.	827.	1034.	35.1	.	.	457.	999.	999.	435.9	[14]	
Kb	25.4	51.0	76.0	.	248.	.	27.1	.	.	229.	999.	999.	62.3	[30]	
Kb	25.4	51.0	127.0	.	248.	.	25.3	.	.	584.	999.	999.	100.1	[30]	
Kb	25.4	102.0	127.0	.	248.	.	25.2	.	.	584.	999.	999.	117.4	[30]	
Kb	12.7	25.4	93.7	.	345.	414.	24.3	.	.	305.	999.	999.	34.7	[47]	
Kb	15.9	31.8	87.3	.	345.	414.	24.3	.	.	305.	999.	999.	62.3	[47]	
Kb	15.9	31.8	87.3	.	345.	414.	24.3	.	.	305.	999.	999.	55.2	[47]	
Kb	15.9	31.8	87.3	.	345.	414.	24.3	.	.	305.	999.	999.	41.8	[47]	
Kb	19.0	38.1	87.3	.	345.	414.	24.3	.	.	305.	999.	999.	62.3	[47]	
Kb	19.0	31.8	88.9	.	345.	414.	24.3	.	.	305.	999.	999.	48.0	[47]	
Kb	19.0	31.8	88.9	.	345.	414.	24.3	.	.	305.	999.	999.	48.0	[47]	
Kb	19.0	31.8	88.9	.	345.	414.	24.3	.	.	305.	999.	999.	55.2	[47]	
Kb	19.0	31.8	88.9	.	345.	414.	24.3	.	.	305.	999.	999.	52.0	[47]	
Kb	22.2	34.9	88.9	.	345.	414.	24.3	.	.	305.	999.	999.	48.0	[47]	
Kb	22.2	34.9	88.9	.	345.	414.	24.3	.	.	305.	999.	999.	55.2	[47]	
Kb	22.2	44.5	88.9	.	345.	414.	24.3	.	.	305.	999.	999.	62.3	[47]	

.fz 3
.sa 1
2Tabelle $n2$1 Versuchsdaten, Axialzug, (USA), Einzelbefestigungen,
Kopfbolzen in der Fläche, c1≥1,0hef

.ue
.nn 15.1
.sa 4

Syst. [-]	d [mm]	dh [mm]	hef [mm]	Tinst [Nm]	fy [MPa]	ft [MPa]	fcc200 [MPa]	fct [MPa]	dagg [mm]	c1 [mm]	s1 [mm]	s2 [mm]	Nu [kN]	Lit.
E	9.5	19.0	42.9	.	350.	450.	13.8	.	.	80.	999.	999.	13.2	[10]
E	9.5	19.0	42.9	.	350.	450.	13.8	.	.	80.	999.	999.	14.0	[10]
E	9.5	19.0	42.9	.	350.	450.	13.8	.	.	80.	999.	999.	14.8	[10]
E	9.5	19.0	42.9	.	350.	450.	28.4	.	.	80.	999.	999.	20.2	[10]
E	9.5	19.0	42.9	.	350.	450.	28.4	.	.	80.	999.	999.	21.2	[10]
E	9.5	19.0	42.9	.	350.	450.	28.4	.	.	80.	999.	999.	21.2	[10]
E	9.5	19.5	42.9	.	350.	450.	27.9	.	.	200.	999.	999.	15.2	[10]
E	9.5	19.5	42.9	.	350.	450.	28.4	.	.	200.	999.	999.	16.0	[10]
E	9.5	19.5	42.9	.	350.	450.	25.1	.	.	200.	999.	999.	18.2	[10]
E	9.5	19.5	42.9	.	350.	450.	25.1	.	.	200.	999.	999.	19.2	[10]
E	9.5	19.5	42.9	.	350.	450.	27.9	.	.	200.	999.	999.	20.6	[10]
E	9.5	19.5	42.9	.	350.	450.	27.9	.	.	200.	999.	999.	20.6	[10]
E	9.5	19.5	42.9	.	350.	450.	25.1	.	.	200.	999.	999.	20.8	[10]
E	9.5	19.5	42.9	.	350.	450.	25.1	.	.	200.	999.	999.	20.8	[10]
E	9.5	19.5	42.9	.	350.	450.	27.9	.	.	200.	999.	999.	21.0	[10]
E	9.5	19.5	42.9	.	350.	450.	27.9	.	.	200.	999.	999.	21.2	[10]
E	9.5	19.5	42.9	.	350.	450.	25.1	.	.	200.	999.	999.	22.0	[10]
E	9.5	19.5	42.9	.	350.	450.	27.9	.	.	200.	999.	999.	22.6	[10]
E	9.5	19.5	42.9	.	350.	450.	35.2	.	.	200.	999.	999.	23.0	[10]
E	9.5	19.5	42.9	.	350.	450.	28.4	.	.	200.	999.	999.	24.0	[10]
E	9.5	19.5	42.9	.	350.	450.	25.1	.	.	200.	999.	999.	24.8	[10]
E	9.5	19.5	42.9	.	350.	450.	36.5	.	.	200.	999.	999.	25.0	[10]
E	9.5	19.5	42.9	.	350.	450.	36.5	.	.	200.	999.	999.	25.0	[10]
E	9.5	19.5	42.9	.	350.	450.	35.2	.	.	200.	999.	999.	25.5	[10]
E	9.5	19.5	42.9	.	350.	450.	36.5	.	.	200.	999.	999.	27.0	[10]

.fz 3
.sa 1
2Tabelle A$n2$1 Versuchsdaten, Axialzug, (D), Einzelbefestigungen,
Kopfbolzen in der Fläche, c1≥1,5 hef

.ns
.sa 4

Syst. [-]	d [mm]	dh [mm]	hef [mm]	Tinst [Nm]	fy [MPa]	ft [MPa]	fcc200 [MPa]	fct [MPa]	dagg [mm]	c1 [mm]	s1 [mm]	s2 [mm]	Nu [kN]	Lit.
E	9.5	19.5	42.9	.	350.	450.	35.2	.	.	200.	999.	999.	27.0	[10]
E	9.5	19.0	42.9	.	350.	450.	35.2	.	.	200.	999.	999.	27.0	[10]
E	9.5	19.5	42.9	.	350.	450.	35.2	.	.	200.	999.	999.	27.5	[10]
E	9.5	19.0	42.9	.	350.	450.	35.2	.	.	200.	999.	999.	29.5	[10]
E	22.2	34.9	65.3	.	350.	450.	30.5	.	.	200.	999.	999.	30.5	[10]
E	22.2	34.9	65.3	.	350.	450.	30.5	.	.	200.	999.	999.	41.4	[10]
E	22.2	34.9	65.3	.	350.	450.	30.5	.	.	200.	999.	999.	42.4	[10]
E	15.9	31.8	67.1	.	350.	450.	13.8	.	.	120.	999.	999.	32.0	[10]
E	15.9	31.8	67.1	.	350.	450.	13.8	.	.	120.	999.	999.	32.8	[10]
E	15.9	31.8	67.1	.	350.	450.	13.8	.	.	120.	999.	999.	33.2	[10]
E	15.9	31.8	67.1	.	350.	450.	28.4	.	.	120.	999.	999.	47.6	[10]
E	15.9	31.8	67.1	.	350.	450.	28.4	.	.	120.	999.	999.	49.6	[10]
E	15.9	31.8	67.1	.	350.	450.	28.4	.	.	120.	999.	999.	52.8	[10]
E	15.9	31.8	67.1	.	350.	450.	22.7	.	.	200.	999.	999.	37.0	[10]
E	15.9	31.8	67.1	.	350.	450.	22.7	.	.	200.	999.	999.	40.5	[10]
E	15.9	31.8	67.1	.	350.	450.	22.7	.	.	200.	999.	999.	42.0	[10]
E	15.9	31.8	67.1	.	350.	450.	22.7	.	.	200.	999.	999.	43.5	[10]
E	15.9	31.8	67.1	.	350.	450.	22.7	.	.	200.	999.	999.	44.0	[10]
E	15.9	31.8	67.1	.	350.	450.	22.7	.	.	200.	999.	999.	49.5	[10]
E	15.9	31.8	67.1	.	350.	450.	11.4	.	.	300.	999.	999.	29.0	[10]
E	15.9	31.8	67.1	.	350.	450.	11.4	.	.	300.	999.	999.	32.0	[10]
E	15.9	31.8	67.1	.	350.	450.	11.4	.	.	300.	999.	999.	37.0	[10]
E	15.9	31.8	67.1	.	350.	450.	22.7	.	.	300.	999.	999.	37.5	[10]
E	15.9	31.8	67.1	.	350.	450.	22.7	.	.	300.	999.	999.	39.0	[10]
E	15.9	31.8	67.1	.	350.	450.	22.7	.	.	300.	999.	999.	40.0	[10]

.fz 3
.sa 1
2Tabelle A$n2$1 Versuchsdaten, Axialzug, (D), Einzelbefestigungen,
Kopfbolzen in der Fläche, c1≥1,5·hef

.ns
.sa 4

Syst. [-]	d [mm]	dh [mm]	hef [mm]	Tinst [Nm]	fy [MPa]	ft [MPa]	fcc200 [MPa]	fct [MPa]	dagg [mm]	c1 [mm]	s1 [mm]	s2 [mm]	Nu [kN]	Lit.
E	15.9	31.8	67.1	.	350.	450.	22.7	.	.	300.	999.	999.	40.0	[10]
E	15.9	31.8	67.1	.	350.	450.	22.7	.	.	300.	999.	999.	42.0	[10]
E	15.9	31.8	67.1	.	350.	450.	22.7	.	.	300.	999.	999.	45.0	[10]
E	15.9	31.8	67.1	.	350.	450.	46.4	.	.	300.	999.	999.	54.0	[10]
E	15.9	31.8	67.1	.	350.	450.	46.4	.	.	300.	999.	999.	56.0	[10]
E	15.9	31.8	67.1	.	350.	450.	46.4	.	.	300.	999.	999.	57.0	[10]
E	15.9	31.8	67.1	.	350.	450.	37.3	.	.	300.	999.	999.	57.5	[10]
E	15.9	31.8	67.1	.	350.	450.	37.3	.	.	300.	999.	999.	58.0	[10]
E	15.9	31.8	67.1	.	350.	450.	37.3	.	.	300.	999.	999.	59.0	[10]
E	15.9	31.8	67.1	.	350.	450.	46.4	.	.	300.	999.	999.	59.0	[10]
E	15.9	31.8	67.1	.	350.	450.	46.4	.	.	300.	999.	999.	60.0	[10]
E	15.9	31.8	67.1	.	350.	450.	46.4	.	.	300.	999.	999.	61.0	[10]
E	22.2	34.9	90.3	.	350.	450.	13.8	.	.	160.	999.	999.	46.2	[10]
E	22.2	34.9	90.3	.	350.	450.	13.8	.	.	160.	999.	999.	46.4	[10]
E	22.2	34.9	90.3	.	350.	450.	13.8	.	.	160.	999.	999.	47.8	[10]
E	22.2	34.9	90.3	.	350.	450.	28.4	.	.	160.	999.	999.	66.8	[10]
E	22.2	34.9	90.3	.	350.	450.	28.4	.	.	160.	999.	999.	70.4	[10]
E	22.2	34.9	90.3	.	350.	450.	28.4	.	.	160.	999.	999.	71.2	[10]
E	22.2	34.9	90.3	.	350.	450.	30.5	.	.	200.	999.	999.	69.2	[10]
E	22.2	34.9	90.3	.	350.	450.	30.5	.	.	200.	999.	999.	71.2	[10]
E	22.2	34.9	90.3	.	350.	450.	30.5	.	.	200.	999.	999.	76.0	[10]
E	22.2	34.9	90.3	.	350.	450.	46.4	.	.	200.	999.	999.	78.5	[10]
E	22.2	34.9	90.3	.	350.	450.	46.4	.	.	200.	999.	999.	80.0	[10]
E	22.2	34.9	90.3	.	350.	450.	46.4	.	.	200.	999.	999.	81.5	[10]
E	22.2	34.9	90.3	.	350.	450.	46.4	.	.	200.	999.	999.	82.0	[10]

.fz 3
.sa 1
2Tabelle A$n2$1 Versuchsdaten, Axialzug, (D), Einzelbefestigungen,
Kopfbolzen in der Fläche, c1≥1,5·hef

.ns
.sa 4

Syst. [-]	d [mm]	dh [mm]	hef [mm]	Tinst [Nm]	fy [MPa]	ft [MPa]	fcc200 [MPa]	fct [MPa]	dagg [mm]	c1 [mm]	s1 [mm]	s2 [mm]	Nu [kN]	Lit.
E	22.2	34.9	90.3	.	350.	450.	46.4	.	.	200.	999.	999.	83.5	[10]
E	22.2	34.9	90.3	.	350.	450.	46.4	.	.	200.	999.	999.	92.0	[10]
E	22.2	34.9	90.3	.	350.	450.	27.9	.	.	300.	999.	999.	62.0	[10]
E	22.2	34.9	90.3	.	350.	450.	27.9	.	.	300.	999.	999.	64.0	[10]
E	22.2	34.9	90.3	.	350.	450.	27.9	.	.	300.	999.	999.	64.8	[10]
E	22.2	34.9	90.3	.	350.	450.	27.9	.	.	300.	999.	999.	65.6	[10]
E	22.2	34.9	90.3	.	350.	450.	25.1	.	.	300.	999.	999.	67.6	[10]
E	22.2	34.9	90.3	.	350.	450.	27.9	.	.	300.	999.	999.	68.4	[10]
E	22.2	34.9	90.3	.	350.	450.	27.9	.	.	300.	999.	999.	68.4	[10]
E	22.2	34.9	90.3	.	350.	450.	28.4	.	.	300.	999.	999.	69.0	[10]
E	22.2	34.9	90.3	.	350.	450.	35.2	.	.	300.	999.	999.	73.0	[10]
E	22.2	34.9	90.3	.	350.	450.	25.1	.	.	300.	999.	999.	73.2	[10]
E	22.2	34.9	90.3	.	350.	450.	28.4	.	.	300.	999.	999.	74.0	[10]
E	22.2	34.9	90.3	.	350.	450.	35.2	.	.	300.	999.	999.	74.0	[10]
E	22.2	34.9	90.3	.	350.	450.	35.2	.	.	300.	999.	999.	74.0	[10]
E	22.2	34.9	90.3	.	350.	450.	25.1	.	.	300.	999.	999.	75.6	[10]
E	22.2	34.9	90.3	.	350.	450.	36.5	.	.	300.	999.	999.	76.0	[10]
E	22.2	34.9	90.3	.	350.	450.	28.4	.	.	300.	999.	999.	76.0	[10]
E	22.2	34.9	90.3	.	350.	450.	25.1	.	.	300.	999.	999.	76.0	[10]
E	22.2	34.9	90.3	.	350.	450.	30.5	.	.	300.	999.	999.	76.8	[10]
E	22.2	34.9	90.3	.	350.	450.	30.5	.	.	300.	999.	999.	77.6	[10]
E	22.2	34.9	90.3	.	350.	450.	35.2	.	.	300.	999.	999.	78.0	[10]
E	22.2	34.9	90.3	.	350.	450.	25.1	.	.	300.	999.	999.	78.8	[10]
E	22.2	34.9	90.3	.	350.	450.	25.1	.	.	300.	999.	999.	79.2	[10]
E	22.2	34.9	90.3	.	350.	450.	35.2	.	.	300.	999.	999.	80.0	[10]

.fz 3
.sa 1
2Tabelle A$n2$1 Versuchsdaten, Axialzug, (D), Einzelbefestigungen,
Kopfbolzen in der Fläche, c1≥1,5 hef

.ns
.sa 4

Syst. [-]	d [mm]	dh [mm]	hef [mm]	Tinst [Nm]	fy [MPa]	ft [MPa]	fcc200 [MPa]	fct [MPa]	dagg [mm]	c1 [mm]	s1 [mm]	s2 [mm]	Nu [kN]	Lit.
E	22.2	34.9	90.3	.	350.	450.	30.5	.	.	300.	999.	999.	80.0	[10]
E	22.2	34.9	90.3	.	350.	450.	36.5	.	.	300.	999.	999.	82.0	[10]
E	22.2	34.9	90.3	.	350.	450.	36.5	.	.	300.	999.	999.	82.5	[10]
E	22.2	34.9	90.3	.	350.	450.	35.2	.	.	300.	999.	999.	85.0	[10]
E	15.9	31.8	92.1	.	350.	450.	15.5	.	.	200.	999.	999.	43.2	[10]
E	15.9	31.8	92.1	.	350.	450.	15.5	.	.	200.	999.	999.	47.6	[10]
E	15.9	31.8	92.1	.	350.	450.	15.5	.	.	200.	999.	999.	50.0	[10]
E	15.9	31.8	92.1	.	350.	450.	11.4	.	.	300.	999.	999.	42.0	[10]
E	15.9	31.8	92.1	.	350.	450.	11.4	.	.	300.	999.	999.	46.0	[10]
E	15.9	31.8	92.1	.	350.	450.	11.4	.	.	300.	999.	999.	51.0	[10]
E	15.9	31.8	92.1	.	350.	450.	37.3	.	.	300.	999.	999.	88.0	[10]
E	15.9	31.8	92.1	.	350.	450.	37.3	.	.	300.	999.	999.	91.0	[10]
E	15.9	31.8	92.1	.	350.	450.	37.3	.	.	300.	999.	999.	98.0	[10]
E	19.0	31.8	115.3	.	350.	450.	20.3	.	.	300.	999.	999.	72.0	[10]
E	19.0	31.8	115.3	.	350.	450.	20.3	.	.	300.	999.	999.	72.0	[10]
E	19.0	31.8	115.3	.	350.	450.	20.3	.	.	300.	999.	999.	87.2	[10]
E	22.2	34.9	115.3	.	350.	450.	30.5	.	.	300.	999.	999.	94.4	[10]
E	22.2	34.9	115.3	.	350.	450.	30.5	.	.	300.	999.	999.	97.6	[10]
E	22.2	34.9	115.3	.	350.	450.	30.5	.	.	300.	999.	999.	100.8	[10]
E	22.0	35.0	130.0	.	350.	450.	27.7	.	.	550.	999.	999.	97.2	[12]
E	22.2	34.9	140.3	.	350.	450.	18.8	.	.	300.	999.	999.	85.6	[10]
E	22.0	35.0	185.0	.	350.	450.	24.8	.	.	400.	.	.	173.5	[13]
E	22.0	35.0	185.0	.	900.	1100.	22.2	1.8	.	447.	.	.	150.6	[12]
E	22.0	35.0	185.0	.	900.	1100.	22.2	1.8	.	449.	.	.	151.7	[12]
E	22.0	35.0	185.0	.	900.	1100.	22.2	1.8	.	450.	.	.	145.6	[12]

.fz 3
.sa 1
2Tabelle A$n2$1 Versuchsdaten, Axialzug, (D), Einzelbefestigungen,
Kopfbolzen in der Fläche, c1≥1,5·hef

.ns
.sa 4

Syst. [-]	d [mm]	dh [mm]	hef [mm]	Tinst [Nm]	fy [MPa]	ft [MPa]	fcc200 [MPa]	fct [MPa]	dagg [mm]	c1 [mm]	s1 [mm]	s2 [mm]	Nu [kN]	Lit.
E	22.0	35.0	185.0	.	350.	450.	27.1	.	.	450.	.	.	187.0	[13]
E	22.0	35.0	185.0	.	350.	450.	27.1	.	.	450.	.	.	200.0	[13]
E	22.0	35.0	185.0	.	350.	450.	28.2	.	.	450.	.	.	207.0	[13]
E	22.0	35.0	185.0	.	350.	450.	29.7	.	.	450.	.	.	223.0	[13]
E	22.0	35.0	185.0	.	350.	450.	29.6	.	.	450.	.	.	223.0	[13]
E	22.0	35.0	185.0	.	350.	450.	33.1	.	.	450.	.	.	223.0	[13]
E	22.0	35.0	185.0	.	350.	450.	27.1	.	.	450.	.	.	226.0	[13]
E	22.0	35.0	185.0	.	350.	450.	29.6	.	.	450.	.	.	228.0	[13]
E	22.0	35.0	185.0	.	350.	450.	27.8	.	.	450.	.	.	230.0	[13]
E	22.0	35.0	185.0	.	350.	450.	27.1	.	.	450.	.	.	236.0	[13]
E	22.0	35.0	185.0	.	350.	450.	29.7	.	.	450.	.	.	239.0	[13]
E	22.0	35.0	185.0	.	350.	450.	30.0	.	.	450.	.	.	241.0	[13]
E	22.0	35.0	185.0	.	350.	450.	29.6	.	.	450.	.	.	259.0	[13]
E	22.0	35.0	185.0	.	900.	1100.	22.2	1.8	.	550.	.	.	148.4	[12]
E	22.0	35.0	185.0	.	350.	450.	15.6	.	.	650.	.	.	128.0	[13]
E	22.0	35.0	185.0	.	350.	450.	16.4	.	.	650.	.	.	128.4	[13]
E	22.0	35.0	185.0	.	350.	450.	16.4	.	.	650.	.	.	135.0	[13]
E	22.0	35.0	185.0	.	350.	450.	15.6	.	.	650.	.	.	138.6	[13]
E	22.0	35.0	185.0	.	350.	450.	20.2	.	.	650.	.	.	181.5	[13]
E	22.0	35.0	185.0	.	350.	450.	20.2	.	.	650.	.	.	182.3	[13]
E	22.0	35.0	185.0	.	350.	450.	19.9	.	.	650.	.	.	182.7	[13]
E	22.0	35.0	185.0	.	350.	450.	19.9	.	.	650.	.	.	201.0	[13]
E	22.0	35.0	185.0	.	900.	1100.	22.2	1.8	.	875.	.	.	141.3	[12]
E	30.0	45.0	250.0	.	953.	1043.	44.0	.	.	999.	999.	999.	411.8	[11]
E	30.0	45.0	250.0	.	953.	1043.	34.0	.	.	999.	999.	999.	412.1	[11]

.fz 3
.sa 1
2Tabelle A$n2$1 Versuchsdaten, Axialzug, (D), Einzelbefestigungen,
Kopfbolzen in der Fläche, c1≥1,5·hef

.ns
.sa 4

Syst. [-]	d [mm]	dh [mm]	hef [mm]	Tinst [Nm]	fy [MPa]	ft [MPa]	fcc200 [MPa]	fct [MPa]	dagg [mm]	c1 [mm]	s1 [mm]	s2 [mm]	Nu [kN]	Lit.
E	30.0	45.0	250.0	.	953.	1043.	44.0	.	.	999.	999.	999.	415.1	[11]
E	30.0	45.0	250.0	.	953.	1043.	44.0	.	.	999.	999.	999.	435.6	[11]
E	30.0	45.0	250.0	.	953.	1043.	34.0	.	.	999.	999.	999.	436.4	[11]
E	30.0	45.0	250.0	.	953.	1043.	70.9	.	.	999.	999.	999.	499.0	[11]
E	30.0	45.0	250.0	.	953.	1043.	70.4	.	.	999.	999.	999.	535.0	[11]
E	30.0	45.0	250.0	.	953.	1043.	70.9	.	.	999.	999.	999.	559.1	[11]
E	30.0	45.0	250.0	.	953.	1043.	71.9	.	.	999.	999.	999.	617.5	[11]
E	30.0	45.0	250.0	.	953.	1043.	71.9	.	.	999.	999.	999.	620.5	[11]
E	30.0	45.0	250.0	.	953.	1043.	71.9	.	.	999.	999.	999.	624.2	[11]
E	30.0	45.0	260.0	.	900.	1100.	22.2	1.8	.	545.	.	.	294.3	[12]
E	30.0	45.0	260.0	.	900.	1100.	22.2	1.8	.	547.	.	.	302.1	[12]
E	30.0	45.0	260.0	.	900.	1100.	22.2	1.8	.	550.	.	.	262.3	[12]
E	30.0	45.0	260.0	.	900.	1100.	22.2	1.8	.	550.	.	.	266.6	[12]
E	30.0	45.0	260.0	.	900.	1100.	22.2	1.8	.	550.	.	.	270.7	[12]
E	30.0	45.0	260.0	.	900.	1100.	22.2	1.8	.	550.	.	.	273.6	[12]
E	30.0	45.0	260.0	.	900.	1100.	22.2	1.8	.	550.	.	.	278.0	[12]
E	30.0	45.0	260.0	.	900.	1100.	22.2	1.8	.	550.	.	.	285.9	[12]
E	30.0	45.0	260.0	.	900.	1100.	27.7	.	.	700.	.	.	290.0	[12]
E	40.0	60.0	355.0	.	900.	1100.	22.2	1.8	.	726.	.	.	450.6	[12]
E	40.0	60.0	355.0	.	900.	1100.	22.2	1.8	.	731.	.	.	452.0	[12]
E	40.0	60.0	355.0	.	900.	1100.	22.2	1.8	.	731.	.	.	465.7	[12]
E	40.0	60.0	355.0	.	900.	1100.	22.2	1.8	.	731.	.	.	468.0	[12]
E	40.0	60.0	355.0	.	900.	1100.	22.2	1.8	.	731.	.	.	479.7	[12]
E	40.0	60.0	355.0	.	900.	1100.	22.2	1.8	.	733.	.	.	470.5	[12]
E	40.0	60.0	355.0	.	900.	1100.	22.2	1.8	.	733.	.	.	475.6	[12]

.fz 3
.sa 1
2Tabelle A$n2$1 Versuchsdaten, Axialzug, (D), Einzelbefestigungen,
Kopfbolzen in der Fläche, c1≥1,5 hef

.ns
.sa 4

Syst. [-]	d [mm]	dh [mm]	hef [mm]	Tinst [Nm]	fy [MPa]	ft [MPa]	fcc200 [MPa]	fct [MPa]	dagg [mm]	c1 [mm]	s1 [mm]	s2 [mm]	Nu [kN]	Lit.
E	40.0	60.0	355.0	.	900.	1100.	22.2	1.8	.	738.	.	.	421.6	[12]
E	40.0	60.0	355.0	.	900.	1100.	22.2	1.8	.	999.	.	.	395.0	[12]
E	40.0	60.0	355.0	.	900.	1100.	22.2	1.8	.	999.	.	.	439.3	[12]
E	50.0	80.0	525.0	.	900.	1100.	27.7	.	.	700.	.	.	868.3	[12]
E	50.0	80.0	525.0	.	900.	1100.	19.1	1.5	.	999.	.	.	731.3	[12]
E	50.0	80.0	525.0	.	900.	1100.	19.1	1.5	.	999.	.	.	770.1	[12]
E	50.0	80.0	525.0	.	900.	1100.	19.1	1.5	.	999.	.	.	841.9	[12]
E	50.0	80.0	525.0	.	900.	1100.	23.7	1.8	.	999.	.	.	843.6	[12]
E	50.0	80.0	525.0	.	900.	1100.	23.7	1.8	.	999.	.	.	860.3	[12]
E	50.0	80.0	525.0	.	900.	1100.	19.1	1.5	.	999.	.	.	861.7	[12]
E	50.0	80.0	525.0	.	900.	1100.	23.7	1.8	.	999.	.	.	884.0	[12]
E	50.0	80.0	525.0	.	900.	1100.	23.7	1.8	.	999.	.	.	917.6	[12]
E	50.0	80.0	525.0	.	900.	1100.	27.7	.	.	999.	.	.	885.2	[12]
E	50.0	80.0	525.0	.	900.	1100.	19.1	1.5	.	999.	.	.	838.6	[12]
E	50.0	80.0	525.0	.	900.	1100.	23.7	1.8	.	999.	.	.	852.4	[12]
E	50.0	80.0	525.0	.	900.	1100.	23.7	1.8	.	999.	.	.	919.3	[12]
E	50.0	80.0	525.0	.	900.	1100.	19.1	1.5	.	999.	.	.	767.2	[12]

.fz 3
.sa 1
2Tabelle A$n2$1 Versuchsdaten, Axialzug, (D), Einzelbefestigungen,
Kopfbolzen in der Fläche, c1≥1,5·hef

.ue
.nn 16.1
.sa 4

Syst. [-]	d [mm]	dh [mm]	hef [mm]	Tinst [Nm]	fy [MPa]	ft [MPa]	fcc200 [MPa]	fct [MPa]	dagg [mm]	c1 [mm]	s1 [mm]	s2 [mm]	Nu [kN]	Lit.
A1	27.0	45.0	140.0	.	736.	840.	30.9	.	.	300.	999.	999.	180.0	[17]
A1	27.0	45.0	142.0	.	736.	840.	30.9	.	.	300.	999.	999.	190.0	[17]
A1	30.0	105.0	130.0	.	736.	840.	56.7	.	.	300.	999.	999.	206.0	[17]

.fz 3
.sa 1
2Tabelle A$n2$1 Versuchsdaten, Axialzug, (S), Einzelbefestigungen,
Kopfbolzen in der Fläche, c1≥1,5 hef

.ue
.nn 18.1
.sa 4

Syst. [-]	d [mm]	dh [mm]	hef [mm]	Tinst [Nm]	fy [MPa]	ft [MPa]	fcc200 [MPa]	fct [MPa]	dagg [mm]	c1 [mm]	s1 [mm]	s2 [mm]	Nu [kN]	Lit.
E	9.5	19.0	42.9	.	350.	450.	13.8	.	.	50.	999.	999.	9.6	[10]
E	9.5	19.0	42.9	.	350.	450.	13.8	.	.	50.	999.	999.	10.6	[10]
E	9.5	19.0	42.9	.	350.	450.	13.8	.	.	50.	999.	999.	11.3	[10]
E	9.5	19.0	42.9	.	350.	450.	28.4	.	.	50.	999.	999.	17.8	[10]
E	9.5	19.0	42.9	.	350.	450.	28.4	.	.	50.	999.	999.	20.0	[10]
E	9.5	19.0	42.9	.	350.	450.	28.4	.	.	50.	999.	999.	20.4	[10]
E	15.9	31.8	67.1	.	350.	450.	22.8	.	.	50.	999.	999.	22.4	[10]
E	15.9	31.8	67.1	.	350.	450.	22.8	.	.	50.	999.	999.	24.8	[10]
E	15.9	31.8	67.1	.	350.	450.	35.1	.	.	50.	999.	999.	26.8	[10]
E	15.9	31.8	67.1	.	350.	450.	22.8	.	.	50.	999.	999.	27.4	[10]
E	15.9	31.8	67.1	.	350.	450.	35.1	.	.	50.	999.	999.	28.8	[10]
E	15.9	31.8	67.1	.	350.	450.	35.1	.	.	50.	999.	999.	29.6	[10]
E	15.9	31.8	67.3	.	350.	450.	20.1	.	.	50.	999.	999.	16.8	[10]
E	15.9	31.8	67.3	.	350.	450.	20.1	.	.	50.	999.	999.	17.6	[10]
E	15.9	31.8	67.3	.	350.	450.	20.1	.	.	50.	999.	999.	19.6	[10]
E	15.9	31.8	67.3	.	350.	450.	47.6	.	.	50.	999.	999.	26.4	[10]
E	15.9	31.8	67.3	.	350.	450.	47.6	.	.	50.	999.	999.	26.4	[10]
E	15.9	31.8	67.3	.	350.	450.	47.6	.	.	50.	999.	999.	29.2	[10]
E	22.2	34.9	90.3	.	350.	450.	47.0	.	.	50.	999.	999.	38.4	[10]
E	22.2	34.9	90.3	.	350.	450.	47.0	.	.	50.	999.	999.	40.8	[10]
E	22.2	34.9	90.3	.	350.	450.	47.0	.	.	50.	999.	999.	44.8	[10]
E	15.9	31.8	67.1	.	350.	450.	22.8	.	.	80.	999.	999.	33.0	[10]
E	15.9	31.8	67.1	.	350.	450.	22.8	.	.	80.	999.	999.	33.4	[10]
E	15.9	31.8	67.1	.	350.	450.	35.1	.	.	80.	999.	999.	33.6	[10]
E	15.9	31.8	67.1	.	350.	450.	22.8	.	.	80.	999.	999.	34.8	[10]

.fz 3
.sa 1
2Tabelle A$n2$1 Versuchsdaten, Axialzug, (D), Einzelbefestigungen,
Kopfbolzen am Bauteilrand, c1≤1,5·hef

.ns
.sa 4

Syst. [-]	d [mm]	dh [mm]	hef [mm]	Tinst [Nm]	fy [MPa]	ft [MPa]	fcc200 [MPa]	fct [MPa]	dagg [mm]	c1 [mm]	s1 [mm]	s2 [mm]	Nu [kN]	Lit.
E	15.9	31.8	67.1	.	350.	450.	35.1	.	.	80.	999.	999.	35.0	[10]
E	15.9	31.8	67.1	.	350.	450.	35.1	.	.	80.	999.	999.	38.4	[10]
E	15.9	31.8	67.3	.	350.	450.	18.4	.	.	80.	999.	999.	18.2	[10]
E	15.9	31.8	67.3	.	350.	450.	18.4	.	.	80.	999.	999.	18.6	[10]
E	15.9	31.8	67.3	.	350.	450.	18.4	.	.	80.	999.	999.	25.4	[10]
E	15.9	31.8	67.3	.	350.	450.	38.9	.	.	80.	999.	999.	30.8	[10]
E	15.9	31.8	67.3	.	350.	450.	38.9	.	.	80.	999.	999.	36.0	[10]
E	15.9	31.8	67.3	.	350.	450.	38.9	.	.	80.	999.	999.	40.8	[10]
E	22.2	34.9	90.3	.	350.	450.	22.8	.	.	80.	999.	999.	49.0	[10]
E	22.2	34.9	90.3	.	350.	450.	22.8	.	.	80.	999.	999.	53.2	[10]
E	22.2	34.9	90.3	.	350.	450.	47.0	.	.	80.	999.	999.	55.2	[10]
E	22.2	34.9	90.3	.	350.	450.	22.8	.	.	80.	999.	999.	58.4	[10]
E	22.2	34.9	90.3	.	350.	450.	47.0	.	.	80.	999.	999.	59.2	[10]
E	22.2	34.9	90.3	.	350.	450.	47.0	.	.	80.	999.	999.	60.8	[10]
E	22.2	34.9	90.3	.	350.	450.	22.8	.	.	120.	999.	999.	62.8	[10]
E	22.2	34.9	90.3	.	350.	450.	22.8	.	.	120.	999.	999.	65.6	[10]
E	22.2	34.9	90.3	.	350.	450.	22.8	.	.	120.	999.	999.	66.8	[10]
E	22.2	34.9	90.3	.	350.	450.	35.1	.	.	120.	999.	999.	69.2	[10]
E	22.2	34.9	90.3	.	350.	450.	35.1	.	.	120.	999.	999.	81.2	[10]
E	22.2	34.9	90.3	.	350.	450.	35.1	.	.	120.	999.	999.	84.2	[10]
E	30.0	45.0	260.0	.	900.	1100.	23.7	1.8	.	220.	.	.	199.6	[12]
E	30.0	45.0	260.0	.	900.	1100.	23.7	1.8	.	220.	.	.	208.5	[12]
E	30.0	45.0	260.0	.	900.	1100.	23.7	1.8	.	220.	.	.	208.7	[12]
E	30.0	45.0	260.0	.	900.	1100.	23.7	1.8	.	220.	.	.	225.6	[12]
E	40.0	60.0	355.0	.	900.	1100.	23.7	1.8	.	220.	.	.	327.2	[12]

.fz 3
.sa 1
2Tabelle A$n2$1 Versuchsdaten, Axialzug, (D), Einzelbefestigungen,
Kopfbolzen am Bauteilrand, c1≤1,5·hef

.ns
.sa 4

Syst. [-]	d [mm]	dh [mm]	hef [mm]	Tinst [Nm]	fy [MPa]	ft [MPa]	fcc200 [MPa]	fct [MPa]	dagg [mm]	c1 [mm]	s1 [mm]	s2 [mm]	Nu [kN]	Lit.
E	40.0	60.0	355.0	.	900.	1100.	23.7	1.8	.	220.	.	.	370.5	[12]
E	22.0	35.0	185.0	.	900.	1100.	22.2	1.8	.	261.	.	.	109.3	[12]
E	22.0	35.0	185.0	.	900.	1100.	22.2	1.8	.	261.	.	.	126.5	[12]
E	22.0	35.0	185.0	.	900.	1100.	22.2	1.8	.	264.	.	.	114.4	[12]
E	22.0	35.0	185.0	.	900.	1100.	22.2	1.8	.	265.	.	.	125.6	[12]
E	30.0	45.0	260.0	.	900.	1100.	19.1	1.5	.	270.	.	.	212.0	[12]
E	30.0	45.0	260.0	.	900.	1100.	19.1	1.5	.	270.	.	.	218.0	[12]
E	40.0	60.0	355.0	.	900.	1100.	19.1	1.5	.	361.	.	.	274.2	[12]
E	40.0	60.0	355.0	.	900.	1100.	19.1	1.5	.	370.	.	.	330.7	[12]
E	40.0	60.0	355.0	.	900.	1100.	19.1	1.5	.	370.	.	.	416.3	[12]
E	40.0	60.0	355.0	.	900.	1100.	19.1	1.5	.	377.	.	.	350.9	[12]

.fz 3
.sa 1
2Tabelle A$n2$1 Versuchsdaten, Axialzug, (D), Einzelbefestigungen,
Kopfbolzen am Bauteilrand, c1≤1,5·hef

.ue
.nn 21.1
.sa 4

Syst. [-]	d [mm]	dh [mm]	hef [mm]	Tinst [Nm]	fy [MPa]	ft [MPa]	fcc200 [MPa]	fct [MPa]	dagg [mm]	c1 [mm]	s1 [mm]	s2 [mm]	Nu [kN]	Lit.
E	40.0	60.0	355.0	.	900.	1100.	23.7	1.8	.	67.	999.	999.	133.9	[12]
E	30.0	45.0	260.0	.	900.	1100.	23.7	1.8	.	70.	999.	999.	104.2	[12]
E	30.0	45.0	260.0	.	900.	1100.	23.7	1.8	.	70.	999.	999.	120.4	[12]
E	30.0	45.0	260.0	.	900.	1100.	23.7	1.8	.	71.	999.	999.	108.4	[12]
E	30.0	45.0	260.0	.	900.	1100.	23.7	1.8	.	75.	999.	999.	113.7	[12]
E	40.0	60.0	355.0	.	900.	1100.	23.7	1.8	.	75.	999.	999.	127.7	[12]
E	40.0	60.0	355.0	.	900.	1100.	23.7	1.8	.	75.	999.	999.	138.2	[12]
E	40.0	60.0	355.0	.	900.	1100.	23.7	1.8	.	75.	999.	999.	145.1	[12]
E	50.0	80.0	525.0	.	900.	1100.	19.1	1.5	.	90.	999.	999.	236.9	[12]
E	50.0	80.0	525.0	.	900.	1100.	19.1	1.5	.	94.	999.	999.	312.8	[12]
E	50.0	80.0	525.0	.	900.	1100.	19.1	1.5	.	95.	999.	999.	235.3	[12]
E	50.0	80.0	525.0	.	900.	1100.	19.1	1.5	.	95.	999.	999.	255.4	[12]
E	50.0	80.0	525.0	.	900.	1100.	19.1	1.5	.	222.	999.	999.	400.3	[12]
E	50.0	80.0	525.0	.	900.	1100.	19.1	1.5	.	223.	999.	999.	380.3	[12]
E	50.0	80.0	525.0	.	900.	1100.	19.1	1.5	.	225.	999.	999.	455.8	[12]
E	50.0	80.0	525.0	.	900.	1100.	19.1	1.5	.	225.	999.	999.	465.4	[12]

.fz 3
.sa 1
2Tabelle A$n2$1 Versuchsdaten, Axialzug, (D), Einzelbefestigungen,
Kopfbolzen mit sehr kleinem c1 ("blow-out")

.ue
.nn 19.1
.sa 4

Syst. [-]	d [mm]	dh [mm]	hef [mm]	Tinst [Nm]	fy [MPa]	ft [MPa]	fcc200 [MPa]	fct [MPa]	dagg [mm]	c1 [mm]	s1 [mm]	s2 [mm]	Nu [kN]	Lit.
A1	27.0	45.0	142.0	.	736.	840.	30.9	.	.	150.	999.	999.	162.0	[17]
A1	27.0	45.0	322.0	.	736.	840.	30.9	.	.	150.	999.	999.	266.0	[17]
A1	27.0	45.0	329.0	.	736.	840.	30.9	.	.	300.	999.	999.	374.0	[17]
A1	27.0	45.0	134.0	.	736.	840.	30.9	.	.	150.	999.	999.	185.0	[17]
A1	30.0	52.0	344.0	.	736.	840.	30.9	.	.	150.	999.	999.	322.0	[17]
A1	30.0	52.0	344.0	.	736.	840.	30.9	.	.	300.	999.	999.	408.0	[17]
A1	30.0	105.0	112.0	.	736.	840.	51.5	.	.	150.	999.	999.	147.0	[17]
A1	30.0	105.0	315.0	.	736.	840.	56.7	.	.	150.	999.	999.	344.0	[17]

.fz 3
.sa 1
2Tabelle A$n2$1 Versuchsdaten, Axialzug, (S), Einzelbefestigungen,
Kopfbolzen mit kleinem Randabstand, c1≤1,5 hef

.ue
.nn 20.1
.sa 4

Syst. [-]	d [mm]	dh [mm]	hef [mm]	Tinst [Nm]	fy [MPa]	ft [MPa]	fcc200 [MPa]	fct [MPa]	dagg [mm]	c1 [mm]	s1 [mm]	s2 [mm]	Nu [kN]	Lit.
Kb	19.5	28.5	88.5	.	345.	414.	44.7	3.5	.	57.	999.	999.	64.0	[14]
Kb	19.5	28.5	114.3	.	345.	414.	44.7	3.5	.	70.	999.	999.	103.1	[14]
Kb	19.5	28.5	88.5	.	345.	414.	44.7	3.5	.	57.	999.	999.	73.8	[14]
Kb	19.5	31.8	92.1	.	345.	414.	39.8	3.2	.	51.	999.	999.	48.9	[14]
Kb	19.5	28.5	88.9	.	345.	414.	39.6	3.2	.	51.	999.	999.	44.0	[14]
Kb	19.5	28.5	88.9	.	345.	414.	35.1	3.0	.	51.	999.	999.	73.8	[14]
Kb	19.5	31.8	168.2	.	345.	414.	42.1	3.3	.	152.	999.	999.	131.2	[14]
Kb	19.5	28.5	88.9	.	345.	414.	39.6	3.2	.	76.	999.	999.	59.1	[14]
Kb	19.5	31.8	168.2	.	345.	414.	42.1	3.3	.	102.	999.	999.	130.7	[14]
Kb	19.5	28.5	88.9	.	345.	414.	35.1	3.0	.	76.	999.	999.	81.4	[14]
Kb	19.5	28.5	114.3	.	345.	414.	37.7	3.1	.	76.	999.	999.	91.1	[14]
Kb	19.5	28.5	139.7	.	345.	414.	35.1	3.0	.	76.	999.	999.	125.4	[14]
Kb	19.5	28.5	114.3	.	345.	414.	37.7	3.1	.	102.	999.	999.	97.8	[14]

.fz 3
.sa 1
2Tabelle $n2$1 Versuchsdaten, Axialzug, (USA), Einzelbefestigungen,
Kopfbolzen am Bauteilrand, c1≤1,0·hef

.ue
.nn 23.1
.sa 4

Syst. [-]	d [mm]	dh [mm]	hef [mm]	Tinst [Nm]	fy [MPa]	ft [MPa]	fcc200 [MPa]	fct [MPa]	dagg [mm]	c1 [mm]	s1 [mm]	s2 [mm]	Nu [kN]	Lit.
E	15.9	31.8	67.3	.	350.	450.	20.1	.	.	40.	80.	80.	59.6	[10]
E	15.9	31.8	67.3	,	350.	450.	47.7	.	.	40.	80.	80.	85.2	[10]
E	15.9	31.8	67.3	.	350.	450.	18.4	.	.	60.	120.	120.	66.0	[10]
E	15.9	31.8	67.3	.	350.	450.	47.7	.	.	60.	120.	120.	87.2	[10]
E	15.9	31.8	67.3	.	350.	450.	17.9	.	.	80.	160.	160.	76.8	[10]
E	15.9	31.8	67.3	.	350.	450.	33.2	.	.	80.	160.	160.	120.8	[10]

.fz 3
.sa 1
2Tabelle A$n2$1 Versuchsdaten, Axialzug, (D), Zweifachbefestigungen,
Kopfbolzen in der Fläche

.ue
.nn 24.1
.sa 4

Syst. [-]	d [mm]	dh [mm]	hef [mm]	Tinst [Nm]	fy [MPa]	ft [MPa]	fcc200 [MPa]	fct [MPa]	dagg [mm]	c1 [mm]	s1 [mm]	s2 [mm]	Nu [kN]	Lit.
E	15.9	31.8	67.3	.	350.	450.	18.4	.	.	40.	80.	80.	72.0	[10]
E	15.9	31.8	67.3	.	350.	450.	33.2	.	.	40.	80.	80.	129.6	[10]
E	22.2	34.9	185.3	.	350.	450.	22.2	.	.	999.	100.	100.	240.0	[11]
E	22.2	34.9	185.3	.	350.	450.	22.6	.	.	999.	100.	100.	253.0	[11]
E	22.2	34.9	185.3	.	350.	450.	25.0	.	.	999.	100.	100.	253.0	[11]
E	22.2	34.9	185.3	.	350.	450.	24.0	.	.	999.	100.	100.	264.0	[11]
E	22.0	35.0	185.0	.	350.	450.	28.6	.	.	850.	100.	100.	275.0	[13]
E	22.2	34.9	185.3	.	350.	450.	27.6	.	.	999.	100.	100.	278.0	[11]
E	22.2	34.9	185.3	.	350.	450.	27.6	.	.	999.	100.	100.	280.0	[11]
E	22.0	35.0	185.0	.	350.	450.	28.6	.	.	850.	100.	100.	290.0	[13]
E	22.0	35.0	185.0	.	350.	450.	25.7	.	.	850.	100.	100.	303.0	[13]
E	22.2	34.9	360.3	.	350.	450.	29.9	.	.	999.	100.	100.	500.0	[11]
E	22.2	34.9	360.3	.	350.	450.	30.8	.	.	999.	100.	100.	518.0	[11]
E	22.2	34.9	360.3	.	350.	450.	27.4	.	.	999.	100.	100.	585.0	[11]
E	15.9	31.8	67.3	.	350.	450.	18.8	.	.	60.	120.	120.	70.4	[10]
E	15.9	31.8	67.3	.	350.	450.	38.9	.	.	60.	120.	120.	157.6	[10]
E	22.0	35.0	185.0	.	350.	450.	30.0	.	.	375.	150.	150.	308.0	[13]
E	22.0	35.0	185.0	.	350.	450.	28.2	.	.	575.	150.	150.	311.0	[13]
E	22.0	35.0	185.0	.	350.	450.	28.2	.	.	575.	150.	150.	313.0	[13]
E	22.0	35.0	185.0	.	350.	450.	28.2	.	.	575.	150.	150.	318.0	[13]
E	22.0	35.0	185.0	.	350.	450.	27.8	.	.	375.	150.	150.	330.0	[13]
E	22.0	35.0	185.0	.	350.	450.	30.0	.	.	375.	150.	150.	335.0	[13]
E	22.0	35.0	185.0	.	350.	450.	33.1	.	.	375.	150.	150.	335.0	[13]
E	22.0	35.0	185.0	.	350.	450.	27.8	.	.	375.	150.	150.	342.0	[13]
E	22.0	35.0	185.0	.	350.	450.	33.1	.	.	375.	150.	150.	351.0	[13]

.fz 3
.sa 1
2Tabelle A$n2$1 Versuchsdaten, Axialzug, (D), Vierfachbefestigungen,
Kopfbolzen in der Fläche

.ns
.sa 4

Syst. [-]	d [mm]	dh [mm]	hef [mm]	Tinst [Nm]	fy [MPa]	ft [MPa]	fcc200 [MPa]	fct [MPa]	dagg [mm]	c1 [mm]	s1 [mm]	s2 [mm]	Nu [kN]	Lit.
E	15.9	31.8	67.3	.	350.	450.	17.9	.	.	80.	160.	160.	118.0	[10]
E	15.9	31.8	67.3	.	350.	450.	33.2	.	.	80.	160.	160.	183.2	[10]
E	22.0	35.0	185.0	.	350.	450.	28.9	.	.	640.	270.	270.	390.0	[13]
E	22.0	35.0	185.0	.	350.	450.	28.9	.	.	640.	270.	270.	433.0	[13]
E	22.0	35.0	185.0	.	350.	450.	28.9	.	.	640.	270.	270.	439.0	[13]
E	22.0	35.0	185.0	.	350.	450.	24.0	.	.	530.	400.	400.	627.0	[13]
E	22.0	35.0	185.0	.	350.	450.	24.0	.	.	530.	400.	400.	628.0	[13]

.fz 3
.sa 1
2Tabelle A$n2$1 Versuchsdaten,Axialzug, (D), Vierfachbefestigungen,
Kopfbolzen in der Fläche

.ue
.nn 33.1
.sa 4

Syst. [-]	d [mm]	do [mm]	hef [mm]	Tinst [Nm]	fy [MPa]	ft [MPa]	fcc200 [MPa]	fct [MPa]	dagg [mm]	c1 [mm]	c2 [mm]	s1 [mm]	Vu [kN]	Lit.
F	20.0	20.0	120.0	.	270.	579.	31.0	.	15.	50.0	100.0	999.	7.0	[15]
F	20.0	20.0	120.0	.	270.	579.	31.0	.	15.	50.0	100.0	999.	8.1	[15]
F	25.0	25.0	150.0	.	286.	606.	31.0	.	15.	50.0	100.0	999.	10.8	[15]
F	25.0	25.0	150.0	.	286.	606.	31.0	.	15.	50.0	100.0	999.	10.8	[15]
F	14.0	14.0	84.0	.	223.	578.	31.0	.	15.	50.4	99.4	999.	5.7	[15]
F	14.0	14.0	84.0	.	223.	578.	31.0	.	15.	50.4	99.4	999.	7.0	[15]
F	14.0	14.0	84.0	.	223.	578.	31.0	.	15.	50.4	99.4	999.	8.3	[15]
F	14.0	14.0	84.0	.	223.	578.	31.0	.	15.	50.4	99.4	999.	8.3	[15]
F	26.5	26.5	212.0	.	1080.	1230.	46.4	.	32.	63.0	112.5	999.	18.6	[15]
F	26.5	26.5	212.0	.	1080.	1230.	46.4	.	32.	63.0	150.0	999.	20.4	[15]
F	26.5	26.5	212.0	.	1080.	1230.	48.5	.	32.	70.0	150.0	999.	28.0	[15]
F	25.0	25.0	150.0	.	286.	606.	31.0	.	15.	75.0	137.5	999.	14.6	[15]
F	25.0	25.0	150.0	.	286.	606.	31.0	.	15.	75.0	137.5	999.	17.2	[15]
F	14.0	14.0	84.0	.	223.	578.	31.0	.	15.	75.6	137.2	999.	13.3	[15]
F	14.0	14.0	84.0	.	223.	578.	31.0	.	15.	75.6	137.2	999.	13.3	[15]
F	20.0	20.0	120.0	.	270.	579.	31.0	.	15.	76.0	138.0	999.	14.6	[15]
F	20.0	20.0	120.0	.	270.	579.	31.0	.	15.	76.0	138.0	999.	15.9	[15]
F	20.0	20.0	120.0	.	270.	579.	31.0	.	15.	76.0	138.0	999.	15.9	[15]
F	20.0	20.0	120.0	.	270.	579.	31.0	.	15.	76.0	138.0	999.	17.2	[15]
F	26.5	26.5	212.0	.	1080.	1230.	46.4	.	32.	84.0	150.0	999.	27.2	[15]
F	26.5	26.5	212.0	.	1080.	1230.	46.4	.	32.	84.0	200.0	999.	26.2	[15]
F	26.5	26.5	212.0	.	1080.	1230.	46.4	.	32.	84.0	267.5	999.	29.5	[15]
F	26.5	26.5	212.0	.	1080.	1230.	46.4	.	32.	85.0	150.0	999.	29.6	[15]
F	26.5	26.5	212.0	.	1080.	1230.	46.4	.	32.	112.5	200.0	999.	40.6	[15]
F	25.0	25.0	150.0	.	286.	606.	32.0	.	15.	125.0	200.0	999.	36.2	[15]

.fz 3
.sa 1
2Tabelle A$n2$1 Versuchsdaten, Querzug, (D), Einzelbefestigungen,
Dollen mit kleinem Randabstand

.ns
.sa4

Syst. [-]	d [mm]	do [mm]	hef [mm]	Tinst [Nm]	fy [MPa]	ft [MPa]	fcc200 [MPa]	fct [MPa]	dagg [mm]	c1 [mm]	c2 [mm]	s1 [mm]	Vu [kN]	Lit.
F	25.0	25.0	150.0	.	286.	606.	32.0	.	15.	125.0	200.0	999.	40.0	[15]
F	25.0	25.0	150.0	.	286.	606.	32.0	.	15.	125.0	200.0	999.	40.0	[15]
F	25.0	25.0	150.0	.	286.	606.	32.0	.	15.	125.0	200.0	999.	40.0	[15]
F	20.0	20.0	120.0	.	270.	579.	32.0	.	15.	126.0	200.0	999.	34.3	[15]
F	20.0	20.0	120.0	.	270.	579.	32.0	.	15.	126.0	200.0	999.	34.3	[15]
F	20.0	20.0	160.0	.	420.	500.	37.6	.	32.	130.0	300.0	999.	55.4	[15]
F	20.0	20.0	160.0	.	420.	500.	40.8	.	32.	130.0	300.0	999.	59.5	[15]
F	26.5	26.5	212.0	.	835.	1030.	40.8	.	32.	133.0	300.0	999.	56.1	[15]
F	28.0	28.0	224.0	.	220.	340.	40.8	.	32.	134.0	300.0	999.	55.1	[15]
F	28.0	28.0	224.0	.	420.	500.	40.8	.	32.	134.0	300.0	999.	68.6	[15]
F	26.5	26.5	212.0	.	1080.	1230.	46.4	.	32.	150.0	267.5	999.	60.0	[15]

.fz 3
.sa 1
2Tabelle A$n2$1 Versuchsdaten, Querzug, (D), Einzelbefestigungen,
Dollen mit kleinem Randabstand

.ue
.nn 30.1
.sa 4

Syst. [-]	d [mm]	dh [mm]	hef [mm]	Tinst [Nm]	fy [MPa]	ft [MPa]	fcc200 [MPa]	fct [MPa]	dagg [mm]	c1 [mm]	c2 [mm]	s1 [mm]	Vu [kN]	Lit.
E	22.0	35.0	185.0	12.5	953.	1043.	28.5	2.2	16.	74.	999.	999.	28.0	[12]
E	22.0	35.0	185.0	9.0	953.	1043.	21.5	1.8	16.	74.	999.	999.	22.7	[12]
E	22.0	35.0	185.0	9.5	953.	1043.	21.5	1.8	16.	75.	999.	999.	27.3	[12]
E	22.0	35.0	185.0	7.0	953.	1043.	21.5	1.8	16.	73.	999.	999.	21.9	[12]

.fz 3
.sa 1
2Tabelle $n2$1 Versuchsdaten, Querzug, (D), Einzelbefestigungen,
Kopfbolzen am Bauteilrand

.ue
.nn 31.1
.sa 4

Syst.	d	d1	hef	Tinst	fy	ft	fcc200	fct	dagg	c1	c2	s1	Vu	Lit.	
[-]	[mm]	[mm]	[mm]	[Nm]		[MPa]	[MPa]	[MPa]	[MPa]	[mm]		[mm]	[mm]	[mm]	[kN]
E	16.0	16.0	200.0	.	250.	.	21.6	.	.	50.	999.	999.	6.7	[25]	
E	16.0	16.0	200.0	.	250.	.	24.7	.	.	50.	999.	999.	9.3	[25]	
E	16.0	16.0	200.0	.	250.	.	24.7	.	.	50.	999.	999.	10.5	[25]	
E	16.0	16.0	200.0	.	250.	.	21.6	.	.	50.	999.	999.	10.7	[25]	
E	16.0	16.0	200.0	.	250.	.	25.5	.	.	50.	999.	999.	10.8	[25]	
E	16.0	16.0	200.0	.	250.	.	25.5	.	.	50.	999.	999.	13.7	[25]	
E	19.0	19.0	203.2	.	345.	414.	34.2	.	.	51.	999.	999.	17.1	[24]	
E	19.0	19.0	203.2	.	345.	414.	34.2	.	.	51.	999.	999.	17.8	[24]	
E	19.0	19.0	203.2	.	345.	414.	34.2	.	.	51.	999.	999.	18.2	[24]	
E	16.0	16.0	200.0	.	250.	.	25.5	.	.	100.	999.	999.	34.3	[25]	
E	16.0	16.0	200.0	.	250.	.	21.6	.	.	100.	999.	999.	36.2	[25]	
E	16.0	16.0	200.0	.	250.	.	24.7	.	.	100.	999.	999.	38.2	[25]	
E	16.0	16.0	200.0	.	250.	.	25.5	.	.	100.	999.	999.	38.2	[25]	
E	16.0	16.0	200.0	.	250.	.	21.6	.	.	100.	999.	999.	39.7	[25]	
E	19.0	19.0	203.2	.	345.	414.	34.2	.	.	102.	999.	999.	26.7	[24]	
E	19.0	19.0	203.2	.	345.	414.	34.2	.	.	102.	999.	999.	26.7	[24]	
E	19.0	19.0	203.2	.	345.	414.	34.2	.	.	102.	999.	999.	30.0	[24]	
E	19.0	19.0	203.2	.	345.	414.	34.2	.	.	102.	999.	999.	33.4	[24]	
E	25.4	25.0	232.2	.	345.	414.	35.7	.	25.	102.	999.	999.	52.0	[24]	
E	25.4	25.0	232.2	.	345.	414.	33.0	.	25.	102.	999.	999.	56.0	[24]	
E	25.4	25.0	232.2	.	345.	414.	33.0	.	25.	102.	999.	999.	73.4	[24]	
E	19.0	19.0	152.4	.	.	.	39.1	.	.	102.	999.	999.	85.0	[24]	
E	19.0	19.0	152.4	.	345.	414.	39.2	.	.	127.	999.	999.	70.3	[24]	
E	19.0	19.0	152.4	.	.	.	39.1	.	.	127.	999.	999.	70.3	[24]	
E	16.0	16.0	200.0	.	250.	.	30.2	.	.	150.	999.	999.	44.1	[25]	

.fz 3
.sa 1
2Tabelle A$n2$1 Versuchsdaten, Querzug, USA, Einzelbefestigungen,
Kopfbolzen am Bauteilrand

.ns
.sa 4

Syst.	d	d1	hef	Tinst	fy	ft	fcc200	fct	dagg	c1	c2	s1	Vu	Lit.	
[-]	[mm]	[mm]	[mm]	[Nm]		[MPa]	[MPa]	[MPa]	[MPa]	[mm]		[mm]	[mm]	[mm]	[kN]
E	16.0	16.0	200.0	.	250.	.	30.2	.	.	150.	999.	999.	59.8	[25]	
E	19.0	19.0	203.2	.	345.	414.	34.2	.	.	152.	999.	999.	41.4	[24]	
E	19.0	19.0	203.2	.	345.	414.	34.2	.	.	152.	999.	999.	44.5	[24]	
E	19.0	19.0	203.2	.	345.	414.	34.2	.	.	152.	999.	999.	64.5	[24]	
E	25.4	25.0	232.2	.	345.	414.	33.2	.	.	152.	999.	999.	76.9	[24]	
E	25.4	25.0	232.2	.	345.	414.	33.2	.	25.	152.	999.	999.	82.7	[24]	
E	25.4	25.0	232.2	.	345.	414.	33.2	.	25.	152.	999.	999.	88.5	[24]	
E	25.4	25.0	232.2	.	345.	414.	33.2	.	25.	152.	999.	999.	89.4	[24]	
E	25.4	25.0	232.2	.	345.	414.	33.2	.	25.	152.	999.	999.	93.4	[24]	
E	25.4	25.0	232.2	.	345.	414.	33.2	.	25.	152.	999.	999.	93.4	[24]	
E	19.0	19.0	152.4	.	.	.	39.3	.	.	152.	999.	999.	100.6	[24]	
E	50.8	50.0	468.3	.	345.	414.	34.4	.	25.	152.	999.	999.	113.0	[24]	
E	50.8	50.0	468.3	.	345.	414.	34.4	.	25.	152.	999.	999.	117.0	[24]	
E	19.0	19.0	203.2	.	345.	414.	34.2	.	.	203.	999.	999.	74.3	[24]	
E	19.0	19.0	203.2	.	345.	414.	34.2	.	.	203.	999.	999.	84.5	[24]	
E	19.0	19.0	203.2	.	345.	414.	34.2	.	.	203.	999.	999.	86.7	[24]	
E	25.4	25.0	232.2	.	345.	414.	33.2	.	25.	203.	999.	999.	144.1	[24]	
E	50.8	50.0	468.3	.	345.	414.	34.9	.	25.	305.	999.	999.	245.1	[24]	
E	50.8	50.0	468.3	.	345.	414.	34.9	.	25.	305.	999.	999.	266.9	[24]	

.fz 3
.sa 1
2Tabelle A$n2$1 Versuchsdaten, Querzug, USA, Einzelbefestigungen,
Kopfbolzen am Bauteilrand

.ue
.nn 28.1
.sa 4

Syst. [-]	d [mm]	do [mm]	hef [mm]	Tinst [Nm]	fy [MPa]	ft [MPa]	fcc200 [MPa]	fct [MPa]	dagg [mm]	c1 [mm]	c2 [mm]	h [mm]	Vu [kN]	Lit.
A1	20.	28.	130.	300.	640.	800.	25.4	1.98	16.	150.	999.	300.	79.6	[28]
A1	20.	28.	130.	300.	640.	800.	25.4	1.98	16.	150.	999.	300.	76.0	[28]
A1	20.	28.	130.	300.	640.	800.	25.4	1.98	16.	150.	999.	300.	61.8	[28]
A1	20.	28.	130.	300.	640.	800.	25.4	1.98	16.	150.	999.	250.	53.2	[28]
A1	20.	28.	130.	300.	640.	800.	25.4	1.98	16.	150.	999.	250.	60.3	[28]
A1	20.	28.	130.	300.	640.	800.	25.4	1.98	16.	150.	999.	250.	57.3	[28]
A1	20.	28.	130.	300.	640.	800.	25.4	1.98	16.	200.	999.	300.	83.8	[28]
A1	20.	28.	130.	300.	640.	800.	25.4	1.98	16.	200.	999.	300.	97.5	[28]
A1	20.	28.	130.	300.	640.	800.	25.4	1.98	16.	200.	999.	300.	94.9	[28]
A1	20.	28.	130.	300.	640.	800.	25.4	1.98	16.	150.	999.	200.	48.4	[28]
A1	20.	28.	130.	300.	640.	800.	25.4	1.98	16.	150.	999.	200.	48.9	[28]
A1	20.	28.	130.	300.	640.	800.	25.4	1.98	16.	150.	999.	200.	46.2	[28]
A1	20.	28.	130.	300.	640.	800.	25.4	1.98	16.	200.	999.	250.	78.0	[28]
A1	20.	28.	130.	300.	640.	800.	25.4	1.98	16.	200.	999.	250.	82.8	[28]
A1	20.	28.	130.	300.	640.	800.	25.4	1.98	16.	200.	999.	250.	81.6	[28]
A1	20.	28.	130.	300.	640.	800.	25.4	1.98	16.	250.	999.	300.	113.5	[28]
A1	20.	28.	130.	300.	640.	800.	25.4	1.98	16.	250.	999.	300.	118.0	[28]
A1	20.	28.	130.	300.	640.	800.	25.4	1.98	16.	250.	999.	300.	117.5	[28]
A1	20.	28.	130.	300.	640.	800.	25.4	1.98	16.	150.	999.	150.	43.6	[28]
A1	20.	28.	130.	300.	640.	800.	25.4	1.98	16.	150.	999.	150.	42.0	[28]
A1	20.	28.	130.	300.	640.	800.	25.4	1.98	16.	150.	999.	150.	38.6	[28]
A1	20.	28.	130.	300.	640.	800.	25.4	1.98	16.	200.	999.	200.	60.2	[28]
A1	20.	28.	130.	300.	640.	800.	25.4	1.98	16.	200.	999.	200.	59.9	[28]
A1	20.	28.	130.	300.	640.	800.	25.4	1.98	16.	250.	999.	250.	102.3	[28]

.fz 3
.sa 1
2Tabelle A$n2$1 Versuchsdaten, Querzug, (D), Einzelbefestigungen,
Metallspreizdübel am Bauteilrand,Einfluß der Bauteildicke

.ns
.sa 4

Syst. [-]	d [mm]	do [mm]	hef [mm]	Tinst [Nm]	fy [MPa]	ft [MPa]	fcc200 [MPa]	fct [MPa]	dagg [mm]	c1 [mm]	c2 [mm]	h [mm]	Vu [kN]	Lit.
A1	20.	28.	130.	300.	640.	800.	25.4	1.98	16.	250.	999.	250.	100.9	[28]
A1	20.	28.	130.	300.	640.	800.	27.6	1.86	16.	300.	999.	300.	109.9	[28]
A1	20.	28.	130.	300.	640.	800.	27.6	1.86	16.	300.	999.	300.	120.3	[28]
A1	20.	28.	130.	300.	640.	800.	27.6	1.86	16.	300.	999.	300.	112.3	[28]
A1	20.	28.	130.	300.	640.	800.	27.6	1.86	16.	300.	999.	250.	101.1	[28]
A1	20.	28.	130.	300.	640.	800.	27.6	1.86	16.	300.	999.	250.	99.4	[28]
A1	20.	28.	130.	300.	640.	800.	25.4	1.98	16.	300.	999.	250.	85.0	[28]
A1	20.	28.	130.	300.	640.	800.	25.4	1.98	16.	250.	999.	200.	75.4	[28]
A1	20.	28.	130.	300.	640.	800.	25.4	1.98	16.	250.	999.	200.	82.3	[28]
A1	20.	28.	130.	300.	640.	800.	25.4	1.98	16.	250.	999.	200.	75.6	[28]
A1	20.	28.	130.	300.	640.	800.	25.4	1.98	16.	200.	999.	150.	46.2	[28]
A1	20.	28.	130.	300.	640.	800.	25.4	1.98	16.	200.	999.	150.	44.6	[28]
A1	20.	28.	130.	300.	640.	800.	25.4	1.98	16.	200.	999.	150.	45.9	[28]
A1	20.	28.	130.	300.	640.	800.	25.4	1.98	16.	150.	999.	100.	21.9	[28]
A1	20.	28.	130.	300.	640.	800.	25.4	1.98	16.	150.	999.	100.	21.0	[28]
A1	20.	28.	130.	300.	640.	800.	25.4	1.98	16.	150.	999.	100.	22.2	[28]
A1	20.	28.	130.	300.	640.	800.	27.6	1.86	16.	300.	999.	200.	73.8	[28]
A1	20.	28.	130.	300.	640.	800.	27.6	1.86	16.	300.	999.	200.	87.4	[28]
A1	20.	28.	130.	300.	640.	800.	27.6	1.86	16.	300.	999.	200.	75.5	[28]
A1	20.	28.	130.	300.	640.	800.	25.4	1.98	16.	250.	999.	150.	53.3	[28]
A1	20.	28.	125.	300.	640.	800.	21.0	1.97	16.	240.	999.	325.	90.7	[28]
A1	20.	28.	125.	300.	640.	800.	21.0	1.97	16.	240.	999.	325.	98.0	[28]
A1	20.	28.	125.	300.	640.	800.	21.0	1.97	16.	240.	999.	325.	97.8	[28]

.fz 3
.sa 1
2Tabelle A$n2$1 Versuchsdaten, Querzug, (D), Einzelbefestigungen,
Metallspreizdübel am Bauteilrand, Einfluß der Bauteildicke

.ns
.sa 4

Syst. [-]	d [mm]	do [mm]	hef [mm]	Tinst [Nm]	fy [MPa]	ft [MPa]	fcc200 [MPa]	fct [MPa]	dagg [mm]	c1 [mm]	c2 [mm]	h [mm]	Vu [kN]	Lit.
A1	20.	28.	125.	300.	640.	800.	21.0	1.97	16.	240.	999.	325.	101.0	[28]
A1	20.	28.	125.	300.	640.	800.	21.0	1.97	16.	240.	999.	325.	98.7	[28]
A1	20.	28.	125.	300.	640.	800.	21.0	1.97	16.	240.	999.	325.	106.0	[28]
A1	20.	28.	125.	300.	640.	800.	36.0	2.87	16.	150.	999.	194.	43.5	[28]
A1	20.	28.	125.	300.	640.	800.	36.0	2.87	16.	150.	999.	194.	49.4	[28]
A1	20.	28.	125.	300.	640.	800.	36.0	2.87	16.	150.	999.	193.	44.5	[28]
A1	20.	28.	125.	300.	640.	800.	34.3	2.77	16.	200.	999.	195.	73.3	[28]
A1	20.	28.	125.	300.	640.	800.	34.3	2.77	16.	200.	999.	195.	56.6	[28]
A1	20.	28.	125.	300.	640.	800.	34.3	2.77	16.	200.	999.	194.	73.1	[28]
A1	20.	28.	125.	300.	640.	800.	21.5	1.96	16.	300.	999.	260.	123.5	[28]
A1	20.	28.	125.	300.	640.	800.	21.5	1.96	16.	300.	999.	260.	121.8	[28]
A1	20.	28.	125.	300.	640.	800.	21.5	1.96	16.	300.	999.	260.	120.0	[28]

.fz 3
.sa 1
2Tabelle A$n2$1 Versuchsdaten, Querzug, (D), Einzelbefestigungen,
Metallspreizdübel am Bauteilrand, Einfluß der Bauteildicke

.ns
.sa 4

Syst. [-]	d [mm]	do [mm]	hef [mm]	Tinst [Nm]	fy [MPa]	ft [MPa]	fcc200 [MPa]	fct [MPa]	dagg [mm]	c1 [mm]	c2 [mm]	h [mm]	Vu [kN]	Lit.
A1	20.	28.	125.	300.	640.	800.	34.3	2.77	16.	250.	999.	197.	73.0	[28]
A1	20.	28.	125.	300.	640.	800.	34.3	2.77	16.	250.	999.	192.	63.9	[28]
A1	20.	28.	125.	300.	640.	800.	34.3	2.77	16.	250.	999.	192.	65.4	[28]
A1	16.	24.	100.	180.	640.	800.	22.1	1.98	16.	200.	999.	262.	69.6	[28]
A1	16.	24.	100.	180.	640.	800.	22.1	1.98	16.	200.	999.	262.	66.8	[28]
A1	16.	24.	100.	180.	640.	800.	22.1	1.98	16.	200.	999.	262.	69.7	[28]
A1	16.	24.	100.	180.	640.	800.	22.1	1.98	16.	200.	999.	262.	72.7	[28]
A1	16.	24.	100.	180.	640.	800.	22.1	1.98	16.	200.	999.	210.	58.9	[28]
A1	16.	24.	100.	180.	640.	800.	22.1	1.98	16.	200.	999.	210.	54.8	[28]
A1	16.	24.	100.	180.	640.	800.	22.1	1.98	16.	200.	999.	210.	59.9	[28]
A1	16.	24.	100.	180.	640.	800.	22.1	1.98	16.	200.	999.	210.	57.9	[28]
A1	16.	24.	100.	180.	640.	800.	28.2	2.26	16.	250.	999.	260.	77.5	[28]
A1	16.	24.	100.	180.	640.	800.	36.0	2.72	16.	150.	999.	154.	41.0	[28]
A1	16.	24.	100.	180.	640.	800.	30.0	2.45	16.	200.	999.	203.	60.2	[28]
A1	16.	24.	100.	180.	640.	800.	30.0	2.45	16.	200.	999.	202.	62.9	[28]
A1	16.	24.	100.	180.	640.	800.	30.0	2.45	16.	200.	999.	201.	60.7	[28]
A1	16.	24.	100.	180.	640.	800.	36.0	2.72	16.	150.	999.	150.	44.1	[28]
A1	16.	24.	100.	180.	640.	800.	36.0	2.72	16.	150.	999.	149.	42.7	[28]
A1	16.	24.	100.	180.	640.	800.	30.0	2.45	16.	200.	999.	195.	53.0	[28]
A1	16.	24.	100.	180.	640.	800.	30.0	2.45	16.	200.	999.	192.	53.4	[28]
A1	16.	24.	100.	180.	640.	800.	29.1	2.34	16.	250.	999.	187.	64.7	[28]
A1	16.	24.	100.	180.	640.	800.	29.1	2.34	16.	250.	999.	187.	59.3	[28]
A1	16.	24.	100.	180.	640.	800.	24.8	2.21	16.	250.	999.	187.	54.7	[28]
A1	16.	24.	100.	180.	640.	800.	24.8	2.21	16.	250.	999.	187.	57.1	[28]
D	10.	16.	80.	80.	900.	1000.	26.9	2.17	16.	160.	999.	160.	36.1	[28]

.fz 3
.sa 1
2Tabelle A$n2$1 Versuchsdaten, Querzug, (D), Einzelbefestigungen,
Metallspreizdübel am Bauteilrand, Einfluß der Bauteildicke

.ns
.sa 4

Syst. [-]	d [mm]	do [mm]	hef [mm]	Tinst [Nm]	fy [MPa]	ft [MPa]	fcc200 [MPa]	fct [MPa]	dagg [mm]	c1 [mm]	c2 [mm]	h [mm]	Vu [kN]	Lit.
D	10.	16.	80.	80.	900.	1000.	27.0	2.15	16.	160.	999.	160.	36.4	[28]
D	10.	16.	80.	80.	900.	1000.	27.0	2.15	16.	160.	999.	160.	42.8	[28]
D	10.	16.	80.	80.	900.	1000.	27.0	2.15	16.	160.	999.	160.	47.7	[28]
D	10.	16.	80.	80.	900.	1000.	29.7	2.53	16.	160.	999.	160.	52.6	[28]
A1	10.	14.	60.	25.	640.	800.	31.0	2.51	16.	130.	999.	120.	33.0	[28]
A1	10.	14.	60.	25.	640.	800.	31.0	2.51	16.	130.	999.	120.	27.8	[28]
A1	10.	14.	60.	25.	640.	800.	31.0	2.51	16.	130.	999.	120.	30.6	[28]
A1	10.	14.	60.	25.	640.	800.	31.0	2.51	16.	130.	999.	120.	33.0	[28]
A1	8.	12.	50.	20.	640.	800.	28.0	2.21	16.	110.	999.	100.	24.6	[28]
A1	8.	12.	50.	20.	640.	800.	28.0	2.21	16.	110.	999.	100.	23.2	[28]
A1	8.	12.	50.	20.	640.	800.	28.0	2.21	16.	110.	999.	100.	19.6	[28]
A1	8.	12.	50.	20.	640.	800.	28.0	2.21	16.	110.	999.	100.	23.4	[28]
D	12.	18.	105.	80.	640.	800.	27.9	1.99	16.	200.	999.	210.	69.3	[28]
D	12.	18.	105.	80.	640.	800.	28.1	2.18	16.	200.	999.	210.	63.6	[28]
D	12.	18.	105.	80.	640.	800.	28.1	2.18	16.	200.	999.	210.	64.8	[28]

.fz 3
.sa 1
2Tabelle A$n2$1 Versuchsdaten, Querzug, (D), Einzelbefestigungen,
Metallspreizdübel am Bauteilrand, Einfluß der Bauteildicke

.ue
.nn 26.1
.sa 4

Syst. [-]	d [mm]	do [mm]	hef [mm]	Tinst [Nm]	fy [MPa]	ft [MPa]	fcc200 [MPa]	fct [MPa]	dagg [mm]	c1 [mm]	c2 [mm]	s1 [mm]	Vu,m [kN]	Lit.
D	10.0	10.0	40.0	40.0	640.	800.	34.8	2.8	16.	40.	999.	999.	7.2	[2]
D	8.0	12.0	50.0	25.0	640.	800.	35.7	2.6	16.	49.	999.	999.	8.1	[2]
D	8.0	12.0	40.0	.	640.	800.	28.0	.	.	50.	999.	100.	8.2	[2]
D	10.0	14.0	40.0	.	640.	800.	28.0	.	.	50.	999.	100.	8.4	[2]
D	8.0	12.0	40.0	.	640.	800.	43.5	.	.	50.	999.	100.	12.5	[2]
C	6.0	10.0	40.0	10.0	640.	800.	28.5	2.5	16.	50.	999.	999.	8.7	[4]
B	6.0	8.0	25.0	5.0	640.	800.	44.0	.	.	50.	999.	999.	6.3	[7]
A1	6.0	9.5	38.0	.	640.	800.	40.0	.	.	53.	999.	999.	10.5	[5]
C	8.0	12.0	50.0	25.0	640.	800.	28.5	2.5	16.	60.	999.	999.	13.3	[4]
C	10.0	14.0	60.0	40.0	640.	800.	26.0	2.3	16.	60.	999.	999.	11.3	[4]
B	8.0	10.0	30.0	11.0	640.	800.	40.0	.	.	60.	999.	999.	9.8	[7]
D	8.0	14.0	40.0	8.0	390.	490.	21.3	.	.	70.	999.	999.	16.7	[7]
D	10.0	16.0	40.0	10.0	390.	490.	21.3	.	.	70.	999.	999.	13.5	[7]
D	10.0	16.0	40.0	10.0	390.	490.	34.8	.	.	70.	999.	999.	21.5	[7]
A1	8.0	12.0	60.0	25.0	640.	800.	34.3	2.6	16.	75.	999.	999.	18.8	[7]
A1	28.0	28.0	130.0	250.0	1080.	1200.	30.5	2.3	16.	75.	999.	999.	16.6	[7]
D	10.0	15.9	102.5	.	724.	862.	42.3	.	.	76.	999.	999.	25.5	[7]
D	12.0	18.0	80.0	80.0	640.	800.	34.3	2.6	16.	80.	999.	999.	23.4	[2]
C	18.0	18.0	80.0	80.0	640.	800.	34.3	2.8	16.	80.	999.	999.	23.4	[4]
A1	12.0	18.0	80.0	80.0	640.	800.	34.3	2.6	16.	80.	999.	999.	38.3	[7]
D	12.0	18.0	80.0	.	640.	800.	24.0	.	.	80.	999.	999.	21.7	[2]
A2	12.0	18.0	80.0	80.0	640.	800.	21.5	.	.	80.	999.	999.	30.4	[7]
D	10.0	14.0	40.0	.	640.	800.	28.0	.	.	100.	999.	200.	20.7	[2]
D	10.0	14.0	40.0	50.0	640.	800.	25.0	.	.	100.	999.	200.	20.9	[2]
D	22.0	22.0	80.0	130.0	640.	800.	30.0	2.4	16.	100.	999.	999.	27.6	[2]

.fz 3
.sa 1
2Tabelle A$n2$1 Versuchsdaten, Querzug, (D), Einzelbefestigungen,
Metallspreizdübel am Bauteilrand

.ns
.sa 4

Syst. [-]	d [mm]	do [mm]	hef [mm]	Tinst [Nm]	fy [MPa]	ft [MPa]	fcc200 [MPa]	fct [MPa]	dagg [mm]	c1 [mm]	c2 [mm]	s1 [mm]	Vu,m [kN]	Lit.
A1	28.0	28.0	130.0	250.0	1080.	1200.	30.5	2.3	16.	100.	999.	999.	28.7	[7]
A2	16.0	24.0	105.0	150.0	640.	800.	53.9	.	.	105.	999.	999.	46.7	[7]
A2	16.0	24.0	105.0	150.0	640.	800.	30.8	.	.	105.	999.	999.	43.3	[7]
A1	18.0	18.0	80.0	80.0	640.	800.	29.8	2.5	16.	120.	999.	999.	32.4	[7]
B	16.0	20.0	60.0	80.0	640.	800.	45.0	.	.	120.	999.	999.	31.7	[7]
D	16.0	25.0	125.0	100.0	902.	997.	32.8	3.0	16.	125.	999.	999.	71.5	[7]
A1	28.0	28.0	130.0	250.0	1080.	1200.	30.5	2.3	16.	125.	999.	999.	38.6	[7]
A1	28.0	28.0	130.0	250.0	1080.	1200.	25.4	2.0	16.	125.	999.	999.	43.5	[7]
A3	16.0	23.0	100.0	180.0	640.	800.	34.3	2.8	16.	130.	999.	999.	50.7	[4]
A1	24.0	24.0	100.0	200.0	640.	800.	28.2	2.5	16.	130.	999.	999.	44.4	[7]
A1	24.0	24.0	100.0	200.0	640.	800.	34.5	2.8	16.	130.	999.	999.	51.5	[7]
A2	20.0	28.0	130.0	250.0	640.	800.	30.8	.	.	130.	999.	999.	50.3	[7]
D	12.0	18.0	80.0	.	640.	800.	25.0	.	.	140.	999.	999.	41.5	[2]
A1	16.0	24.0	100.0	200.0	640.	800.	34.3	2.6	16.	150.	999.	999.	58.9	[7]
A1	28.0	28.0	130.0	250.0	1080.	1200.	30.5	2.3	16.	150.	999.	999.	52.5	[7]
A1	28.0	28.0	130.0	250.0	1080.	1200.	25.4	2.0	16.	150.	999.	999.	56.9	[7]
A1	28.0	28.0	130.0	250.0	1080.	1200.	27.6	1.9	16.	150.	999.	999.	60.4	[7]
A2	16.0	24.0	105.0	150.0	640.	800.	53.9	.	.	158.	999.	999.	82.8	[7]
A2	16.0	24.0	105.0	150.0	640.	800.	30.8	.	.	158.	999.	999.	78.6	[7]
A2	12.0	18.0	80.0	80.0	640.	800.	21.5	.	.	160.	999.	999.	66.0	[7]
D	20.0	30.0	170.0	200.0	1047.	1134.	29.6	2.4	16.	170.	999.	999.	149.7	[7]
B	16.0	20.0	60.0	80.0	640.	800.	45.0	.	.	180.	999.	999.	41.6	[7]
A2	20.0	28.0	130.0	250.0	640.	800.	21.5	.	.	195.	999.	999.	86.1	[7]
A2	20.0	28.0	130.0	250.0	640.	800.	30.8	.	.	195.	999.	999.	91.7	[7]
A3	20.0	20.0	100.0	80.0	640.	800.	32.7	2.7	16.	200.	999.	999.	65.7	[4]

.fz 3
.sa 1
2Tabelle A$n2$1 Versuchsdaten, Querzug, (D), Einzelbefestigungen,
Metallspreizdübel am Bauteilrand

.ns
.sa 4

Syst. [-]	d [mm]	do [mm]	hef [mm]	Tinst [Nm]	fy [MPa]	ft [MPa]	fcc200 [MPa]	fct [MPa]	dagg [mm]	c1 [mm]	c2 [mm]	s1 [mm]	Vu,m [kN]	Lit.
A1	28.0	28.0	130.0	250.0	1080.	1200.	30.5	2.3	16.	200.	999.	999.	87.5	[7]
A3	28.0	28.0	200.0	330.0	640.	800.	30.9	2.7	16.	200.	999.	999.	92.0	[4]
A3	28.0	28.0	200.0	330.0	640.	800.	34.4	2.6	16.	200.	999.	999.	123.1	[4]
A2	16.0	24.0	105.0	150.0	640.	800.	30.8	.	.	210.	999.	999.	103.5	[7]
D	24.0	32.0	220.0	300.0	1144.	1242.	32.7	2.6	16.	220.	999.	999.	226.0	[7]
A3	24.0	24.0	125.0	180.0	640.	800.	30.0	2.4	16.	250.	999.	999.	80.9	[4]
A1	28.0	28.0	130.0	250.0	1080.	1200.	27.4	2.2	16.	250.	999.	999.	114.9	[7]
A2	20.0	28.0	130.0	250.0	640.	800.	21.5	.	.	260.	999.	999.	121.8	[7]
A1	28.0	28.0	130.0	250.0	1080.	1200.	27.3	2.2	16.	300.	999.	999.	140.2	[7]
A1	28.0	28.0	130.0	250.0	1080.	1200.	27.4	2.2	16.	300.	999.	999.	140.3	[7]

.fz 3
.sa 1
2Tabelle A$n2$1 Versuchsdaten, Querzug, (D), Einzelbefestigungen,
Metallspreizdübel am Bauteilrand

.ue
.nn 29.1
.sa 4

Syst. [-]	d [mm]	d1 [mm]	hef [mm]	Tinst [Nm]	fy [MPa]	ft [MPa]	fcc200 [MPa]	fct [MPa]	dagg [mm]	c1 [mm]	c2 [mm]	s1 [mm]	Vu [kN]	Lit.
A1	18.	12.	80.	80.	640.	800.	20.5	1.91	16.	80.	999.	200.	33.0	[7]
A1	18.	12.	80.	80.	640.	800.	20.5	1.91	16.	200.	999.	80.	95.0	[7]
A1	24.	16.	100.	180.	640.	800.	20.5	1.91	16.	105.	999.	263.	60.0	[7]
A1	24.	16.	100.	180.	640.	800.	20.5	1.91	16.	105.	999.	263.	65.0	[7]
A1	24.	16.	100.	180.	640.	800.	20.5	1.91	16.	105.	999.	263.	70.0	[7]
A1	18.	12.	80.	80.	640.	800.	26.0	2.26	16.	120.	999.	120.	56.0	[7]
A1	18.	12.	80.	80.	640.	800.	26.0	2.26	16.	120.	999.	120.	57.2	[29]
A1	18.	12.	80.	80.	640.	800.	26.0	2.26	16.	120.	999.	120.	48.8	[29]
D	18.	12.	80.	80.	640.	800.	26.0	2.26	16.	80.	999.	120.	24.1	[29]
D	18.	12.	80.	80.	640.	800.	26.0	2.26	16.	80.	999.	120.	23.5	[29]
D	18.	12.	80.	80.	640.	800.	26.0	2.26	16.	80.	999.	120.	27.2	[29]
A1	18.	12.	80.	80.	640.	800.	26.0	2.26	16.	200.	999.	120.	72.1	[29]
A1	18.	12.	80.	80.	640.	800.	26.0	2.26	16.	200.	999.	120.	75.0	[29]
A1	18.	12.	80.	80.	640.	800.	26.0	2.26	16.	200.	999.	120.	74.0	[29]
A1	18.	12.	80.	80.	640.	800.	26.0	2.26	16.	200.	999.	120.	82.0	[29]
A1	18.	12.	80.	80.	640.	800.	26.0	2.26	16.	200.	999.	120.	96.6	[29]
D	22.	16.	80.	130.	640.	800.	27.2	2.41	16.	200.	999.	150.	100.0	[28]
D	22.	16.	80.	130.	640.	800.	27.2	2.41	16.	200.	999.	150.	89.2	[28]
D	22.	16.	80.	130.	640.	800.	24.1	2.30	16.	200.	999.	150.	96.6	[28]
D	22.	16.	80.	130.	640.	800.	24.1	2.30	16.	200.	999.	150.	97.9	[28]
D	22.	16.	80.	130.	640.	800	24.1	2.30	16.	200.	999.	100.	90.0	[28]
D	22.	16.	80.	130.	640.	800	24.1	2.30	16.	200.	999.	100.	79.2	[28]
D	22.	16.	80.	130.	640.	800	27.2	2.41	16.	200.	999.	100.	84.0	[28]
D	22.	16.	80.	130.	640.	800	27.2	2.41	16.	200.	999.	100.	85.8	[28]
D	22.	16.	80.	130.	640.	800	24.1	2.30	16.	200.	999.	200.	104.4	[28]

.fz 3
.sa 1

2Tabelle A$n2$1 Versuchsdaten, Querzug, (D), Zweifachbefestigungen,
Metallspreizdübel am Bauteilrand

.ns
.sa 4

Syst. [-]	d [mm]	d1 [mm]	hef [mm]	Tinst [Nm]	fy [MPa]	ft [MPa]	fcc200 [MPa]	fct [MPa]	dagg [mm]	c1 [mm]	c2 [mm]	s1 [mm]	Vu [kN]	Lit.
D	22.	16.	80.	130.	640.	800	24.1	2.30	16.	200.	999.	200.	93.9	[28]
D	22.	16.	80.	130.	640.	800	24.1	2.30	16.	200.	999.	200.	102.2	[28]
D	22.	16.	80.	130.	640.	800	24.3	2.26	16.	200.	999.	250.	110.1	[28]
D	22.	16.	80.	130.	640.	800	24.3	2.26	16.	200.	999.	250.	101.2	[28]
D	22.	16.	80.	130.	640.	800	24.3	2.26	16.	200.	999.	250.	102.4	[28]
D	22.	16.	80.	130.	640.	800	26.1	2.46	16.	200.	999.	300.	125.6	[28]
D	22.	16.	80.	130.	640.	800	26.1	2.46	16.	200.	999.	300.	123.5	[28]
D	22.	16.	80.	130.	640.	800	24.3	2.30	16.	200.	999.	300.	129.8	[28]
D	22.	16.	80.	130.	640.	800	26.1	2.46	16.	200.	999.	400.	147.7	[28]
D	22.	16.	80.	130.	640.	800	26.1	2.46	16.	200.	999.	400.	143.1	[28]
D	22.	16.	80.	130.	640.	800	24.1	2.30	16.	200.	999.	400.	138.2	[28]

.fz 3
.sa 1
Tabelle A$n2$1 Versuchsdaten, Querzug, (D), Zweifachbefestigungen, Metallspreizdübel am Bauteilrand

.ue
.nn 27.1
.sa 4

Syst. [-]	d [mm]	do [mm]	hef [mm]	Tinst [Nm]	fy [MPa]	ft [MPa]	fcc200 [MPa]	fct [MPa]	dagg [mm]	c1 [mm]	c2 [mm]	s1 [mm]	Vu,m [kN]	Lit.
A3	6.3	6.0	27.4	11.0	.	.	18.6	.	25.	38.	999.	999.	4.5	[37]
A3	6.3	6.0	27.7	11.0	745.	.	17.1	.	25.	38.	999.	999.	4.5	[37]
A3	6.3	6.0	29.7	11.0	.	.	18.6	.	25.	38.	999.	999.	4.6	[37]
A3	6.3	6.0	29.2	11.0	.	.	18.6	.	25.	38.	999.	999.	4.8	[37]
A1	7.9	8.0	34.2	27.0	.	.	18.9	.	25.	48.	999.	999.	8.6	[35]
A3	6.3	6.0	27.7	.	565.	.	17.0	.	25.	51.	999.	999.	8.8	[39]
A3	9.5	9.5	40.3	48.0	745.	.	17.0	.	25.	57.	999.	999.	11.2	[38]
A3	9.5	9.5	40.0	48.0	565.	.	17.0	.	25.	57.	999.	999.	12.1	[38]
A3	9.5	9.5	39.2	48.0	565.	.	34.8	.	25.	57.	999.	999.	12.5	[38]
A3	9.5	9.5	39.4	48.0	745.	.	34.8	.	25.	57.	999.	999.	12.8	[38]
A3	9.5	9.5	39.5	54.0	.	.	18.6	.	25.	57.	999.	999.	9.4	[37]
A3	9.5	9.5	39.3	54.0	.	.	18.6	.	25.	57.	999.	999.	10.0	[37]
A3	9.5	9.5	39.4	54.0	.	.	18.6	.	25.	57.	999.	999.	11.7	[37]
A3	9.5	9.5	39.4	54.0	745.	.	17.1	.	25.	57.	999.	999.	11.7	[38]
A3	9.5	9.5	38.3	54.0	.	.	36.9	.	25.	57.	999.	999.	12.1	[37]
A3	9.5	9.5	41.7	54.0	.	.	36.9	.	25.	57.	999.	999.	12.4	[37]
A3	9.5	9.5	41.9	54.0	.	.	36.9	.	25.	57.	999.	999.	12.6	[37]
A3	9.5	9.5	41.4	54.0	745.	.	34.3	.	25.	57.	999.	999.	12.6	[38]
A3	9.5	9.5	38.6	68.0	483.	565	44.3	.	25.	57.	999.	999.	15.8	[38]
A3	9.5	10.0	41.3	27.0	345.	483.	18.3	.	.	64.	999.	999.	9.1	[44]
A3	9.5	10.0	41.3	27.0	345.	483.	33.8	.	.	64.	999.	999.	13.1	[44]
A3	9.5	10.0	63.5	34.0	345.	483.	18.3	.	.	64.	999.	999.	13.0	[44]
A3	9.5	10.0	63.5	34.0	345.	483.	33.8	.	.	64.	999.	999.	14.8	[44]
A3	9.5	9.0	35.8	.	565.	.	17.0	.	25.	76.	999.	999.	17.0	[39]
A1	12.7	13.0	57.5	48.0	.	.	18.7	.	25.	76.	999.	999.	19.3	[35]
A3	12.7	13.0	50.8	68.0	745.	.	16.1	.	25.	76.	999.	999.	15.6	[38]
A3	12.7	13.0	57.2	88.0	.	.	16.9	.	25.	76.	999.	999.	17.9	[37]

.fz 3
.sa 1
2Tabelle $n2$1 Versuchsdaten, Querzug, (USA), Einzelbefestigungen,
Dübel am Bauteilrand

.ns
.sa 4

Syst. [-]	d [mm]	do [mm]	hef [mm]	Tinst [Nm]	fy [MPa]	ft [MPa]	fcc200 [MPa]	fct [MPa]	dagg [mm]	c1 [mm]	c2 [mm]	s1 [mm]	Vu,m [kN]	Lit.
A3	12.7	13.0	57.2	88.0	.	.	16.9	.	25.	76.	999.	999.	19.3	[38]
A3	12.7	13.0	57.2	88.0	.	.	16.9	.	25.	76.	999.	999.	20.9	[37]
A3	12.7	13.0	60.5	95.0	745.	.	16.9	.	25.	76.	999.	999.	19.3	[38]
A3	12.7	13.0	58.4	95.0	.	.	32.6	.	25.	76.	999.	999.	20.4	[37]
A3	12.7	13.0	72.6	95.0	.	.	32.6	.	25.	76.	999.	999.	22.1	[37]
A3	12.7	13.0	61.2	95.0	.	.	32.6	.	25.	76.	999.	999.	22.2	[37]
A3	12.7	13.0	61.0	95.0	745.	.	32.6	.	25.	76.	999.	999.	22.2	[38]
A3	12.7	13.0	56.3	108.0	483.	565.	44.3	.	25.	76.	999.	999.	22.2	[38]
A3	12.7	13.0	101.6	108.0	483.	565.	44.3	.	25.	76.	999.	999.	22.8	[38]
A3	12.7	13.0	61.0	122.0	745.	.	25.5	.	25.	76.	999.	999.	17.1	[35]
A3	15.9	16.0	78.2	136.0	.	.	16.7	.	25.	95.	999.	999.	26.6	[37]
A3	15.9	16.0	73.7	136.0	.	.	32.6	.	25.	95.	999.	999.	28.2	[37]
A3	15.9	16.0	78.5	136.0	745.	.	25.5	.	25.	95.	999.	999.	29.0	[38]
A3	15.9	16.0	81.3	136.0	.	.	16.7	.	25.	95.	999.	999.	29.2	[37]
A3	15.9	16.0	79.2	136.0	.	.	16.7	.	25.	95.	999.	999.	30.5	[37]
A3	15.9	16.0	80.5	136.0	745.	.	17.1	.	25.	95.	999.	999.	30.5	[38]
A3	15.9	16.0	76.2	136.0	.	.	32.6	.	25.	95.	999.	999.	32.2	[37]
A3	15.9	16.0	78.7	136.0	.	.	32.6	.	25.	95.	999.	999.	34.9	[37]
A3	15.9	16.0	80.4	136.0	745.	.	32.6	.	25.	95.	999.	999.	35.0	[38]
A3	15.9	16.0	71.1	136.0	483.	565.	44.3	.	25.	95.	999.	999.	37.4	[38]
A3	15.9	16.0	125.7	136.0	483.	565.	44.3	.	25.	95.	999.	999.	39.9	[38]
A3	12.7	13.0	59.5	68.0	.	.	16.5	.	25.	102.	999.	999.	21.2	[40]
A3	12.7	13.0	60.0	68.0	745.	.	32.7	.	25.	102.	999.	999.	22.2	[38]
A3	12.7	13.0	73.2	68.0	565.	.	32.6	.	25.	102.	999.	999.	26.1	[38]
A1	19.0	19.0	57.5	149.0	.	.	18.9	.	25.	102.	999.	999.	37.2	[35]
A3	19.0	19.0	85.1	203.0	.	.	17.7	.	25.	114.	999.	999.	31.4	[37]
A3	19.0	19.0	81.2	203.0	.	.	17.7	.	25.	114.	999.	999.	31.4	[37]

.fz 3
.sa 1
2Tabelle$n2$1 Versuchsdaten, Querzug, (USA), Einzelbefestigungen,
Dübel am Bauteilrand

.ns
.sa 4

Syst. [-]	d [mm]	do [mm]	hef [mm]	Tinst [Nm]	fy [MPa]	ft [MPa]	fcc200 [MPa]	fct [MPa]	dagg [mm]	c1 [mm]	c2 [mm]	s1 [mm]	Vu,m [kN]	Lit.
A3	19.0	19.0	88.9	203.0	.	.	17.7	.	25.	114.	999.	999.	35.7	[37]
A3	19.0	19.0	88.8	203.0	745.	.	17.1	.	25.	114.	999.	999.	35.7	[38]
A3	19.0	19.0	84.5	203.0	.	.	32.6	.	25.	114.	999.	999.	37.1	[37]
A3	19.0	19.0	86.9	203.0	745.	.	25.5	.	25.	114.	999.	999.	41.8	[38]
A3	19.0	19.0	83.8	203.0	.	.	32.6	.	25.	114.	999.	999.	42.8	[37]
A3	19.0	19.0	83.8	203.0	483.	565.	44.3	.	25.	114.	999.	999.	45.8	[38]
A3	19.0	19.0	87.1	203.0	.	.	32.6	.	25.	114.	999.	999.	46.6	[37]
A3	19.0	19.0	86.3	203.0	745.	.	32.6	.	25.	114.	999.	999.	46.6	[38]
A3	19.0	19.8	82.6	203.0	345.	483.	20.6	.	.	124.	999.	999.	45.8	[44]
A3	19.0	19.8	82.6	203.0	345.	483.	40.7	.	.	124.	999.	999.	44.7	[44]
A3	19.0	19.8	120.7	305.0	345.	483.	20.6	.	.	124.	999.	999.	41.6	[44]
A3	19.0	19.8	120.7	305.0	345.	483.	40.7	.	.	124.	999.	999.	50.2	[44]
A3	15.9	16.0	70.6	.	565.	.	16.7	.	25.	127.	999.	999.	43.6	[39]
A3	15.9	16.0	83.9	.	565.	.	34.6	.	25.	127.	999.	999.	51.1	[39]
A3	15.9	16.0	71.6	81.0	.	.	16.5	.	25.	127.	999.	999.	29.8	[40]
A1	15.9	16.0	58.5	81.0	.	.	16.5	.	25.	127.	999.	999.	31.9	[40]
A3	15.9	16.0	70.6	81.0	573.	599.	17.8	.	25.	127.	999.	999.	37.2	[39]
A3	12.7	13.0	76.5	81.0	323.	622.	18.4	.	25.	127.	999.	999.	40.0	[39]
A3	19.0	19.0	86.7	.	565.	.	34.6	.	25.	152.	999.	999.	60.8	[39]
A1	19.0	19.0	63.4	122.0	.	.	16.5	.	25.	152.	999.	999.	43.8	[40]
A3	19.0	19.0	84.3	162.0	.	.	16.5	.	25.	152.	999.	999.	49.3	[40]
A3	19.0	19.0	167.6	203.0	745.	.	25.5	.	25.	165.	999.	999.	74.4	[38]

.fz 3
.sa 1
2Tabelle $n2$1 Versuchsdaten, Querzug, (USA), Einzelbefestigungen,
Dübel am Bauteilrand

.ns
.sa 4

Syst. [-]	d [mm]	do [mm]	hef [mm]	Tinst [Nm]	fy [MPa]	ft [MPa]	fcc200 [MPa]	fct [MPa]	dagg [mm]	c1 [mm]	c2 [mm]	s1 [mm]	Vu,m [kN]	Lit.
A3	25.4	26.3	114.3	271.0	517.	607.	18.4	.	.	172.	999.	999.	54.4	[44]
A3	25.4	26.3	114.3	271.0	517.	607.	48.4	.	.	172.	999.	999.	67.7	[44]
A3	25.4	26.3	114.3	475.0	517.	607.	18.4	.	.	172.	999.	999.	67.6	[44]
A3	22.2	22.2	103.7	203.0	.	.	16.5	.	25.	178.	999.	999.	54.0	[40]
A3	22.2	22.2	100.6	271.0	573.	599.	17.8	.	25.	178.	999.	999.	69.6	[39]
A3	22.2	22.2	102.2	285.0	573.	599.	28.4	.	25.	178.	999.	999.	64.3	[39]
A3	19.0	19.0	103.1	163.0	323.	622.	34.4	.	25.	191.	999.	999.	106.6	[39]
A3	25.4	25.0	113.9	406.0	.	.	16.5	.	25.	203.	999.	999.	82.9	[39]

.fz 3
.sa 1
2Tabelle $n2$1 Versuchsdaten, Querzug, (USA), Einzelbefestigungen,
Dübel am Bauteilrand

Permission to Include References for **Appendix C** was not received by time of document publication.

APPENDIX D: ORIGINAL DATA BASE FOR STEEL FAILURES (U.S. UNITS)

TEST NO.	REFERENCE	REF. NO.	TYPE	DIAMETER	LENGTH	EMBEDMENT	HEAD	CONCRETE	TYPE	EDGE DISTANCE	ULT. LOAD	MODE	REMARK
1	10	A1-1	STUD	.750	7.000	6.625	1.250	5270.	NWT	12.000	28.3	S	
2	10	A1-2	STUD	.750	7.000	6.625	1.250	5270.	NWT	12.000	28.5	S	
3	10	A1-3	STUD	.750	7.000	6.625	1.250	5270.	NWT	12.000	28.0	S	
6	10	A2-4	STUD	.750	7.000	6.625	1.250	5270.	NWT	4.000	31.5	S	
7	10	A2-5	STUD	.750	7.000	6.625	1.250	5270.	NWT	4.000	29.3	S	
8	10	A3-4	STUD	.750	7.000	6.625	1.250	5270.	NWT	6.000	29.3	S	
9	10	A3-5	STUD	.750	7.000	6.625	1.250	5270.	NWT	6.000	28.8	S	
12	10	B3-4	STUD	.750	7.000	6.625	1.250	4900.	NWT	6.000	31.5	S	
13	10	B3-5	STUD	.750	7.000	6.625	1.250	4900.	NWT	4.000	29.4	S	
19	10	C3-5	STUD	.750	7.000	6.625	1.250	5180.	NWT	6.000	27.3	S	
26	12	1/4HLA	STUD	.250	2.500	2.313	.500	2950.	NWT	12.000	3.7	S	
27	12	1/4HLB	STUD	.250	2.500	2.313	.500	2950.	NWT	12.000	3.0	S	WELD BROKE
28	12	3/8HLA	STUD	.375	3.875	3.594	.750	2950.	NWT	12.000	8.5	S	
29	12	3/8HLB	STUD	.375	3.875	3.594	.750	2950.	NWT	12.000	8.7	S	
30	12	1/2HLA	STUD	.500	5.000	4.688	1.000	2950.	NWT	12.000	12.5	S	
31	12	1/2HLB	STUD	.500	5.000	4.688	1.000	2950.	NWT	12.000	15.0	S	
32	12	5/8HLA	STUD	.625	6.250	5.938	1.250	2950.	NWT	12.000	23.7	S	
33	12	5/8HLB	STUD	.625	6.250	5.938	1.250	2950.	NWT	12.000	25.0	S	
34	12/13	5/8HLA	STUD	.625	6.250	5.938	1.125	3110.	NWT	12.000	22.0	S	

35	12/13	5/8HLB	STUD	.625	6.250	5.938	1.125	3110.	NWT	12.000	25.0	S	
36	12	3/4HLA	STUD	.750	7.500	7.125	1.500	2950.	NWT	12.000	33.0	S	WELD BROKE
37	12	3/4HLB	STUD	.750	7.500	7.125	1.500	2950.	NWT	12.000	34.5	S	WELD BROKE
38	12	3/4HLA	STUD	.750	7.500	7.125	1.250	3110.	NWT	12.000	33.2	S	MACH.BROKE
39	12	3/4HLB	STUD	.750	7.500	7.125	1.250	3110.	NWT	12.000	38.1	S	
40	12	7/8HLA	STUD	.875	7.500	7.125	1.750	2950.	NWT	12.000	50.5	S	WELD BROKE
41	12	7/8HLB	STUD	.875	7.500	7.125	1.750	2950.	NWT	12.000	42.5	S	MACH.BROKE
42	12	1/2THA	STUD	.500	5.000	4.688	.875	3110.	NWT	12.000	14.5	S	THR.STUD
43	12	1/2THB	STUD	.500	5.000	4.688	.875	3110.	NWT	12.000	16.8	S	THR.STUD
44	12	5/8THA	STUD	.625	6.250	5.938	1.125	3110.	NWT	12.000	23.1	S	THR.STUD
45	12	5/8THB	STUD	.625	6.250	5.938	1.125	3110.	NWT	12.000	24.3	S	THR.STUD
46	12	3/4THA	STUD	.750	7.500	7.125	1.250	3110.	NWT	12.000	35.0	S	THR.STUD
47	12	3/4THB	STUD	.750	7.500	7.125	1.250	3110.	NWT	12.000	35.0	S	MACH.BROKE
51	7		A490	1.000	12.600	12.000	1.625	4300.	NWT	18.000	116.0	S	
52	7		A490	1.000	14.700	14.100	1.625	4245.	NWT	18.000	118.0	S	
53	7		A490	1.000	16.800	16.200	1.625	4200.	NWT	18.000	118.0	S	
54	7		A307	.750	6.000	5.500	1.125	5050.	NWT	5.000	26.1	S	
55	7		A307	.750	6.000	5.500	1.125	5050.	NWT	6.000	26.2	S	
57	7		A307	.750	7.000	6.500	1.125	4000.	NWT	2.000	25.4	S	
58	7		A307	.750	7.000	6.500	1.125	5050.	NWT	4.000	26.3	S	
59	7		A307	.750	7.000	6.500	1.125	5050.	NWT	5.000	29.6	S	
60	7		A307	.750	8.000	7.500	1.125	3500.	NWT	2.000	23.2	S	
61	7		A307	.750	8.000	7.500	1.125	3500.	NWT	4.000	24.4	S	

67	7	A307	.750	5.000	4.500	1.125	5500.	NWT	3.750	29.9	S	GROUTED
68	7/14	A307	.750	6.000	5.500	1.125	5500.	NWT	2.500	25.4	S	GROUTED
78	7	A307	.750	5.000	4.500	1.125	4635.	NWT	5.000	21.0	S	
82	7	A307	.750	6.000	5.500	1.125	5050.	NWT	3.000	26.0	S	
83	7	A307	.750	6.000	5.500	1.125	5050.	NWT	4.000	26.1	S	
84	7	A307	.750	6.000	5.500	1.125	5500.	NWT	3.000	26.0	S	GROUTED
86	7	A307	.750	7.000	6.500	1.125	5500.	NWT	2.750	30.4	S	GROUTED
87	7	A307	.750	8.000	7.500	1.125	5500.	NWT	2.750	29.3	S	GROUTED
88	7	A307	.750	8.000	7.500	1.125	5500.	NWT	2.750	27.7	S	GROUTED

REFERENCES FOR APPENDIX D

7. Cannon, R. W., Burdette, E. G., and Funk, R. R., "Anchorage to Concrete," Tennessee Valley Authority, Knoxville, Tennessee, Dec. 1975.

10. McMackin, P. J., Slutter, R. G., and Fisher, J. W., "Headed Steel Anchors under Combined Loading," AISC Engineeering Journal, Second Quarter, Apr. 1973, pp. 43-52.

12. "Concrete Anchor Design Data," Manual No. 21, Nelson Stud Welding Company, Lorain, Aug. 1961.

13. "Nelson Stud Project No. 87," Report No. 1960-16: Concrete Arctests No. 5, Nelson Stud Welding Company, Lorain, 1960.

14. Bailey, John W., and Burdette, Edwin G., "Edge Effects on Anchorage to Concrete," Civil Engineering Research Series No. 31, The University of Tennessee, Knoxville, Aug. 1977, 120 pp.

APPENDIX E: SPREADSHEET DATA BASE FOR CONCRETE FAILURES OF SINGLE ANCHORS NEAR A FREE EDGE, FAR FROM OTHER ANCHORS (SI UNITS)

d (mm)	do or dh (mm)	hef (mm)	fcc200 (MPa)	c1 (mm)	s1 (mm)	s2 (mm)	Nu,m (kN)	Normalized Actual Capacity sq(N)*mm	Normalized Predicted Capacity CC Method sq(N)*mm	Normalized Predicted Capacity ACI 349-85 sq(N)*mm	Normalized Predicted Capacity VCA sq(N)*mm
15.9	31.8	67.1	22.8	50	999	999	24.8	5194	5173	4753	7289
15.9	31.8	67.1	35.1	50	999	999	26.8	4524	5173	4753	7289
15.9	31.8	67.1	22.8	50	999	999	27.4	5738	5173	4753	7289
15.9	31.8	67.1	35.1	50	999	999	28.8	4861	5173	4753	7289
15.9	31.8	67.1	35.1	50	999	999	29.6	4996	5173	4753	7289
12.7		151.4	32.9	114	999	999	73.8	12866	15360	21846	21846
15		193.8	25.2	159	999	999	131.4	26176	23386	36670	36670
12.7		151.4	32.9	127	999	999	78.3	13651	16366	22654	22654
12.7		151.4	25.9	127	999	999	90.3	17743	16366	22654	22654
12.7		151.4	25.9	127	999	999	84.5	16604	16366	22654	22654
30	45	260	23.7	220			199.6	41000	42512	68606	68606
30	45	260	23.7	220			208.5	42828	42512	68606	68606
30	45	260	23.7	220			208.7	42869	42512	68606	68606
30	45	260	23.7	220			225.6	46341	42512	68606	68606
19.5	28.5	88.9	39.6	76	999	999	59.1	9392	8554	8656	11352
19.5	28.5	88.9	35.1	76	999	999	81.4	13739	8554	8656	11352
30	52	344	30.9	300	999	999	408	73397	65920	118686	118686
12.7		145	29.6	127	999	999	81	14888	15755	21121	21121
12.7		145	29.6	127	999	999	85.9	15789	15755	21121	21121
22.2	34.9	90.3	22.8	80	999	999	49	10262	8954	9197	11919
22.2	34.9	90.3	22.8	80	999	999	53.2	11142	8954	9197	11919
22.2	34.9	90.3	47	80	999	999	55.2	8052	8954	9197	11919
22.2	34.9	90.3	22.8	80	999	999	58.4	12231	8954	9197	11919
22.2	34.9	90.3	47	80	999	999	59.2	8635	8954	9197	11919
22.2	34.9	90.3	47	80	999	999	60.8	8869	8954	9197	11919
19.5	28.5	114.3	37.7	102	999	999	97.8	15928	12810	14035	15396
19.5	31.8	168.2	42.1	152	999	999	131.2	20221	23052	29315	29315
27	45	329	30.9	300	999	999	374	67281	63429	109540	109540
19		82.6	24.4	76	999	999	54.2	10972	6990	7709	10592
19		82.6	30.1	76	999	999	55	10025	6990	7709	10592
19		82.6	24.4	76	999	999	57.1	11560	6990	7709	10592
6	6.8	34.2	18.6	32	999	999	7.4	1716	1883	1279	2568
6	6.8	34.2	34.1	32	999	999	7.6	1301	1883	1279	2568
17	17.5	53	25	50	999	999	26.7	5340	3652	3390	5715
25	25.4	83	25	80	999	999	40.3	8060	7260	8270	11260
12	12	62	25	60	999	999	18.1	3620	4700	4299	6941
12.7		51.6	26	51	999	999	25.8	5060	3620	3106	5379
12.7		51.6	24.4	51	999	999	26.1	5284	3620	3106	5379
8	12	63.5	18.4	63	999	999	17.3	4033	4954	4314	7005
8	12	63.5	18.4	63	999	999	18	4196	4954	4314	7005
12	18.4	80	24	80	999	999	39.8	8124	7044	6988	9968
16		125	37.7	125	999	999	114.3	18616	13757	16771	17037

d (mm)	do or dh (mm)	hef (mm)	fcc200 (MPa)	c1 (mm)	s1 (mm)	s2 (mm)	Nu,m (kN)	Normalized Actual Capacity sq(N)*mm	Normalized Predicted Capacity CC Method sq(N)*mm	Normalized Predicted Capacity ACI 349-85 sq(N)*mm	Normalized Predicted Capacity VCA sq(N)*mm
30	52	344	30.9	150	999	999	322	57926	46845	93573	93573
27	45	322	30.9	150	999	999	266	47852	43514	83553	83553
30	105	315	56.7	150	999	999	344	45684	42472	81231	81231
25	25.4	83	25	40	999	999	24.2	4840	5028	6492	8897
19		222.3	29.5	114	999	999	164.6	30305	22612	41177	41177
19.5	28.5	139.7	35.1	76	999	999	125.4	21166	13270	17259	17259
22.2	34.9	90.3	47	50	999	999	38.4	5601	6951	7785	10115
22.2	34.9	90.3	47	50	999	999	40.8	5951	6951	7785	10115
22.2	34.9	90.3	47	50	999	999	44.8	6535	6951	7785	10115
19.5	31.8	92.1	39.8	51	999	999	48.9	7751	7160	7924	10187
17	17.5	53	25	30	999	999	12	2400	2750	2827	4817
15		193.8	29.5	111	999	999	131.4	24193	19331	32325	32325
19.5	28.5	88.9	39.6	51	999	999	44	6992	6901	7512	9874
19.5	28.5	88.9	35.1	51	999	999	73.8	12457	6901	7512	9874
19		222.3	29.5	133	999	999	164.6	30305	24241	43454	43454
19.5	31.8	168.2	42.1	102	999	999	130.7	20143	18437	25560	25560
19.5	28.5	114.3	44.7	70	999	999	103.1	15421	10378	12305	13478
40	60	355	23.7	220			327.2	67211	57133	114473	114473
40	60	355	23.7	220			370.5	76105	57133	114473	114473
19.5	28.5	88.5	44.7	57	999	999	64	9573	7249	7762	10209
19.5	28.5	88.5	44.7	57	999	999	73.8	11038	7249	7762	10209
15		193.8	25.2	127	999	999	130.6	26016	20641	33911	33911
19.5	28.5	114.3	37.7	76	999	999	91.1	14837	10815	12673	13877
12.7		151.4	29.6	102	999	999	81	14888	14458	21004	21004
12.7		151.4	32.9	102	999	999	38.3	6677	14458	21004	21004
12.7		151.4	25.9	102	999	999	74.7	14678	14458	21004	21004
12.7		151.4	32.9	102	999	999	80.1	13965	14458	21004	21004
15		187.5	25	127	999	999	129.7	25940	19982	32182	32182
19		222.3	29.5	152	999	999	169	31115	25924	45575	45575
19		222.3	29.5	152	999	999	197.9	36436	25924	45575	45575
19		82.6	24.4	57	999	999	47.2	9555	5900	6975	9559
19		82.6	24.4	57	999	999	41.6	8422	5900	6975	9559
12.7		145	29.6	102	999	999	78.7	14465	13865	19618	19618
12.7		51.6	24.4	38	999	999	20.2	4089	3018	2815	4849
15		193.8	25	143	999	999	129.9	25980	21993	35370	35370
15.9	31.8	67.3	20.1	50	999	999	16.8	3747	5187	4774	7312
15.9	31.8	67.3	20.1	50	999	999	17.6	3926	5187	4774	7312
15.9	31.8	67.3	20.1	50	999	999	19.6	4372	5187	4774	7312
15.9	31.8	67.3	47.6	50	999	999	26.4	3826	5187	4774	7312
15.9	31.8	67.3	47.6	50	999	999	26.4	3826	5187	4774	7312
15.9	31.8	67.3	47.6	50	999	999	29.2	4232	5187	4774	7312
15.9	31.8	67.1	22.8	50	999	999	22.4	4691	5173	4753	7289

d (mm)	do or dh (mm)	hef (mm)	fcc200 (MPa)	c1 (mm)	s1 (mm)	s2 (mm)	Nu,m (kN)	Normalized Actual Capacity sq(N)*mm	Normalized Predicted Capacity CC Method sq(N)*mm	Normalized Predicted Capacity ACI 349-85 sq(N)*mm	Normalized Predicted Capacity VCA sq(N)*mm
20		170	24.7	170	999	999	159.8	32154	21819	30766	30766
12	18.4	80	24	80	999	999	39.7	8104	7044	6988	9968
24		220	27.6	220	999	999	223.4	42523	32121	51171	51171
40	60	355	19.1	361			274.2	62741	76475	134035	134035
30	45	260	19.1	270			212	48509	48640	72277	72277
30	45	260	19.1	270			218	49882	48640	72277	72277
28	28	125	25	130	999	999	91.2	18240	14137	18178	18455
40	60	355	19.1	370			330.7	75669	77802	134491	134491
40	60	355	19.1	370			416.3	95255	77802	134491	134491
24	24	100	25	105	999	999	55.3	11060	10184	11792	14395
27	45	142	30.9	150	999	999	162	29143	19870	22946	22946
40	60	355	19.1	377			350.9	80291	78842	134616	134616
16	16	75	25	80	999	999	34.4	6880	6689	6525	9634
12	12	37	25	40	999	999	9.7	22920	18722	25516	25516
32	32	148	25	160	999	999	114.6	1940	2340	1721	3307
24	24	100	25	110	999	999	58.2	11640	10530	11887	14592
27	45	134	30.9	150	999	999	185	33281	18995	20711	20711
19.5	28.5	88.9	39.6	102	999	999	88.5	14064	10454	9251	12521
9.5	19	42.9	13.8	50	999	999	9.6	2584	3546	2158	4167
9.5	19	42.9	13.8	50	999	999	10.6	2853	3546	2158	4167
9.5	19	42.9	13.8	50	999	999	11.3	3042	3546	2158	4167
9.5	19	42.9	28.4	50	999	999	17.8	3340	3546	2158	4167
9.5	19	42.9	28.4	50	999	999	20	3753	3546	2158	4167
9.5	19	42.9	28.4	50	999	999	20.4	3828	3546	2158	4167
15.9	31.8	67.3	18.4	80	999	999	18.2	4243	7073	5375	8620
15.9	31.8	67.3	18.4	80	999	999	18.6	4336	7073	5375	8620
15.9	31.8	67.3	18.4	80	999	999	25.4	5921	7073	5375	8620
15.9	31.8	67.3	38.9	80	999	999	30.8	4938	7073	5375	8620
15.9	31.8	67.3	38.9	80	999	999	36	5772	7073	5375	8620
15.9	31.8	67.3	38.9	80	999	999	40.8	6542	7073	5375	8620
15.9	31.8	67.1	22.8	80	999	999	33	6911	7057	5347	8593
15.9	31.8	67.1	22.8	80	999	999	33.4	6995	7057	5347	8593
15.9	31.8	67.1	35.1	80	999	999	33.6	5671	7057	5347	8593
15.9	31.8	67.1	22.8	80	999	999	34.8	7288	7057	5347	8593
15.9	31.8	67.1	35.1	80	999	999	35	5908	7057	5347	8593
15.9	31.8	67.1	35.1	80	999	999	38.4	6482	7057	5347	8593
16	16	67	25	80	999	999	30.9	6180	6140	5339	8586
12	12	100	23	120	999	999	50	10426	11239	10752	13671
8	8	65	23	80	999	999	23	4796	6006	4555	7767
22	22	87	25	110	999	999	46.6	9320	9500	9104	12710
14	14	55	25	70	999	999	20.1	4020	4800	3643	6523
12	12	47	25	60	999	999	16.4	3280	3801	2662	5075

d (mm)	do or dh (mm)	hef (mm)	fcc200 (MPa)	c1 (mm)	s1 (mm)	s2 (mm)	Nu,m (kN)	Normalized Actual Capacity sq(N)*mm	Normalized Predicted Capacity CC Method sq(N)*mm	Normalized Predicted Capacity ACI 349-85 sq(N)*mm	Normalized Predicted Capacity VCA sq(N)*mm
10	10	38	25	50	999	999	11.1	2220	2831	1751	3609
22.2	34.9	90.3	22.8	120	999	999	62.8	13152	12005	9752	13335
22.2	34.9	90.3	22.8	120	999	999	65.6	13738	12005	9752	13335
22.2	34.9	90.3	22.8	120	999	999	66.8	13990	12005	9752	13335
22.2	34.9	90.3	35.1	120	999	999	69.2	11680	12005	9752	13335
22.2	34.9	90.3	35.1	120	999	999	81.2	13706	12005	9752	13335
22.2	34.9	90.3	35.1	120	999	999	84.2	14212	12005	9752	13335
10	10	30	25	40	999	999	6.7	1340	2008	1152	2482
50	80	525	27.7	700			868.3	164979	168758	289800	289800
30	105	112	51.5	150	999	999	147	20484	16689	15268	17316
16	16	67	25	90	999	999	29.7	5940	6742	5339	8869
6	10.7	37	24	50	999	999	13.1	2674	2780	1527	3317
6	10.7	37	59	50	999	999	17.9	2330	2780	1527	3317
6	12	37	25.5	50	999	999	13	2574	2780	1740	3317
12	12	37	25	50	999	999	5.6	1120	2780	1527	3576
8	12.7	36.5	56	50	999	999	21.3	2846	2755	1559	3345
8	12.7	36.5	25	50	999	999	13.9	2780	2755	1559	3345
10	14.7	36	24	50	999	999	11.9	2429	2730	1590	3372
10	14.7	36	59	50	999	999	19.9	2591	2730	1590	3372
8.9	8.5	34.2	18.6	48	999	999	8.9	2064	2550	1415	3073
8.9	8.5	34.2	34.1	48	999	999	10	1712	2550	1415	3073
22	35	185	22.2	261			109.3	23198	36999	36763	36763
22	35	185	22.2	261			126.5	26848	36999	36763	36763
9.5		40	17.2	57	999	999	13.8	3327	3267	1901	3986
9.5		40	17.2	57	999	999	15.2	3665	3267	1901	3986
22	35	185	22.2	264			114.4	24280	37359	36763	36763
22	35	185	22.2	265			125.6	26657	37480	36763	36763
25	25.4	83	25	120	999	999	56.1	11220	9888	8605	12456
14	14	55	25	80	999	999	28.3	5660	5361	3643	6758
10	10	40	25	60	999	999	10.9	2180	3415	1920	4065
20		170	28.3	255	999	999	183.2	34438	29923	31008	31008
24		220	33.2	330	999	999	235.3	40837	44052	51533	51533
20		170	28.3	255	999	999	183.2	34438	29923	31008	31008
24		220	33.2	330	999	999	235.3	40837	44052	51533	51533

APPENDIX F: SPREADSHEET DATA BASE FOR CONCRETE FAILURES OF MULTIPLE CLOSELY SPACED ANCHORS FAR FROM A FREE EDGE (SI UNITS)

d (mm)	do or dh (mm)	hef (mm)	fcc200 (MPa)	c1 (mm)	s1 (mm)	s2 (mm)	Nu,m (kN)	Normalized Actual Capacity sq(N)*mm	Normalized Predicted Capacity CC Method sq(N)*mm	Normalized Predicted Capacity ACI Method sq(N)*mm	Normalized Predicted Capacity VCA Method sq(N)*mm	Normalized Predicted Capacity Peripheral Shear sq(N)*mm
16.00	31.75	153.92	27.58	381	50.8	50.8	267	12732	9118	8932	8932	3143
15.90	63.50	161.90	32.50	406	51	51	266	11643	9747	9699	9699	3311
16.00	31.75	162.05	27.58	999	50.8	50.8	266	12641	9752	9706	9706	3309
15.90	24.80	193.70	39.50	999	76	76	409	16269	11634	14795	14795	5442
15.90	24.80	227.00	34.60	999	102	102	529	22462	15260	21248	21248	8182
15.88		228.60	29.44	999	101.6	101.6	519	23929	15377	21443	21443	8210
15.88		228.60	29.44	999	101.6	101.6	538	24783	15377	21443	21443	8210
19.05		234.95	29.44	999	101.6	101.6	575	26492	15911	22581	22581	8666
19.05		234.95	29.44	999	101.6	101.6	603	27774	15911	22581	22581	8666
19.00	29.80	285.80	34.60	999	102	102	821	34889	20417	30795	30795	10572
19.05		292.10	29.44	999	101.6	101.6	807	37175	20982	31856	31856	10773
19.05		292.10	29.44	999	101.6	101.6	835	38457	20982	31856	31856	10773
22.20	34.90	360.30	29.90	999	100	100	500	22860	31632	45066	45066	13460
22.20	34.90	360.30	30.80	999	100	100	518	23334	31632	45066	45066	13460
22.20	34.90	360.30	27.40	999	100	100	585	27940	31632	45066	45066	13460
9.50	10.00	77.40	14.90	999	38	999	32	4119	5349	4163	6209	1349
12.70	13.40	105.40	14.90	999	51	999	42	5414	8482	7682	9121	2462
15.90	16.70	129.50	35.40	999	64	999	120	10051	11586	11671	11671	3793
15.90	16.70	131.90	15.20	999	64	999	74	9465	11879	12038	12038	3863
19.00	19.80	150.70	15.20	999	76	999	74	9452	14587	15917	15917	5252
16.00	31.75	153.92	27.58	381	76.2	76.2	282	13436	10044	10410	10410	4339
15.90	63.50	161.90	32.50	381	76	76	280	12288	10676	11216	11216	4548
16.00	31.75	162.05	27.58	999	76.2	76.2	280	13340	10696	11249	11249	4568
22.00	35.00	185.00	28.60	850	100	100	275	12856	13581	15791	15791	6900
22.00	35.00	185.00	28.60	850	100	100	290	13557	13581	15791	15791	6900
22.00	35.00	185.00	25.70	850	100	100	303	14942	13581	15791	15791	6900
22.20	34.90	185.30	22.20	999	100	100	240	12734	13607	15839	15839	6922
22.20	34.90	185.30	25.00	999	100	100	253	12650	13607	15839	15839	6922
22.20	34.90	185.30	22.60	999	100	100	253	13305	13607	15839	15839	6922
22.20	34.90	185.30	24.00	999	100	100	264	13472	13607	15839	15839	6922
22.20	34.90	185.30	27.60	999	100	100	278	13229	13607	15839	15839	6922
22.20	34.90	185.30	27.60	999	100	100	280	13324	13607	15839	15839	6922
15.90	24.80	188.90	34.60	999	102	102	394	16754	12201	16100	16100	6808
15.88		190.50	29.44	999	101.6	101.6	390	17946	12310	16272	16272	6841
15.88		190.50	29.44	999	101.6	101.6	399	18374	12310	16272	16272	6841
19.00	29.80	225.40	34.60	999	102	102	589	25033	15126	21215	21215	8337
12.70		152.40	29.44	999	101.6	101.6	297	13674	9485	11641	11641	5325
12.70		152.40	29.44	999	101.6	101.6	314	14485	9485	11641	11641	5325
16.00	31.75	153.92	27.58	381	101.6	101.6	284	13521	11015	11963	11963	5534
12.70	19.80	154.00	34.60	999	102	102	306	12988	9612	11839	11839	5400
22.00	35.00	160.00	24.80	999	100	100	160	8032	11451	12816	12816	5967

d (mm)	do or dh (mm)	hef (mm)	fcc200 (MPa)	c1 (mm)	s1 (mm)	s2 (mm)	Nu,m (kN)	Normalized Actual Capacity sq(N)*mm	Normalized Predicted Capacity CC Method sq(N)*mm	Normalized Predicted Capacity ACI Method sq(N)*mm	Normalized Predicted Capacity VCA Method sq(N)*mm	Normalized Predicted Capacity Peripheral Shear sq(N)*mm
22.00	35.00	160.00	24.80	999	100	100	196	9839	11451	12816	12816	5967
15.90	63.50	161.90	35.80	356	102	102	282	11766	11687	12871	12871	5835
16.00	31.75	162.05	30.34	999	101.6	101.6	282	12800	11684	12867	12867	5826
9.50	10.00	42.60	14.90	999	38	999	20	2565	2435	1589	3025	742
9.53		114.30	29.44	999	101.6	101.6	203	9373	6930	7750	8385	3883
9.53		114.30	29.44	999	101.6	101.6	213	9799	6930	7750	8385	3883
10.00	16.60	117.50	34.60	999	102	102	208	8845	7146	8077	8569	4023
16.00		117.60	29.44	381	101.6	101.6	214	9869	7140	8304	8797	4228
22.35	35.00	184.91	20.50	381	152.4	152.4	300	16549	15833	19779	19779	9878
22.00	35.00	185.00	30.00	375	150	150	308	14058	15733	19582	19582	9727
22.00	35.00	185.00	28.20	575	150	150	311	14641	15733	19582	19582	9727
22.00	35.00	185.00	28.20	575	150	150	313	14735	15733	19582	19582	9727
22.00	35.00	185.00	28.20	575	150	150	318	14971	15733	19582	19582	9727
22.00	35.00	185.00	27.80	375	150	150	330	15647	15733	19582	19582	9727
22.00	35.00	185.00	33.10	375	150	150	335	14557	15733	19582	19582	9727
22.00	35.00	185.00	30.00	375	150	150	335	15291	15733	19582	19582	9727
22.00	35.00	185.00	27.80	375	150	150	342	16216	15733	19582	19582	9727
22.00	35.00	185.00	33.10	375	150	150	351	15252	15733	19582	19582	9727
22.00	35.00	185.00	26.00	999	150	150	490	6006	7993	17149	17149	6673
22.00	35.00	185.00	26.00	999	150	150	508	6227	7993	17149	17149	6673
22.00	35.00	185.00	26.00	999	150	150	520	6374	7993	17149	17149	6673
9.50	10.00	38.50	36.20	999	38	999	23	1870	2143	1362	2654	671
9.50	10.00	41.30	33.80	999	41	999	23	1969	2384	1554	2965	758
12.70	13.40	57.80	36.20	999	57	999	46	3781	3941	3016	5050	1456
12.70	13.40	61.00	14.90	999	57	999	34	4378	4218	3276	5370	1537
9.50	10.00	63.50	33.80	999	64	999	42	3612	4563	3498	5649	1611
15.90	16.70	71.40	36.20	999	70	999	64	5327	5403	4602	6929	2222
15.90	16.60	71.50	14.90	999	70	999	47	6036	5413	4612	6939	2225
12.00	18.00	80.00	25.00	999	80	999	61	6090	6440	5539	7865	2543
12.00	18.40	80.00	25.00	999	80	999	61	6090	6440	5539	7865	2543
16.00	24.00	100.00	19.90	999	105	999	101	11343	9113	8861	10795	4188
16.00	24.00	100.00	22.00	999	105	999	103	10937	9113	8861	10795	4188
16.00	24.00	100.00	61.70	999	105	999	175	11152	9113	8861	10795	4188
20.00	28.00	125.00	24.20	999	130	999	163	16588	12704	13800	14001	6496
16.00		125.00	34.10	999	125	999	176	15044	12578	13316	13513	5999
20.00	28.00	125.00	48.20	999	130	999	242	17457	12704	13800	14001	6496
22.00	35.00	190.00	35.90	999	175	175	377	15730	17337	22318	22318	11442
22.00	35.00	190.00	35.90	999	175	175	395	16481	17337	22318	22318	11442
12.00	15.00	46.00	20.00	999	50	999	39	4383	2869	2026	3685	1041
12.00	15.00	46.00	40.00	999	50	999	40	3162	2869	2026	3685	1041
16.00	31.75	67.06	14.72	999	80.01	80.01	72	4692	4157	3524	4993	1968

d (mm)	do or dh (mm)	hef (mm)	fcc200 (MPa)	c1 (mm)	s1 (mm)	s2 (mm)	Nu,m (kN)	Normalized Actual Capacity sq(N)*mm	Normalized Predicted Capacity CC Method sq(N)*mm	Normalized Predicted Capacity ACI Method sq(N)*mm	Normalized Predicted Capacity VCA Method sq(N)*mm	Normalized Predicted Capacity Peripheral Shear sq(N)*mm
16.00	31.75	67.06	25.76	999	80.01	80.01	130	6384	4157	3524	4993	1968
12.00	18.00	75.00	21.40	999	80	999	59	6420	5943	5011	7370	2384
12.00	18.00	75.00	29.30	999	80	999	70	6429	5943	5011	7370	2384
12.00	18.00	75.00	57.00	999	80	999	126	8358	5943	5011	7370	2384
19.00	19.90	85.70	36.20	999	95	999	77	6424	7334	6908	9302	3484
19.00	19.80	87.60	14.90	999	95	999	57	7344	7535	7141	9491	3562
12.70		88.90	39.10	999	102	999	108	8604	7822	7136	9443	3462
12.70		88.90	31.72	381	101.6	999	108	9625	7813	7126	9431	3451
12.70		88.90	34.48	999	101.6	101.6	171	7276	5395	5738	7172	3106
12.70		88.90	40.70	999	102	102	176	6881	5407	5754	7191	3117
12.70		88.90	34.48	999	101.6	101.6	180	7672	5395	5738	7172	3106
22.00	35.00	90.00	38.20	999	100	100	103	4158	6213	6051	7491	3357
22.00	35.00	90.00	38.20	999	100	100	105	4255	6213	6051	7491	3357
22.00	35.00	90.00	38.20	999	100	100	115	4668	6213	6051	7491	3357
22.00	35.00	90.00	38.20	999	100	100	117	4712	6213	6051	7491	3357
19.05		82.55	33.10	381	101.6	999	126	10968	7140	6688	9188	3525
19.05		82.55	33.10	381	101.6	999	135	11704	7140	6688	9188	3525
19.05		82.55	34.48	999	101.6	101.6	201	8541	5034	5442	7005	3045
19.05		82.55	34.48	999	101.6	101.6	219	9318	5034	5442	7005	3045
19.00		82.60	39.10	999	102	999	125	10019	7153	6701	9202	3535
19.00		82.60	39.10	999	102	999	134	10691	7153	6701	9202	3535
19.00		82.60	40.70	999	102	102	210	8221	5049	5460	7024	3055
22.00	35.00	160.00	24.80	999	200	200	303	15211	15739	19777	19777	10858
22.00	35.00	160.00	24.80	999	200	200	342	17169	15739	19777	19777	10858
12.70		51.56	34.48	999	76.2	76.2	109	4623	2784	2453	3747	1401
12.70		51.56	34.48	999	76.2	76.2	114	4862	2784	2453	3747	1401
12.70		51.60	39.10	381	76	999	65	5190	3730	2815	4849	1599
12.70		51.60	39.10	381	76	999	70	5557	3730	2815	4849	1599
12.70		51.60	40.70	999	76	76	111	4365	2781	2450	3743	1399
10.00	15.00	71.00	13.60	999	100	999	34	4556	5934	4890	7384	2605
10.00	15.00	71.00	27.90	999	100	999	39	3663	5934	4890	7384	2605
22.35	35.00	184.91	20.50	381	269.24	269.24	404	22313	21497	29402	29402	16483
22.00	35.00	185.00	28.90	640	270	270	390	18137	21545	29454	29454	16514
22.00	35.00	185.00	28.90	640	270	270	433	20136	21545	29454	29454	16514
22.00	35.00	185.00	28.90	640	270	270	439	20415	21545	29454	29454	16514
22.00	35.00	185.00	23.60	999	270	270	1320	16982	14745	26019	26019	11763
22.00	35.00	185.00	23.60	999	270	270	1450	18655	14745	26019	26019	11763
22.00	35.00	185.00	24.30	999	270	270	1460	18511	14745	26019	26019	11763
12.00	15.00	46.00	20.00	999	75	999	40	4439	3250	2342	4195	1392
12.00	15.00	46.00	40.00	999	75	999	46	3605	3250	2342	4195	1392
16.00	31.75	67.06	15.04	999	119.888	119.888	70	4539	5420	4778	6613	2786

d (mm)	do or dh (mm)	hef (mm)	fcc200 (MPa)	c1 (mm)	s1 (mm)	s2 (mm)	Nu,m (kN)	Normalized Actual Capacity sq(N)*mm	Normalized Predicted Capacity CC Method sq(N)*mm	Normalized Predicted Capacity ACI Method sq(N)*mm	Normalized Predicted Capacity VCA Method sq(N)*mm	Normalized Predicted Capacity Peripheral Shear sq(N)*mm
16.00	31.75	67.06	31.12	999	119.888	119.888	158	7063	5420	4778	6613	2786
19.05		82.55	20.69	381	165.1	999	113	12436	8438	7892	10902	5128
19.05		82.55	20.69	381	165.1	999	116	12746	8438	7892	10902	5128
19.05		82.55	33.10	381	165.1	999	158	13737	8438	7892	10902	5128
19.05		82.55	27.92	999	165.1	165.1	173	8207	7031	7732	10003	4647
19.05		82.55	33.10	381	165.1	999	180	15610	8438	7892	10902	5128
19.05		82.55	27.92	999	165.1	165.1	182	8628	7031	7732	10003	4647
19.00		82.60	24.40	999	165	999	112	11367	8441	7895	10903	5126
19.00		82.60	24.40	999	165	999	115	11651	8441	7895	10903	5126
19.00		82.60	33.00	999	165	165	178	7746	7031	7733	10001	4646
19.00		82.60	39.10	999	165	999	178	14257	8441	7895	10903	5126
12.70		88.90	24.40	999	152	999	77	7794	8883	8211	10859	4821
12.70		88.90	20.69	381	152.4	999	78	8525	8891	8218	10869	4832
12.70		88.90	20.69	381	152.4	999	80	8831	8891	8218	10869	4832
16.00	24.00	100.00	22.30	999	158	999	109	11499	10305	10239	12443	5808
22.00	35.00	160.00	24.80	999	300	300	361	18133	20709	26532	26532	15750
22.00	35.00	160.00	24.80	999	300	300	472	23675	20709	26532	26532	15750
9.50	10.00	41.30	33.80	999	83	999	28	2442	2992	1977	3724	1288
12.00	15.00	46.00	20.00	999	100	999	45	4986	3632	2550	647	1744
12.00	15.00	46.00	40.00	999	100	999	49	3905	3632	2550	4647	1744
12.70		51.56	27.92	999	127	127	105	4966	4144	3181	5459	2202
12.70		51.56	26.89	999	127	127	109	5275	4144	3181	5459	2202
12.70		51.60	24.40	381	127	999	49	4970	4555	3185	5807	2404
12.70		51.60	24.40	381	127	999	58	5911	4555	3185	5807	2404
12.70		51.60	39.10	381	127	999	86	6901	4555	3185	5807	2404
12.70		51.60	39.10	381	127	999	99	7940	4555	3185	5807	2404
12.70		51.60	33.00	999	127	127	105	4570	4146	3185	5463	2204
12.70		51.60	31.70	999	127	127	109	4858	4146	3185	5463	2204
16.00	31.75	67.06	14.32	999	160.02	160.02	118	7796	6859	5347	8205	3608
16.00	31.75	67.06	26.56	999	160.02	160.02	183	8888	6859	5347	8205	3608
12.00	18.00	75.00	29.30	999	160	999	88	8092	7502	6259	9351	4219
12.00	18.00	75.00	57.00	999	160	999	139	9192	7502	6259	9351	4219
20.00	28.00	125.00	24.20	999	260	999	204	20734	15974	17326	17603	11464
22.00	35.00	160.00	24.80	999	400	400	359	18042	26359	27955	27955	20641
22.00	35.00	160.00	24.80	999	400	400	480	24087	26359	27955	27955	20641
22.35	35.00	184.91	20.50	381	401.32	401.32	638	35226	28941	36793	36793	23949
22.00	35.00	185.00	24.00	530	400	400	627	31996	28870	36763	36763	23866
22.00	35.00	185.00	24.00	530	400	400	628	32047	28870	36763	36763	23866
10.00	14.70	36.00	28.00	999	100	999	28	2665	2808	1590	3372	1321
10.00	14.70	36.00	56.00	999	100	999	40	2666	2808	1590	3372	1321
8.00	12.70	36.50	25.00	999	100	999	27	2660	2848	1559	3345	1294

d (mm)	do or dh (mm)	hef (mm)	fcc200 (MPa)	c1 (mm)	s1 (mm)	s2 (mm)	Nu,m (kN)	Normalized Actual Capacity sq(N)*mm	Normalized Predicted Capacity CC Method sq(N)*mm	Normalized Predicted Capacity ACI Method sq(N)*mm	Normalized Predicted Capacity VCA Method sq(N)*mm	Normalized Predicted Capacity Peripheral Shear sq(N)*mm
8.00	12.70	36.50	56.00	999	100	999	40	2699	2848	1559	3345	1294
6.00	10.70	37.00	28.00	999	100	999	28	2684	2888	1527	3317	1267
12.00	15.00	46.00	20.00	999	125	999	49	5445	4013	2561	5010	2095
12.00	15.00	46.00	40.00	999	125	999	55	4317	4013	2561	5010	2095
12.00	18.00	75.00	21.40	999	200	999	66	7177	8281	6264	9911	5136
12.00	18.00	75.00	29.30	999	200	999	94	8720	8281	6264	9911	5136
12.00	18.00	75.00	57.00	999	200	999	150	9960	8281	6264	9911	5136
19.05		82.55	31.72	381	228.6	999	151	13368	9736	8052	11802	6730
19.05		82.55	31.72	381	228.6	999	154	13698	9736	8052	11802	6730
19.05		82.55	20.69	999	228.6	228.6	223	12281	9361	8052	11802	6250
19.05		82.55	33.10	999	228.6	228.6	278	12087	9361	8052	11802	6250
19.05		82.55	33.10	999	228.6	228.6	283	12284	9361	8052	11802	6250
19.00		82.60	24.40	999	229	229	223	11307	9380	8056	11805	6262
19.00		82.60	39.10	999	229	229	280	11211	9380	8056	11805	6262
16.00	24.00	100.00	22.30	999	263	999	132	14008	12668	11136	14106	9018
16.00	24.00	100.00	19.90	999	263	999	132	14840	12668	11136	14106	9018
16.00	24.00	100.00	22.00	999	263	999	133	14210	12668	11136	14106	9018
16.00	24.00	100.00	61.70	999	263	999	268	17059	12668	11136	14106	9018
20.00	28.00	125.00	24.20	999	325	999	202	20572	17609	17400	17705	13948
16.00		125.00	34.10	999	375	999	228	19548	18867	16920	17221	15552
20.00	28.00	125.00	48.20	999	325	999	347	25005	17609	17400	17705	13948

APPENDIX G: SPREADSHEET DATA BASE FOR HIGH STRENGTH STEEL FAILURES (SI UNITS)

Test Number	d (in.)	do or dh (in.)	hef (in.)	fc (psi)	Actual Capacity (kips)	fy (ksi)	fult (ksi)	Normalized Actual Capacity sq(lb.)*in.	Normalized Predicted Capacity ACI 349-85 sq(lb)*in.
51	1	1.625	12	4300	116	120	150	116000	72689
52	1	1.625	14.1	4245	118	120	150	118000	72689
53	1	1.625	16.2	4200	118	120	150	118000	72689
2a	.625		7	5430	37.5	96	120	37500	19093
2b	.625		7	5430	37.4	96	120	37400	19093
2c	.625		7	5430	37.4	96	120	37400	19093
8a	.625		8	4050	30.9	120	150	30900	23866
8b	.625		8	4050	31.1	120	150	31100	23866
12a	.625		8	4050	31.7	120	150	31700	23866
12b	.625		8	4050	31.2	120	150	31200	23866
15a	.625		8	4050	31.1	120	150	31100	23866
15b	.625		8	4050	31.1	120	150	31100	23866
17a	.625		8	5760	30.9	120	150	30900	23866
17b	.625		8	5760	30.9	120	150	30900	23866
22e	.625		12	4810	31.4	120	150	31400	23866
4a	.625		8	4050	31.1	120	150	31100	23866
5a	.625		8	4050	31.3	120	150	31300	23866
5b	.625		8	4050	31.1	120	150	31100	23866
28a	.625		6	5760	26.3	80	100	26300	15910
28c	.625		6	4520	24.5	80	100	24500	15910
28d	.625		6	4520	23.3	80	100	23300	15910
30a	.625		7	4810	30.6	88	110	30600	17502
30b	.625		7	4810	29.9	88	110	29900	17502
33b	.625		7.5	4520	29.2	120	150	29200	23866
33c	.625		7.5	4520	28.3	120	150	28300	23866
33d	.625		7.5	4520	29.2	120	150	29200	23866
16a	.625		8	5760	30.9	120	150	30900	23866
16b	.625		8	5760	30.8	120	150	30800	23866
21d	.625		7	5130	32.2	120	150	32200	23866
21e	.625		7	5130	32.1	120	150	32100	23866
21f	.625		7	5130	32.1	120	150	32100	23866

APPENDIX H: COMPUTER PROGRAMS FOR CONDUCTING MONTE CARLO ANALYSIS

```
$large
$nofloatcalls
C**  PROGRAM SAFETY3
C****************************************************
C    THIS PROGRAM USES THE MONTE CARLO TECHNIQUE TO COMPUTE THE
C    PROBABILITY OF FAILURE OF A SINGLE TENSILE ANCHOR DESIGNED
C    USING THE APPROACH OF ACI 349 APPENDIX B.  THE METHOD CAN BE
C    APPLIED TO ANY DESIGN APPROACH.  THE FOLLOWING STEPS ARE
C    CARRIED OUT:
C
C    1)   THE LOAD IS ASSUMED TO REPRESENT A 95-PERCENTILE
C         VALUE.  IT IS USED WITH A LOAD FACTOR OF 1.7.
C         BASED ON THIS HISTOGRAM, 1000 LOAD VALUES ARE GENERATED.
C         THE NUMBER OF LOAD VALUES CORRESPONDING TO EACH LOAD
C         DEPENDS ON THE ORDINATES OF THE PROBABILITY FUNCTION.
C
C    2)   AN ANCHOR IS DESIGNED TO HAVE SUFFICIENT STEEL AREA TO
C         RESIST THE FACTORED LOAD.  THE DESIGN STEEL STRENGTH
C         IS A FUNCTION OF THE 95-PERCENTILE LOAD, THE LOAD
C         FACTOR, AND THE PHI FACTOR FOR STEEL.
C
C    3)   THE ANCHOR IS DESIGNED TO HAVE SUFFICIENT EMBEDMENT
C         TO DEVELOP THE STEEL IN TENSION, USING THE 45 DEGREE
C         CONE FORMULA OF ACI 349 APPENDIX B.
C
C    4)   BASED ON THE RESULTS OF PREVIOUS U.S. RESEARCH (SEE
C         KLINGNER AND MENDONCA), THE STATISTICAL DISTRIBUTION
C         OF ACTUAL TO PREDICTED CAPACITY IS KNOWN FOR STEEL
C         AND ALSO FOR CONCRETE FAILURE.  EACH DISTRIBUTION IS
C         REPRESENTED BY A SMOOTHED NORMAL DISTRIBUTION.  AS
C         WITH THE LOADS, 10000 STEEL AND CONCRETE RESISTANCE
C         VALUES ARE GENERATED.  THE NUMBER OF RESISTANCE VALUES
C         CORRESPONDING TO EACH VALUE DEPENDS ON THE
C         STATISTICAL DISTRIBUTION FOR STEEL AND FOR CONCRETE.
C
C    5)   THREE GROUPS OF 10000 RANDOM NUMBERS ARE GENERATED
C         (ZERO TO 999), ONE FOR THE LOAD, ONE FOR STEEL,
C         AND ONE FOR CONCRETE CAPACITY.  EACH SET OF THREE
C         RANDOM NUMBERS REPRESENTS SOME COMBINATION OF LOAD,
C         STEEL STRENGTH, AND CONCRETE STRENGTH.  EACH NUMBER
C         CORRESPONDS RESPECTIVELY TO A PARTICULAR VALUE
C         ON THE STATISTICAL DISTRIBUTION FOR STEEL FAILURE
C         AND FOR CONCRETE FAILURE.  BECAUSE THE NUMBERS ARE
C         RANDOM, THE DISTRIBUTION OF VALUES FOR STEEL AND
C         CONCRETE FAILURE WILL FOLLOW THE EXPERIMENTALLY
C         DETERMINED DISTRIBUTIONS FOR EACH TYPE OF FAILURE.
C
C    6)   BASED ON THOSE VALUES, THE MINIMUM RESISTANCE (STEEL
C         OR CONCRETE) IS COMPUTED, AND THE QUANTITY
```

```
C         (RESISTANCE - LOAD) IS ALSO COMPUTED.
C
C    7)   THE STATISTICAL DISTRIBUTION OF (RESISTANCE - LOAD),
C         OBTAINED BY THIS MONTE CARLO TECHNIQUE, IS ALSO
C         TREATED AS NORMAL.
C         THE NUMBER OF CASES FOR WHICH RESISTANCE IS LESS THAN
C         LOAD, DIVIDED BY THE TOTAL NUMBER OF CASES, REPRESENTS
C         THE PROBABILITY OF FAILURE.
C
C***************************************************************
      IMPLICIT REAL*8 (A-H,O-Z)
      PARAMETER (NMAX = 10000)
      CHARACTER*15 FILOUT
      COMMON / STAT / AVGLOD, COVLOD, AVGSTL, COVSTL, STRSTL,
     1              AVGCONC, COVCONC, STRCONC
      COMMON / RAN / NRAN(NMAX,3),DISTLOD(NMAX),
     1              DISTSTL(NMAX), DISTCON(NMAX), DIFF(NMAX)
      DATA AVGLOD / 1.D0 /
      DATA COVLOD / 0.2D0 /
      DATA AVGSTL / 1.444 /
      DATA COVSTL / 0.156 /
C
C    SET UP OUTPUT FILES
C
      WRITE (*,2001)
 2001 FORMAT (/,5X,'Enter name of output file'/)
      READ (*,1000) FILOUT
 1000 FORMAT (A15)
      OPEN (6,FILE=FILOUT,STATUS='UNKNOWN')
      write (*,5000)
 5000 format(/,5x,'enter mean and cov of concrete data'/)
      read (*,*) avgconc,covconc
C
C    GENERATE THREE SETS OF RANDOM NUMBERS
C
      CALL RANDM
C
C    SET UP STATISTICAL DISTRIBUTION OF LOAD.  DESIGN LOAD
C    IS AT 95% VALUE (1.924 COEFFICIENTS OF VARIATION AWAY
C    FROM AVERAGE).  THIS SUBROUTINE RETURNS NMAX VALUES
C    OF LOAD, DISTRIBUTED ACCORDING TO THE ABOVE.
C
      CALL LOAD
C
C    CHECK DISTRIBUTION OF LOADS
C
      KOUNT = 0
      SUM = 0.D0
      SUM2 = 0.D0
      DO 5 I=1,NMAX
      KOUNT = KOUNT + 1
      SUM = SUM + DISTLOD(I)
      SUM2 = SUM2 + DISTLOD(I)**2
    5 CONTINUE
C
      AVLOD = SUM/DFLOAT(KOUNT)
      STLOD = DSQRT ((SUM2 - SUM**2/DFLOAT(KOUNT))/
     1        DFLOAT(KOUNT - 1))
      COLOD = STLOD/AVLOD
C
C     PRINT CHECK ON DISTRIBUTION OF LOADS
C
      WRITE (6,2002) AVGLOD, COVLOD, AVLOD, COLOD
 2002 FORMAT (1X,// 'TARGET LOADS:',//,
     1        5X, 'AVERAGE LOAD =', F8.3/,
     2        5X, 'COV OF LOADS =',F8.3///,
     3        1X, 'ACTUAL LOADS:',//,
     4        5X, 'AVERAGE LOAD =',F8.3/,
     5        5X, 'COV OF LOADS =', F8.3///)
C
C     SET UP STATISTICAL DISTRIBUTION OF STEEL RESISTANCES.
C     THIS SUBROUTINE RETURNS NMAX VALUES OF STEEL
C     RESISTANCE, DISTRIBUTED ACCORDING TO THE ABOVE.
C
      CALL RESSTL
C
C     CHECK DISTRIBUTION OF STEEL RESISTANCES
C
      KOUNT = 0
      SUM = 0.D0
      SUM2 = 0.D0
      DO 10 I=1,NMAX
      KOUNT = KOUNT + 1
      SUM = SUM + DISTSTL(I)
      SUM2 = SUM2 + DISTSTL(I)**2
   10 CONTINUE
C
      AVSTL = SUM/DFLOAT(KOUNT)
      STSTL = DSQRT ((SUM2 - SUM**2/DFLOAT(KOUNT))/
     1        DFLOAT(KOUNT - 1))
      COSTL = STSTL/AVSTL
C
C     PRINT CHECK ON DISTRIBUTION OF STEEL RESISTANCES
C
      WRITE (6,2003) STRSTL, COVSTL, AVSTL, COSTL
 2003 FORMAT (1X,// 'TARGET STEEL RESISTANCE:',//,
     1        5X, 'AVERAGE STEEL RESISTANCE =',F8.3,/,
     2        5X, 'COV OF STEEL RESISTANCES =', F8.3///
   3        1X, 'ACTUAL STEEL RESISTANCES:',//,
   4        5X, 'AVERAGE STEEL RESISTANCE =', F8.3,/,
   5        5X, 'COV OF STEEL RESISTANCES =',F8.3,///)
C
C    SET UP STATISTICAL DISTRIBUTION OF CONCRETE RESISTANCES.
C    THIS SUBROUTINE RETURNS NMAX VALUES OF CONCRETE
C    RESISTANCE, DISTRIBUTED ACCORDING TO THE ABOVE.
C
      CALL RESCONC
C
C    CHECK DISTRIBUTION OF CONCRETE RESISTANCES
C
      KOUNT = 0
      SUM = 0.D0
      SUM2 = 0.D0
      DO 15 I=1,NMAX
      KOUNT = KOUNT + 1
      SUM = SUM + DISTCON(I)
      SUM2 = SUM2 + DISTCON(I)**2
   15 CONTINUE
C
      AVCONC = SUM/DFLOAT(KOUNT)
      STCONC = DSQRT ((SUM2 - SUM**2/DFLOAT(KOUNT))/
     1         DFLOAT(KOUNT - 1))
      COCONC = STCONC/AVCONC
C
C    PRINT CHECK ON DISTRIBUTION OF CONCRETE RESISTANCES
C
      WRITE (6,2004) STRCONC, COVCONC, AVCONC, COCONC
 2004 FORMAT (1X,// 'TARGET CONCRETE RESISTANCE:',//,
     1        5X, 'AVERAGE CONCRETE RESISTANCE =', F8.3,/,
     2        5X, 'COV OF CONCRETE RESISTANCES =',F8.3,///,
     3        1X, 'ACTUAL CONCRETE RESISTANCES:',//,
     4        5X, 'AVERAGE CONCRETE RESISTANCE =', F8.3/,
     5        5X, 'COV OF CONCRETE RESISTANCES =', F8.3,///)
C
C    APPLY MONTE CARLO TECHNIQUE NMAX TIMES.  EACH TIME,
C    DETERMINE THE LESSER OF STEEL OR CONCRETE RESISTANCE.
C    CALCULATE (RESISTANCE - LOAD), AND ACCUMULATE THE
C    STATISTICS NECESSARY TO DETERMINE THE MEAN AND
C    STANDARD DEVIATION OF (RESISTANCE - LOAD).
C
      KOUNT = 0
      SUM = 0.D0
      SUM2 = 0.D0
C
      DO 20 I=1,NMAX
      DIFF(I) = DMIN1(DISTSTL(NRAN(I,2)),DISTCON(NRAN(I,3)))
     1        - DISTLOD(NRAN(I,1))
```

```
C
      KOUNT = KOUNT + 1
      SUM = SUM + DIFF(I)
      SUM2 = SUM2 + DIFF(I)**2
   20 CONTINUE
C
      AVGDIFF = SUM/DFLOAT(KOUNT)
      STDDIFF = DSQRT ((SUM2 - SUM**2/DFLOAT(KOUNT))/
     1          DFLOAT(KOUNT - 1))
C
C     GIVEN THE STATISTICAL CHARACTERISTICS OF THE
C     (RESISTANCE - LOAD) CURVE, COMPUTE THE SAFETY
C     INDEX BETA, AND THE PROBABILITY OF FAILURE.
C
      BETA = AVGDIFF/STDDIFF
      PROB = AREA(0.D0,AVGDIFF,STDDIFF)/AREA(10.D0,AVGDIFF,STDDIFF)
C
C     WRITE OUTPUT
C
      WRITE (6,2005)
 2005 FORMAT (/,8X,'BETA',10X,'PROBABILITY OF FAILURE'//)
      WRITE (6,2006) BETA, PROB
 2006 FORMAT (1X,F10.2,15X,E10.3)
      STOP
      END
C*****************************************************
      SUBROUTINE RANDM
      IMPLICIT REAL*8 (A-H,O-Z)
      INTEGER*2 IHR, IMIN, ISEC, I100TH
      PARAMETER (NMAX = 10000)
      REAL*4 RANVAL
      COMMON / RAN / NRAN(NMAX,3), DISTLOD(NMAX),
     1          DISTSTL(NMAX), DISTCON(NMAX), DIFF(NMAX)
C
C     GENERATE 3 DIFFERENT SETS OF
C     PSEUDO-RANDOM NUMBERS, USING A DIFFERENT SEED EACH TIME.
C
      DO 20 J=1,3
      CALL GETTIM (IHR,IMIN,ISEC,I100TH)
      CALL SEED(I100TH)
      DO 10 I=1,NMAX
C
C     RANVAL RETURNS A SINGLE RANDOM NUMBER GREATER THAN OR EQUAL
C     TO ZERO AND LESS THAN 1.0.
C
      CALL RANDOM (RANVAL)
      NRAN(I,J) = INT4(RANVAL*DFLOAT(NMAX))
   10 CONTINUE
   20 CONTINUE
```

```
C
      RETURN
      END
C***********************************************************
      SUBROUTINE LOAD
      IMPLICIT REAL*8 (A-H,O-Z)
      PARAMETER (NMAX = 10000)
      COMMON / STAT / AVGLOD, COVLOD, AVGSTL, COVSTL, STRSTL,
     1          AVGCONC, COVCONC, STRCONC
      COMMON / RAN / NRAN(NMAX,3), DISTLOD(NMAX),
     1          DISTSTL(NMAX), DISTCON(NMAX), DIFF(NMAX)
C
C     SET UP STATISTICAL DISTRIBUTION OF LOADS.
C     COEFFICIENT OF VARIATION DOES NOT CHANGE.
C
      XSTART = AVGLOD*(1.D0 - 5.D0*COVLOD)
      XEND = AVGLOD*(1.D0 + 5.D0*COVLOD)
      DX = (XEND - XSTART)/DFLOAT(NMAX/50 + 1)
      KOUNT = 0
      SUM = 0.D0
C
      DO 20 I=1,NMAX/50 + 1
      X = XSTART + DX/2.D0 + DFLOAT(I-1)*DX
      SUM = SUM + GAUSS(X,AVGLOD,AVGLOD*COVLOD)
   20 CONTINUE
C
      FACTOR = DFLOAT(NMAX)/SUM
      KOUNT = 0
C
      DO 30 J=1,NMAX/50 + 1
      X = XSTART + DX/2.D0 + DFLOAT(J-1)*DX
      NHIST = INT4(FACTOR * GAUSS(X,AVGLOD,AVGLOD*COVLOD))
      DO 29 K=1,NHIST
      KOUNT = KOUNT+1
      DISTLOD(KOUNT) = X
   29 CONTINUE
   30 CONTINUE
C
      IF (KOUNT.LT.NMAX) THEN
         DO 35 I=KOUNT+1,NMAX
         DISTLOD(I) = AVGLOD
   35    CONTINUE
      ENDIF
C
      RETURN
      END
C***********************************************************
      SUBROUTINE RESSTL
      IMPLICIT REAL*8 (A-H,O-Z)
      PARAMETER (NMAX = 10000)
      COMMON / STAT / AVGLOD, COVLOD, AVGSTL, COVSTL, STRSTL,
     1           AVGCONC, COVCONC, STRCONC
      COMMON / RAN / NRAN(NMAX,3), DISTLOD(NMAX),
     1           DISTSTL(NMAX), DISTCON(NMAX), DIFF(NMAX)
C
C     SET UP STATISTICAL DISTRIBUTION OF RESISTANCE.  DESIGN
C     RESISTANCE EQUAL DESIGN LOAD TIMES LOAD FACTOR, DIVIDED
C     BY PHI FACTOR.
C
      DESLOD = AVGLOD*(1.D0 + COVLOD*1.924D0)
      PHISTL = 0.9D0
C
C     DETERMINE DESIGN STRENGTH OF STEEL
C     COEFFICIENT OF VARIATION WILL BE
C     AS GIVEN IN DATA STATEMENTS ABOVE.
C
      STRSTL = (DESLOD*1.7D0/PHISTL)*AVGSTL
C
C     SET UP STATISTICAL DISTRIBUTION OF STEEL
C     RESISTANCES.  COEFFICIENT OF VARIATION
C     DOES NOT CHANGE.
C
      XSTART = STRSTL*(1.D0 - 5.D0*COVSTL)
      XEND = STRSTL*(1.D0 + 5.D0*COVSTL)
      DX = (XEND - XSTART)/DFLOAT(NMAX/50 + 1)
      KOUNT = 0
      SUM = 0.D0
C
      DO 20 J=1,NMAX/50 + 1
      X = XSTART + DX/2.D0 + DFLOAT(J-1)*DX
      SUM = SUM + GAUSS(X,STRSTL,STRSTL*COVSTL)
   20 CONTINUE
C
      FACTOR = DFLOAT(NMAX)/SUM
      KOUNT = 0
C
      DO 30 J=1,NMAX/50 + 1
      X = XSTART + DX/2.D0 + DFLOAT(J-1)*DX
      NHIST = INT4(FACTOR * GAUSS(X,STRSTL,STRSTL*COVSTL))
      DO 29 K=1,NHIST
      KOUNT = KOUNT+1
      DISTSTL(KOUNT) = X
   29 CONTINUE
   30 CONTINUE
C
      IF (KOUNT.LT.NMAX) THEN
          DO 35 I=KOUNT+1,NMAX
          DISTSTL(I) = STRSTL
```

```
 35      CONTINUE
       ENDIF
C
       RETURN
       END
C**************************************************************
       SUBROUTINE RESCONC
       IMPLICIT REAL*8 (A-H,O-Z)
       PARAMETER (NMAX = 10000)
       COMMON / STAT / AVGLOD, COVLOD, AVGSTL, COVSTL, STRSTL,
      1          AVGCONC, COVCONC, STRCONC
       COMMON / RAN / NRAN(NMAX,3), DISTLOD(NMAX),
      1          DISTSTL(NMAX), DISTCON(NMAX), DIFF(NMAX)
C
C   SET UP STATISTICAL DISTRIBUTION OF CONCRETE RESISTANCE.
C   DESIGN RESISTANCE EQUALS THE DESIGN STEEL STRENGTH
C   (DESLOD/PHISTEEL), MULTIPLIED BY AVERAGE RATIO OF STEEL
C   ULTIMATE STRENGTH TO STEEL YIELD STRENGTH, DIVIDED
C   BY THE PHI FACTOR FOR CONCRETE, AND MULTIPLIED BY THE
C   AVERAGE RATIO OF ACTUAL CONCRETE STRENGTH TO COMPUTED
C   CONCRETE STRENGTH.  THE AVERAGE RATIO OF STEEL ULTIMATE
C   STRENGTH TO STEEL YIELD STRENGTH IS CONSERVATIVELY
C   TAKEN AS 1.20.
C
       PHISTL = 0.9D0
       PHICONC = 0.65D0
C
C   DETERMINE DESIGN STRENGTH OF CONCRETE
C   COEFFICIENT OF VARIATION WILL BE
C   AS GIVEN IN DATA STATEMENTS ABOVE.
C
       DESLOD = AVGLOD*(1.D0 + COVLOD*1.924D0)
       STRCONC = ((DESLOD*1.7D0)/PHISTL)*1.2D0*AVGCONC/PHICONC
C
C   SET UP STATISTICAL DISTRIBUTION OF CONCRETE
C   RESISTANCES.  COEFFICIENT OF VARIATION
C   DOES NOT CHANGE.
C
       XSTART = STRCONC*(1.D0 - 5.D0*COVCONC)
       XEND = STRCONC*(1.D0 + 5.D0*COVCONC)
       DX = (XEND - XSTART)/DFLOAT(NMAX/50 + 1)
       KOUNT = 0
       SUM = 0.D0
C
       DO 20 J=1,NMAX/50 + 1
       X = XSTART + DX/2.D0 + DFLOAT(J-1)*DX
       SUM = SUM + GAUSS(X,STRCONC,STRCONC*COVCONC)
 20 CONTINUE
C
```

```
      FACTOR = DFLOAT(NMAX)/SUM
      KOUNT = 0
      SUM = 0.D0
C
      DO 30 J=1,NMAX/50 + 1
      X = XSTART + DX/2.D0 + DFLOAT(J-1)*DX
      NHIST = INT4(FACTOR * GAUSS(X,STRCONC,STRCONC*COVCONC))
      DO 29 K=1,NHIST
      KOUNT = KOUNT+1
      DISTCON(KOUNT) = X
   29 CONTINUE
   30 CONTINUE
C
      IF (KOUNT.LT.NMAX) THEN
          DO 35 I=KOUNT+1,NMAX
          DISTCON(I) = STRCONC
   35     CONTINUE
      ENDIF
C
      RETURN
      END
C*************************************************************
      FUNCTION AREA(XEND,AVG,STD)
C
C     THIS FUNCTION SUBPROGRAM COMPUTES THE AREA UNDER A GAUSSIAN
C     CURVE BETWEEN -10 AND XEND.
C
      IMPLICIT REAL*8 (A-H,O-Z)
C
C     SET UP LIMITS OF NUMERICAL INTEGRATION
      START = -10.D0
      DX  = (XEND - START)/1000.D0
      AREA = 0.D0
C
      DO 10 N=1,1000
      X1 = START + DFLOAT(N-1)*DX
      X2 = X1 + DX
      DA = DX*(GAUSS(X1,AVG,STD) + GAUSS(X2,AVG,STD))/2.D0
      AREA = AREA + DA
   10 CONTINUE
C
      RETURN
      END
C*************************************************************
      FUNCTION GAUSS(X,AVG,STD)
      IMPLICIT REAL*8 (A-H,O-Z)
C
C    THIS FUNCTION SUBPROGRAM RETURNS THE VALUE OF A GAUSSION CURVE
C     FOR ANY AVERAGE (AVG) AND STANDARD DEVIATION (STD).
```

```
C
      PI = 2.D0*DASIN(1.D0)
      GAUSS = 1.D0/(STD*DSQRT(2.D0*PI))*
     1        DEXP(-((X - AVG)**2)/(2.D0*STD**2))
C
      RETURN
      END
```

```
$large
$nofloatcalls
C**   PROGRAM SAFETY4
C******************************************************
C     THIS PROGRAM USES THE MONTE CARLO TECHNIQUE TO COMPUTE THE
C     PROBABILITY OF DUCTILE FAILURE OF A SINGLE TENSILE ANCHOR
C     DESIGNED USING THE APPROACH OF ACI 349 APPENDIX B.
C     THE METHOD CAN BE APPLIED TO ANY DESIGN APPROACH.
C     THE FOLLOWING STEPS ARE CARRIED OUT:
C
C     1)   AN ANCHOR IS DESIGNED TO HAVE SUFFICIENT STEEL AREA TO
C          RESIST SOME LOAD.
C
C     2)   THE ANCHOR IS DESIGNED TO HAVE SUFFICIENT EMBEDMENT
C          TO DEVELOP THE STEEL IN TENSION, USING THE 45 DEGREE
C          CONE FORMULA OF ACI 349 APPENDIX B.
C
C     3)   BASED ON THE RESULTS OF PREVIOUS U.S. RESEARCH (SEE
C          KLINGNER AND MENDONCA), THE STATISTICAL DISTRIBUTION
C          OF ACTUAL TO PREDICTED CAPACITY IS KNOWN FOR STEEL
C          AND ALSO FOR CONCRETE FAILURE.  EACH DISTRIBUTION IS
C          REPRESENTED BY A SMOOTHED NORMAL DISTRIBUTION.  AS
C          WITH THE LOADS, 10000 STEEL AND CONCRETE RESISTANCE
C          VALUES ARE GENERATED.  THE NUMBER OF RESISTANCE VALUES
C          CORRESPONDING TO EACH VALUE DEPENDS ON THE
C          STATISTICAL DISTRIBUTION FOR STEEL AND FOR CONCRETE.
C
C     4)   TWO GROUPS OF 10000 RANDOM NUMBERS ARE GENERATED
C          (ZERO TO 999), ONE FOR STEEL, AND ONE FOR CONCRETE
C          CAPACITY.  EACH SET OF TWO RANDOM NUMBERS REPRESENTS
C          SOME COMBINATION OF STEEL STRENGTH, AND CONCRETE STRENGTH.

C        EACH NUMBER CORRESPONDS RESPECTIVELY TO A PARTICULAR VALUE
C          ON THE STATISTICAL DISTRIBUTION FOR STEEL FAILURE
C          AND FOR CONCRETE FAILURE.  BECAUSE THE NUMBERS ARE
C          RANDOM, THE DISTRIBUTION OF VALUES FOR STEEL AND
C          CONCRETE FAILURE WILL FOLLOW THE EXPERIMENTALLY
C          DETERMINED DISTRIBUTIONS FOR EACH TYPE OF FAILURE.
C
C     5)   BASED ON THOSE VALUES, DISCRETE HISTOGRAMS ARE
C          GENERATED FOR STEEL AND CONCRETE RESISTANCE,
C          AND THE QUANTITY (CONCRETE - STEEL) IS COMPUTED.
C
C     6)   THE STATISTICAL DISTRIBUTION OF (CONCRETE - STEEL),
C          OBTAINED BY THIS MONTE CARLO TECHNIQUE, IS ALSO
C          TREATED AS NORMAL.  THE NUMBER OF CASES FOR WHICH
C          CONCRETE RESISTANCE IS LESS THAN STEEL RESISTANCE,
C          DIVIDED BY THE TOTAL NUMBER OF CASES, REPRESENTS
C          THE PROBABILITY OF BRITTLE FAILURE.
```

```
C
C***************************************************************
      IMPLICIT REAL*8 (A-H,O-Z)
      PARAMETER (NMAX = 10000)
      CHARACTER*15 FILOUT
      COMMON / STAT / AVGLOD, COVLOD, AVGSTL, COVSTL, STRSTL,
     1              AVGCONC, COVCONC, STRCONC
      COMMON / RAN / NRAN(NMAX,2),DISTLOD(NMAX),
     1             DISTSTL(NMAX), DISTCON(NMAX), DIFF(NMAX)
      DATA AVGLOD / 1.D0 /
      DATA COVLOD / 0.2D0 /
      DATA AVGSTL / 1.444 /
      DATA COVSTL / 0.156 /
C
C     SET UP OUTPUT FILES
C
      WRITE (*,2001)
 2001 FORMAT (/,5X,'Enter name of output file'/)
      READ (*,1000) FILOUT
 1000 FORMAT (A15)
      OPEN (6,FILE=FILOUT,STATUS='UNKNOWN')
      write(*,5000)
 5000 format(/,5x,'enter mean and cov of concrete'/)
      read(*,*) avgconc,covconc
C
C     GENERATE TWO SETS OF RANDOM NUMBERS
C
      CALL RANDM
C
C     SET UP STATISTICAL DISTRIBUTION OF STEEL RESISTANCES.
C     THIS SUBROUTINE RETURNS NMAX VALUES OF STEEL
C     RESISTANCE, DISTRIBUTED ACCORDING TO THE ABOVE.
C
      CALL RESSTL
C
C     CHECK DISTRIBUTION OF STEEL RESISTANCES
C
      KOUNT = 0
      SUM = 0.D0
      SUM2 = 0.D0
      DO 10 I=1,NMAX
      KOUNT = KOUNT + 1
      SUM = SUM + DISTSTL(I)
      SUM2 = SUM2 + DISTSTL(I)**2
   10 CONTINUE
C
      AVSTL = SUM/DFLOAT(KOUNT)
      STSTL = DSQRT ((SUM2 - SUM**2/DFLOAT(KOUNT))/
     1           DFLOAT(KOUNT - 1))
```

```
      COSTL = STSTL/AVSTL
C
C      PRINT CHECK ON DISTRIBUTION OF STEEL RESISTANCES
C
      WRITE (6,2003) STRSTL, COVSTL, AVSTL, COSTL
 2003 FORMAT (1X,// 'TARGET ULTIMATE STEEL RESISTANCE:',//,
     1      5X, 'AVERAGE ULTIMATE STEEL RESISTANCE =',F8.3,/,
     2      5X, 'COV OF ULTIMATE STEEL RESISTANCES =', F8.3///
     3      1X, 'ACTUAL ULTIMATE STEEL RESISTANCES:',//,
     4      5X, 'AVERAGE ULTIMATE STEEL RESISTANCE =', F8.3,/,
     5      5X, 'COV OF ULTIMATE STEEL RESISTANCES =',F8.3,///)
C
C      SET UP STATISTICAL DISTRIBUTION OF CONCRETE RESISTANCES.
C      THIS SUBROUTINE RETURNS NMAX VALUES OF CONCRETE
C      RESISTANCE, DISTRIBUTED ACCORDING TO THE ABOVE.
C
      CALL RESCONC
C
C      CHECK DISTRIBUTION OF CONCRETE RESISTANCES
C
      KOUNT = 0
      SUM = 0.D0
      SUM2 = 0.D0
      DO 15 I=1,NMAX
      KOUNT = KOUNT + 1
      SUM = SUM + DISTCON(I)
      SUM2 = SUM2 + DISTCON(I)**2
   15 CONTINUE
C
      AVCONC = SUM/DFLOAT(KOUNT)
      STCONC = DSQRT ((SUM2 - SUM**2/DFLOAT(KOUNT))/
     1         DFLOAT(KOUNT - 1))
      COCONC = STCONC/AVCONC
C
C      PRINT CHECK ON DISTRIBUTION OF CONCRETE RESISTANCES
C
      WRITE (6,2004) STRCONC, COVCONC, AVCONC, COCONC
 2004 FORMAT (1X,// 'TARGET CONCRETE RESISTANCE:',//,
     1      5X, 'AVERAGE CONCRETE RESISTANCE =', F8.3,/,
     2      5X, 'COV OF CONCRETE RESISTANCES =',F8.3,///,
     3      1X, 'ACTUAL CONCRETE RESISTANCES:',//,
     4      5X, 'AVERAGE CONCRETE RESISTANCE =', F8.3/,
     5      5X, 'COV OF CONCRETE RESISTANCES =', F8.3,///)
C
C      APPLY MONTE CARLO TECHNIQUE NMAX TIMES.  EACH TIME,
C      DETERMINE THE LESSER OF STEEL OR CONCRETE RESISTANCE.
C      CALCULATE (CONCRETE - STEEL), AND ACCUMULATE THE
C      STATISTICS NECESSARY TO DETERMINE THE MEAN AND
C      STANDARD DEVIATION OF (CONCRETE - STEEL).
```

```
C
      KOUNT = 0
      SUM = 0.D0
      SUM2 = 0.D0
C
      DO 20 I=1,NMAX
      DIFF(I) = DISTCON(NRAN(I,2)) - DISTSTL(NRAN(I,2))
C
      KOUNT = KOUNT + 1
      SUM = SUM + DIFF(I)
      SUM2 = SUM2 + DIFF(I)**2
   20 CONTINUE
C
      AVGDIFF = SUM/DFLOAT(KOUNT)
      STDDIFF = DSQRT ((SUM2 - SUM**2/DFLOAT(KOUNT))/
     1          DFLOAT(KOUNT - 1))
C
C     GIVEN THE STATISTICAL CHARACTERISTICS OF THE
C     (CONCRETE - STEEL) CURVE, COMPUTE THE SAFETY
C     INDEX BETA, AND THE PROBABILITY OF BRITTLE
C     FAILURE.
C
      BETA = AVGDIFF/STDDIFF
      PROB = AREA(0.D0,AVGDIFF,STDDIFF)/AREA(10.D0,AVGDIFF,STDDIFF)
C
C     WRITE OUTPUT
C
      WRITE (6,2005)
 2005 FORMAT (/,8X,'BETA',10X,'PROBABILITY OF BRITTLE FAILURE'//)
      WRITE (6,2006) BETA, PROB
 2006 FORMAT (1X,F10.2,15X,E10.3)
      STOP
      END
C*****************************************************
      SUBROUTINE RANDM
      IMPLICIT REAL*8 (A-H,O-Z)
      INTEGER*2 IHR, IMIN, ISEC, I100TH
      PARAMETER (NMAX = 10000)
      REAL*4 RANVAL
      COMMON / RAN / NRAN(NMAX,2), DISTLOD(NMAX),
     1          DISTSTL(NMAX), DISTCON(NMAX), DIFF(NMAX)
C
C     GENERATE 2 DIFFERENT SETS OF
C     PSEUDO-RANDOM NUMBERS, USING A DIFFERENT SEED EACH TIME.
C
      DO 20 J=1,2
      CALL GETTIM (IHR,IMIN,ISEC,I100TH)
      CALL SEED(I100TH)
      DO 10 I=1,NMAX
```

```
C
C   RANVAL RETURNS A SINGLE RANDOM NUMBER GREATER THAN OR EQUAL
C    TO ZERO AND LESS THAN 1.0.
C
      CALL RANDOM (RANVAL)
      NRAN(I,J) = INT4(RANVAL*DFLOAT(NMAX))
   10 CONTINUE
   20 CONTINUE
C
      RETURN
      END
C**********************************************************
      SUBROUTINE RESSTL
      IMPLICIT REAL*8 (A-H,O-Z)
      PARAMETER (NMAX = 10000)
      COMMON / STAT / AVGLOD, COVLOD, AVGSTL, COVSTL, STRSTL,
     1            AVGCONC, COVCONC, STRCONC
      COMMON / RAN / NRAN(NMAX,2), DISTLOD(NMAX),
     1            DISTSTL(NMAX), DISTCON(NMAX), DIFF(NMAX)
C
C   SET UP STATISTICAL DISTRIBUTION OF ULTIMATE RESISTANCE.
C   ULTIMATE RESISTANCE EQUALS DESIGN LOAD TIMES LOAD FACTOR,
C   DIVIDED BY DIVIDED BY PHI FACTOR, MULTIPLIED BY RATIO OF
C   SPECIFIED ULTIMATE RESISTANCE TO SPECIFIED YIELD
C   RESISTANCE, AND FINALLY MULTIPLIED BY AVERAGE RATIO
C   OF ACTUAL TO PREDICTED STEEL CAPACITY.
C
      DESLOD = AVGLOD*(1.D0 + COVLOD*1.924D0)
      PHISTL = 0.9D0
C
C   DETERMINE DESIGN STRENGTH OF STEEL
C   COEFFICIENT OF VARIATION WILL BE
C   AS GIVEN IN DATA STATEMENTS ABOVE.
C
      STRSTL = (DESLOD*1.7D0/PHISTL)*AVGSTL
C
C   SET UP STATISTICAL DISTRIBUTION OF STEEL
C   RESISTANCES.  COEFFICIENT OF VARIATION
C   DOES NOT CHANGE.
C
      XSTART = STRSTL*(1.D0 - 5.D0*COVSTL)
      XEND = STRSTL*(1.D0 + 5.D0*COVSTL)
      DX = (XEND - XSTART)/DFLOAT(NMAX/50 + 1)
      KOUNT = 0
      SUM = 0.D0
C
      DO 20 J=1,NMAX/50 + 1
      X = XSTART + DX/2.D0 + DFLOAT(J-1)*DX
      SUM = SUM + GAUSS(X,STRSTL,STRSTL*COVSTL)
```

```
 20 CONTINUE
C
    FACTOR = DFLOAT(NMAX)/SUM
    KOUNT = 0
C
    DO 30 J=1,NMAX/50 + 1
    X = XSTART + DX/2.D0 + DFLOAT(J-1)*DX
    NHIST = INT4(FACTOR * GAUSS(X,STRSTL,STRSTL*COVSTL))
    DO 29 K=1,NHIST
    KOUNT = KOUNT+1
    DISTSTL(KOUNT) = X
 29 CONTINUE
 30 CONTINUE
C
    IF (KOUNT.LT.NMAX) THEN
        DO 35 I=KOUNT+1,NMAX
        DISTSTL(I) = STRSTL
 35      CONTINUE
    ENDIF
C
    RETURN
    END
C*************************************************************
    SUBROUTINE RESCONC
    IMPLICIT REAL*8 (A-H,O-Z)
    PARAMETER (NMAX = 10000)
    COMMON / STAT / AVGLOD, COVLOD, AVGSTL, COVSTL, STRSTL,
   1              AVGCONC, COVCONC, STRCONC
    COMMON / RAN / NRAN(NMAX,2), DISTLOD(NMAX),
   1             DISTSTL(NMAX), DISTCON(NMAX), DIFF(NMAX)
C
C    SET UP STATISTICAL DISTRIBUTION OF CONCRETE RESISTANCE.
C    DESIGN RESISTANCE EQUALS THE DESIGN STEEL STRENGTH
C    (DESLOD/PHISTEEL), MULTIPLIED BY AVERAGE RATIO OF STEEL
C    ULTIMATE STRENGTH TO STEEL YIELD STRENGTH, DIVIDED
C    BY THE PHI FACTOR FOR CONCRETE, AND MULTIPLIED BY THE
C    AVERAGE RATIO OF ACTUAL CONCRETE STRENGTH TO COMPUTED
C    CONCRETE STRENGTH.  THE AVERAGE RATIO OF STEEL ULTIMATE
C    STRENGTH TO STEEL YIELD STRENGTH IS CONSERVATIVELY
C    TAKEN AS 1.20.
C
    PHISTL = 0.9D0
    PHICONC = 0.65D0
C
C    DETERMINE DESIGN STRENGTH OF CONCRETE
C    COEFFICIENT OF VARIATION WILL BE
C    AS GIVEN IN DATA STATEMENTS ABOVE.
C
    DESLOD = AVGLOD*(1.D0 + COVLOD*1.924D0)
```

```
      STRCONC = ((DESLOD*1.7D0)/PHISTL)*1.2D0*AVGCONC/PHICONC
C
C      SET UP STATISTICAL DISTRIBUTION OF CONCRETE
C      RESISTANCES.  COEFFICIENT OF VARIATION
C      DOES NOT CHANGE.
C
      XSTART = STRCONC*(1.D0 - 5.D0*COVCONC)
      XEND = STRCONC*(1.D0 + 5.D0*COVCONC)
      DX = (XEND - XSTART)/DFLOAT(NMAX/50 + 1)
      KOUNT = 0
      SUM = 0.D0
C
      DO 20 J=1,NMAX/50 + 1
      X = XSTART + DX/2.D0 + DFLOAT(J-1)*DX
      SUM = SUM + GAUSS(X,STRCONC,STRCONC*COVCONC)
   20 CONTINUE
C
      FACTOR = DFLOAT(NMAX)/SUM
      KOUNT = 0
      SUM = 0.D0
C
      DO 30 J=1,NMAX/50 + 1
      X = XSTART + DX/2.D0 + DFLOAT(J-1)*DX
      NHIST = INT4(FACTOR * GAUSS(X,STRCONC,STRCONC*COVCONC))
      DO 29 K=1,NHIST
      KOUNT = KOUNT+1
      DISTCON(KOUNT) = X
   29 CONTINUE
   30 CONTINUE
C
      IF (KOUNT.LT.NMAX) THEN
          DO 35 I=KOUNT+1,NMAX
          DISTCON(I) = STRCONC
   35     CONTINUE
      ENDIF
C
      RETURN
      END
C*************************************************************
      FUNCTION AREA(XEND,AVG,STD)
C
C     THIS FUNCTION SUBPROGRAM COMPUTES THE AREA UNDER A GAUSSIAN
C     CURVE BETWEEN -10 AND XEND.
C
      IMPLICIT REAL*8 (A-H,O-Z)
C
C     SET UP LIMITS OF NUMERICAL INTEGRATION
      START = -10.D0
      DX  = (XEND - START)/1000.D0
      AREA = 0.D0
C
      DO 10 N=1,1000
      X1 = START + DFLOAT(N-1)*DX
      X2 = X1 + DX
      DA = DX*(GAUSS(X1,AVG,STD) + GAUSS(X2,AVG,STD))/2.D0
      AREA = AREA + DA
   10 CONTINUE
C
      RETURN
      END
C******************************************************************
      FUNCTION GAUSS(X,AVG,STD)
      IMPLICIT REAL*8 (A-H,O-Z)
C
C     THIS FUNCTION SUBPROGRAM RETURNS THE VALUE OF A GAUSSION CURVE
C      FOR ANY AVERAGE (AVG) AND STANDARD DEVIATION (STD).
C
      PI = 2.D0*DASIN(1.D0)
      GAUSS = 1.D0/(STD*DSQRT(2.D0*PI))*
     1     DEXP(-((X - AVG)**2)/(2.D0*STD**2))
C
      RETURN
      END
```

REFERENCES

1. ACI Committee 349, Code Requirements for Nuclear Safety Related Structures (ACI 349-85), American Concrete Institute, Detroit, 1985.

2. Farrow, C. B., Frigui, I., and Klingner, R. E., "Tensile Capacity of Single Headed Anchors in Concrete: Evaluation of Existing Formulas on an LRFD Basis", A Report to the Tennessee Valley Authority, The University of Texas at Austin, March 1992.

3. CEB Task Group VI/5, Fastenings to Reinforced Concrete and Masonry Structures: Design and Detailing; Volume 1 (Behavior under Monotonic, Sustained, Fatigue, Seismic and Impact Loadings, Task Group/5 (Embedments), Euro-International Concrete Committee (CEB), August 1991.

4. Eligehausen, R., Fuchs, W., and Mayer, B., "Tragverhalten von Dubelbefestigungen bei Zugbeanspruchung" ("Load-bearing Behavior of Anchor Fastenings in Tension"), Betonwerk + Fertigteil-Technik, Berlin, no. 12 (1987). pp. 826-832 (German) and no. 1 (1988), pp. 29-35 (English), 1987/88.

5. Rehm, G., Eligehausen, R., and Mallee, R., "Befestigungstechnik," Beitrag zum Betonkalendar 1988 ("Fastening Technique," contribution to 1988 Concrete Calendar), Verlag Enst & Sohn, Berlin, 1988.

6. Klingner, R. E. and Mendonca, J. A., "Tensile Capacity of Short Anchor Bolts and Welded Studs: A Literature Review," Journal of the American Concrete Institute, Proceedings Vol. 79, No. 4, July-August 1982, pp. 270-279.

7. Collins, D. M., Klingner, R. E., and Polyzois, D., "Load-Deflection Behavior of Cast-in-Place and Retrofit Concrete Anchors Subjected to Static, Fatigue, and Impact Tensile Loads," Research Report CTR 1126-1, Center for Transportation Research, The University of Texas at Austin, February 1989.

8. Eligehausen, R. and Sawade, G., "A Fracture Mechanics-Based Description of the Pull-Out Behavior of Headed Studs Embedded in Concrete," University of Stuttgart, 1989. (Especially see Fig. 10).

9. "General Anchorage to Concrete," TVA Civil Design Standard No. DS-C.1.7.1, Tennessee Valley Authority, Knoxville, Tennessee, 1984.

10. Eligehausen, R., "Report to ACI 355," 1989.

11. Breen, J. E., Eligehausen, R., and Fuchs, W., "Comparison of Procedures For Concrete Capacity", Draft Report No. 12/14-91/10, September 1991.

12. Correspondence with Werner Fuchs. June 1991.

13. Correspondence with Rolf Eligehausen. December 23, 1991.

14. Correspondence with Robert W. Cannon. December 26, 1991.

15. Correspondence with Richard Orr. December 2, 1991.

16. Avram, Constantin, et al, Concrete Strength and Strains, Elsevier Scientific Publishing Company, Oxford, England, 1981.

17. Lee D. W., and Breen, J. E., "Factors Affecting Anchor Bolt Development," Research Report No. 88-1F, Center for Highway Research, The University of Texas at Austin, Aug. 1966.

18. Hasselwander, G. B., Jirsa, J. O., Breen, J. E., and Lo, K., "Strength and Behavior of Anchor Bolts Embedded near Edges of Concrete Piers," Research Report No. 29-2F, Center for Highway Research, The University of Texas at Austin, May 1977.

19. UEAtc - European Union of Agrément, UEAtc Directives for Assessment of Anchor Bolts, M.O.A.T. No. 42, London, 1986.

20. Eligehausen, R., "Report to ACI 355," 1991.

21. MacGregor, J. G., Reinforced Concrete Mechanics and Design, Prentice-Hall, Englewood Cliffs, New Jersey, 1988.

22. Klingner, R.E., "Development of a Load and Resistance Factor Basis for Anchorage Design by ACI 349-85, Appendix B", Report to ACI Committee 355, September 1990.

VITA

Charles Benjamin Farrow, son of Charles Aubrey and Jerry Shreve Farrow, was born in Montgomery, Alabama, on March 7, 1969. Farrow attended Benjamin Russell High School in Alexander City, Alabama. One year prior to his May 1987 graduation, he participated in Duke University's Precollege Program. Subsequently, he continued his undergraduate studies at Duke. During the summer of 1989 he attended the University of North Carolina at Chapel Hill. He received the degree of Bachelor of Science in Engineering along with a second major in mathematics from Duke University in May 1991. In June 1991 he entered the Graduate School of the University of Texas.

Farrow has interned in the engineering departments of Russell Corporation, Alexander City, Alabama, and of Moffatt and Nichol, Raleigh, North Carolina. As a research assistant at the University of Texas at Austin, he has also worked on two projects cooperatively evaluating standard design methodologies for concrete anchors loaded in tension.

Permanent Address: 807 Cherokee Road
Alexander City, Alabama 35010

This thesis was typed by the author.